Webb Institute

wind support

MARIN
BETTER SHIPS, BLUE OCEANS

UNITED STATES MERCHANT MARINE ACADEMY
ACTA NON VERBA
1943
KINGS POINT

Proceedings of the 6th

Sustainability *and* Innovation *in* Ship Design *and* Operations

Conference



October 19-20, 2026

Volume 4: Presentations

Conference Information

The Sustainability and Innovation in Ship Design and Operations (SISDO) conference aims to bring together industry and academia to discuss the concepts, technologies, case studies, and success stories related to sustainability in ship design and the greater maritime industry. Academic and technical presentations are shared by experts and practitioners, bringing innovative ideas and information to a wider audience. The presentation slide decks are collected in these conference proceedings.

The ultimate goal of maritime sustainability is to create and operate ships and infrastructure that are more efficient and environmentally friendly, making the maritime industry more sustainable in the long term.

Disclaimer

The views and viewpoints expressed during the Sustainability and Innovation in Ship Design and Operations conference and through the following papers and presentation slides are those of the authors and/or speakers and do not necessarily reflect the opinions, policies, or endorsements of the conference organizers, partner institutions, sponsor organizations, U.S. Government or of the non-Federal entities (NFE). References to NFEs, trade names, or commercial products do not constitute their endorsement by the U.S. Government and are meant for illustrative and educational purposes only.

Open Access License – CC BY 4.0

Unless otherwise noted, material provided in this document is licensed under a Creative Commons Attribution 4.0 License (CC BY). This license enables the copy, distribution, transmission, or adaptation of material in any medium or format, so long as attribution and credit is given to the original author(s). This license allows for commercial use. Additional licensing information may be found at: https://creativecommons.org/licenses/by/4.0/

Citation Information

Papers or presentations from this publication may be cited with the following information, adapted to the citation format of choice.

LastName, F.I., Second Name, "Title of presentation," *Proceedings of the 6th Sustainability and Innovation in Ship Design and Operations Conference*, Glen Cove, NY, October 19-20, 2026, Volume 4, pp. XX-XX.

Table of Contents

Risk Mitigation for Innovative Designs and Novel Ships, Part 1

Ian Busch 1

Large-Area Additive Manufacturing for High-Speed Uncrewed Surface Vessels

Addie Lindyberg, Troy Zangle 33

Risk Mitigation for Innovative Designs and Novel Ships, Part 2

Ian Busch 73

Air Layer Drag Reduction Systems

Alex Taber 118

Bay State Sail Freight

Steven Woods 149

Improved Ship Engine Emissions Mitigation through Optimized Propeller Design for Reduced Cavitation

Lubomir Ribarov 174

WINDCOOP: A New Perspective on Hydrodynamic Optimization

Bastien Abeil 240

A Prototype Human-Powered Electric-Drive Small Boat for Long-Distance Cruising on Rivers and Lakes

Isaac Lee, Erik Lunn, Sergio E. Perez 260

Reassessing the 32°C Tropical Seawater Design Condition for Ship Machinery Cooling Under Ocean Warming

M. Spenser Boyd 299

The Case for Powered Propellers on Ship Wingsails

Sergio E. Perez 347

GENERAL DYNAMICS

NASSCO

Risk Mitigation for Innovative Designs and Novel Ships Part 1

- 19 October 2026



SUSTAINABILITY AND INNOVATION IN SHIP DESIGN AND OPERATIONS CONFERENCE 2026

October 19-20, 2026

Who Am I?

The Basics

- Webb Institute, 1988
- Right away to MIT
  - MS, NA&ME 1990
  - MS, Ocean Sys Mgmt, 1990
- NASSCO for 36 years and counting

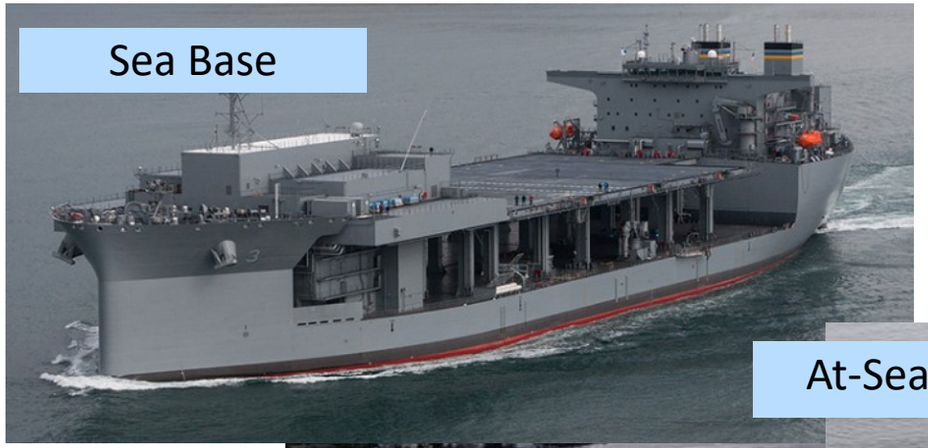
What Have I Seen?

- 3 classes of commercial ships built that were designed in house
- 6 classes of Navy ships built that were designed in house
- 4 classes of commercial ships built that had Korean design leadership
- Dozens of in-house concept designs

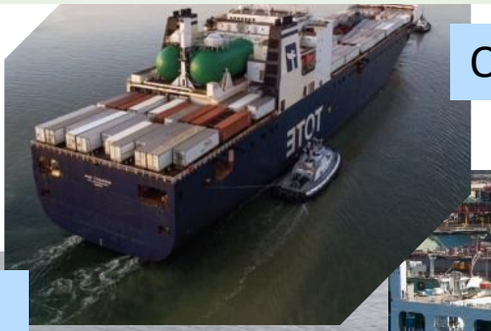
Sequence at NASSCO

- Naval Architect: undockings, stability, structural analysis
- Marketing: Proposal writing
- Contracts: Claims and contract changes
- Steel Production: Interpret drawings and facility Improvement support
- Structural detail design supervisor
- Manager of Initial Design & Naval Architecture: concept through sea trials
- Director: added marine & electrical
- Director Hull, Innovation, & Quality: gave up most marine & electrical, gained structural detail, test, quality, design improvement, and the Council of Principals

Innovative Design Work at NASSCO 1990-Present (a sampler)



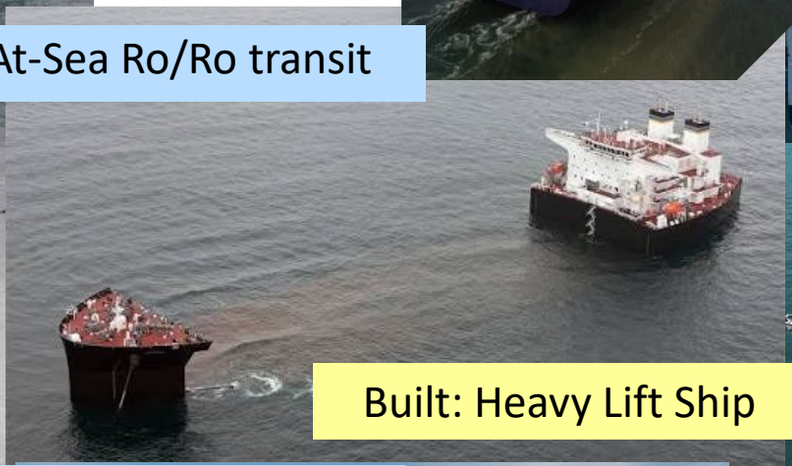
Integrated AC Diesel Electric



Oceangoing LNG Propulsion



At-Sea Ro/Ro transit

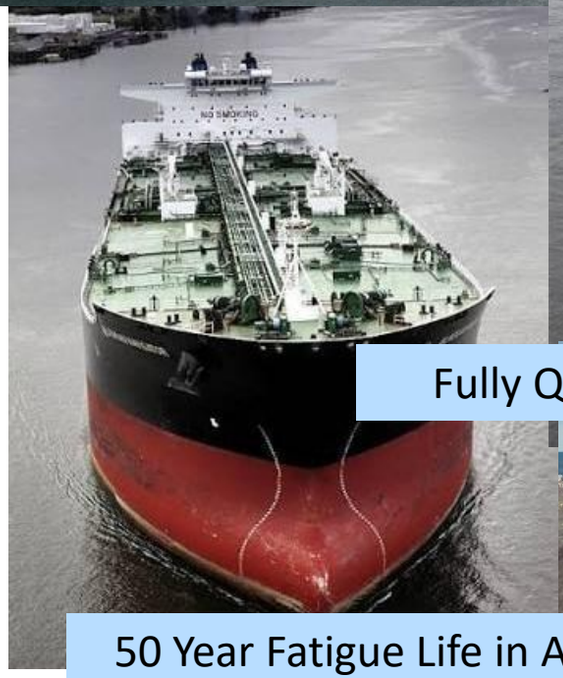




First to NASSCO

First for USA

First in World



Built: Heavy Lift Ship

Fully Qualified for V-22



Commercial Standard Tenders



50 Year Fatigue Life in Alaska

Presentation Overview

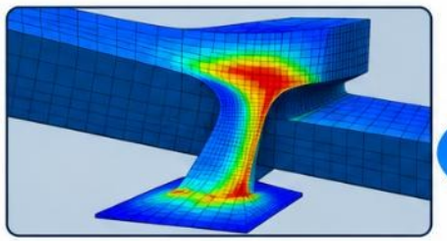
Strange ships can be tough to design (well).

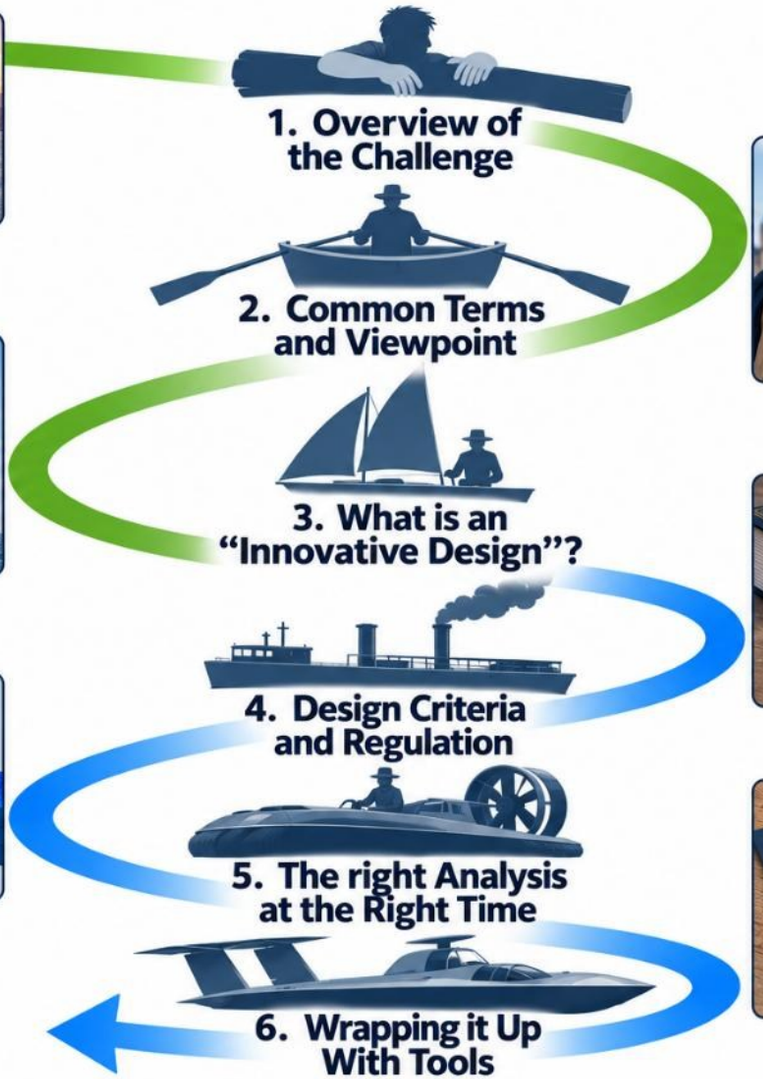
“Doing new” is a trip into the unknown, where prior designs, existing rules, and established practice can lead us astray.

But ship design is a risky business. As designers and builders, we must overcome the risk, while staying in business.















Same Toll Booth, Different Bridge.



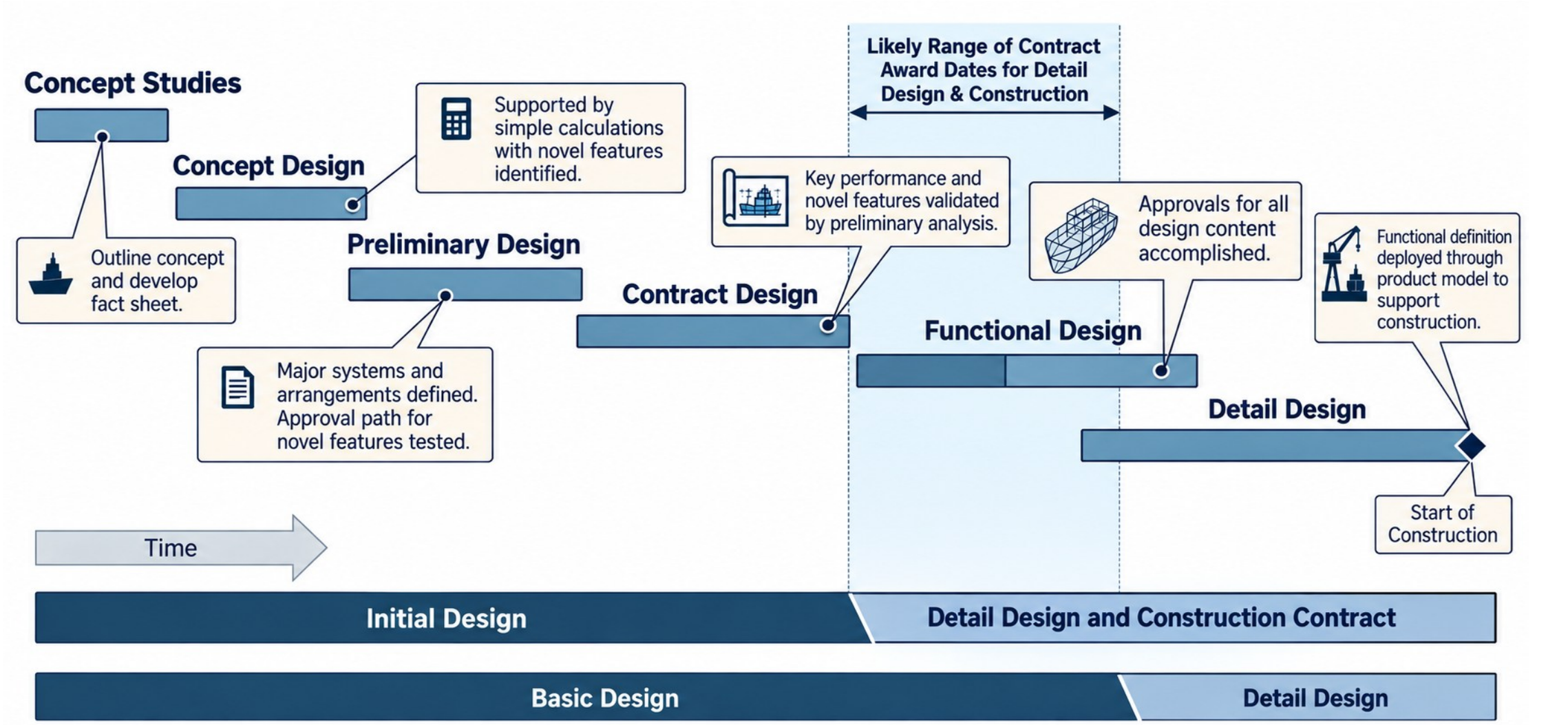
What Makes a Ship Novel?

- Don’t ask: “Has this feature been built before?”
- Ask: “Does this feature or combination impact how this project gets approved in service?

- What everyone worries about:
  - Risk of approval
  - Cost of the project
  - Time to in service
- How do we gain the advantage we seek while we avoid the pitfalls of the real world?



Design Stages



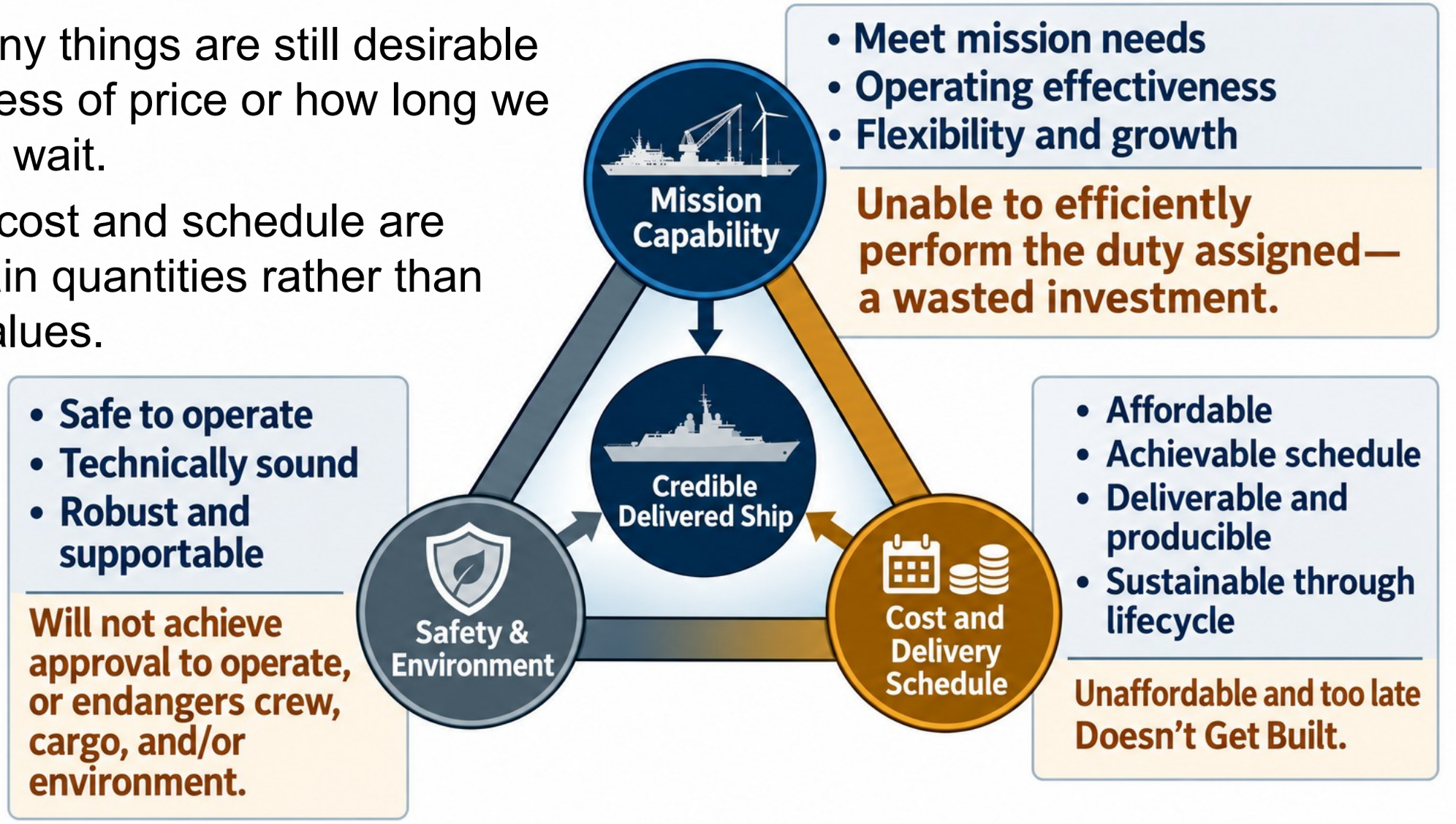
Data Inventory



Generate the minimum information necessary to support the next design decision and generate it as late as possible without affecting the schedule.

Cost and Schedule Are Design Requirements

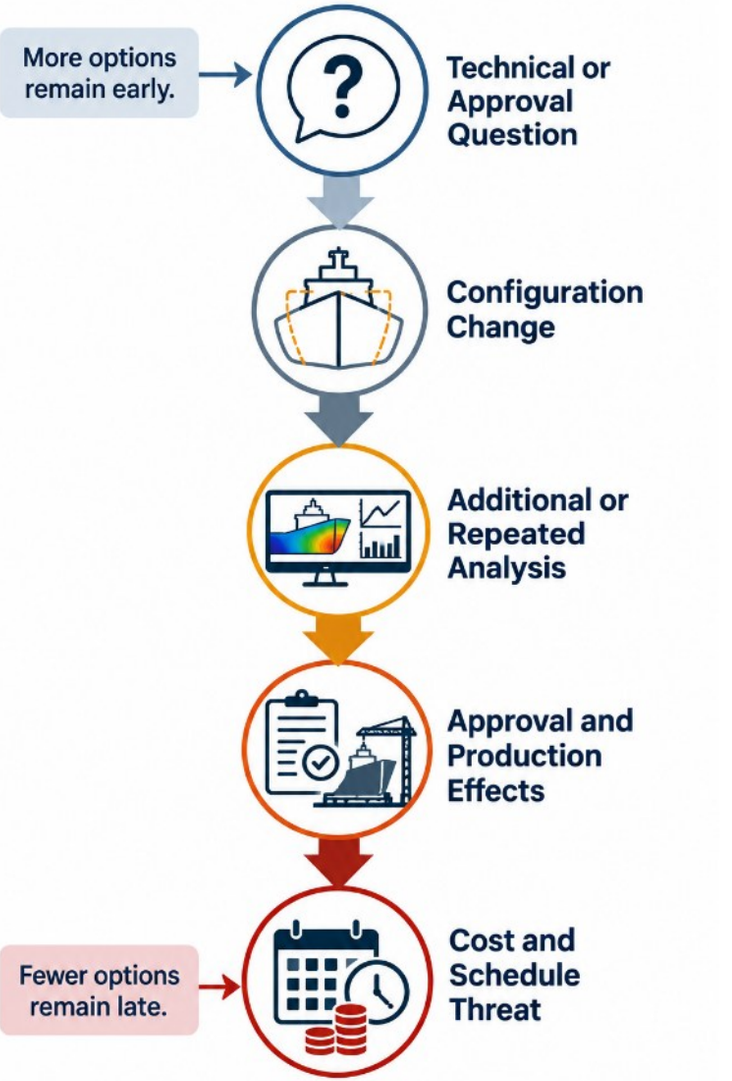
- Not many things are still desirable regardless of price or how long we have to wait.
- Future cost and schedule are uncertain quantities rather than fixed values.



What Failure Means in Shipbuilding Programs

- Risk affects the sequence of design decisions, not only the completed vessel.
- The design objective is a ship that is: achievable, safe; approvable; producible; and capable of performing its mission.
- Technical, approval, production, cost, and schedule risks can each contribute to the same project-level failure.
- For this presentation, failure means that the ship is not built, delivered, and placed into its intended productive service.

Every ship project begins with a business case that involves a mission and money.
Risk and Failure are about invalidating that business case.



The Business Environment

Alignment of strategy and risk appetite should minimize exposure to unexpected losses.
– Jerome Powell

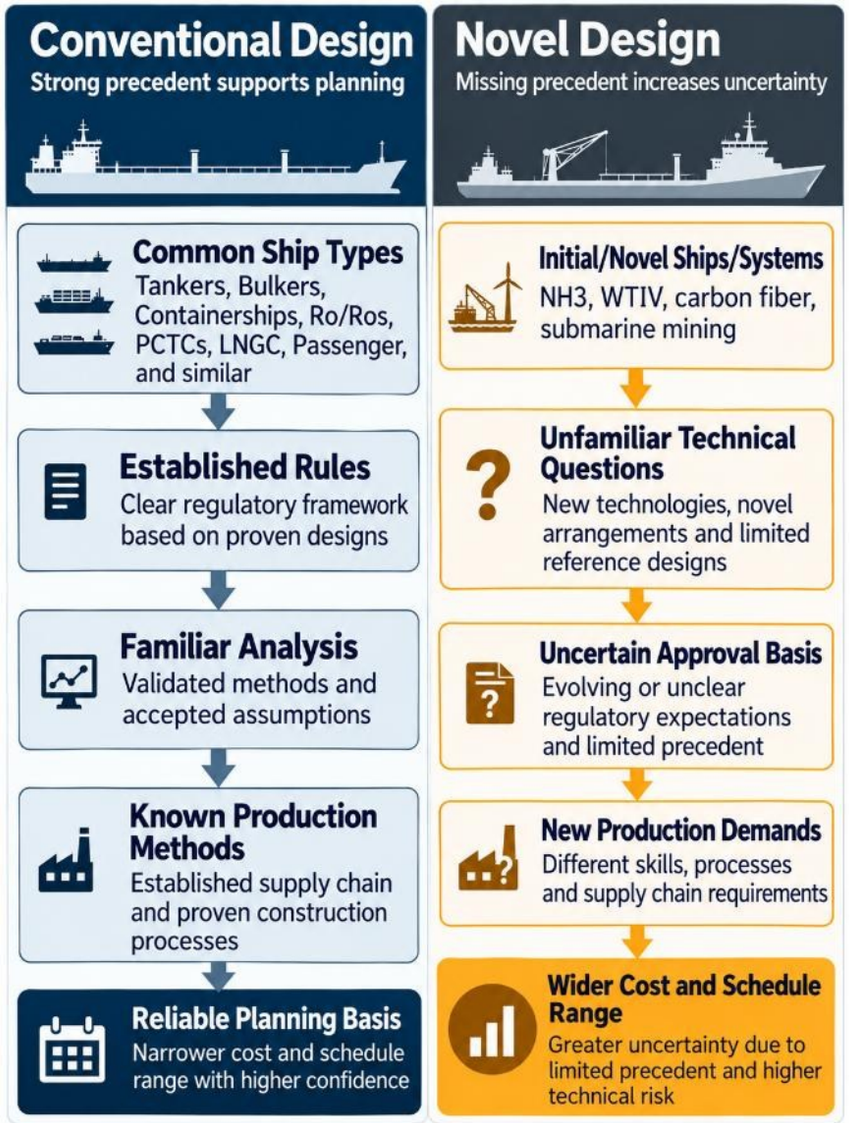
- Risk that is present in a project can't be contracted away.
- Best case is it is held by the party that has the most ability to control it (they should price it cheapest!)
- Regardless of who has the risk hot potato, that party must account for it in bids and estimates.

Terms	Owner Viewpoint	Contractor Viewpoint	Advantage	Risk	Exposure	Failure Mode
Fixed price	Known cost. Get everything you can out of that fixed price.	Must cover every possible risk in initial bid. Save every penny.	Cost predictability after award	All Contractor	Unresolved uncertainty becomes contractor exposure.	Contractor defaults, bankruptcy.
Fixed Price Incentive	Shared pain and Gain – both parties have an interest to control cost & risk.		Shares benefits from improved performance	Mix of Contractor & Owner	Both contractor and owner may absorb costs, need to be aware of risks	Early program termination.
Cost plus Award Fee	Cost risk, but award fee can drive performance	Won't go out of business, but customer perception of performance is key.	Owner control contractor is covered.	Mostly Owner	Owner exposed to full cost risk. Contractor exposed to owner whim for profit.	Costs exceed funding, stop work.
Cost plus Fixed Fee	Total cost & risk at mercy of contractor. Strong owner control.	Cost growth is covered but tough to stop change and dilutes profit.	Allows technical evolution	Mostly Owner	Owner absorb risk. May squeeze out other, better work for contractor.	Costs exceed funding, stop work.
Time and Material	All costs/risks borne by the controlling owner, No cost reduction incentive	Little control but steady pay and profit. Just handling flexible manning.	Owner control, and contractor fully covered	All Owner	Nobody has incentive to control costs or account for risk.	Costs exceed funding, stop work.

INADEQUATELY ADDRESSED RISK FEELS GREAT IN THE BEGINNING BUT HURTS EVERYONE IN THE END.

Why Novelty Creates Risk

- Novelty weakens the precedent to plan and control a ship design effort:
  - technical analysis;
  - regulatory approval production methods;
  - owner, shipyard, or
  - supplier history
- It's not just more work. A design can be technically promising but difficult to
  - price,
  - schedule,
  - approve, or
  - build.
- The risk is greatest when several unfamiliar conditions occur together.



Why Novelty Creates Risk

Risk source	Immediate problem	Possible effect on ship delivery
Technical performance	Required performance is not demonstrated	Redesign, added analysis, or unacceptable ship performance
Regulatory approval	Existing rules or approval path do not fit	Additional work, delay, or inability to obtain approval
Design process	Analysis or verification takes longer than planned	Schedule loss and increased design cost
Production	Design is difficult or expensive to build	Construction delay, cost growth, or redesign
Program constraints	Cost or schedule limits are exceeded	Project no longer supports the intended service

Establish the Path Before Commitment

- Novel ship design should advance at a pace supported by the quality of available information.
- Early work should preserve flexibility while establishing the path to a buildable, approvable, mission-capable ship.
- More durable commitments to detailed-design and construction cost and schedule should follow increasing confidence.
- The goal is not to resolve every detail early, but to resolve the issues most likely to change the path.

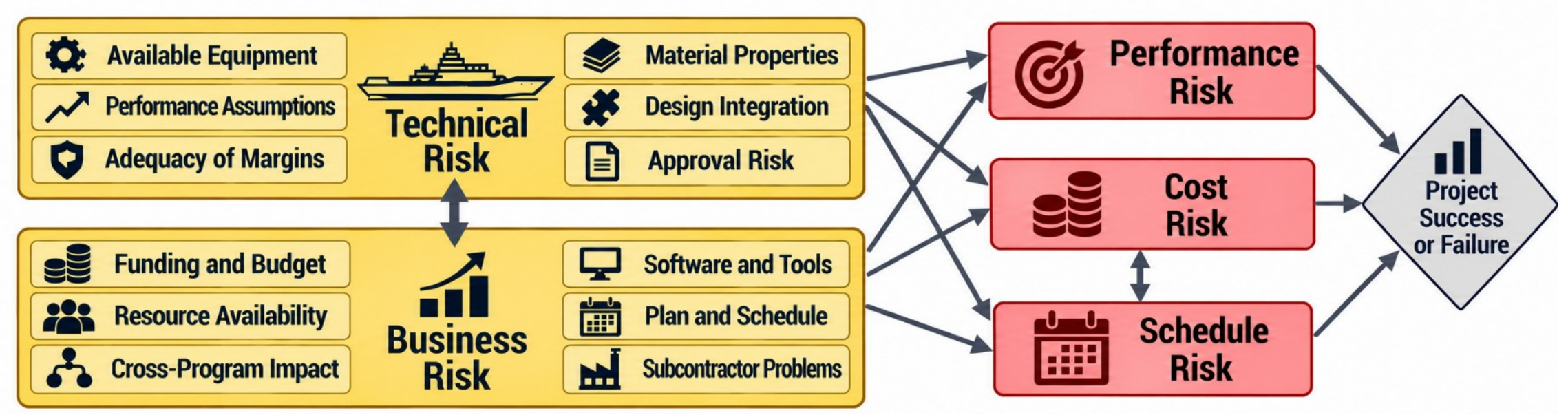


Increasing confidence does not mean every uncertainty disappears; it means the uncertainties most likely to change the design, approval path, production approach, cost, or schedule have been addressed sufficiently for the next commitment.

Risk in Ship Design Is More Than Technical Risk

- Technical risk: The design, system, material, method, or interface may not have the design contribution intended.
- Business risk: External financial, labor, tools, cross-program, planning/sequencing or other conditions may disrupt execution.
- Cost risk: Actual expenditure may exceed the planned or expected cost.
- Schedule risk: Activities may take longer or occur in a different sequence.
- Performance risk: The delivered design may not provide the capabilities desired.

- Example of Technical Integration risk: the potential that structural adequacy might not be achieved without exceeding weight values that imperil buoyancy and stability limits.
- Example of Program Risk: the initial plan for design omitted a critical predecessor-successor relationship, and now the design must proceed making substantial assumptions with little justification in order to maintain schedule.



Risk Grows Through the Design Sequence



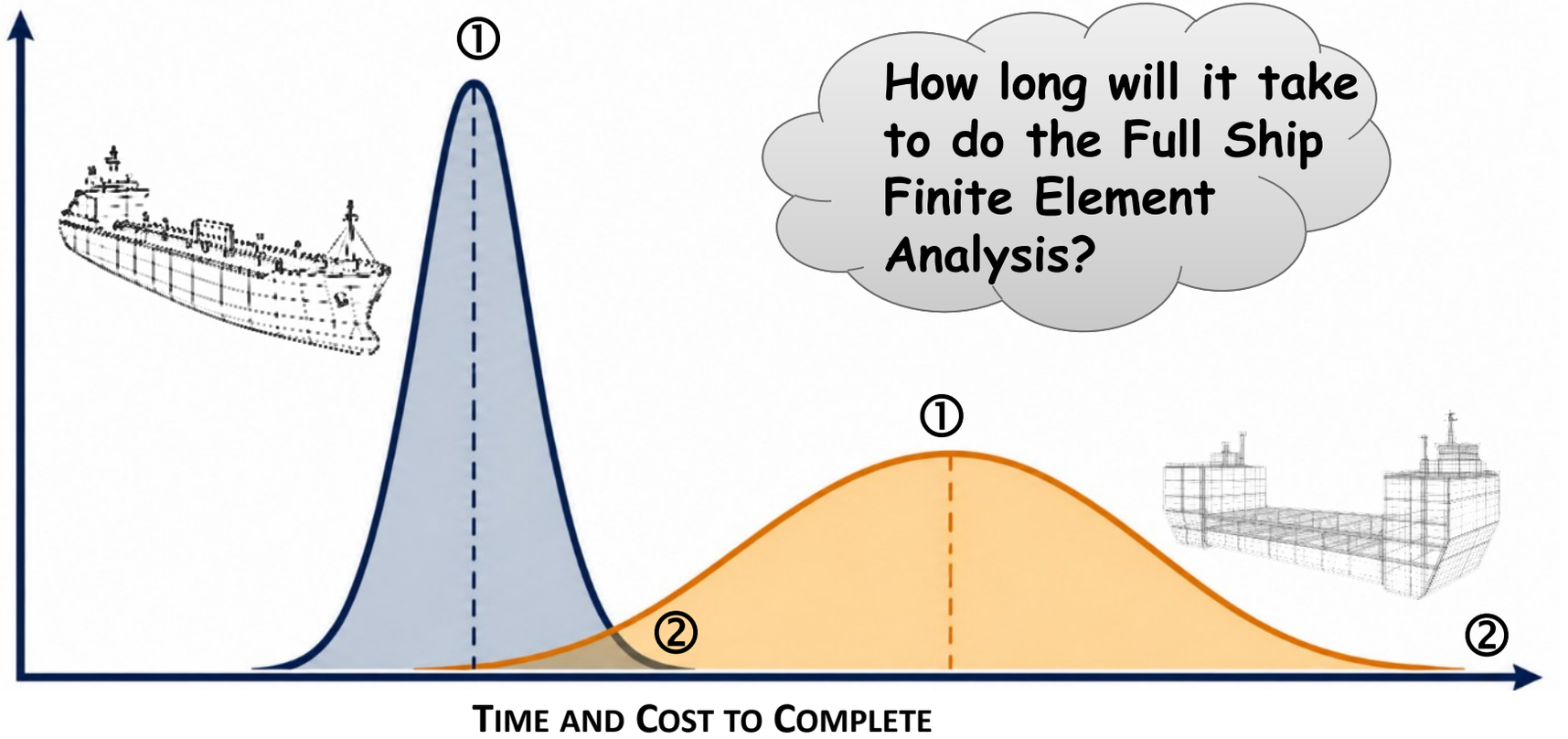
- Risk in one design activity can increase the risk of later activities.
- An unresolved technical or approval question may delay later work;
  - force a configuration change; or
  - require earlier work to be repeated.

Cost and Schedule Are Ranges, Not Points

A Tale of Two Ships



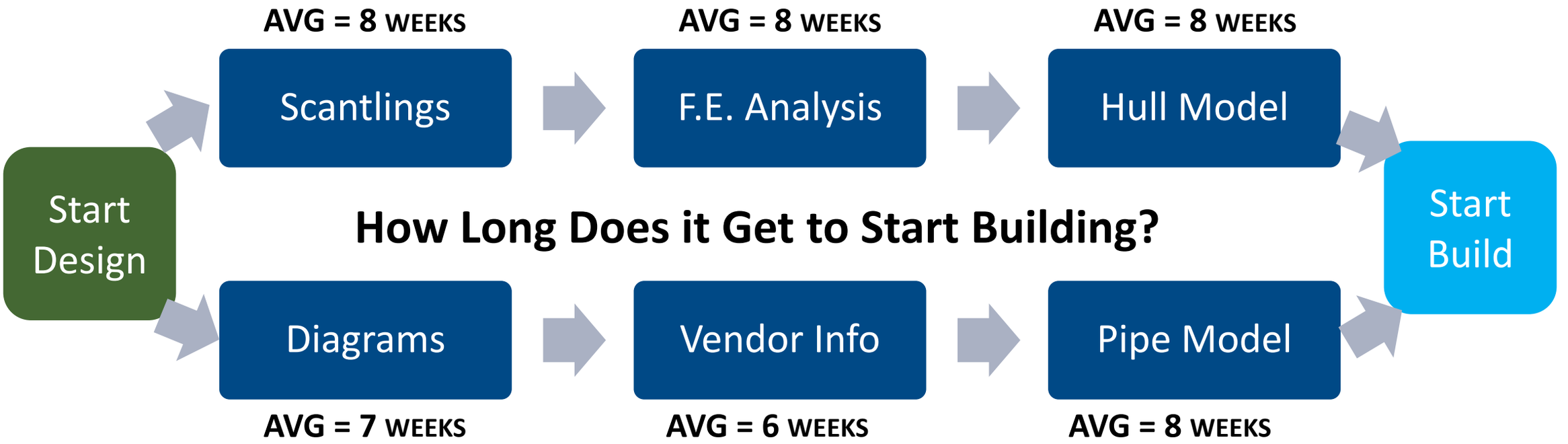




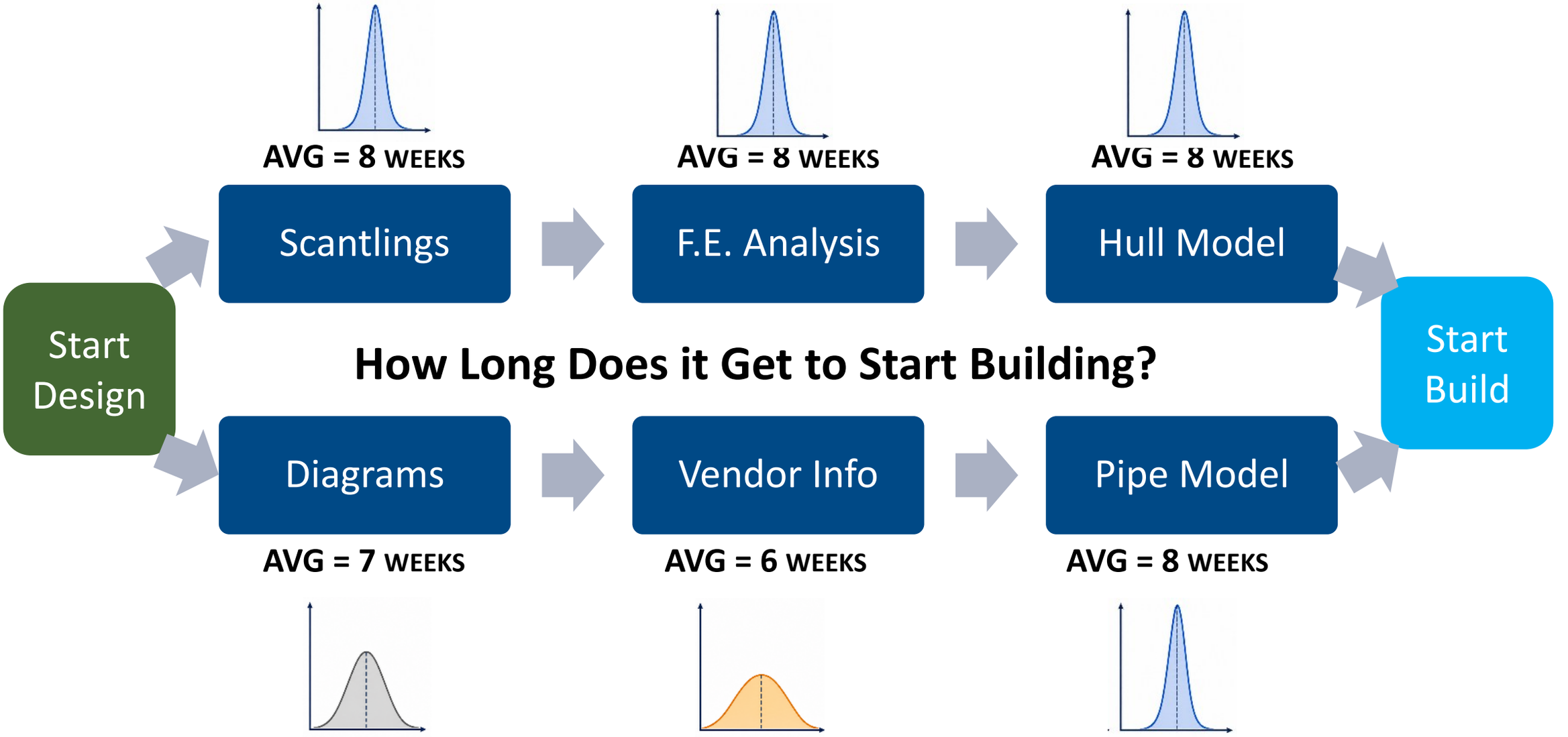
- Each design, analysis, verification, and approval activity has a range of possible effort.
- Novelty often increases the average expected effort.
- May greatly increase the spread of possible effort.

- On Average (①①) it takes 2x as long
- Worst case (②②) maybe its 2.5x as long
- Or, it could be that the novel ship is actually easier (but that would be a really rare occurrence!)

A Notional Engineering Plan



The Variability of Novel Ships and Systems



Impact of Novel Designs on Engineering Plans



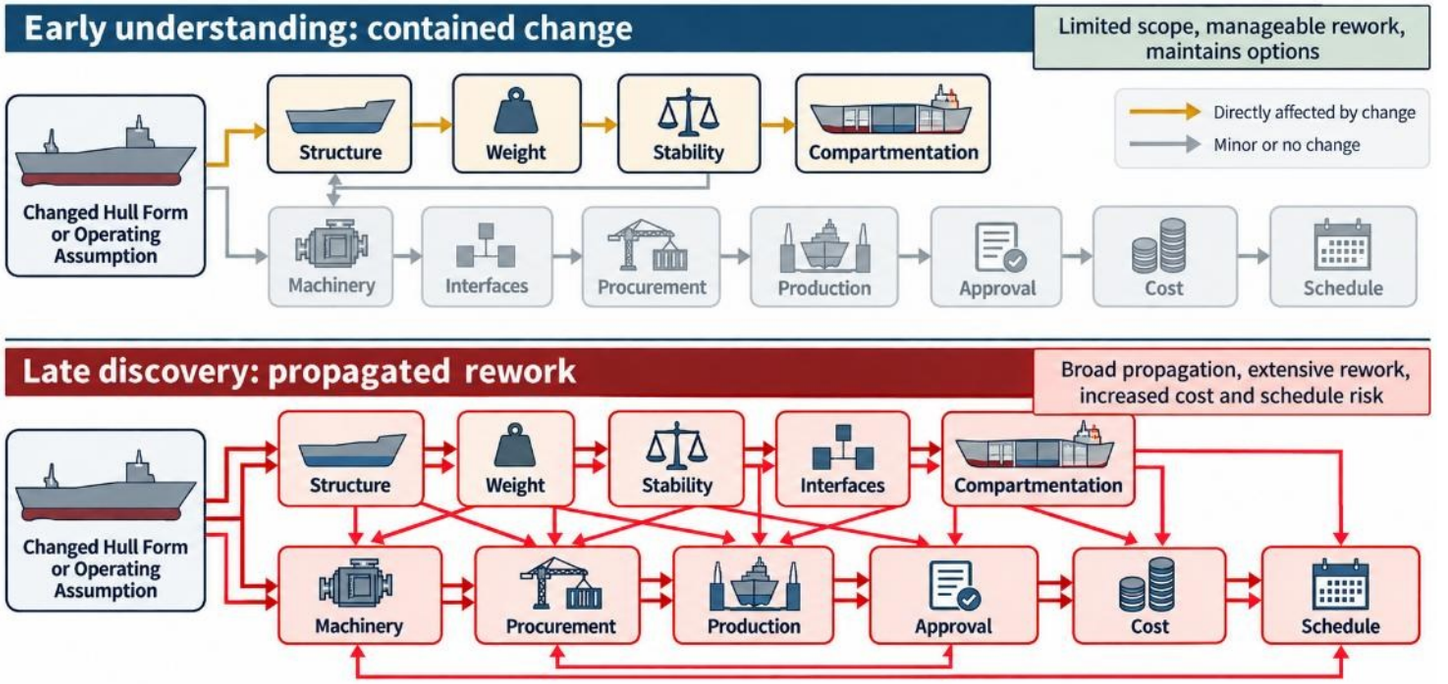


Characteristic	Conventional design	Novel design
Expected analysis and approval effort	Usually based on established precedent	May be higher because unfamiliar work is required
Range of possible effort	Relatively narrow	May be substantially wider
Cost estimate	More closely tied to previous work	More dependent on assumptions that may change
Schedule estimate	More predictable	More exposed to delays and repeated work
Estimating the work	Set price and schedule from established information	Reduce major unknowns before fixing price and schedule

Early work should narrow the most important ranges before major commitments are made.

Design Progression and Change Impact

- Design decisions are connected across disciplines.
- The earlier these relationships are understood, the more alternatives remain available.
- Early design should expose important interactions without creating excessive design inventory.
- Progressive commitment is the path between premature certainty and indefinite delay.



A hull-form change may affect:	An equipment-change may affect:	An operating profile change may affect:
• stability; • structural strength; • Compartment arrangement & layout • weight; • cost; and • production.	• vibration; • fatigue; • local structure; • procurement; and • testing.	• fatigue environment; • damage stability; • equipment requirements; and • approval evidence.

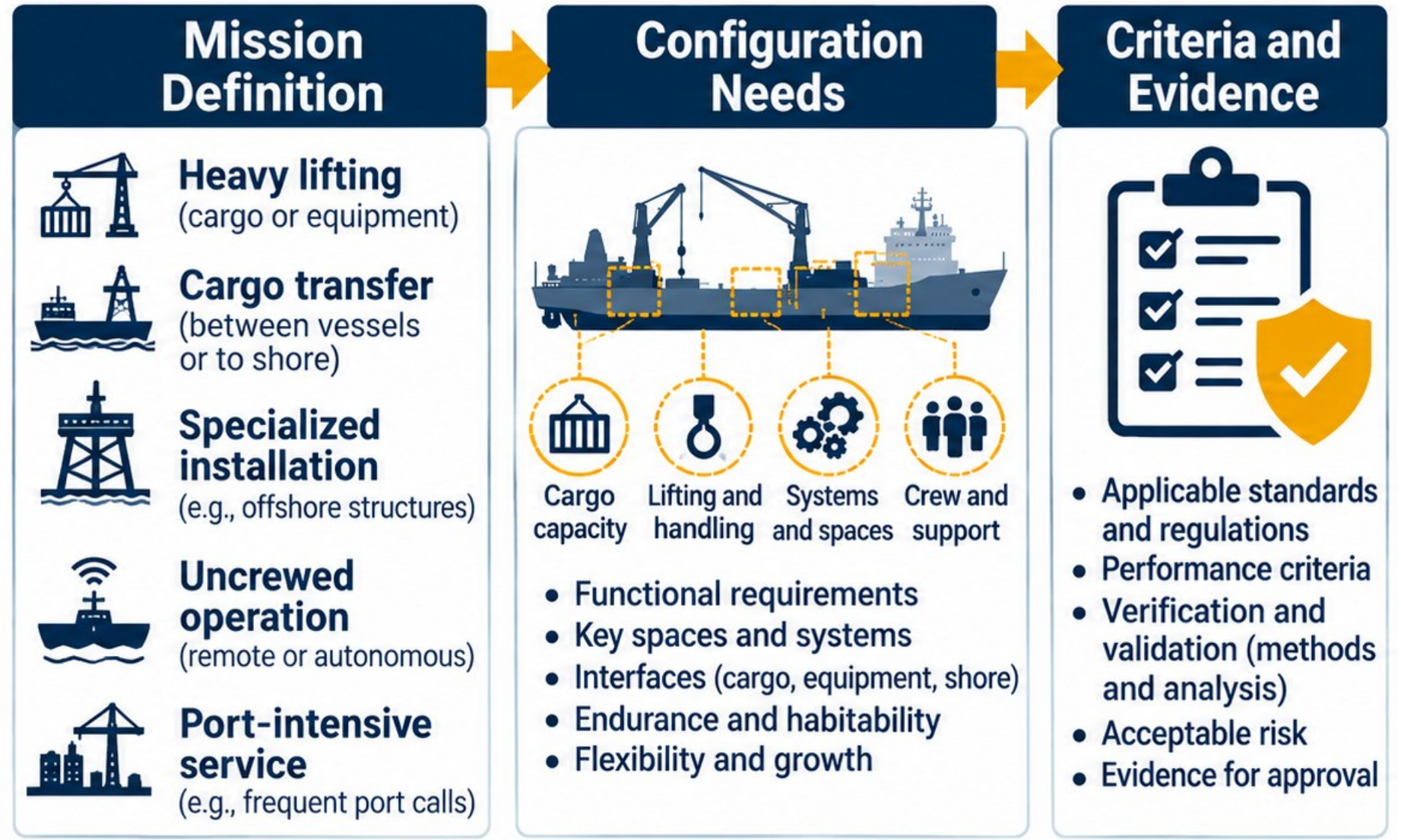
What Is Innovation in Ship Design?

- Innovation may occur in one dimension or several at once.
- A new mission may require:
  - a new hull form;
  - a new loading pattern;
  - new mission equipment; or
  - a new operating envelope.
- A new system may alter the ship's system and interfaces without much visible change.
- Familiar elements can become innovative when combined in an unfamiliar way.
- The purpose of categorizing innovation is to focus attention, not to label the whole vessel experimental.



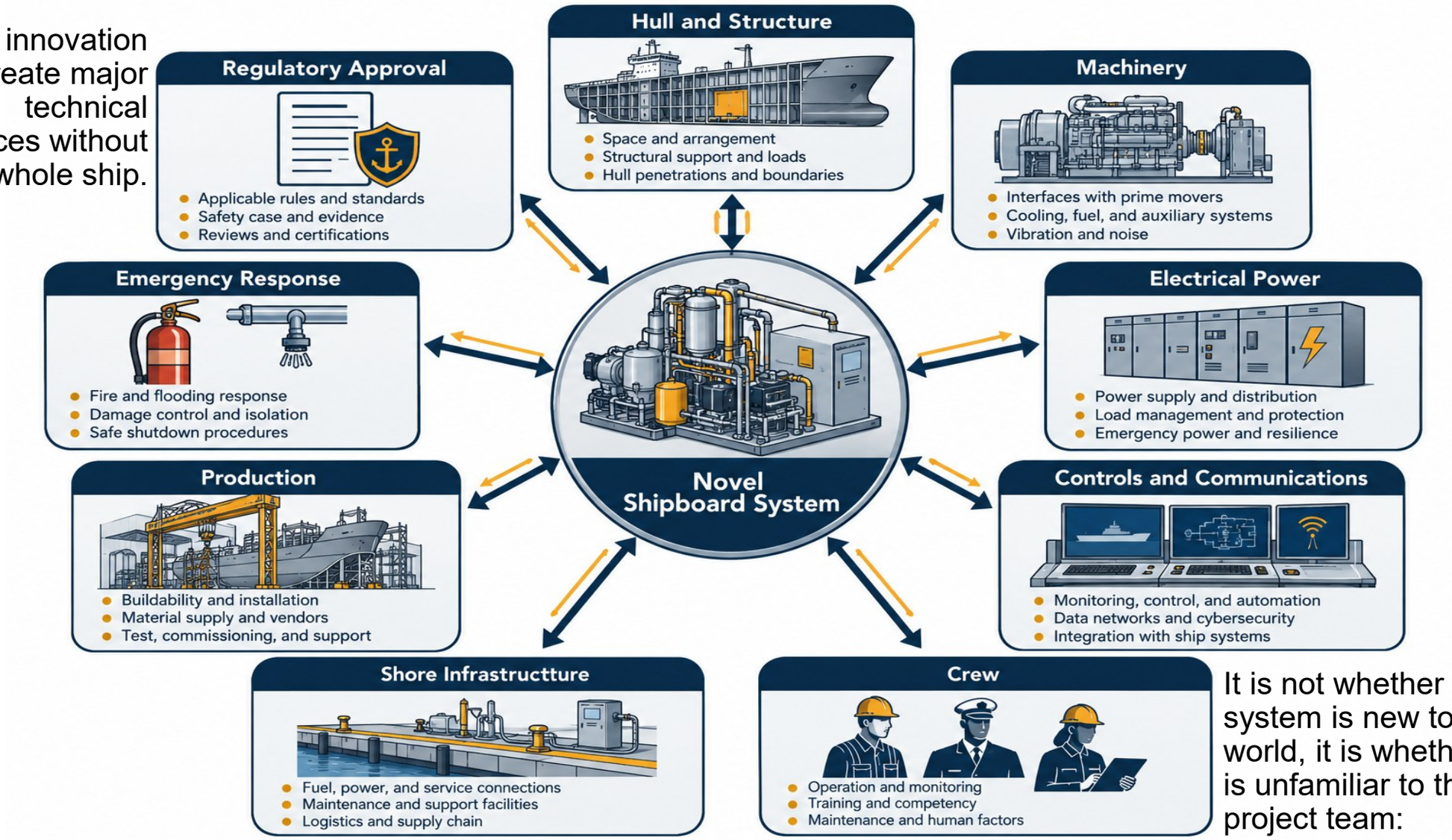
Categories May Overlap

Mission Innovation



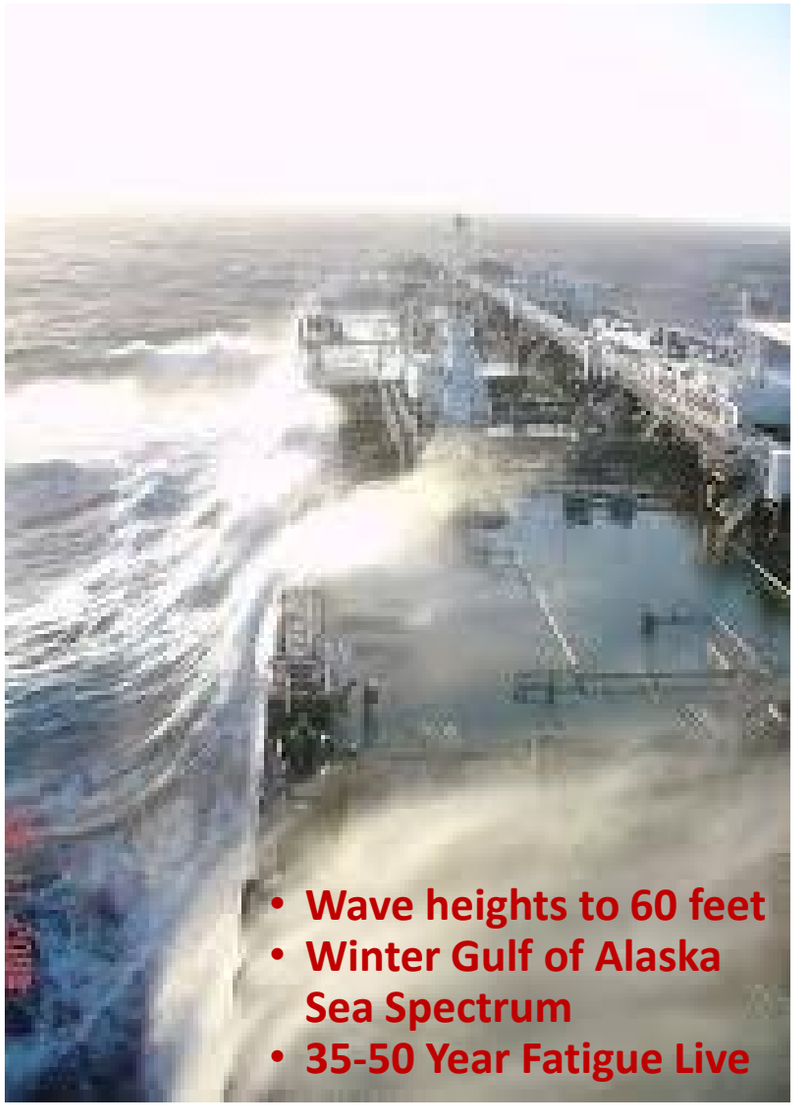
Shipboard-System Innovation

System innovation can create major technical consequences without changing whole ship.



It is not whether the system is new to the world, it is whether it is unfamiliar to the project team:

Operating Environment Innovation



The six commercial ships delivered from 2003 to 2006 shared two things in common:

- Both were designed as well as built at NASSCO
- Both were designed for some of the harshest conditions for commercial cargo carriers.

None of these conditions are unique in world shipbuilding, but each was new to NASSCO, especially in combination



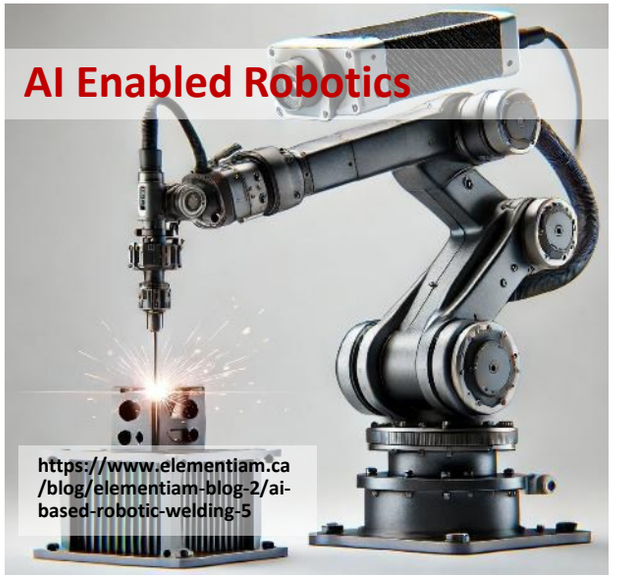
Production Innovation

Composite Materials



© FIBRESHIP Consortium

AI Enabled Robotics



https://www.elementiam.ca/blog/elementiam-blog-2/ai-based-robotic-welding-5

Additive Manufacturing



https://www.thefabricator.com/thefabricator/article/additive/metal-additive-manufacturing-goes-big

Friction Stir Welding



www.shapesbyhydro.com

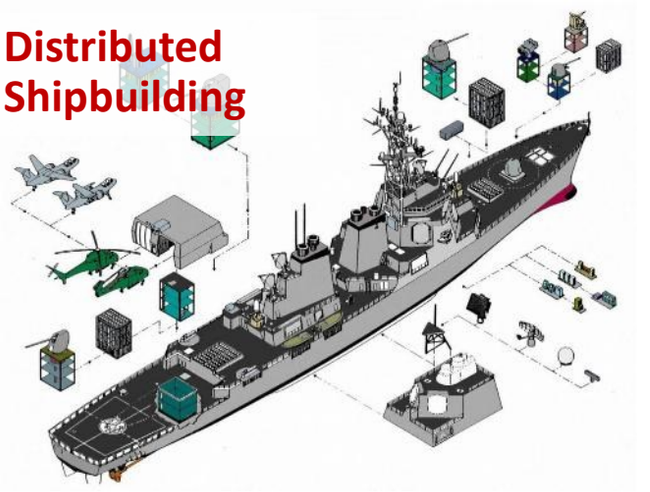
Digital Videography



Artificial Intelligence Applications in Ship Design and Production (Marine Technology October 2026)

All manner of new ship production innovations are coming to pass

Distributed Shipbuilding



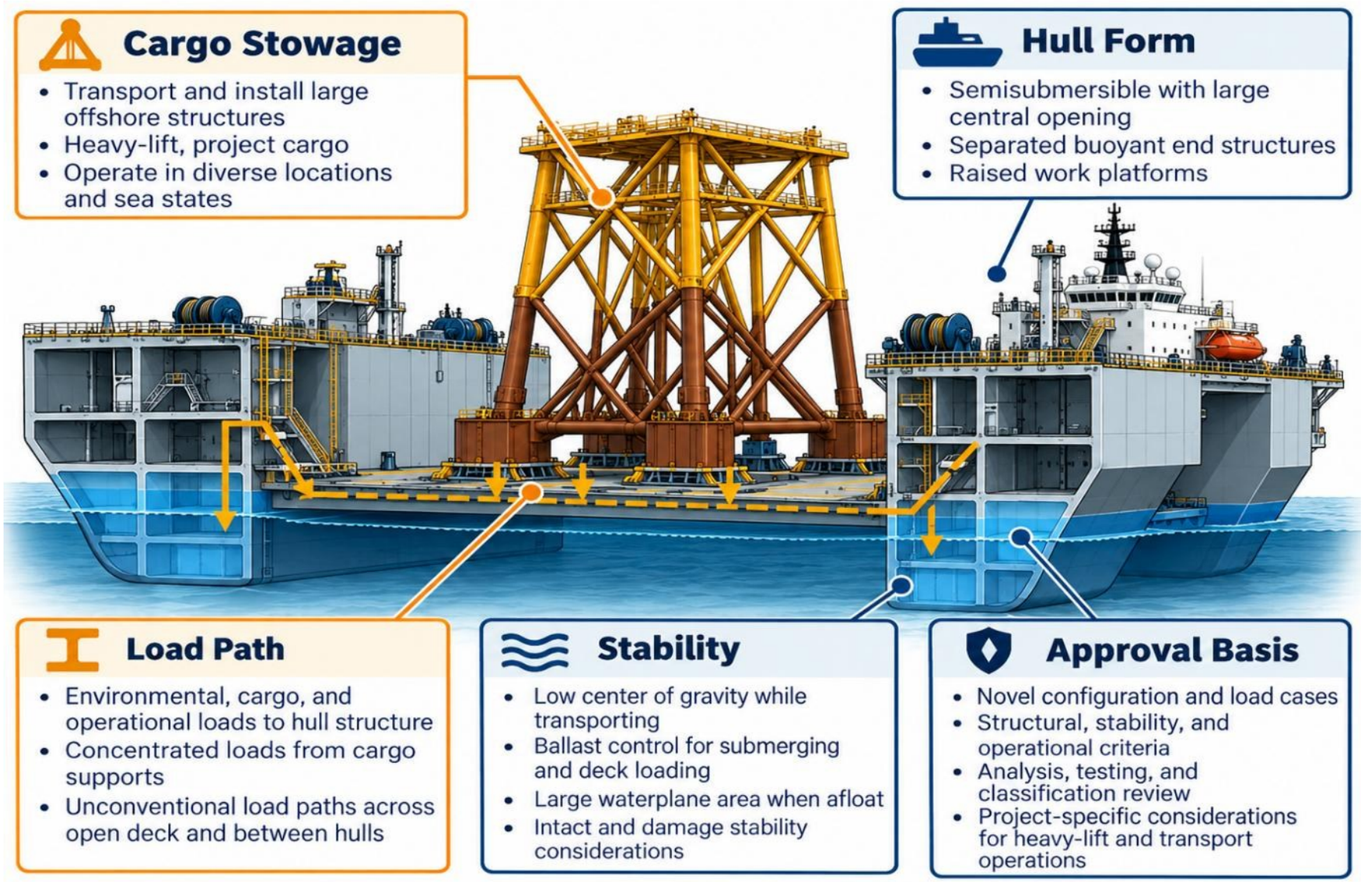
- Friction Stir Welding

Configuration Innovation

Examples of past innovations include:

- Semisubmersible heavy-lift,
- SWATH,
- Moonpools,
- Jack ups,
- Pure car/truck carriers,
- Containerization.

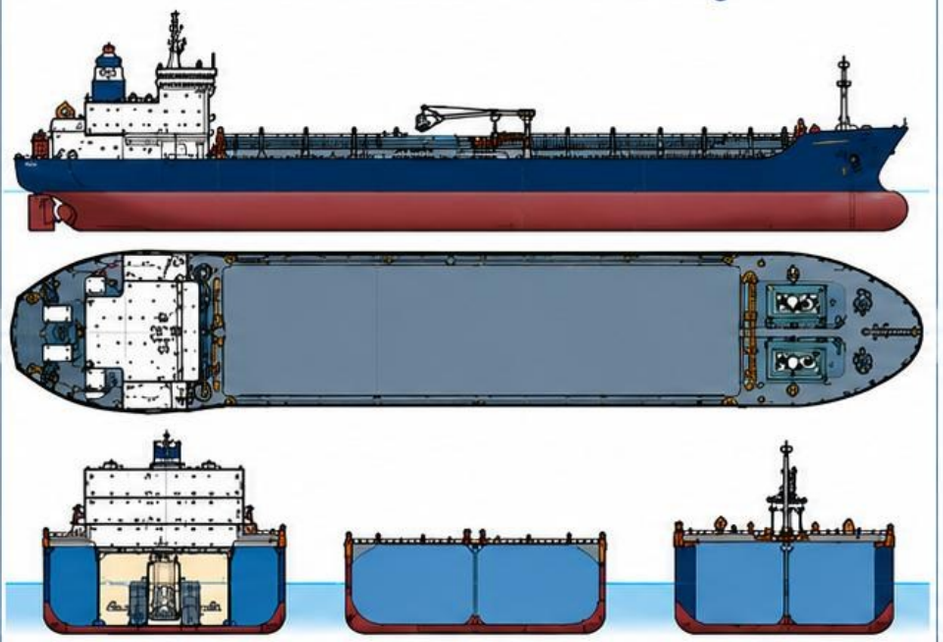
A configuration need not be globally unprecedented to be innovative for a particular project.



Tanker-to-Heavy-Lift Conversion

1. ORIGINAL TANKER

Conventional tanker – continuous hull girder

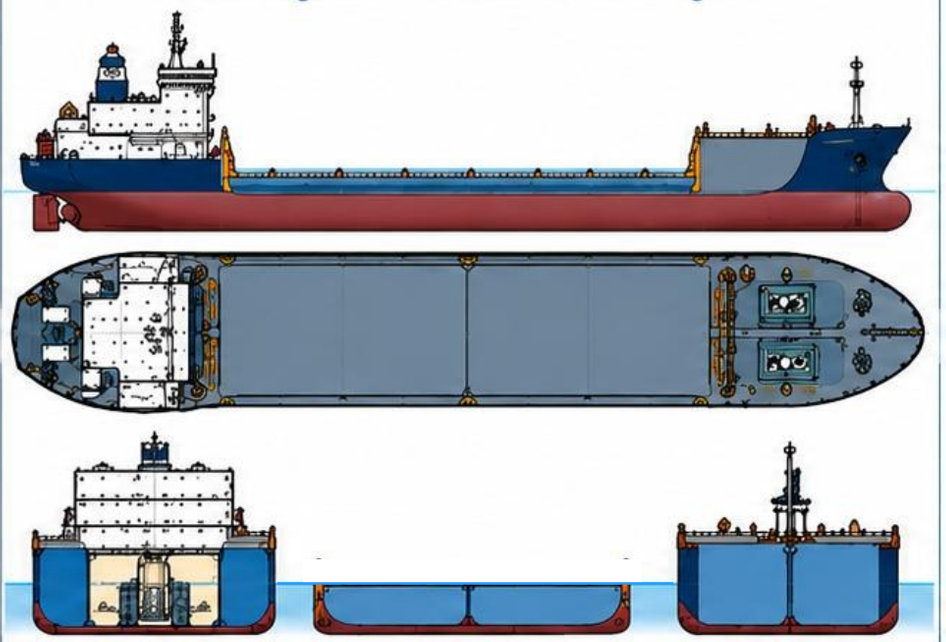


Aft section (at deckhouse front) | Midship section (cargo tanks) | Forward section (forecastle)

Mission	Carry liquid cargo (oil/chemicals) between ports.
Stability	Conventional intact and damage stability criteria for single-hull tanker.
Flooding	Designed with subdvision per tanker rules (limited progressive flooding).
Load Path	Continuous hull girder; global longitudinal strength for wave and still-water loads.
Approval Basis	Built to tanker rules (e.g., IACS), conventional service.

2. CONVERTED HEAVY-LIFT VESSEL

Lowered cargo deck – semisubmersible configuration



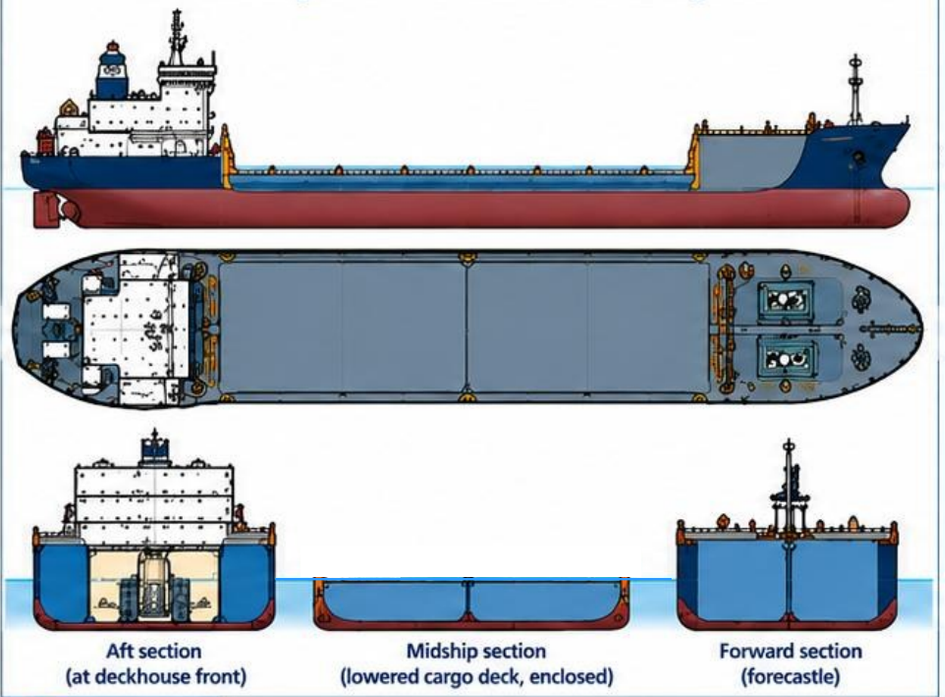
Aft section (at deckhouse front) | Midship section (lowered cargo deck, enclosed) | Forward section (forecastle)

Mission	Transport and install large, heavy structures (e.g., offshore platforms, modules).
Stability	Altered stability characteristics; low freeboard when submerged; assess multiple loading and ballast conditions (transit, submerged, lifting, deck cargo).
Flooding	Multiple buoyant regions with longitudinal subdvision; assess flooding for lowered deck configuration and interface with end structures.
Load Path	Discontinuous hull girder; loads transferred through end structures; local and global strength checks for lowered cargo deck and transitions.
Approval Basis	Conversion and new service approval; project-specific criteria, special-purpose rules, and assessment of stability, structure, and flooding for new operating envelope.

Added Platforms and Berthing Spaces

2. CONVERTED HEAVY-LIFT VESSEL

Lowered cargo deck – semisubmersible configuration

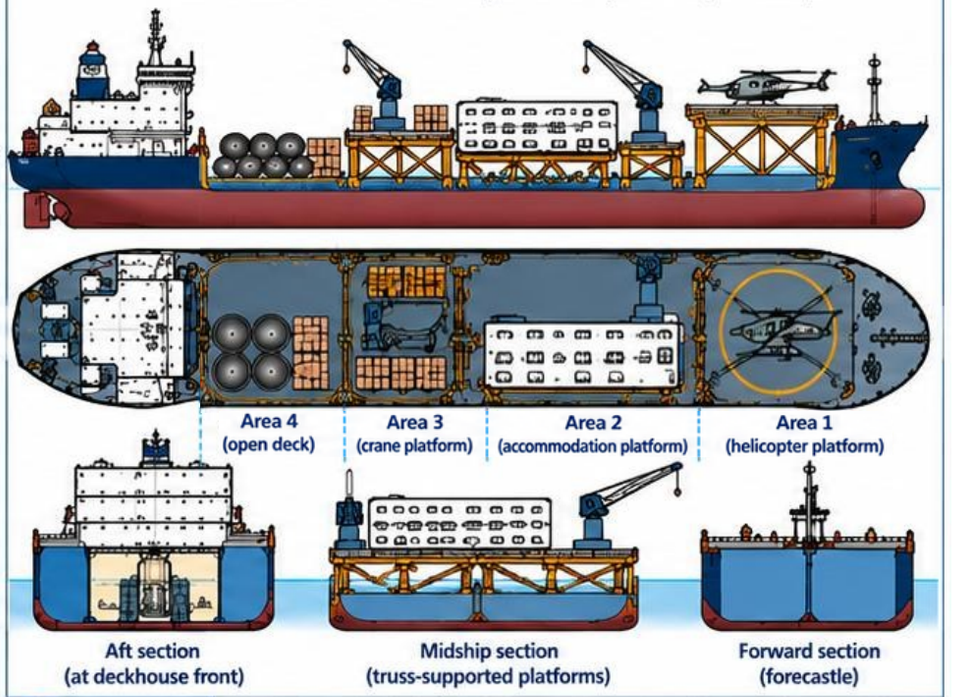


Aft section (at deckhouse front) | Midship section (lowered cargo deck, enclosed) | Forward section (forecastle)

Mission	Transport and install large, heavy structures (e.g., offshore platforms, modules).
Stability	Altered stability characteristics; low freeboard when submerged; assess multiple loading and ballast conditions (transit, submerged, lifting, deck cargo).
Flooding	Multiple buoyant regions with longitudinal subdvision; assess flooding for lowered deck configuration and interface with end structures.
Load Path	Discontinuous hull girder; loads transferred through end structures; local and global strength checks for lowered cargo deck and transitions.
Approval Basis	Conversion and new service approval; project-specific criteria, special-purpose rules, and assessment of stability, structure, and flooding for new operating envelope.

3. TRUSS-SUPPORTED PLATFORM

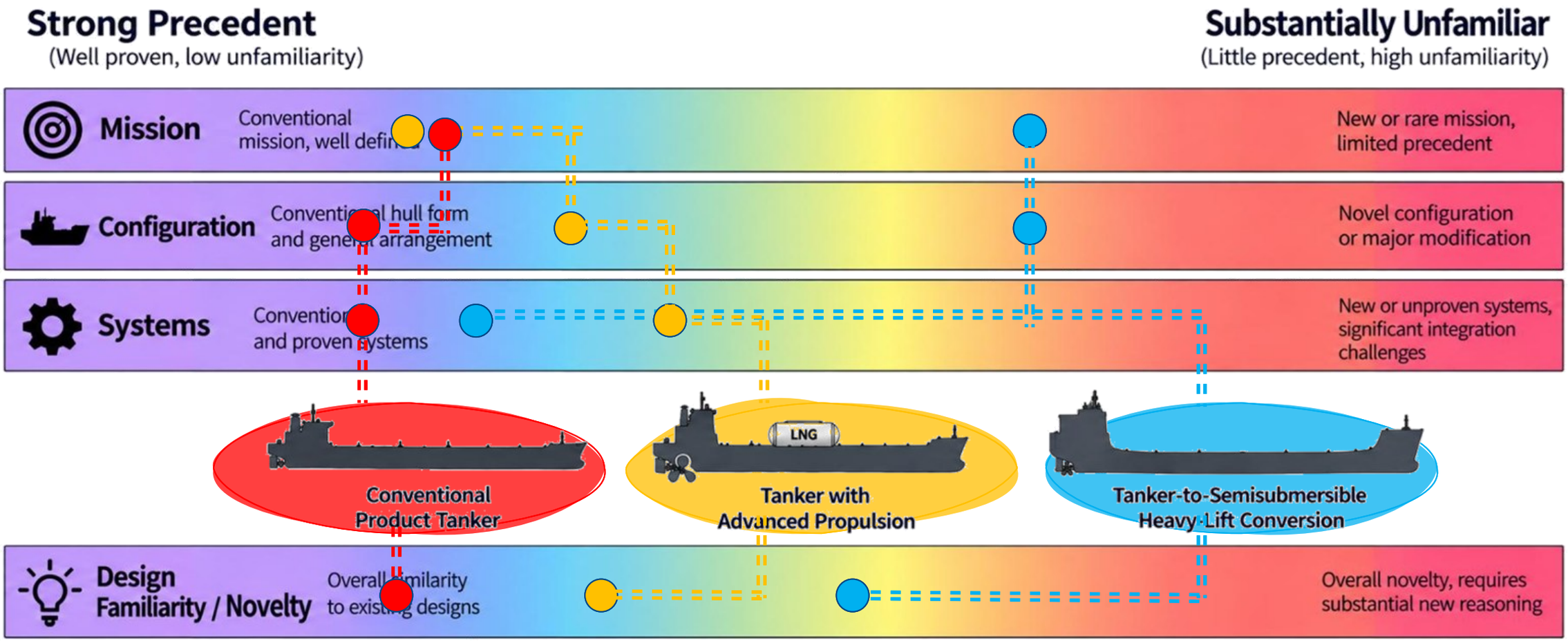
Three modules on raised truss platforms (Area 4 open deck)



Aft section (at deckhouse front) | Midship section (truss-supported platforms) | Forward section (forecastle)

Mission	Provide elevated work platform for heavy structures (e.g., offshore platforms, modules). Includes helicopter operations, cranes, equipment, and deck cargo.
Stability	Altered by increased vertical center due to platforms, wind effects, and crane overturning; assess multiple loading and ballast conditions (transit, installed cargo, lifting, operations).
Flooding	Multiple buoyant regions with longitudinal subdivision; assess flooding for lowered deck configuration and platform supports, and interface with end structures.
Load Path	Platform loads transferred to hull through stiff transverse trusses; truss structures and take longitudinal bending loads; assess local and global strength. assess local and global strength.
Approval Basis	Project-specific criteria for platform structures, cranes, and operations; assessment of stability, structure, and flooding for raised platform arrangement.

Innovation as a Spectrum

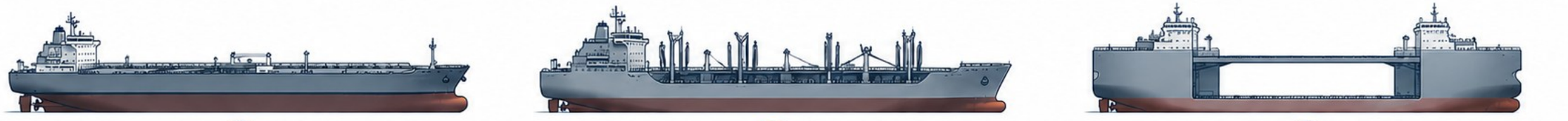


When Does Innovation Require Special Treatment?

Disciplined Compliance
Use established criteria and standard approval approach.

Focused Early Analysis
Targeted studies to address key uncertainties and demonstrate adequacy.

Adapted or Project-Specific Criteria
Tailored criteria, methods, or approval approach for novel features or behavior.



ECO-Class Tanker
Primarily disciplined compliance
(well established design and precedent)

Common Naval Auxiliary
Focused analysis and adapted evidence
(evolving design, some novel features)

Tanker-to-Heavy-Lift Conversion
Project-specific criteria and focused analysis
(novel configuration and behavior)

Key Screening Questions

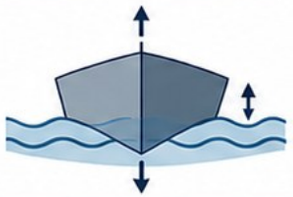
Does precedent fit the new design?



Do inherited criteria represent the actual hazard?



Is the physical behavior familiar and well understood?



Are interfaces and production methods stable?



Would a focused study change a consequential decision?



Is the evidence proportionate to the uncertainty?



SUSTAINABILITY AND INNOVATION
IN SHIP DESIGN AND OPERATIONS
CONFERENCE 2026

GENERAL DYNAMICS

Risk Mitigation for Innovative Designs and Novel Ships

Coming soon... Part 2

The views expressed are those of the author and do not reflect the official policy or position of the Department of War or the U.S. Government

Large-Area Additive Manufacturing for High-Speed Uncrewed Surface Vessels

Presenters: Addie Lindyberg and Troy Zangle

SISDO 2026

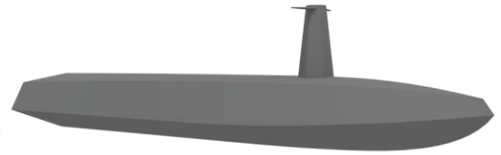
ONR-331, N000142612346

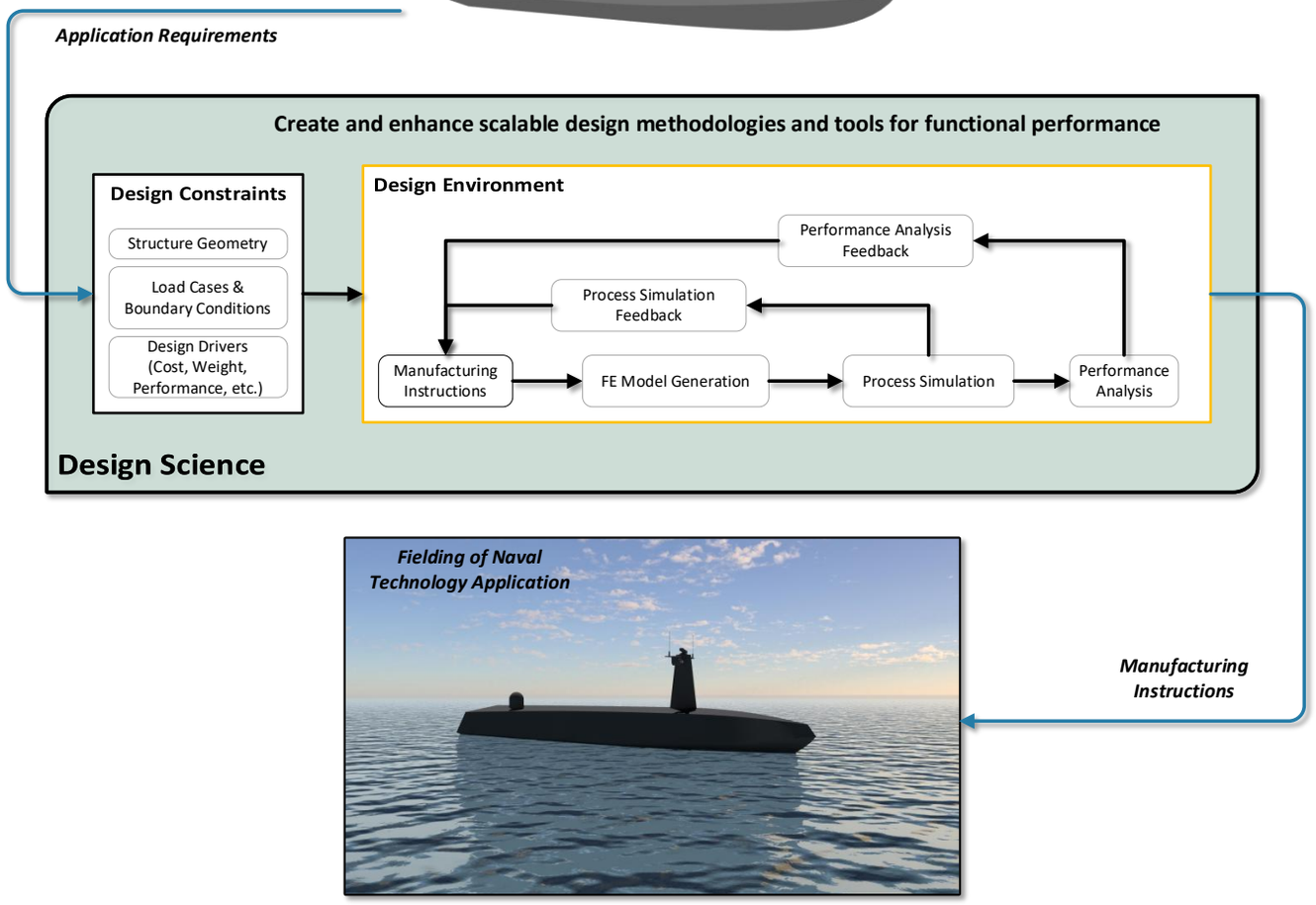
Composites for Advanced Maritime Structures (CAMS)

UMaine is researching robotic advanced manufacturing (RAM) methods to rapidly explore vessel structural design space to reduce the cost and build time for small/medium composite uncrewed vessels.

Program Focus Areas:

- ***Explore robotic advanced manufacturing*** for uncrewed surface vessels to address vessel cost and build time.
- ***Manufacturing technology advancements*** to enable efficient use of thermoplastic material systems for small/medium-scale vessels with multi-process, multi-material path planning.
- ***Design and analysis tool development*** to close the gap between efficient design and manufacturability.
- ***Validate design tools and methods*** through manufacturing and experimental evaluation of structures with increasing complexity and scale.





Overview

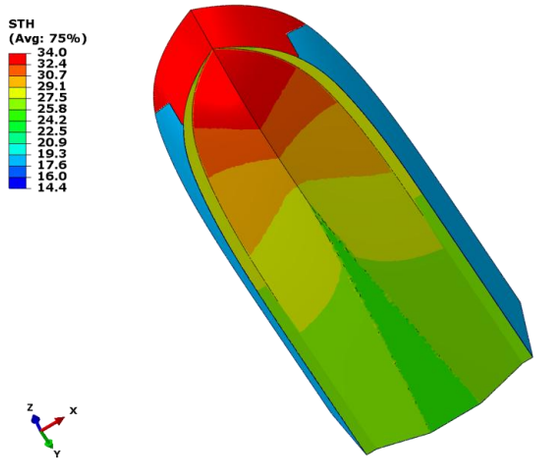
- **University of Maine Advanced Structures and Composites Center**

- **Vessel Design for Additive Manufacturing**
  - Hull Design Efforts
  - Previous Builds
  - Design Considerations



- **Materials and Demonstrator Testing**
  - Material Characterization
  - On-water testing

- **Design Space Exploration Efforts**
  - Design methods
  - AM-specific process
  - Cost and build time optimization



1865 THE UNIVERSITY OF MAINE





- 11,000 Student Enrollment
- 866 Faculty
- Carnegie R1 Top-Tier Research University
- 16:1 Student to Faculty Ratio
- 3.35 Avg. First Year Student GPA
- $245.7M R&D expenditures in FY22
- 150+ Research Institutes, Centers and Labs
- Maine's leading engineering program
- Engineering excellence since 1865



ADVANCED STRUCTURES & composites center

THE UNIVERSITY OF MAINE

Mission

Expanding the frontiers of materials and technologies to engineer solutions in national security, infrastructure, energy and manufacturing while preparing future leaders to solve society's emerging challenges

Vision

To engineer a secure, sustainable, and prosperous world.

- **Founded through the NSF in 1996**
- **Over 400 Personnel**
- **150,000 ft² lab**
- **Largest Univ.-based research Center in Maine**
- **2,900+ students funded from 35 majors**
- **10+ spinoff companies**
- **1,000 publications**
- **130+ patents**
- **30,000 Visitors**
- **1,600 media stories**

ADVANCED STRUCTURES & COMPOSITES CENTER | 30 YEARS

Research Areas

Civil Infrastructure



National Security



Material Development



Ocean Engineering



Additive Manufacturing



Civil Infrastructure & Structural Testing

- Ultimate (failure) and fatigue (cyclic) testing of bridge girders, wind blades, towers
- Development of composite bridge girders



"Bridge in a Backpack" Composite Beams



Wind Blade Testing Lab



Structural Testing Lab

National Security

- Mark V/MAKO
  - 83ft fully carbon fiber Special Operations Craft for Navy Seals
  - Designed with DLBA, built by Hodgdon Yachts
- Army Command Shelter
- Secure Shipping Containers
- Blast Resistant Structures & Origami Structures



Command Shelter


MAKO


Blast Resistant Panels

Offshore Wind Testing

- VolturnUS+ 1:4.5 scale floating offshore wind turbine
  - Vestas V27 225kW turbine
  - Deployed 2025
  - Goal: validate platform design, mooring testing (materials, sensors, entanglement, fishing)





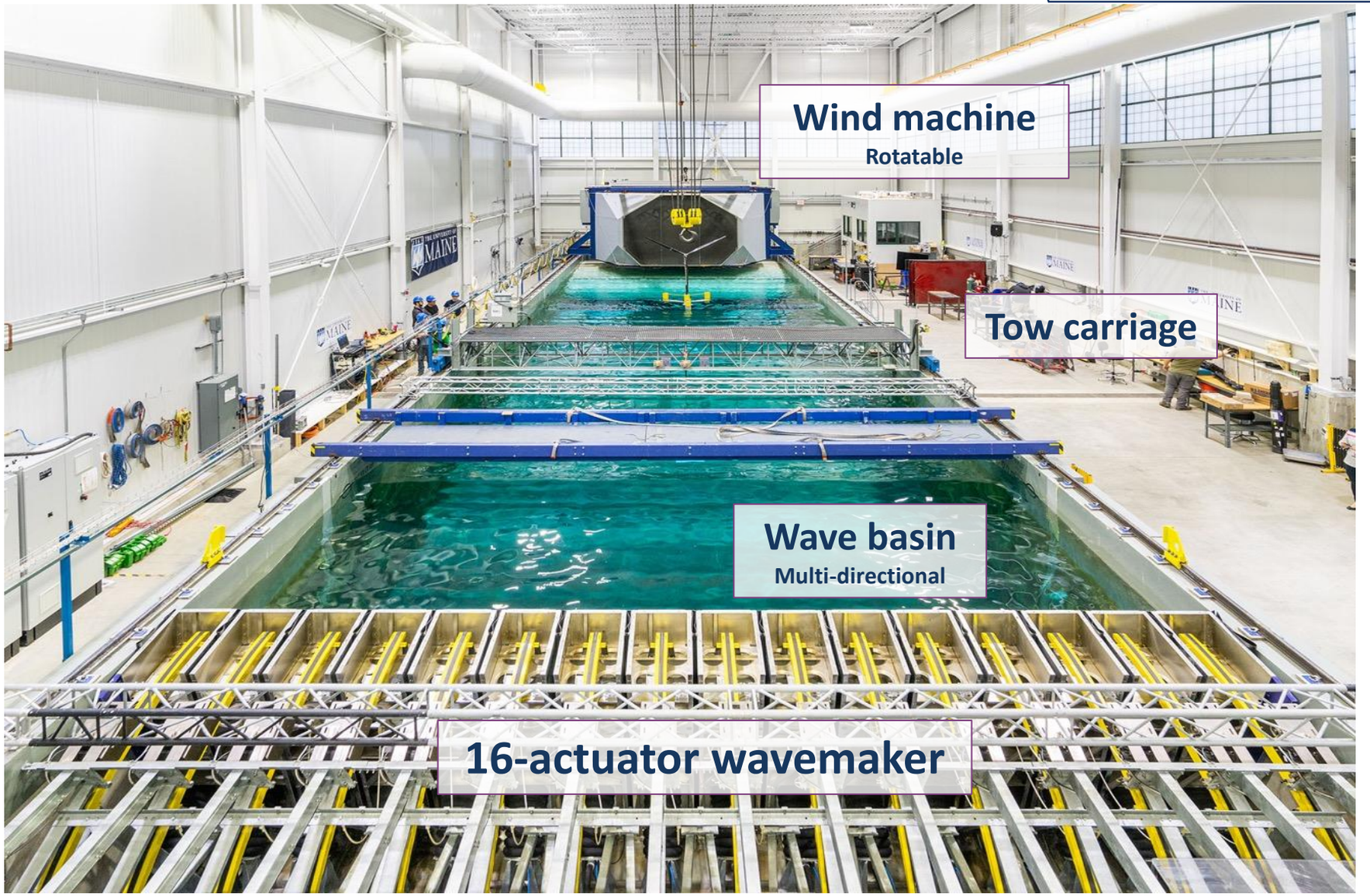
W2 Wind-Wave Basin

- 0.8m waves
- 15m/s wind
- Directional winds and waves
- Changing water depths

Length	98 ft
Width	30 ft
Height	5 ft

Types of Testing

- Floating Offshore Wind
- Wave Energy Converters
- Coastal Protection Systems
- Low-Speed Towing (1 m/s max)



Large-Area Additive Manufacturing (LAAM)

AKA Large-Format Additive Manufacturing (LFAM), Big Area Additive Manufacturing (BAAM)



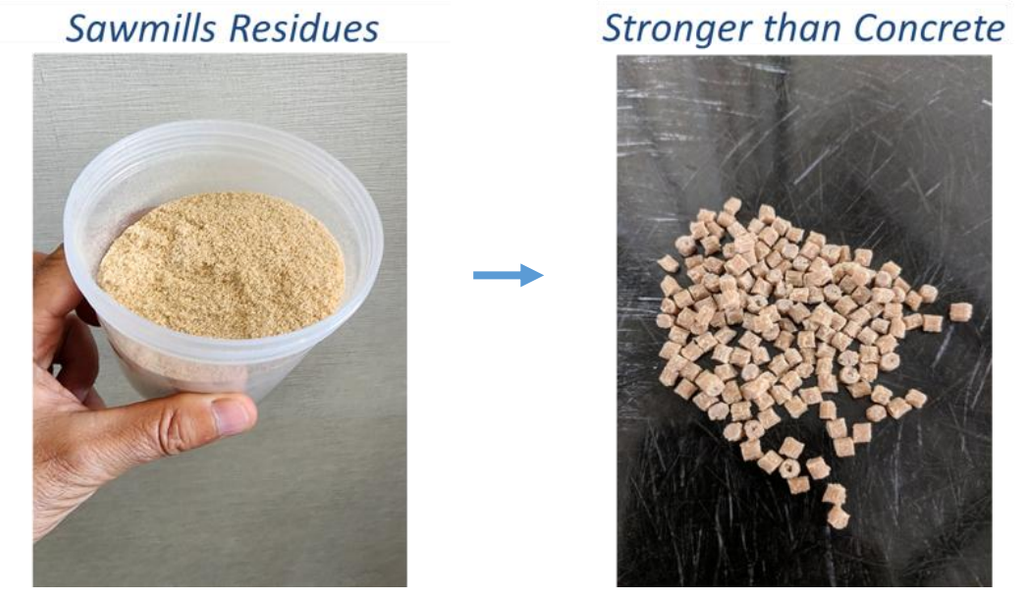


Applications include:

- Molds & formworks
- Houses & shelters
- Boats

LAAM Materials

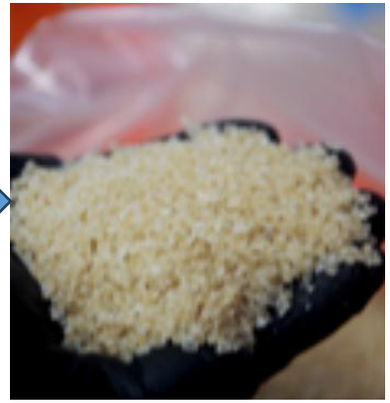
- Thermoplastic polymer pellets
- Processed at 200-400℃
- Additives – glass, carbon fiber, wood



Wind Blade Recycling:



Old Wind Turbine Blade



Wood Flour & rPETG



Pellets for additive manufacturing

Advanced Manufacturing Equipment

- Ingersoll MasterPrint
  - 60'x 22'x12' build volume
  - 150-500 lb/hr throughput
  - 8 x ¼" AFP with IR + HUMM3
  - Milling Spindle
- CEAD AM Flexbot
  - 6-axis robotic work cell
  - 2m x 8m bed
  - Pellet fed additive (60 kg/hr)
  - Milling Spindle



Ingersoll MasterPrint

- Cincinnati BAAM
- Juggerbot Tradesman
- Stratasys Fortus 900mc
- Numerous Small Machines


CEAD AM Flexbot



Juggerbot

GEM Facility and Factory of the Future

- New 50,000 sq ft lab
- Opening Fall 2026
- 1000 lb/hr











Demand Signal

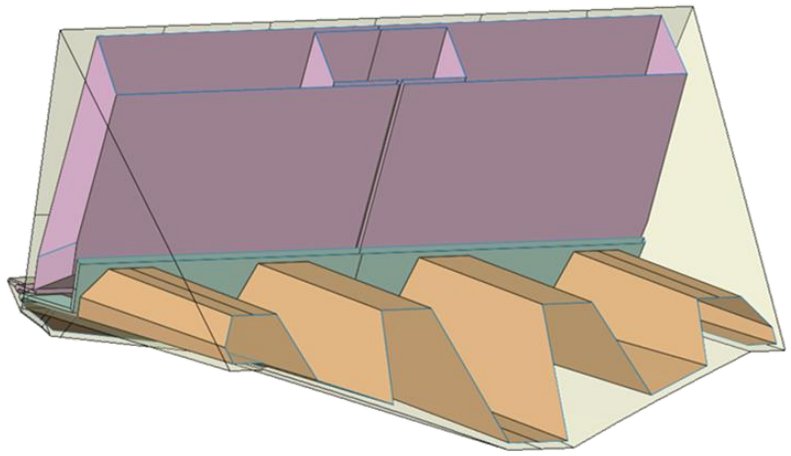
- Demand for small, fast, low-cost unmanned surface vessels is accelerating across defense, security, and maritime operations.
- Conventional FRP construction relies on expensive tooling, long lead times, and a shrinking skilled labor pool.
- Each new hull form requires a new mold – cost and schedule are locked in before a single layer of fiber is laid.

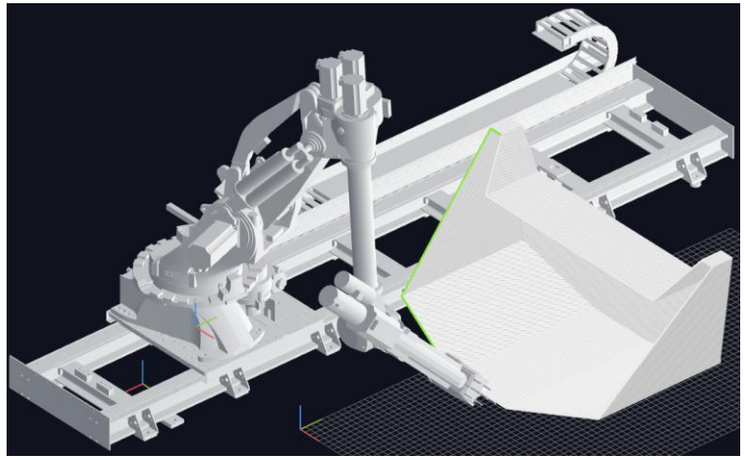


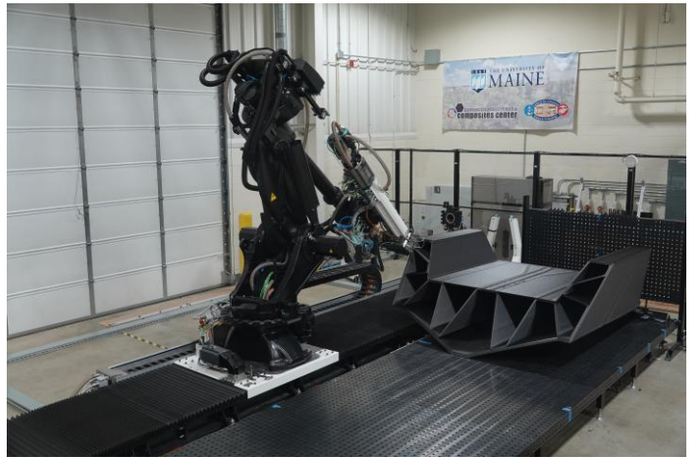
G. Gardiner, "Composites take the hit in U.S. Navy patrol boat," CompositesWorld, Jan. 1, 2008. [Online]. Available: https://www.compositesworld.com/articles/composites-take-the-hit-in-us-navy-patrol-boat

Demand Signal

- Modern, advanced manufacturing technologies (*e.g.*, LAAM) have the potential to significantly reduce cost and build time compared to traditional methods.
- Objective: Establish a repeatable digital-to-production pipeline using robotic advanced manufacturing and thermoplastic/thermoset composite technologies to design, optimize, and build small-to-medium unmanned surface vessels, achieving quantified reductions in unit cost, build time, and structural risk.







3Dirigo - Proof of Concept - 2019

Particulars	
LOA	7.62 m
Weight	2,268 kg

- Printed in 72 hours
- 2 Guinness World Records
  - Largest 3D Printed Boat
  - Largest 3D Printed Object
- Proof of concept for boat manufacturing
  - Lab float testing
  - Qualitative print accuracy





Video

USV1 – Modular Displacement Vessel



Particulars	
LOA	6.0m
B	1.95m
T	0.44m
Disp.	3,300 kg
Payload	340 kg
Max. Speed	13 kts

Description

- Verify and validate performance models through field testing USV built as a scientific demonstrator with advanced manufacturing technologies
- 4 modules manufactured with LAAM and reinforced continuous glass fiber, joined with bolts and adhesive
- Cost & build time data collected & compared to other manufacturing technologies
- Vessel instrumented with accelerometers, IMUs, and strain gauge to measure structural behavior

Scientific Demonstrator Information

- Engine: 90HP Yamaha
- Remote control system designed and installed by Maribotics
- Designed to handle 2 personnel on deck for maintenance while docked
- Fuel tank sized for 8 hours of continuous testing
- Low profile vessel with deckhouse to hold research data acquisition systems
- Hull Structure and design pressure: ISO 12155-5:2019
- System: ABYC H-22

USV2 – Monolithic Planing Hull



Particulars	
LOA	6.0m
B	2.4m
T	0.29m
Disp.	2,600 kg
Max. Speed	23 kts

Objective

- Verify and validate performance models through field testing USV built as a scientific demonstrator with advanced manufacturing technologies
- Single print hull form of only polymer AM material
- Planing hull
- Cost & build time data collected & compared to other manufacturing technologies
- Vessel instrumented with accelerometers, IMUs, and strain gauges, to measure structural behavior

Scientific Demonstrator Information

- Engine: 150HP Suzuki
- Remote control system designed and installed by Maribotics
- Fuel tank sized for 8 hours of continuous testing
- Designed to handle 2 personnel on deck for maintenance while docked
- Hull Structure and design pressure: ISO 12155-5:2019

Military USV Use

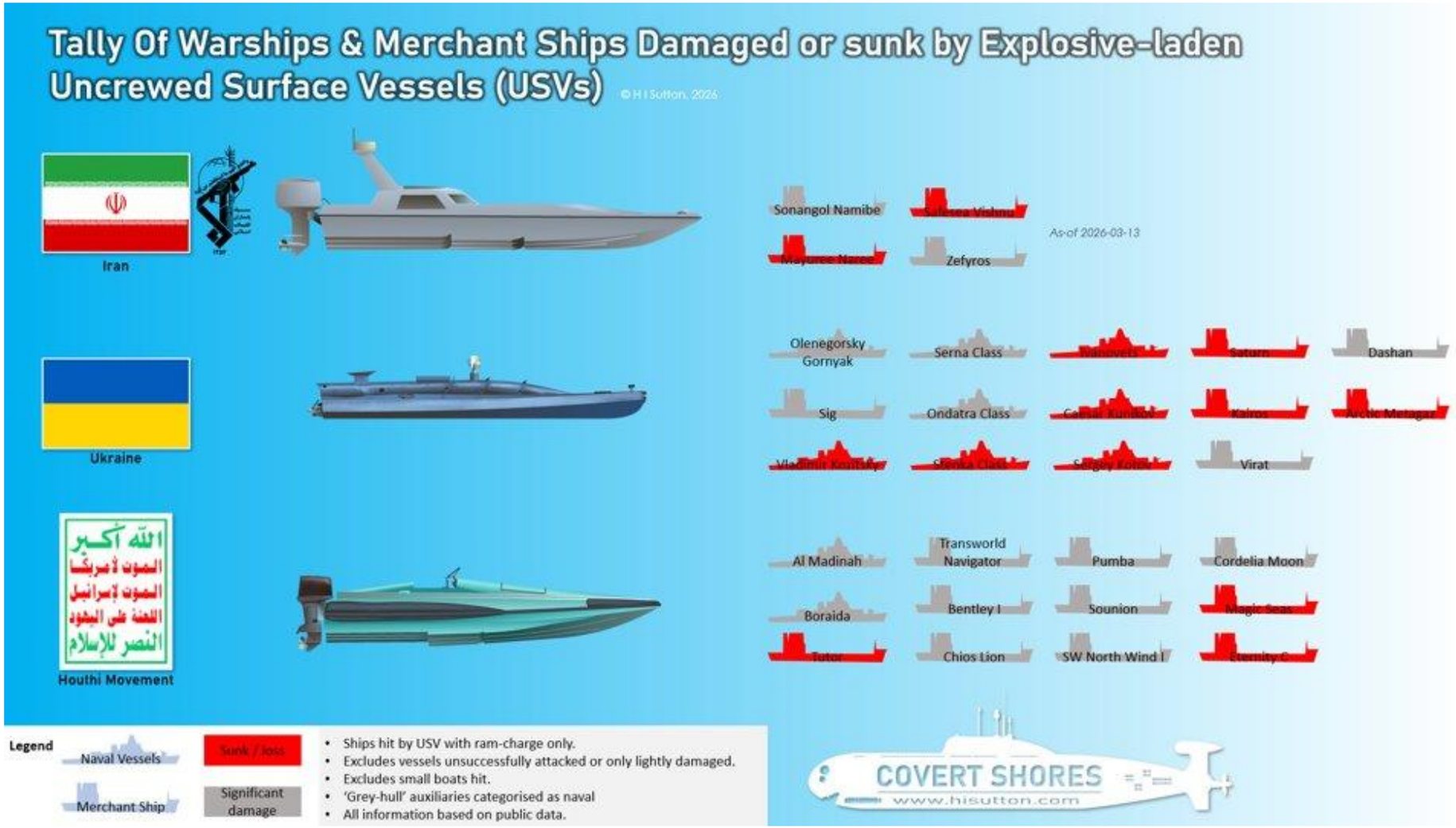
Used for:

- Surveillance
- Patrol
- Clearing mines
- Attack

Payloads 150-1000kg

Evolving quickly

Often very specialized



Other USV Use



Firefighting
Zycroft Longrunner USV
54’ LOA

Spill Response
6M Prozero OSR USV
20’ LOA





Target Boats
L3 Harris C-Target 3 USV
14’ LOA

Comparable USVs

Name	GARC	Magura V5	Zycraft M75
L (ft)	15.75	18.00	17.06
B (ft)	5.74	-	4.72
Disp (lbs)	4,800	2,205	1,984
Payload (lbs)	1,000	706	-
Speed (kt)	40	42	35
HP	200	-	115



GARC
(US Navy)



Magura V5
(Ukraine)



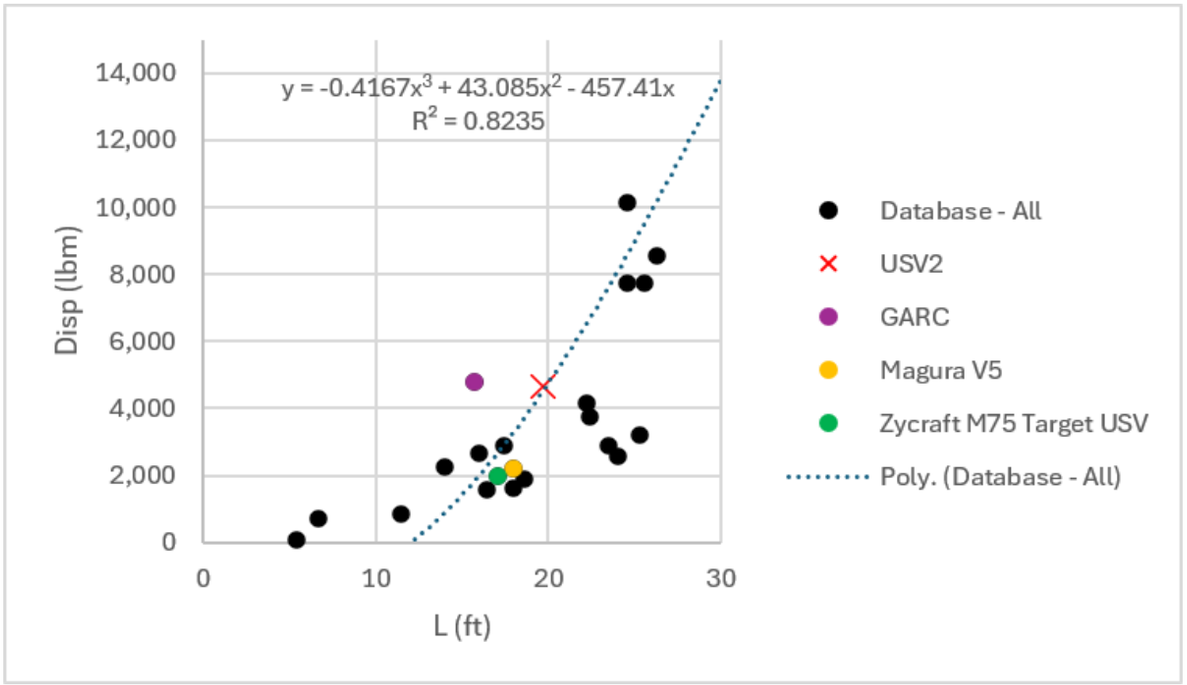
M75 Target Boat
(Zycroft)

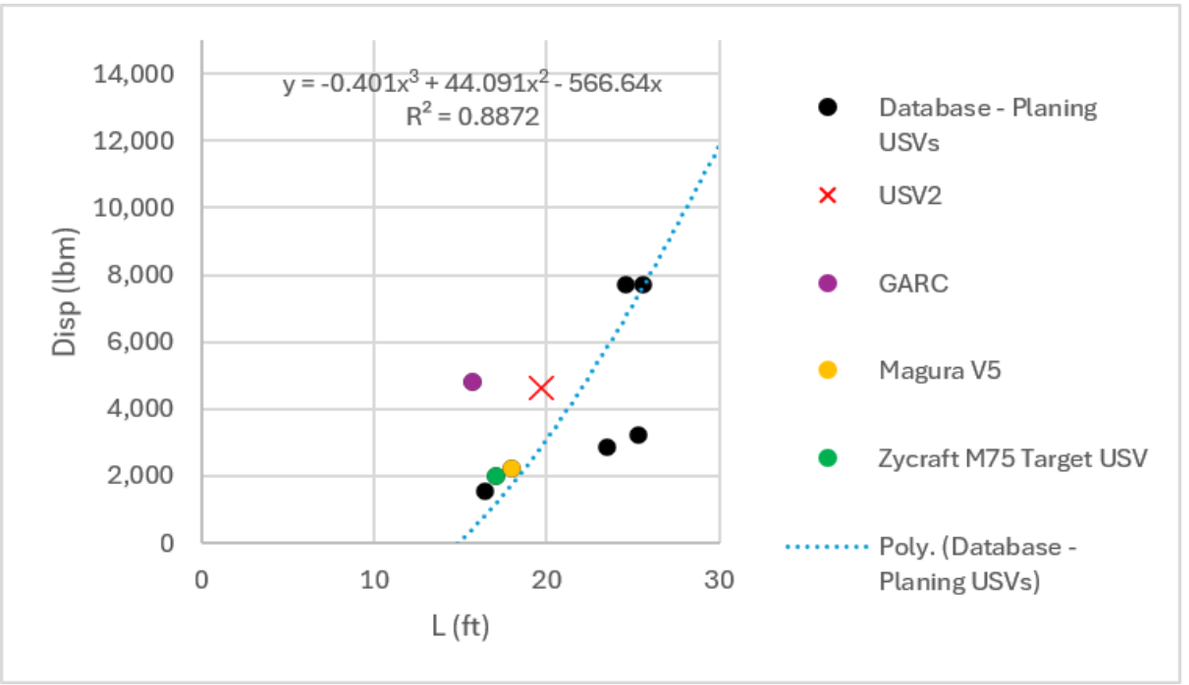
Parametric Analysis – Weight

- Length has the strongest relationship to displacement – cubic regression used

USV2 Predictions by Length

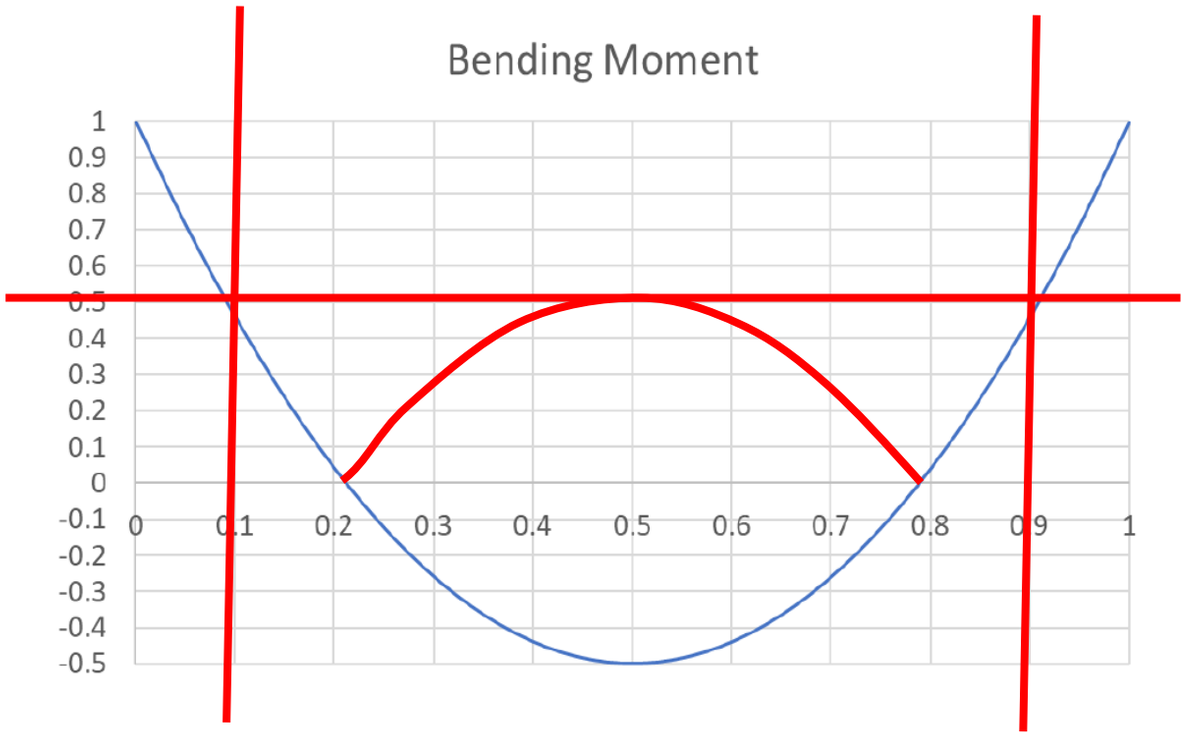
	Disp.	% Change
All	4513 lbs	3% reduction
Planing USVs Only	2872 lbs	38% reduction





Variable Bead Thickness

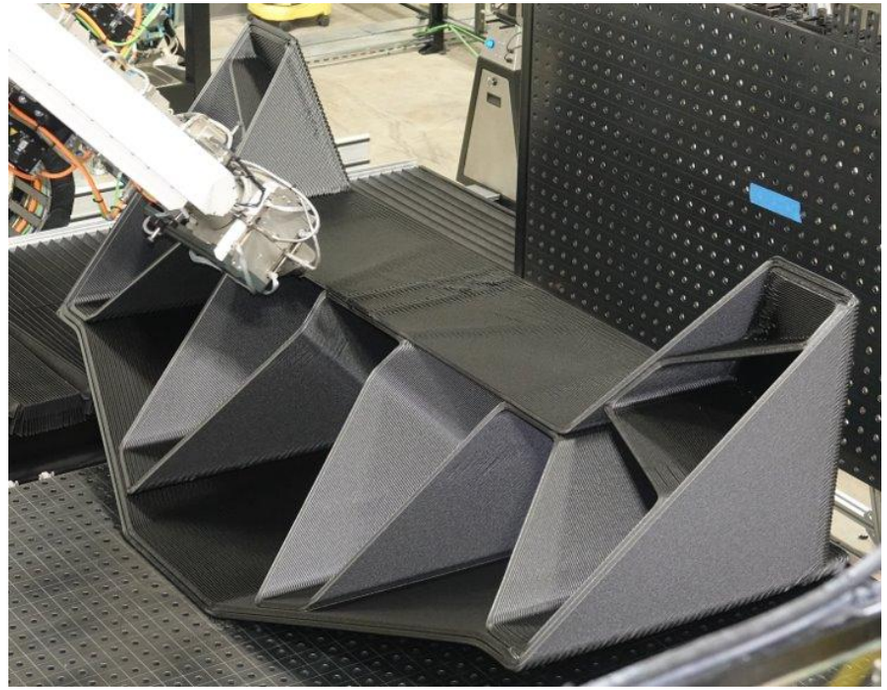
- Customize thickness of hull panels
- Customize thickness across panel



Panel	Current Panel Thickness	Minimum Panel Thickness	Savings
	mm	mm	%
Hull Bottom under fuel tank inner	16.5	14.2	14%
Hull Bottom under fuel tank outer	16.5	14.0	15%
Hull bottom panel mid inner	16.5	14.2	14%
Hull bottom panel mid outer	16.5	14.0	15%
Hull bottom panel fwd inner	16.5	13.3	20%
Hull bottom panel fwd outer	16.5	12.9	22%
Topsides aft lower	10	6.9	31%
Topsides aft upper	10	12.3	-23%
Topsides mid lower	10	8.0	20%
Topsides mid upper	10	13.9	-39%
Topsides fwd Upper	10	11.3	-13%

Additive Manufacturing Considerations

- Print time
  - Layer Time depends on:
    - Path length
    - Stops and starts
  - Time between layers
- Software compatibility
- Roughness
  - Increases resistance
  - Surface machining or coatings



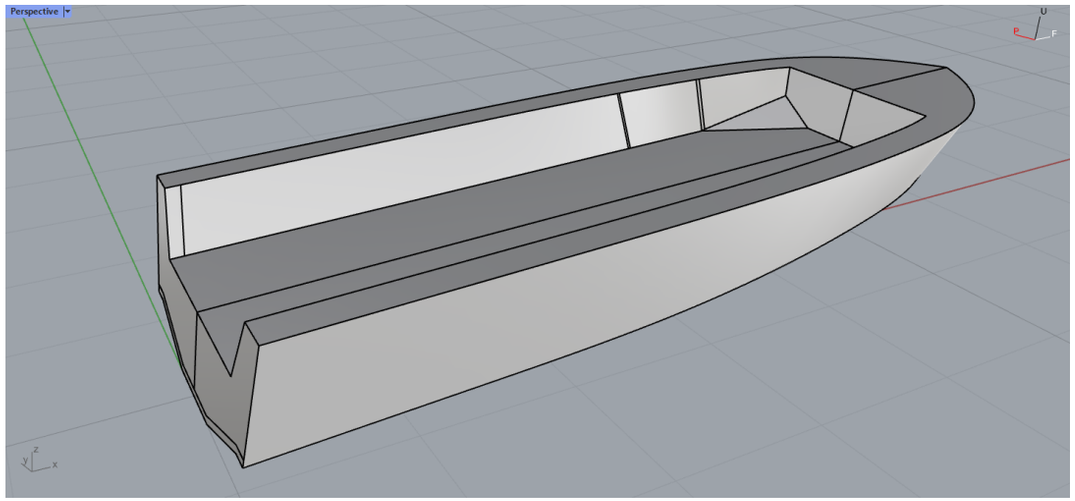




Design Goals

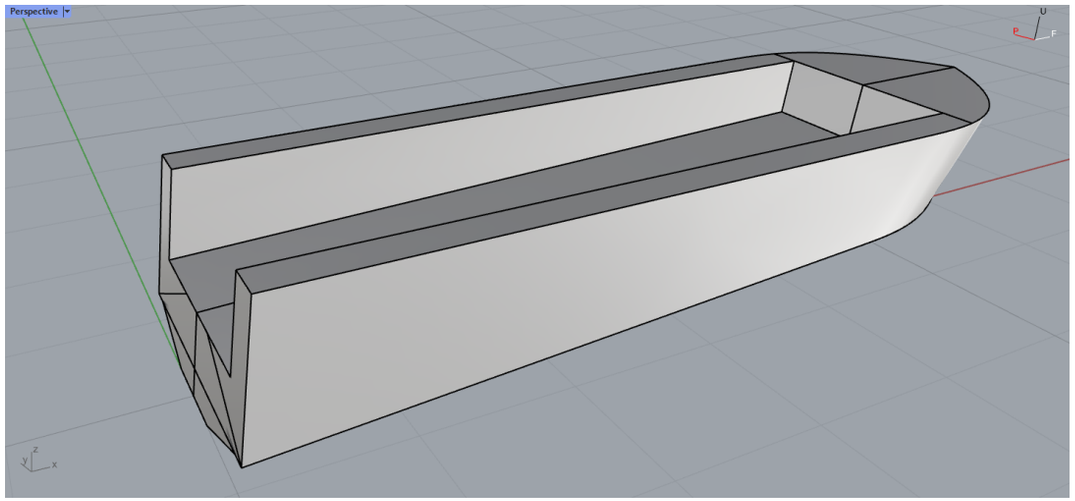
USV2

- Stock hull design
- Structure overdesigned



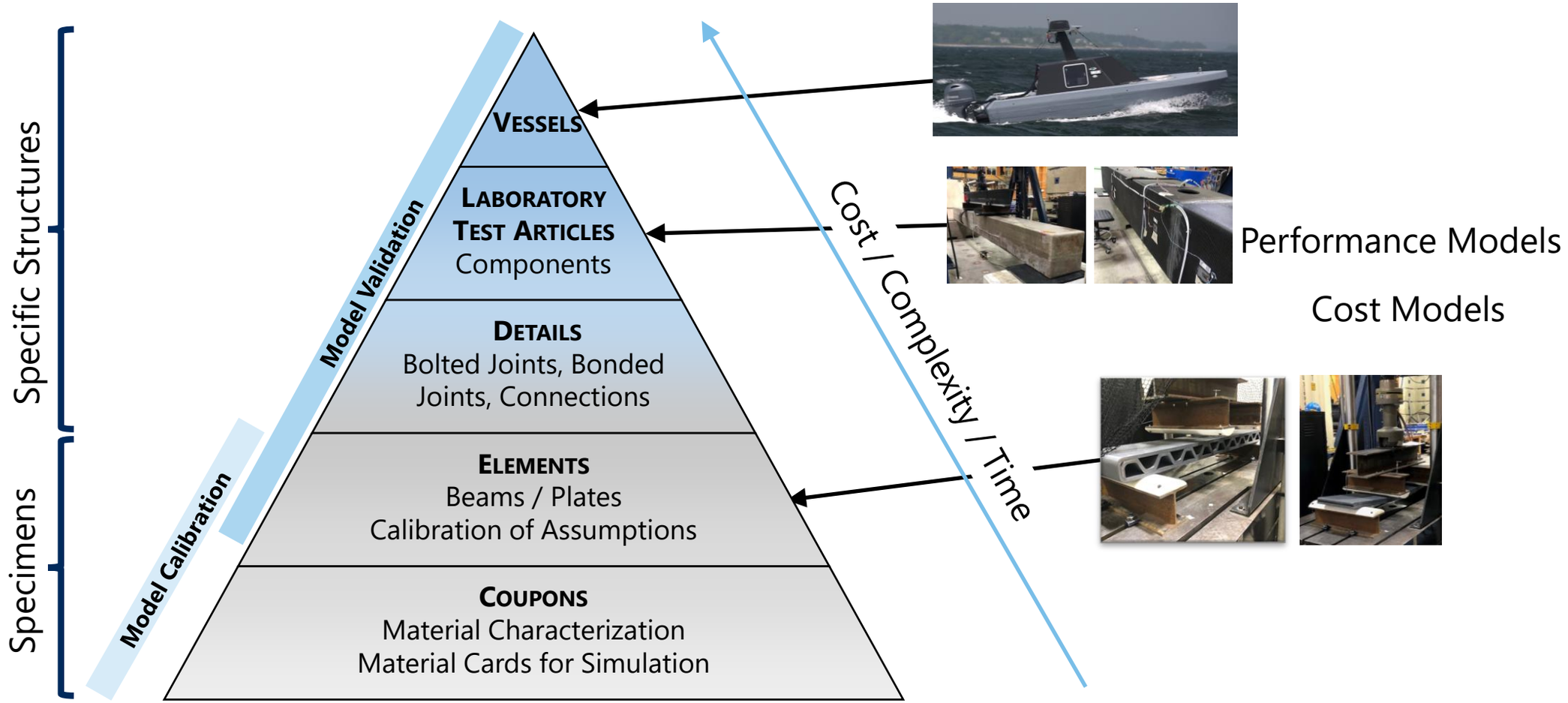
Updated

- Customize hull for AM
- Optimize panel thickness & internal structure
- Reduce weight, print time, and cost



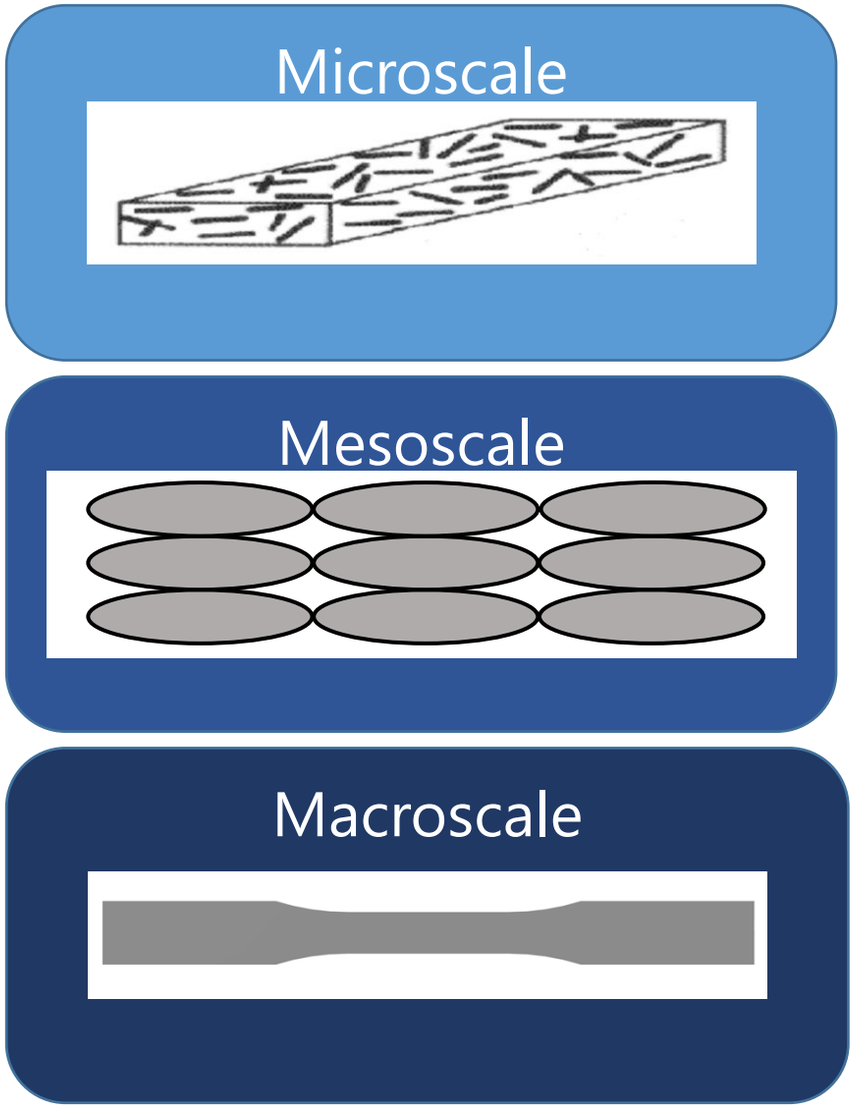
Material and Demonstrator Testing

Utilize a building block approach for identifying and evaluating vessel structures to systematically increase confidence through evaluation of performance at increasingly larger and more complex scales. Performance and cost models increase in complexity with each structure manufactured and experimentally evaluated.



Validate design tools and methods through manufacturing and experimental evaluation of structures with increasing complexity and scale.

Coupon Level AM Structures



Issue: Multiple property scales are at work within a 3D printed structure

Materials must be characterized relative to print process

- Nozzle type
- Bead geometry
- Print path
- Print Temperatures

Specific testing must be accomplished on each material used for printing to understand manufactured strength

On Water Testing

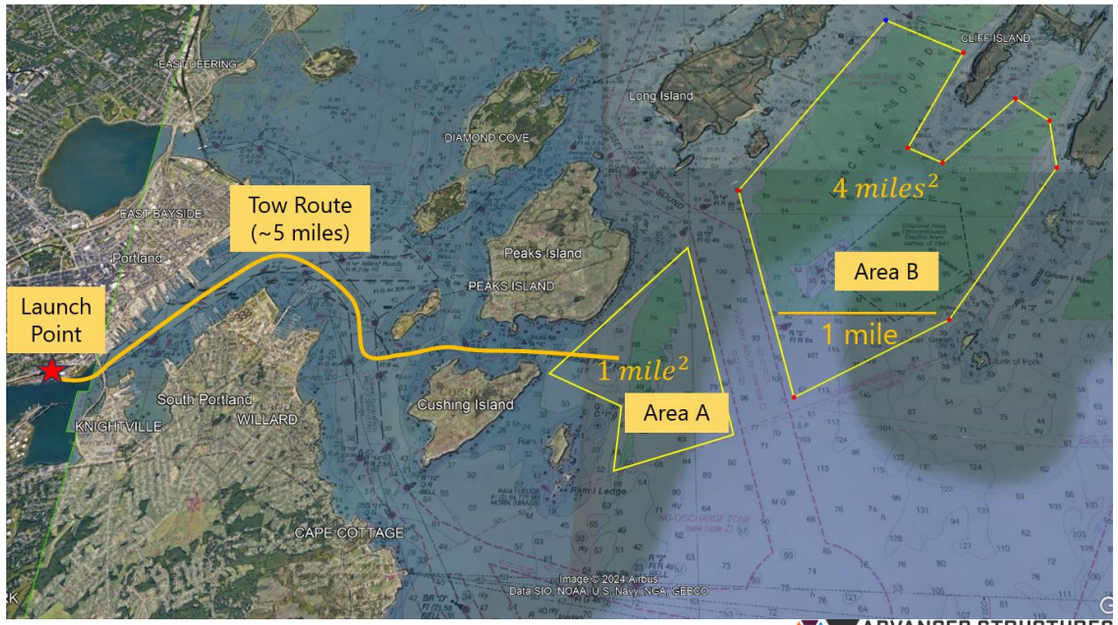
Protected Area

- The Fore River, upstream of the Casco Bay Bridge offers protected flat waters with only light boat and shipping traffic
- Local test area close to boat ramp and support vessel dock location
- Half-mile calm water testing area
- Testing Capabilities
  - Commissioning of remote systems
  - Calm water speed testing

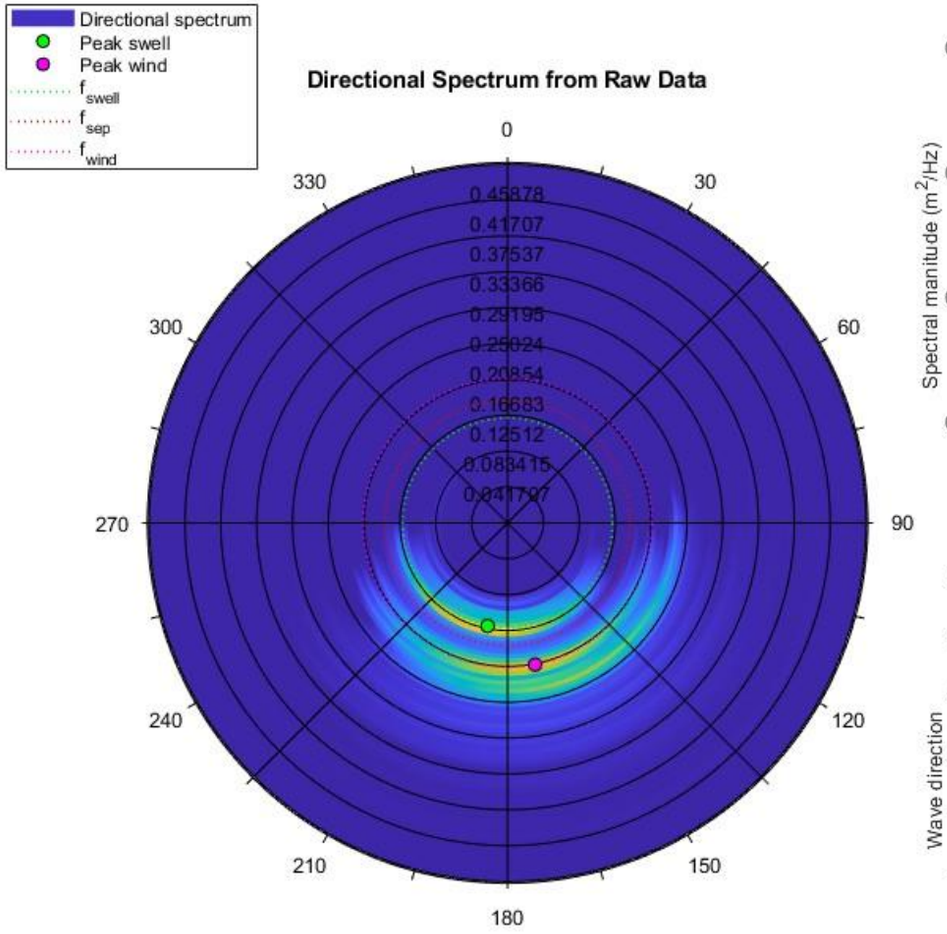


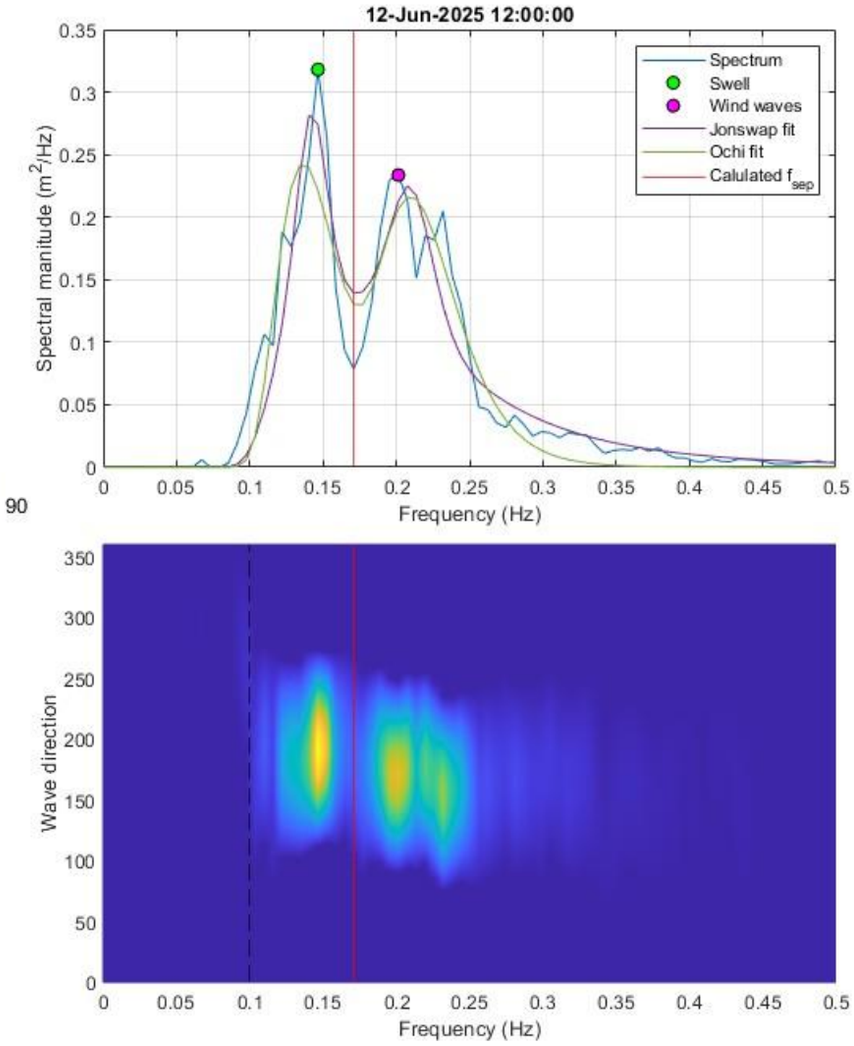
Casco Bay Test Area

- At sea testing area to showcase operations in waves
- Two testing areas with up to SS3 conditions
- Outlined with help form USCG for uncrewed ops
- Testing Capabilities
  - Calm-water testing
  - Seakeeping



Sea State Definition





Wave Statistics		
m_{m1}	0.173	m^2Hz^{-2}
m_0	0.0321	m^2
m_1	0.00735	m^2Hz
m_2	0.00232	m^2Hz^2
m_4	0.00062	m^2Hz^4
$H_{s,total}$	0.717	m
$H_{s,wind}$	0.555	m
$H_{s,swell}$	0.445	m
f_p	0.146	Hz
T_p	6.83	s
$T_{p,wind}$	4.96	s
$T_{p,swell}$	6.83	s
T_{m01}	4.37	s
T_{m02}	3.72	s
T_{m10}	5.39	s
γ_{wind}	2.8	-
γ_{swell}	2.36	-

of

Rough Water Testing

Tests Performed

- Head seas and following seas runs at incrementally increasing speeds in ~SS2 (H_s .325m):
  - ~5 knots (displacement mode)
  - ~10 knots (semi-displacement mode)
  - ~15 knots (planing mode)
  - Top Speed (~20-22knots) (planing mode)

Test Data Collected

- Strain
- Temperature
- Accelerations

Test Goals

- Qualitative performance at sea
- Quantitative measurements of operations

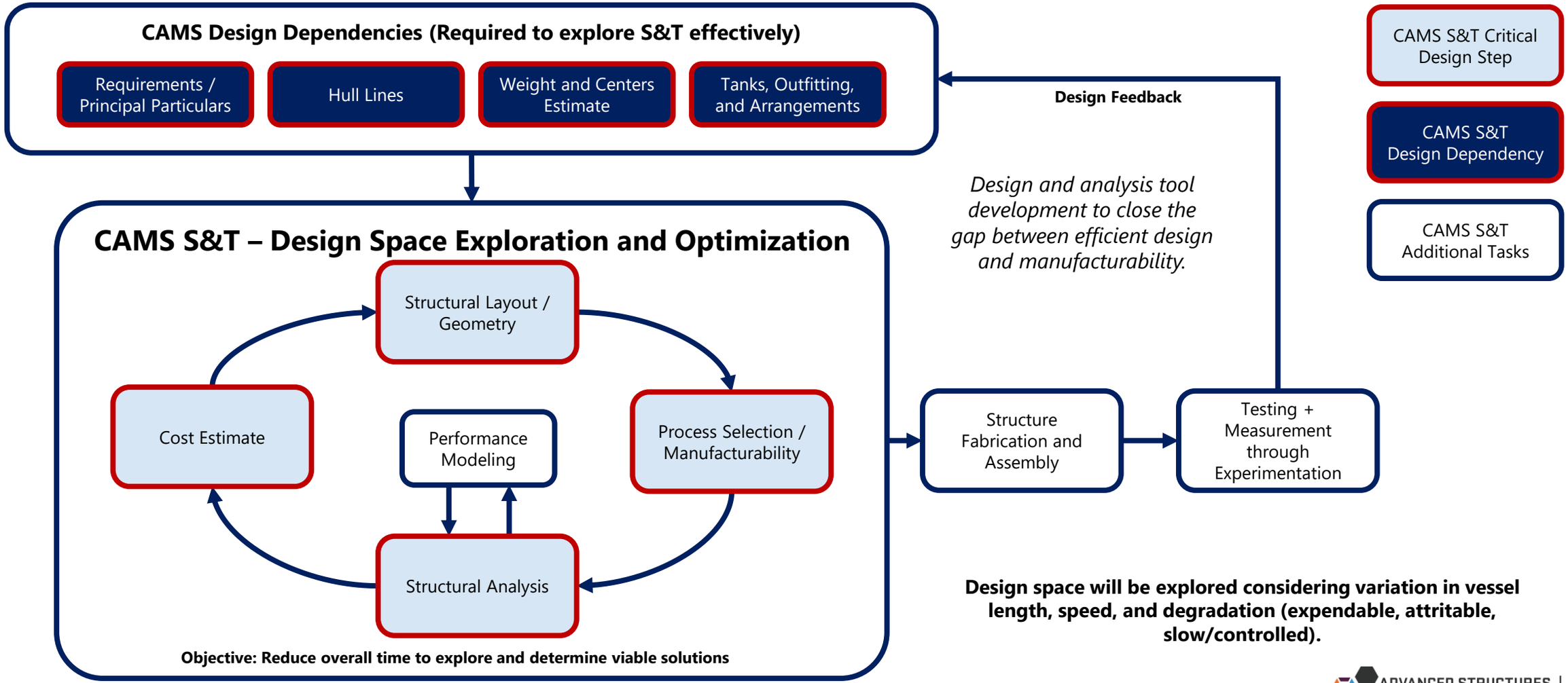
Sea State 2, Top Speed



Design Tool and Method Development

Design and analysis tool development to close the gap between efficient design and manufacturability.

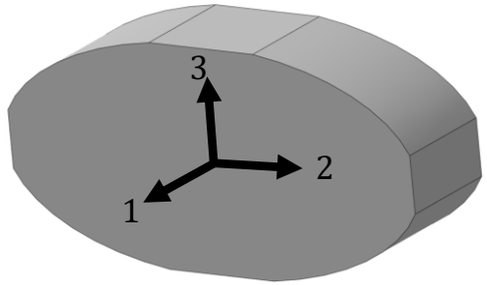
Focused on the rapid exploration and optimization of the design space considering robotic advanced manufacturing methods. An outcome of this S&T work is an improved understanding of how this design and manufacturing process can be appropriately benchmarked with existing methods. By integrating structural analysis and manufacturing process constraints into the iterative design process, overall time to generate a viable design decreases.

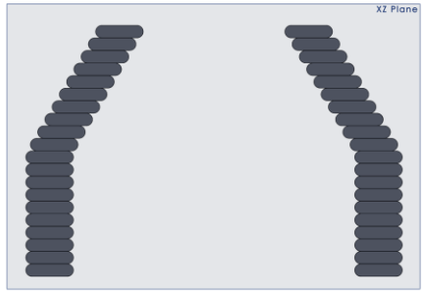


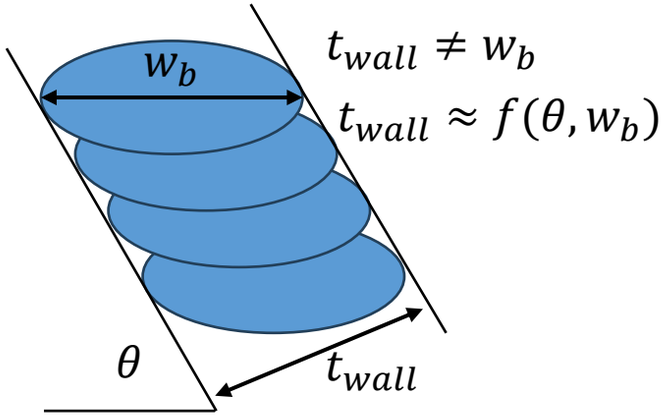
Structural Analysis

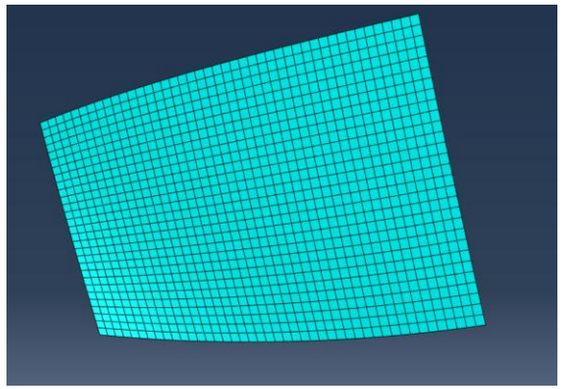
How to include AM process in structural evaluation?

- Treat AM material as **transversely isotropic**
- Create a **shell model** of the hull structure
- Capture **as-printed properties** using nozzle direction relative to shell element normal
  - **Transform** properties to match global coordinates
  - **Panel thickness** based on stacking direction
- User specified **factor of safety** to define feasible design space

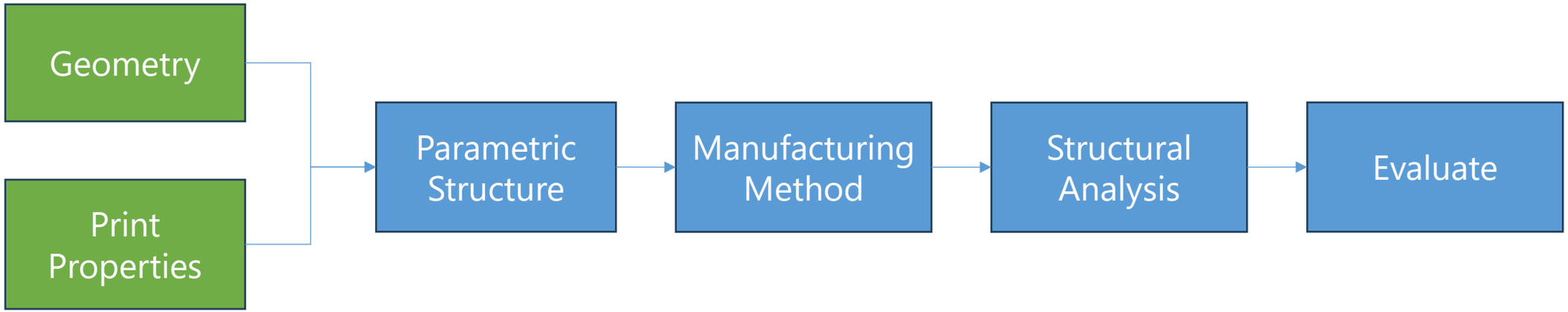








AM Analysis Workflow



Goal: *Enact design space exploration framework using simplest path through design workflow.*

Key Points:

- *Automate structural property search*
- *Determine manufacturing method*
- *Analyze AM structure*
- *Evaluate for cost and build time*

AM Design Exploration

- Analyze relation between print and structural parameters on end cost and build time
- Additively manufactured Generic Prismatic Planing Hull (GPPH)
- Targets
  - CEAD Printer
  - 6 meter hullform
- Compare results in a pareto front analysis

CEAD AM Flexbot



Generic Prismatic Planing Hullform

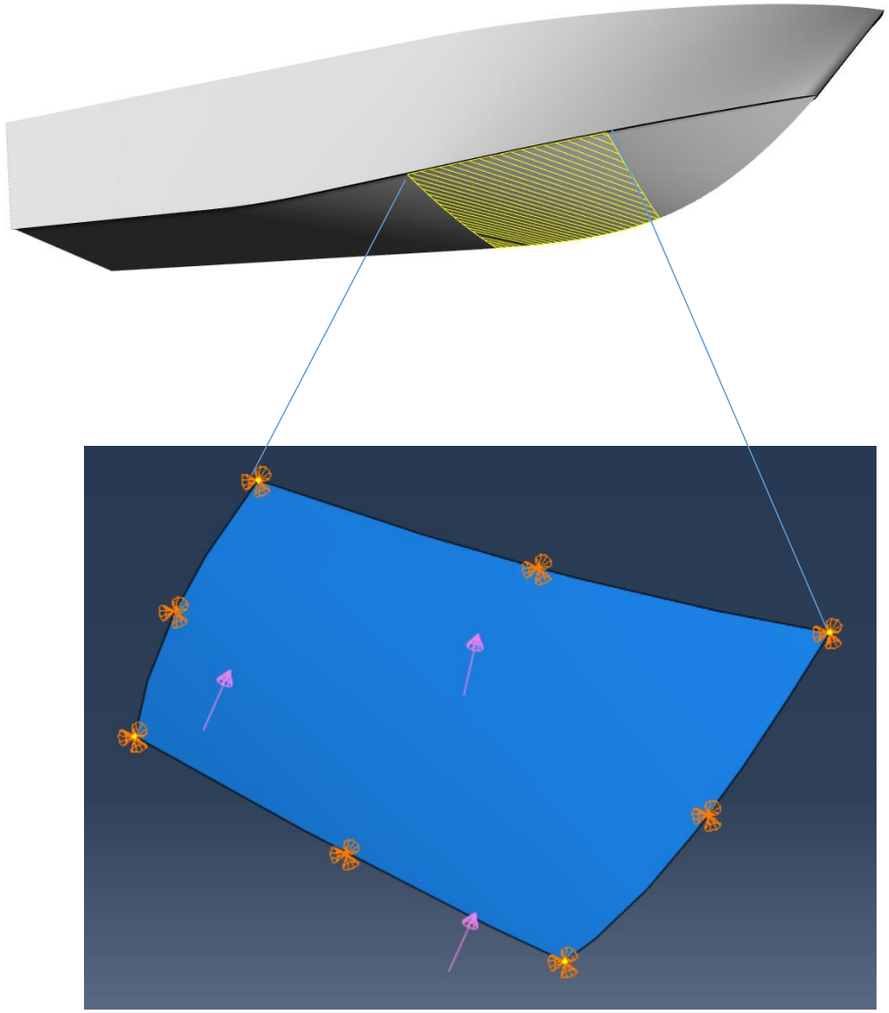


Principle Characteristics		
L_{OA}	6.00	m
L_{WL}	5.36	m
B	1.65	m
B_c	1.55	m
B_{WL}	1.67	m
B_T	1.65	m
D	0.99	m
T	0.43	m
T_T	0.43	m
L/B	3.64	
Δ	2.09	m^3

AM Design Exploration

Geometry and Loading:

- Bow panel from GPPH
- Taken from area between two bulkheads in the hull
- Loaded according to ISO small craft structural standards



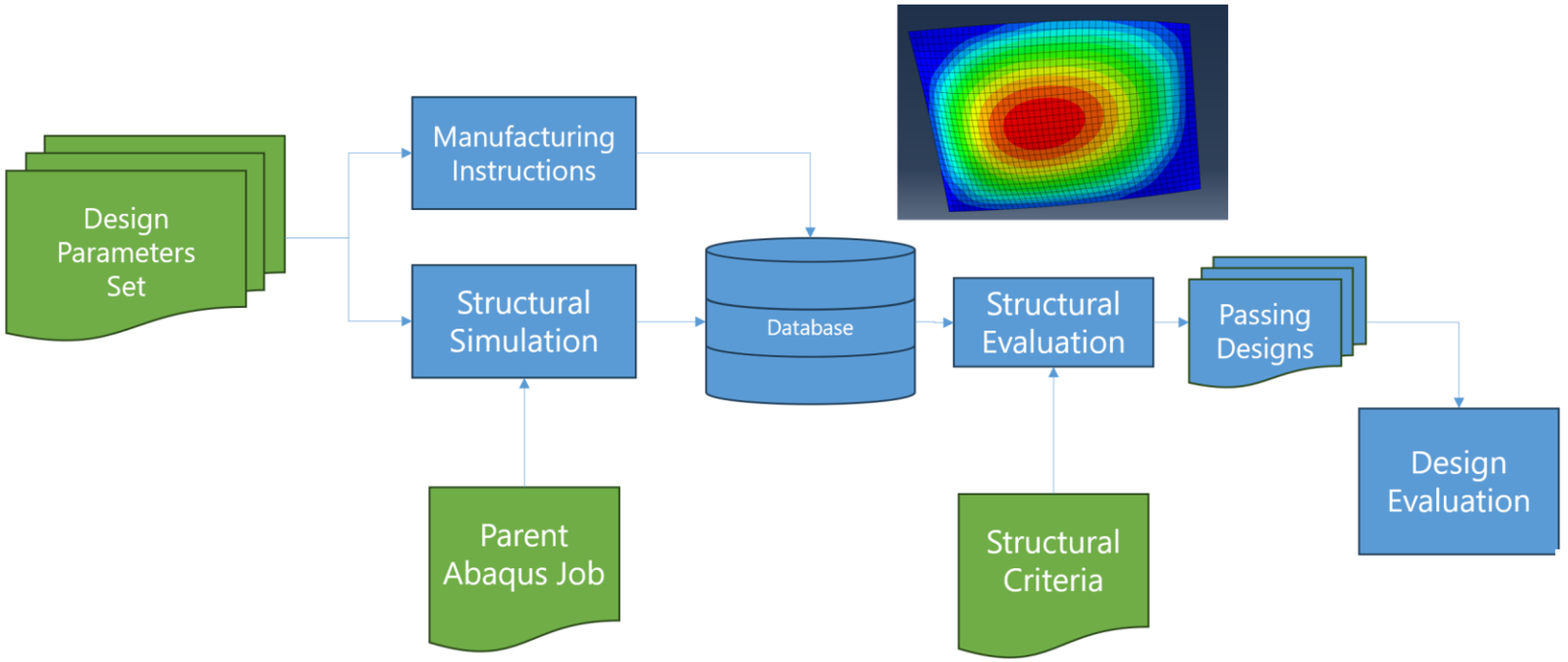
Objective:

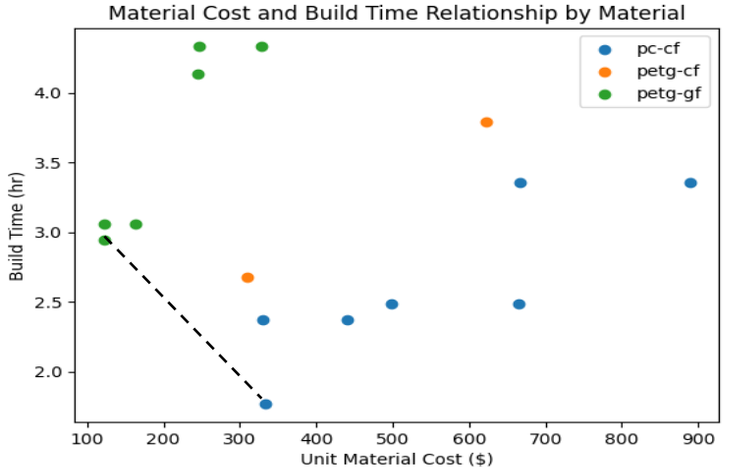
- Explore manufacturing parameters for minimum cost and build time given structural constraints

Design Space:

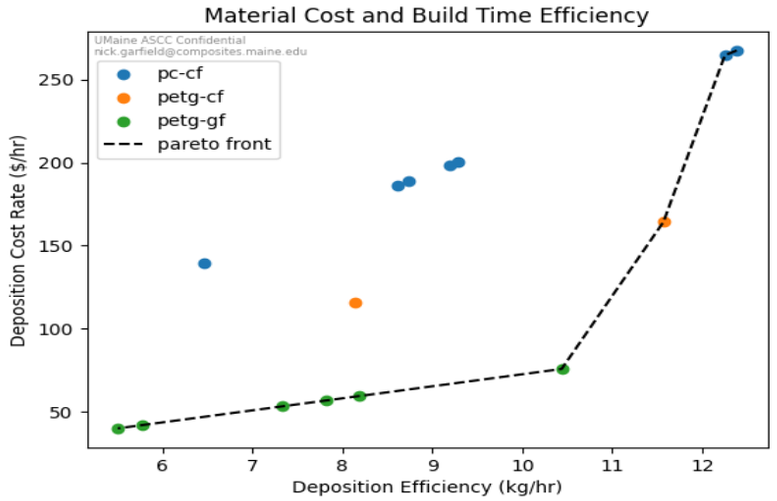
- Nozzle Diameters (mm): 4, 6, 9, 12
- Bead Orientations (deg): 90, 45
- Number of Beads: 1, 2, 3, 4
- Materials: pc-cf, petg-cf, petg-gf

AM Design Exploration



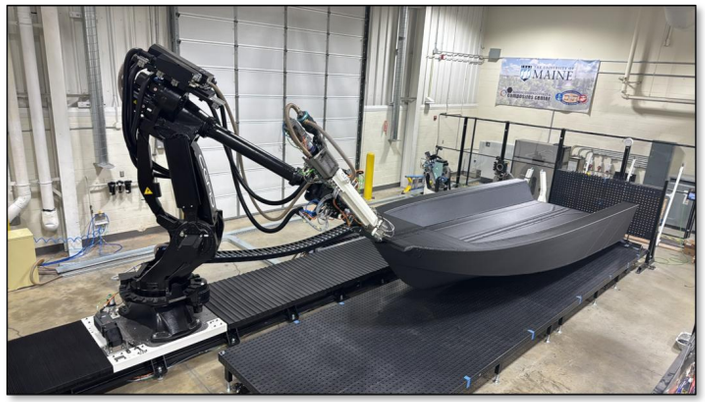


- Set based design approach
- Python notebook
- Shell mapper for structural analysis
- JSON file used for optimization storage
- Safety factor criteria for plate

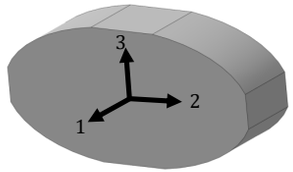


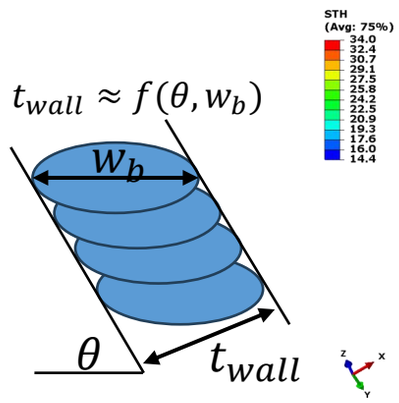
Conclusions

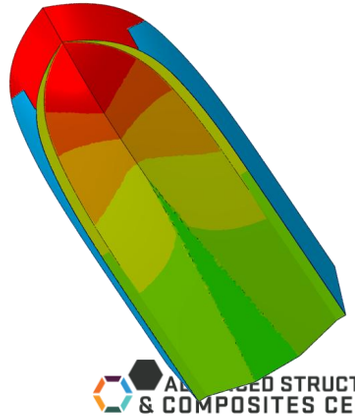
- Design to production method targets understanding of LAAM for high-speed vessels
  - Aims to ground our designs against currently available vessels
  - Identifying AM specific design concerns
- Coupon testing aims to characterize our as-printed material properties and strengths
- On water testing shows ability to deploy and operate additively manufactured USV
  - Identified issues with hull roughness on performance
  - Hull materials are capable of operation in real ocean environments
- Design tools and methods can capture complexities of AM
  - Allows for generalization of design process
  - Improves early-stage analysis





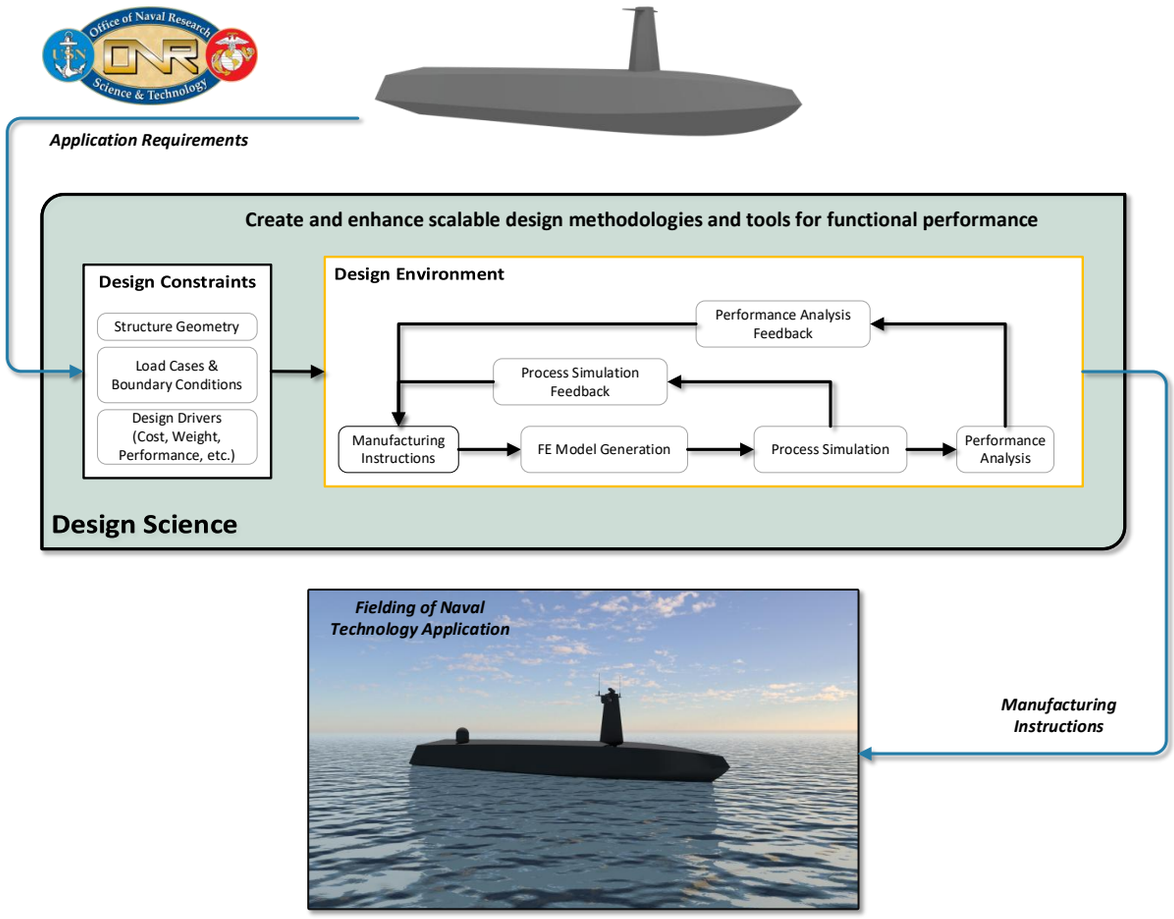






Next Steps

- **Improve vessel manufacturing methods**
  - Lower cost and build time
  - Explore larger vessel scales
  - Identify AM specific build characteristics
- **Increase coupling of on-water testing to design feedback**
  - Digital twin capability to explain on water phenomenon with simulation tool feedback
  - Continue to identify real world operations
- **Advance design methods**
  - Allow for early-stage design to be cognizant of manufacturability
  - Automate analysis process for closed loop optimization of hull structural design
  - Increase inclusion of process-structure-property relationships in analysis
- **Work with operators, acquisition offices, and industry to turn these demonstrators into an actionable manufacturing option for future USVs**



Questions

SUSTAINABILITY AND INNOVATION
IN SHIP DESIGN AND OPERATIONS
CONFERENCE 2026

GENERAL DYNAMICS

Risk Mitigation for Innovative Designs and Novel Ships

Coming soon... Part 2

GENERAL DYNAMICS

NASSCO

Risk Mitigation for Innovative Designs and Novel Ships Part 2

- 19 October 2026



SUSTAINABILITY AND INNOVATION IN SHIP DESIGN AND OPERATIONS CONFERENCE 2026

October 19-20, 2026

Session 2 Overview

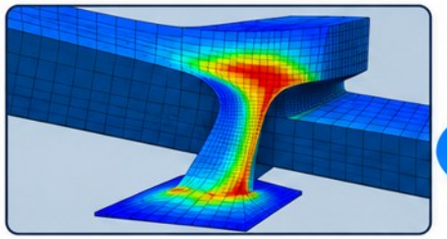
We've done a lot of introduction… why are we here, what the background is and what an innovative design looks like.

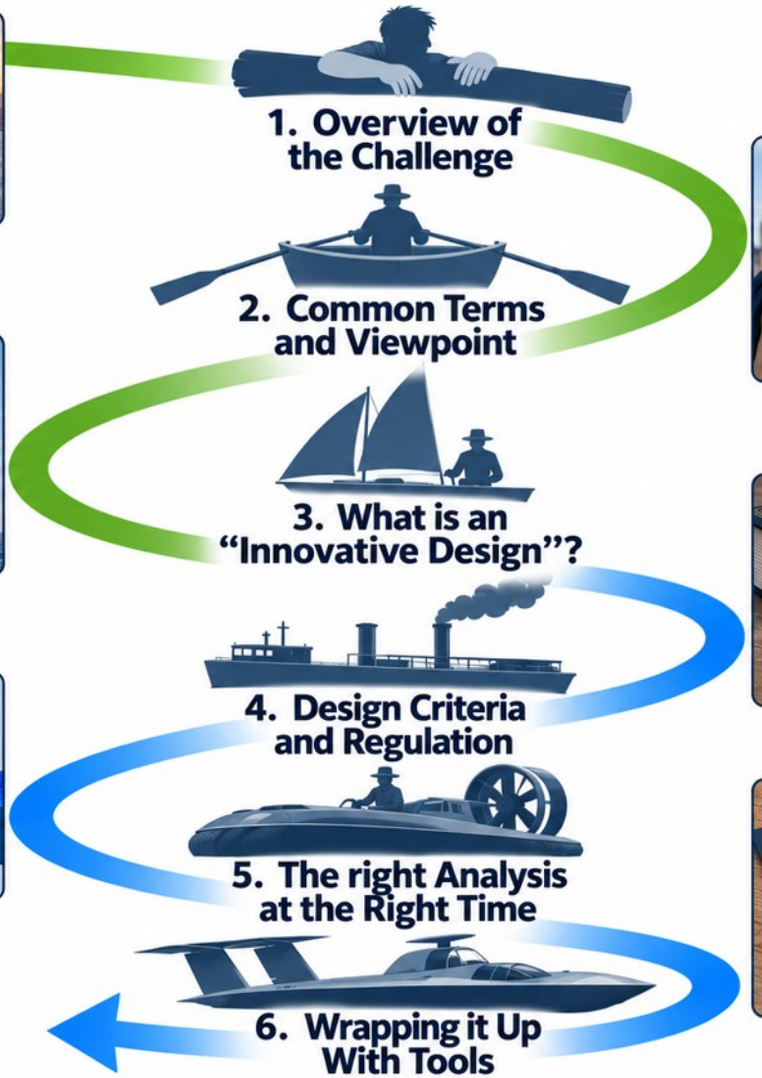
Now for the meat of the matter. What to do with it.

We will look at regulations and design criteria, then making sure we are on the right path, and wrap it up with some tools.







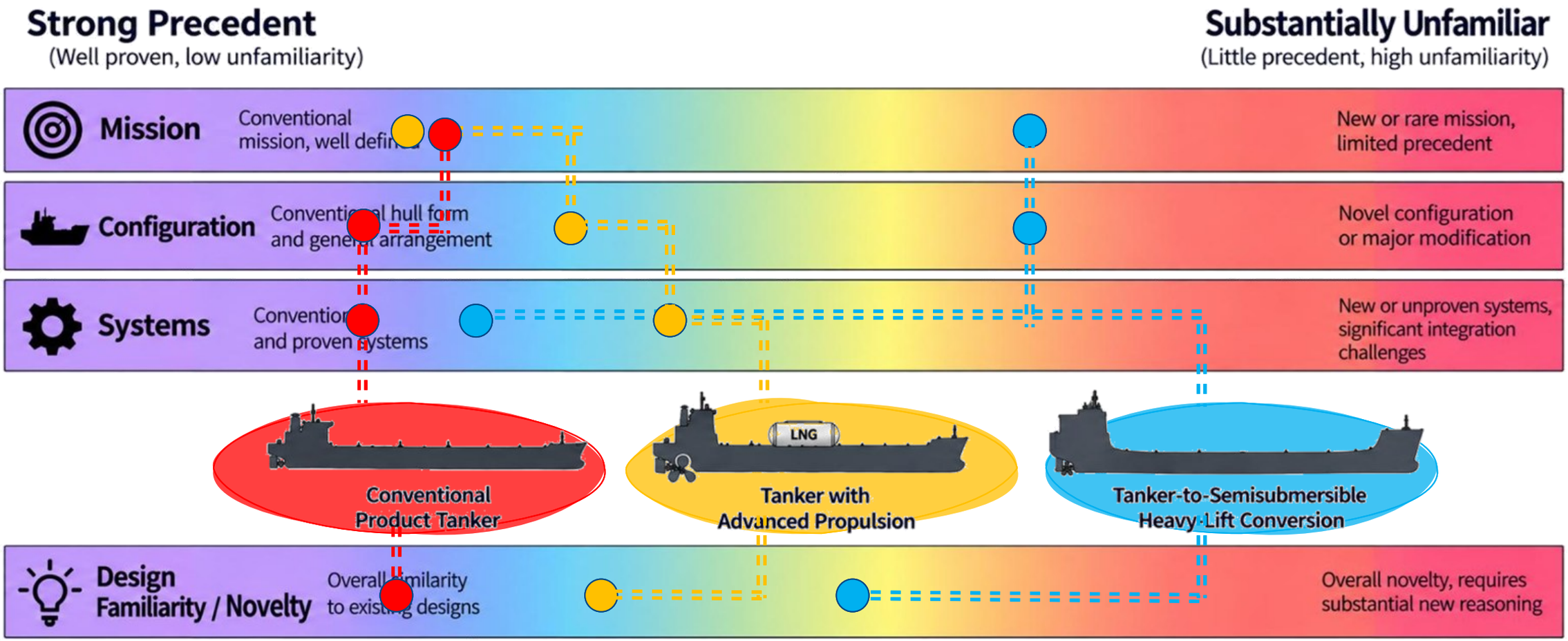








Innovation as a Spectrum

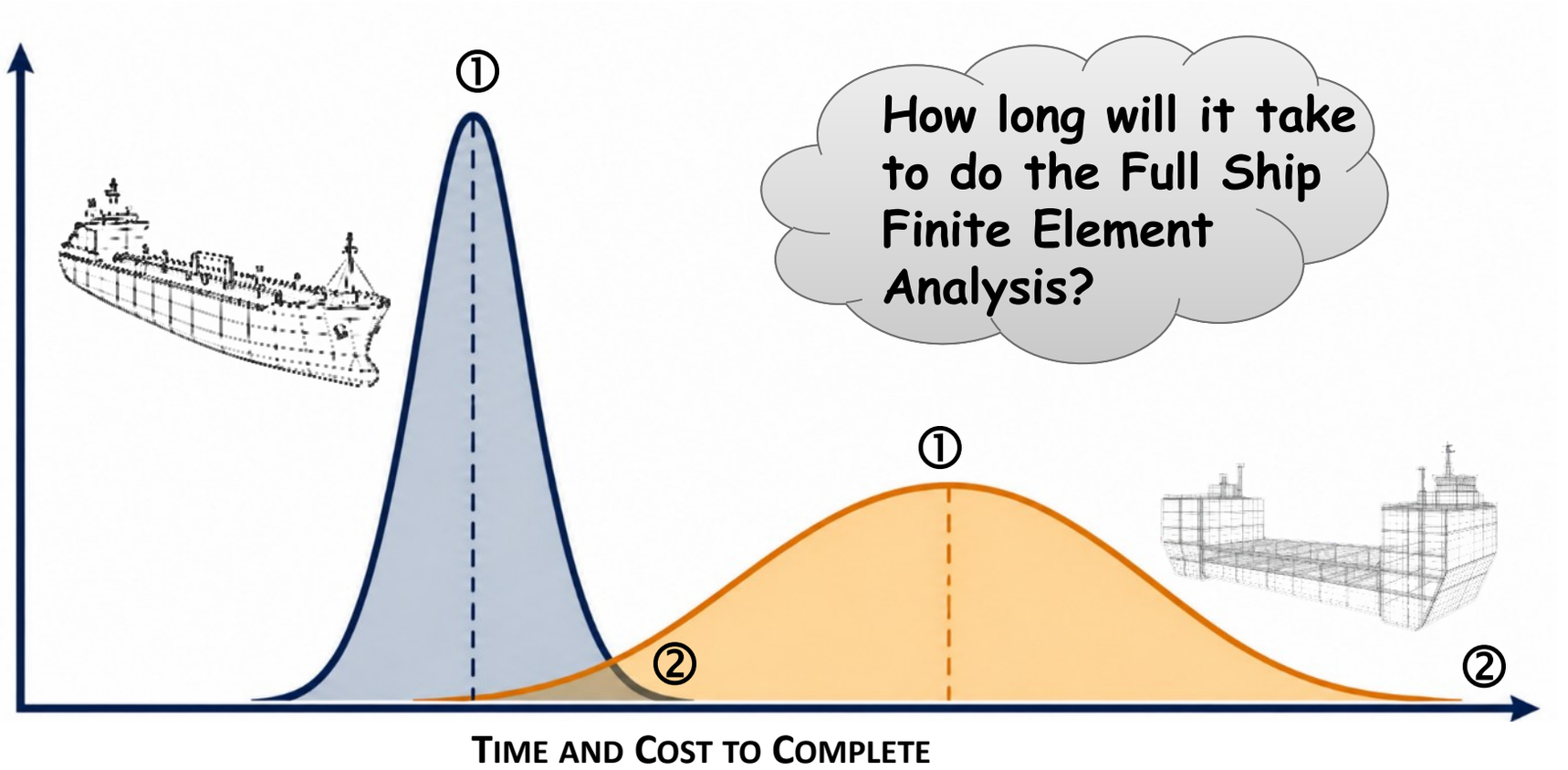


Cost and Schedule Are Ranges, Not Points

A Tale of Two Ships







- Each design, analysis, verification, and approval activity has a range of possible effort.
- Novelty often increases the average expected effort.
- May greatly increase the spread of possible effort.

- On Average (①①) it takes 2x as long
- Worst case (②②) maybe its 2.5x as long
- Or, it could be that the novel ship is actually easier (but that would be a really rare occurrence!)

Data Inventory



Generate the minimum information necessary to support the next design decision and generate it as late as possible without affecting the schedule.

The Titanic and SOLAS



- In response to the Titanic disaster, The Text of International Convention for the Safety of Life at Sea was signed in January of 1914
- Only ships that check all boxes are affected:
  - ❑ 12+ passengers
  - ❑ Engine propelled
  - ❑ Leave or return to certain ports

CHAPTER II.—SHIPS TO WHICH THIS CONVENTION APPLIES.

Article 2.

Except where otherwise provided by this Convention, the merchant ships of any of the States of the High Contracting Parties, which are mechanically propelled, which carry more than 12 passengers and which proceed from a port of one of the said States to a port situated outside that State, or conversely, are subject to the provisions of this Convention. Ports situated in the Colonies, Possessions or Protectorates of the High Contracting Parties are considered to be ports outside the States of the High Contracting Parties.

Observed Accident or Hazard



- Accidents
- Incidents
- Recurring hazards
- Operational experience

Safety Objective

- Protect people
- Protect the environment
- Prevent loss of the vessel
- Reduce risk to an acceptable level

Rule or Standard



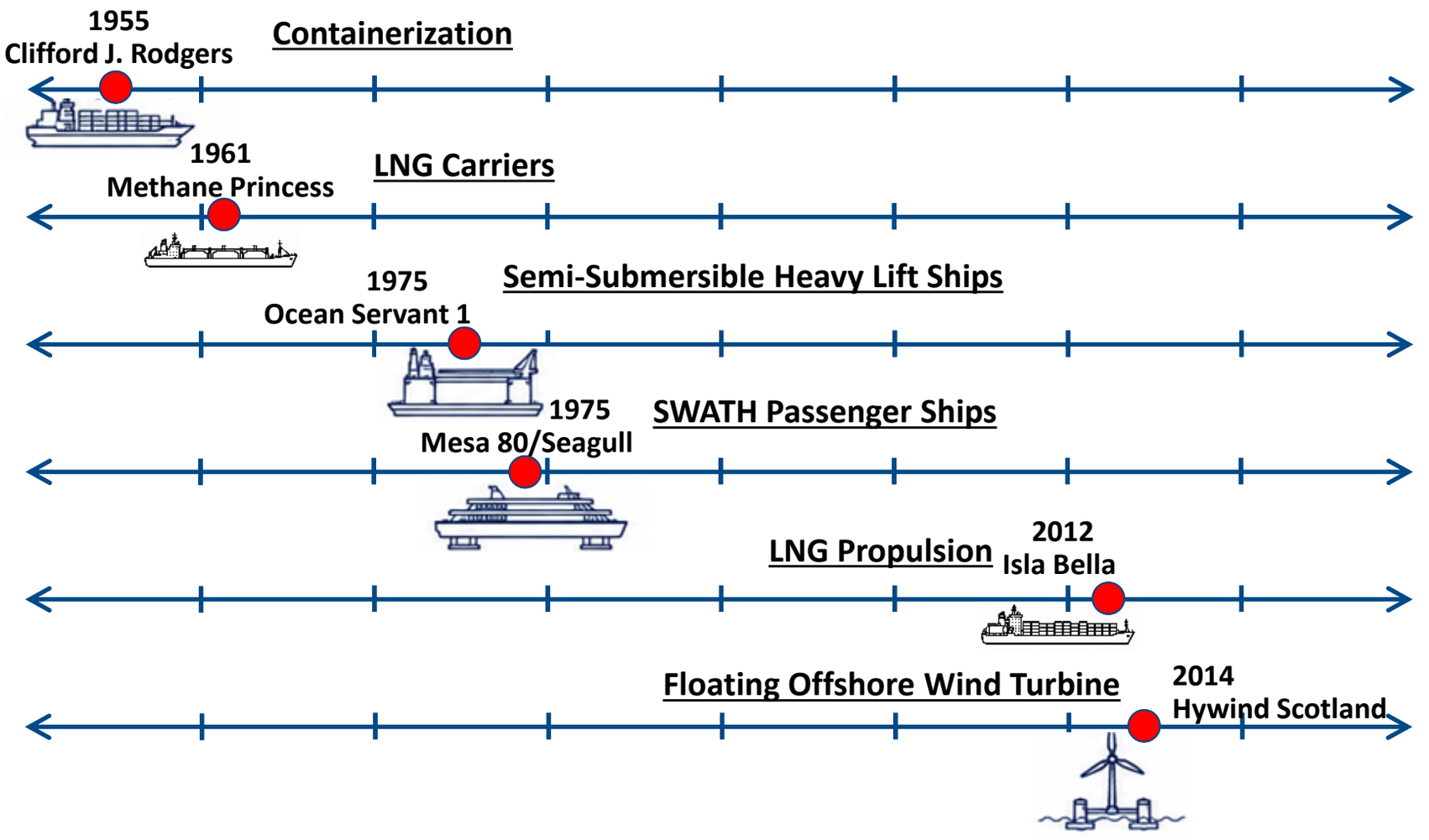
- Performance or prescriptive requirements
- Design, construction, equipment, and operation
- Based on the safety objective and past experience

So, Daddy, Where do Regulations Come From?

- Most regulations arise like the first traffic lights: A bad thing happens and a rule is created to prevent that accident from happening again.
- Changes in the regulation tend to occur because
  - The initial regulation did not provide for performance under similar conditions
  - A new condition has occurred that needs to be similarly addressed
- Once established and tested through several designs across the covered range of the regulation, they form a foundation for rapid, low risk design.



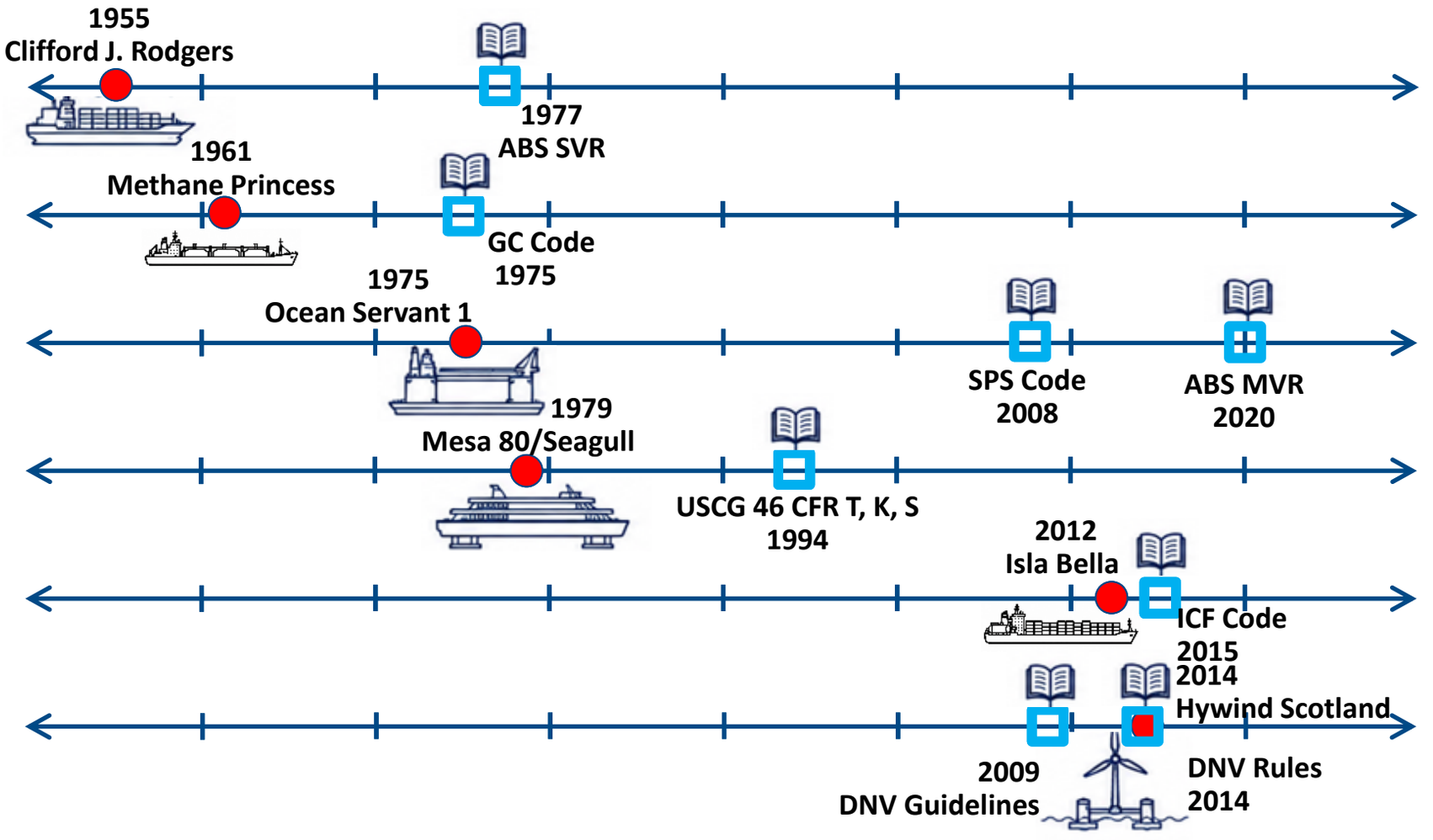
Constant Forward Pace of Marine Design Innovation



A sample of some significant innovations in marine design over the past 80 years.

Dates shown are contract award dates, where available.

Initial Implementation of Comprehensive Rule Sets

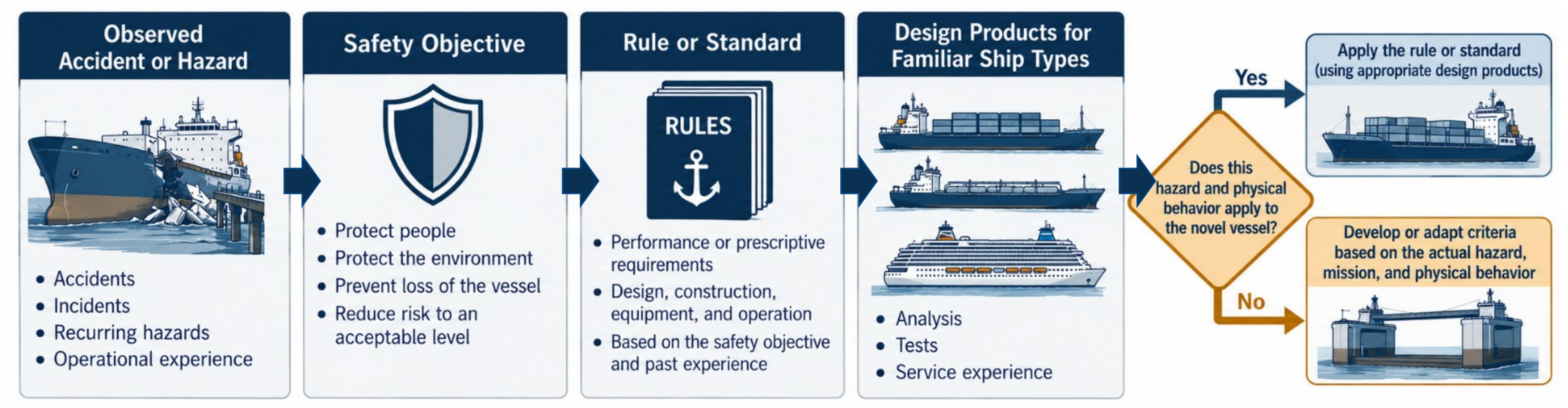


Comprehensive rulesets lead help the owner, designer, and builder quickly arrive at a closed-form design solution that is buildable and affordable, where costs of construction and operation facilitate continuing profitable commercial service.

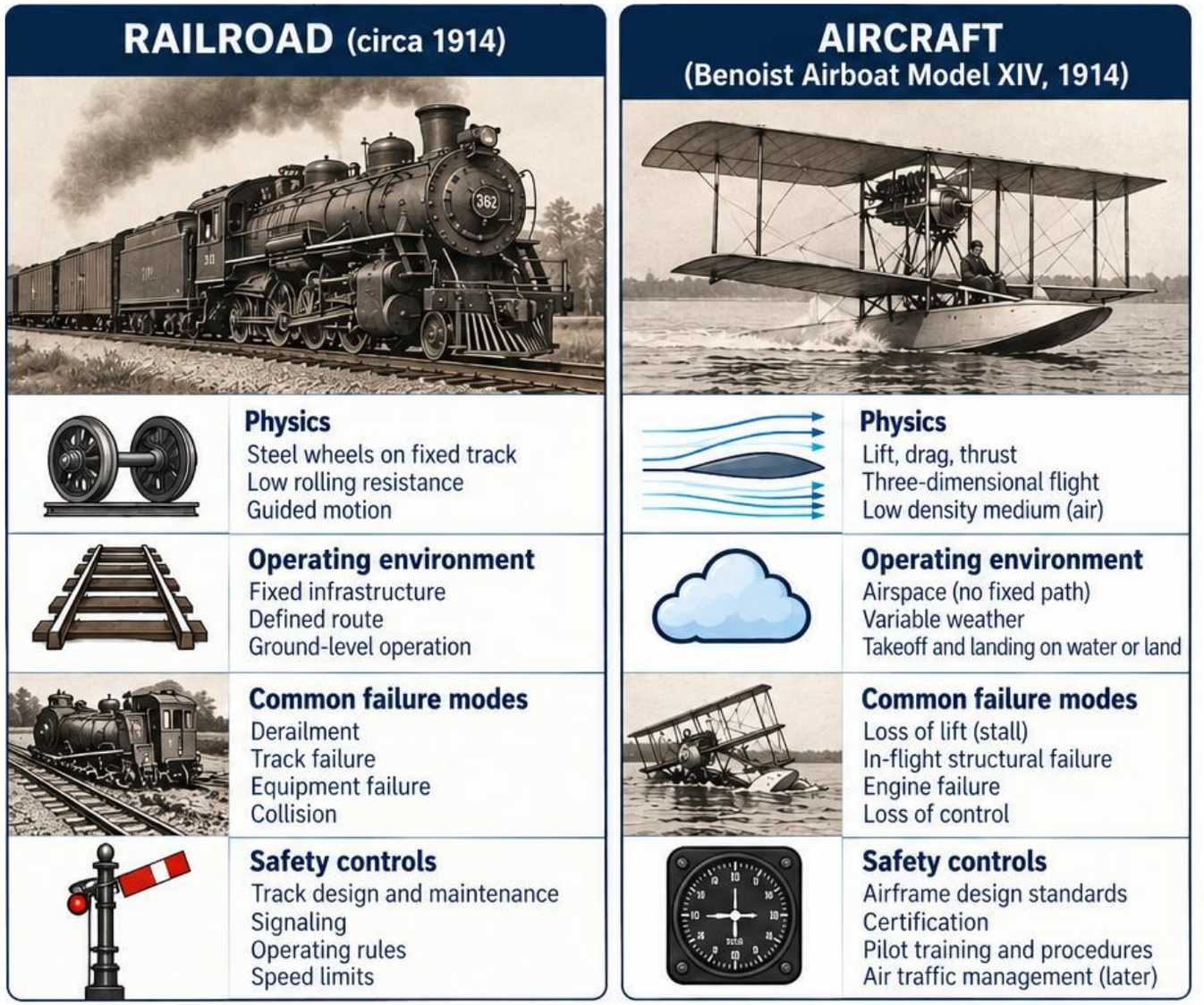
When Regulations and Novelty Collide

- Established rules and standards:
  - collect accumulated experience;
  - define minimum expectations;
  - provide a common technical language; and
  - reduce unnecessary reinvention.
- They are most effective when the ship fits the assumptions behind them.
- Many conventional systems may remain directly governed by established requirements.

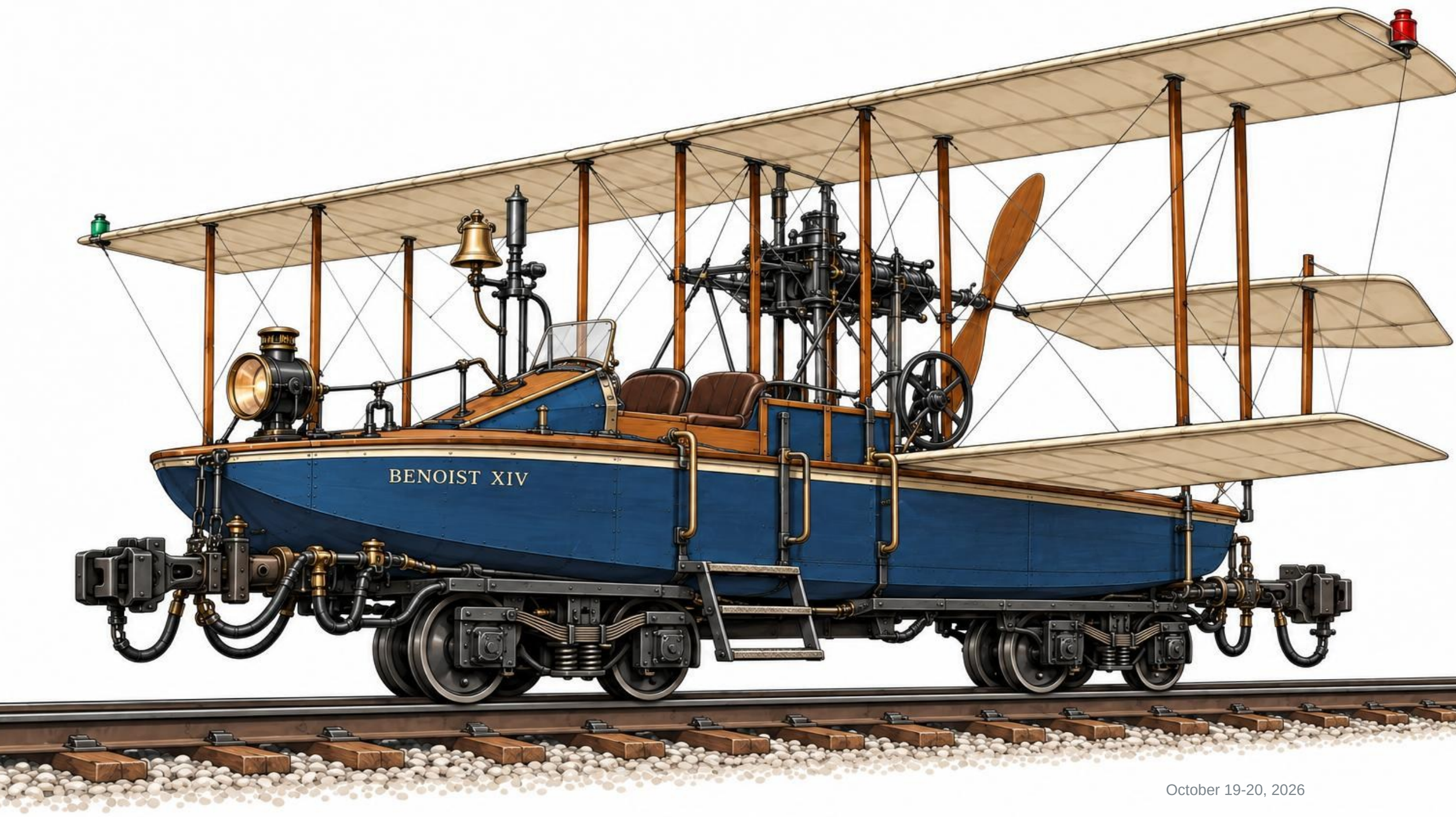
- Established rules and standards:
  - Assume every ship matches a template
  - Can be unresponsive to differences
  - Burden novelty with unintentionally
- IACS Common Structural Rules (CSR) are a strong ruleset for very traditional ships.
- But a seemingly simple change—like engine room location, cannot be handled effectively by them.



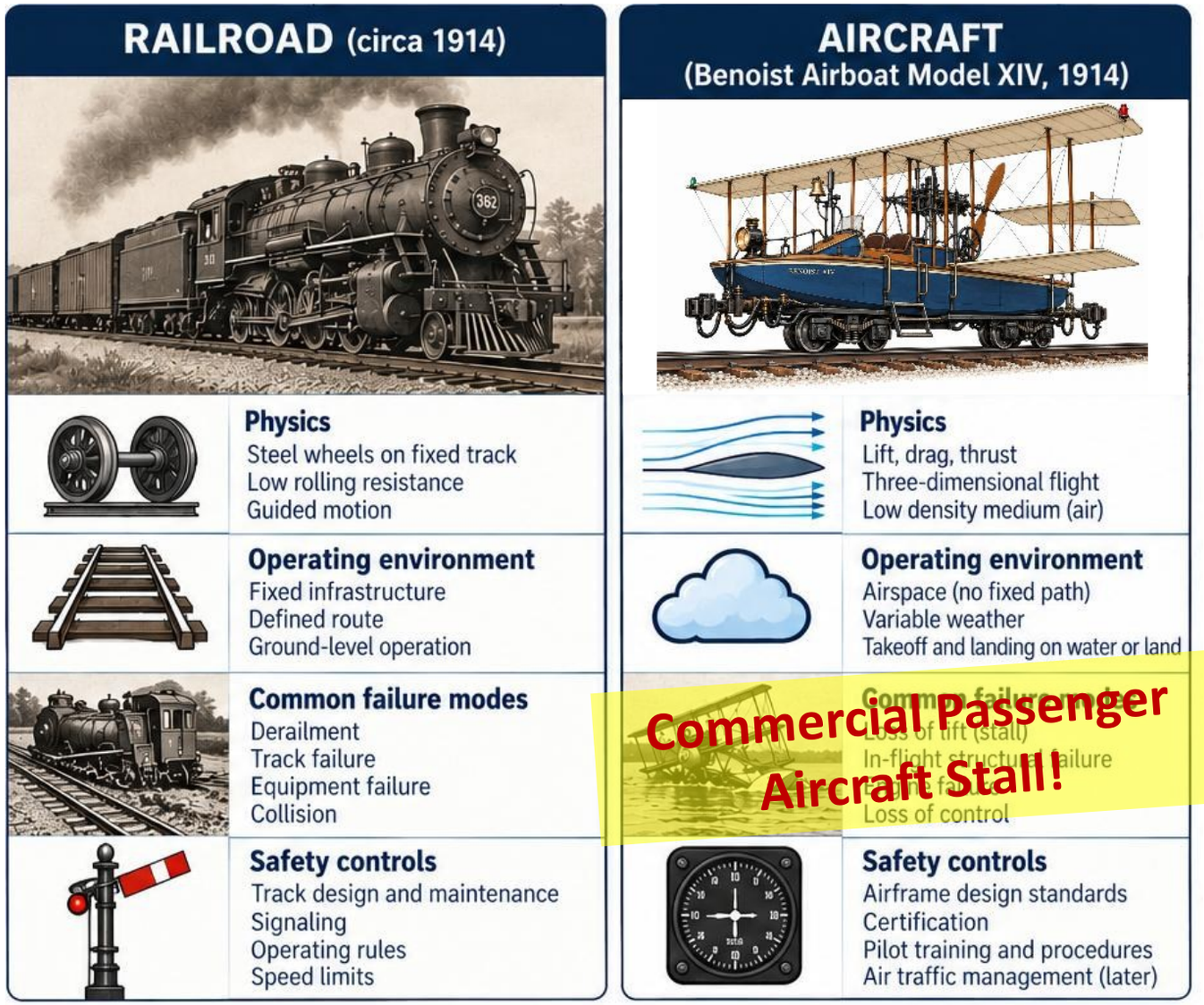
Transportation Safety a Century Ago



- Transportation regulations tend to surround two things:
  - The safety of the people and goods on board the vehicle
  - The safety of people, property, and environment surrounding the area of operation of the vehicle.
- Enter a new technology for transporting people and goods. Do we apply the same regulations and expect a reasonable result?
- Applying railroad criteria to an aircraft would not be conservative; it would be irrelevant to the aircraft's actual hazards and behavior.


BENOIST XIV

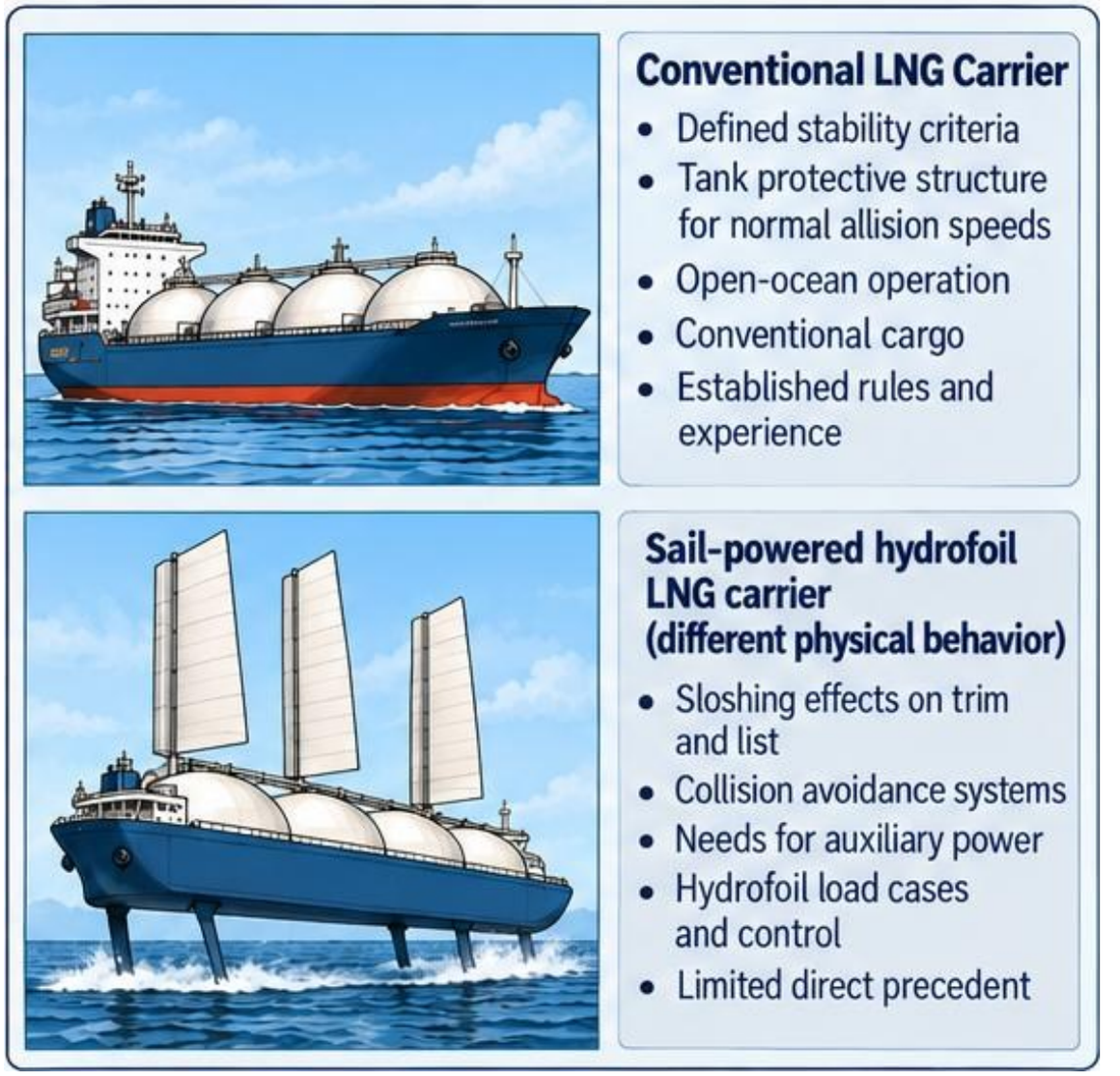
Transportation Safety a Century Ago



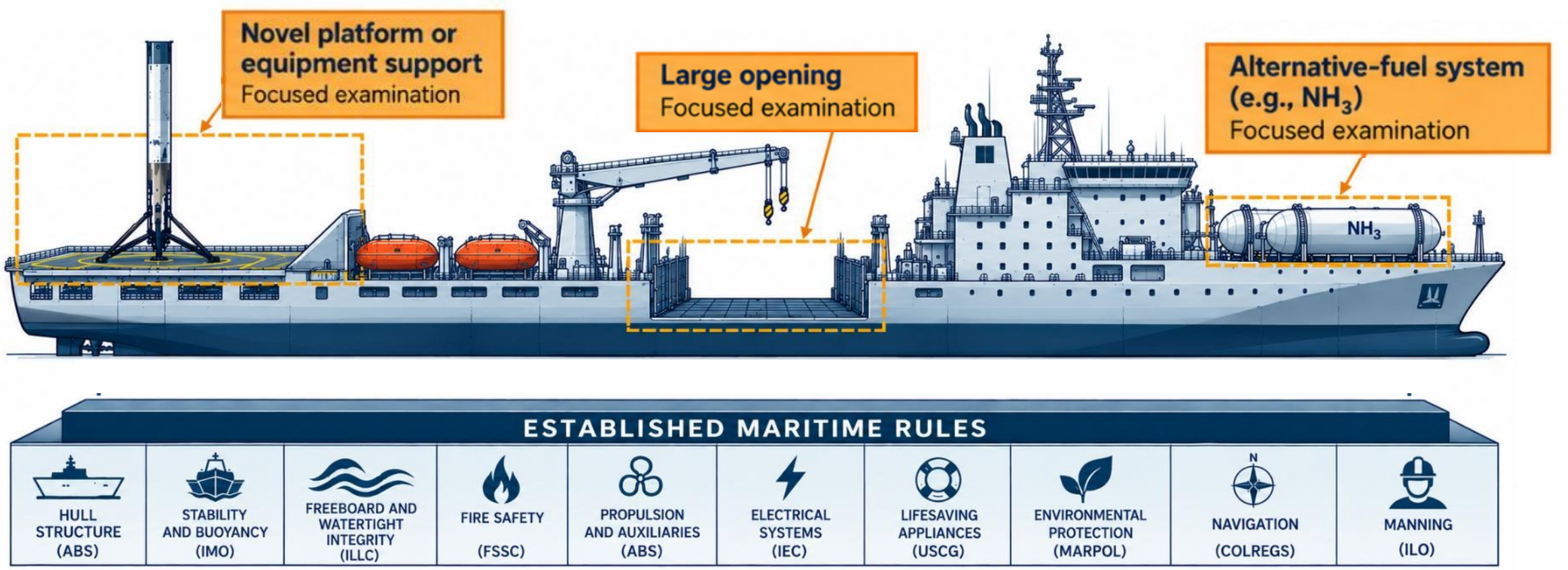
- Transportation regulations tend to surround two things:
  - The safety of the people and goods on board the vehicle
  - The safety of people, property, and environment surrounding the area of operation of the vehicle.
- Enter a new technology for transporting people and goods. Do we apply the same regulations and expect a reasonable result?
- Applying railroad criteria to an aircraft would not be conservative; it would be irrelevant to the aircraft's actual hazards and behavior.

Modern Application

- Novel ships present a narrower version of the same problem.
- Novel features and configurations inevitably come up against the assumptions implicit in existing regulations.
- Rules may reflect a configuration or condition that doesn't match the new reality. While existing regulation is unlikely to be as out of context as railroad regulations for aircraft, blindly applied, they can still halt a promising technology in its tracks.
- The responsible answer is to use physics and sound engineering to establish an acceptable safety basis.

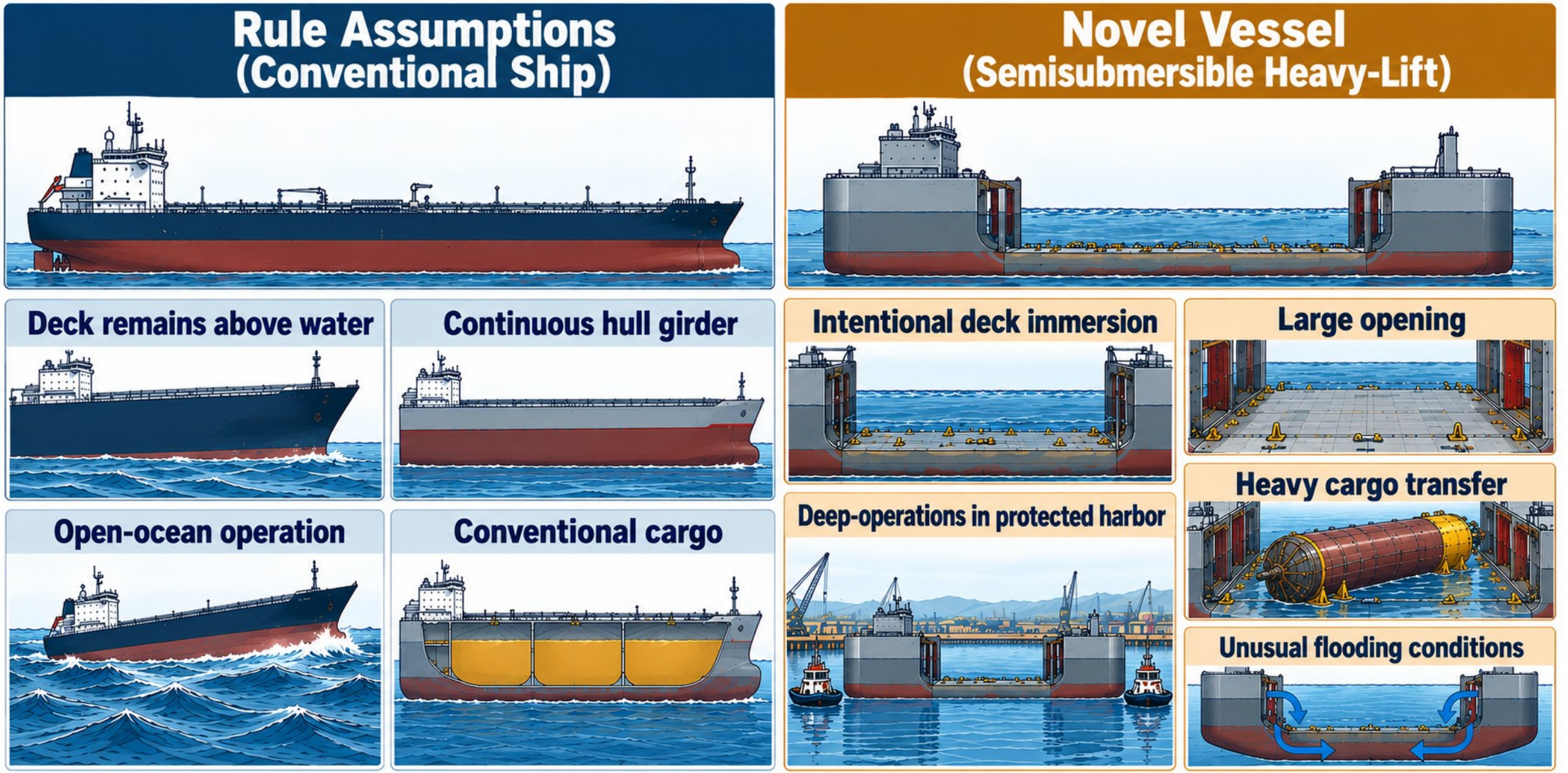


Rules: High Value and Real Limitations



- Most of the ship can remain within established practice.
- But the ship shown above will need exceptions to most of these regulations.
- Even combinations of known attributes can make the whole ship “novel”

Recognizing Rule–Design Misfit



From Mission to Criteria

Analysis may require reconsideration of mission or operating assumptions

When rule assumptions do not fit, physics and engineering judgment help establish the basis
.
Goal-based rules are founded in the idea that innovation can be accepted with appropriate validation.

1 Mission and Operating Conditions

- Mission (e.g., heavy lift, cargo transfer)
- Operating environment (e.g., sea state, temperature)
- Areas of operation (ocean, coastal, port)
- Loading, ballast, and operational profiles
- Interfaces (port facilities, other vessels, subsea)



2 Physical Behavior and Credible Failure Modes

- What is response to various load profiles?
- What are the credible failure modes?
- What are the consequences?
- How do systems and interfaces interact?





3 Safety Objective and Acceptable Performance

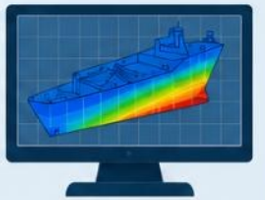
- What needs to be prevented or limited?
- Target level of safety (e.g., risk or performance target)
- Acceptable performance criteria
- Margins and robustness



4 Criteria, Methods, and Approval Documents

- Applicable regulations and standards
- Project-specific criteria (as needed)
- Analysis, testing, and modeling
- Engineering judgment
- Approval documents to demonstrate acceptable performance







Results and insights may refine safety objectives and identified failure modes.

Develop the Design and Criteria Together



- Configuration affects physical behavior, analysis, production, and approval.
- Criteria and analysis methods can affect which configurations are feasible.
- Select the simplest criteria path that provides credible evidence for the actual vessel.

Develop the Design and Criteria Together

Situation	Path	Use when	Typical output
Existing basis fits	Direct application	Existing assumptions fit	Conventional compliance evidence
Interpretation is uncertain	Clarification	Boundaries or interpretation are uncertain	Documented interpretation
Safety objective fits but method needs change	Adaptation	Safety objective fits but implementation must change	Project-specific application
Several useful partial bases	Combination	Multiple sources address different aspects	Integrated criteria basis
Inherited method doesn't represent the vessel	Supplement	Existing basis is useful but incomplete	Existing basis plus focused evidence
	Replace	Inherited method does not represent the vessel	Alternative technical method
	Develop new	No existing approach addresses the hazard	New project-specific criteria

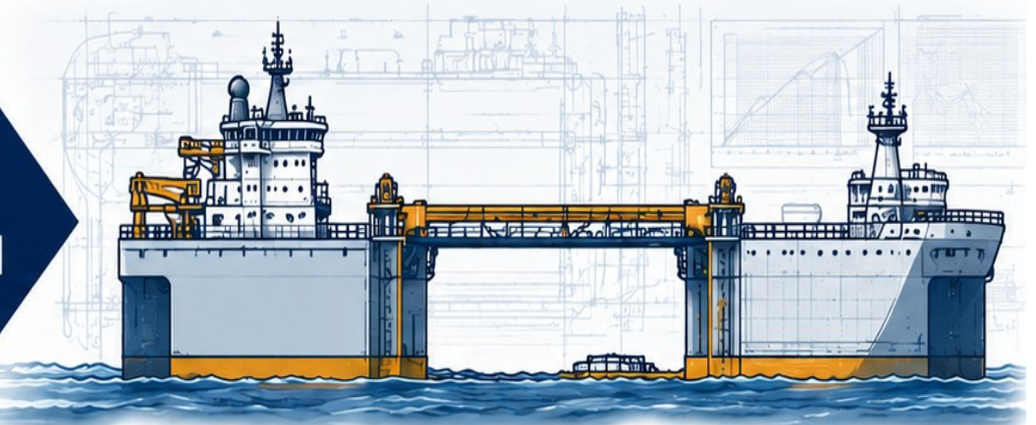
Physics and First-Principles Engineering



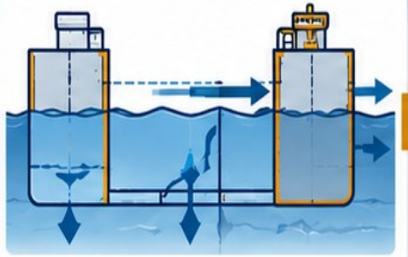
When requirements do not fit,

RETURN TO THE PHYSICAL PROBLEM

Use engineering to determine acceptable limits.

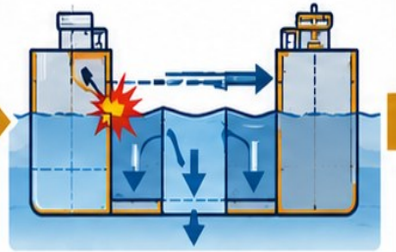


1 BEHAVIOR



- What behavior must be understood?
- What are the governing physical phenomena?

2 CREDIBLE FAILURE MODE



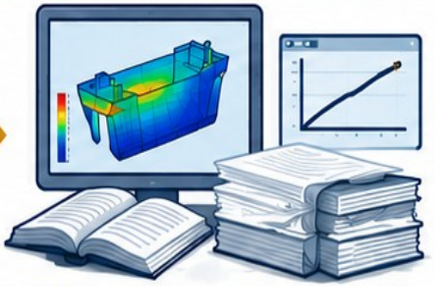
- What failures are credible?
- How could the behavior change?

3 CONSEQUENCE



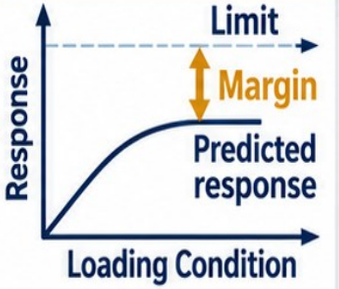
- What consequences could follow?
- What is the effect on safety, mission, and the environment?

4 RELEVANT EVIDENCE



- What evidence is relevant?
  - analysis
  - tests or experience
  - comparison with similar vessels
  - simplified calculations (when they represent the governing behavior)

5 ACCEPTABLE MARGIN



- What margin is needed to address uncertainties?
- Is the design robust across the relevant conditions?


DESIGN OFFICE
REGULATORS
MY OWN RULES
OUT WITH THE OLD
DOWN WITH REGS
MORE CREATIVITY
RIVERDALE SHIPYARD
THIS IS NOT WHAT WE ARE AFTER!
SUGGESTIONS
46CFR
SOLAS
IMO
ABS SVR
NVIC
MARPOL
DNVGL
ICLL
SHIP OWNER
RULES SUCK

Engage Regulatory Approval Authorities Early

Sequential Review

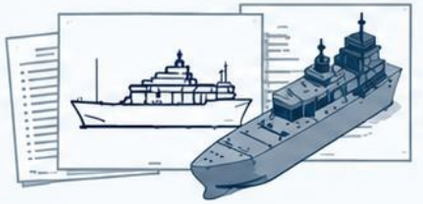
Design completed before significant regulatory engagement

Designer



Develops design based on assumptions and interpretation of requirements

Completed Design



Design finalized and documented

Review



Regulatory review of completed design

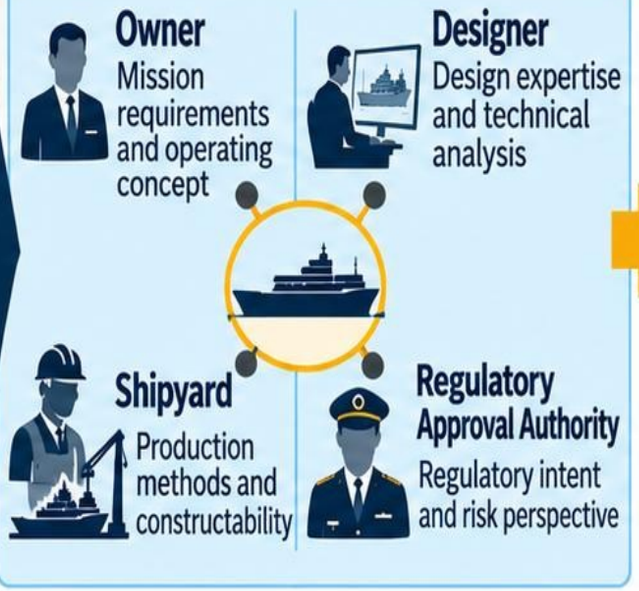
Late Disagreement



- Significant issues identified
- Redesign or rework required
- Cost and schedule impact
- Adversarial outcome

Early Cooperative Development

Early and continued engagement to solve the right problem



Common Technical Problem



Shared understanding of mission, hazards, physical behavior, and constraints

Alternatives and Evidence



Develop and compare feasible alternatives with targeted analyses and evidence

Formal Determination



Documented, risk-informed determination on an acceptable solution

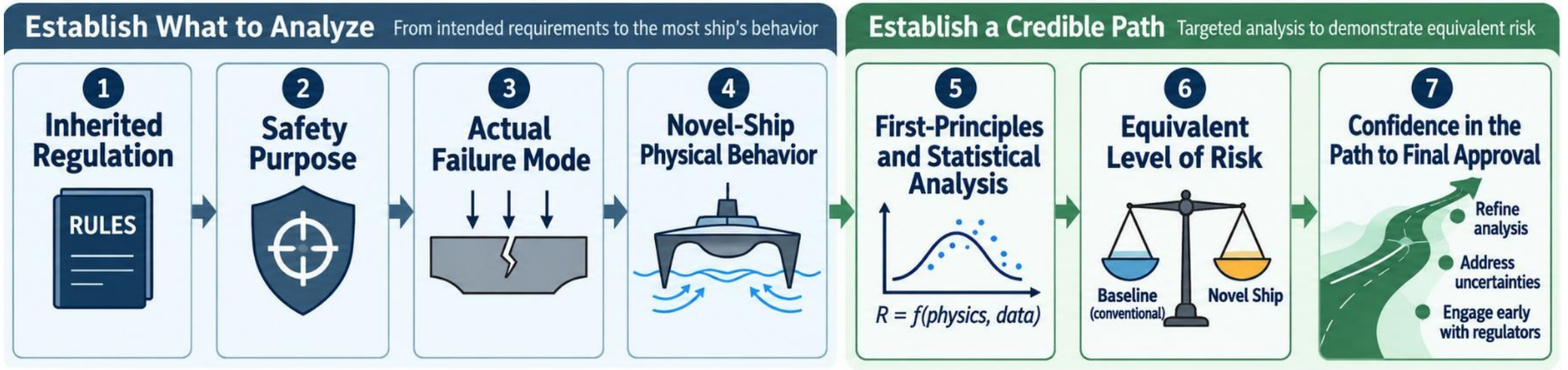
Establish a Predictable Basis for Design Assurance

- Safety and environmental protection are governing requirements—not quantities to trade against cost or schedule.
- Establish a suitable combination of standards, criteria, first-principles analyses, and approval methods for the actual design.
- Use mission requirements, cost, schedule, and producibility to shape a design-assurance process that can be carried out predictably.
- Achieve a narrower range of variation in:
  - the work leading to validation; and
  - the final validation and approval result.



Early Focused Analysis Establishes the Path

- Use the inherited safety purpose as a starting point—not its method.
- Analyze the actual failure mode and physical behavior of the novel ship.
- Use first principles unless it is clear inherited criteria are representative.
- Establish confidence in the path to final approval; do not finish the entire analysis early.
- Compare the result with an equivalent level of risk and control risk creep.

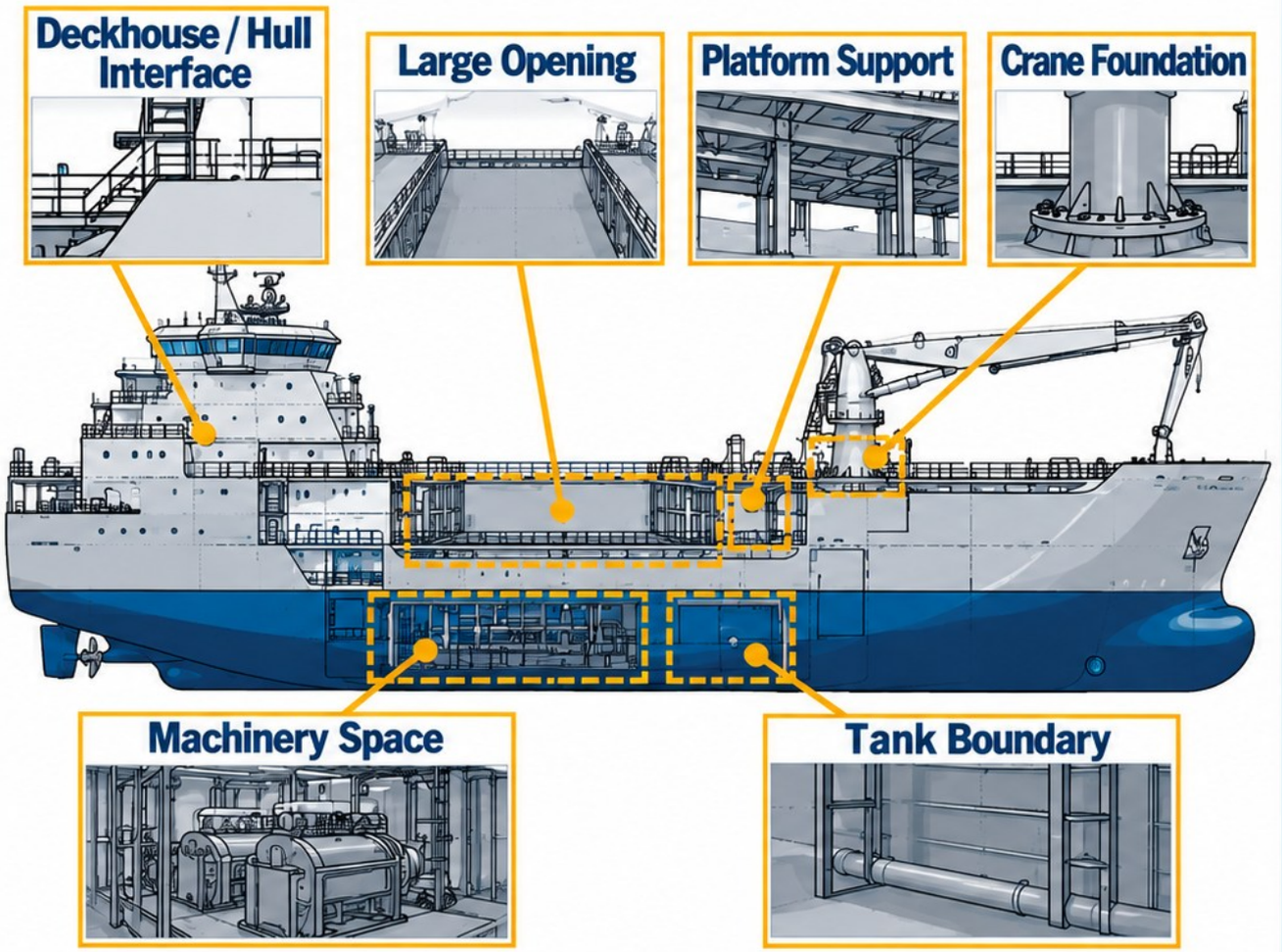


Types and Scope of Early Focused Analyses

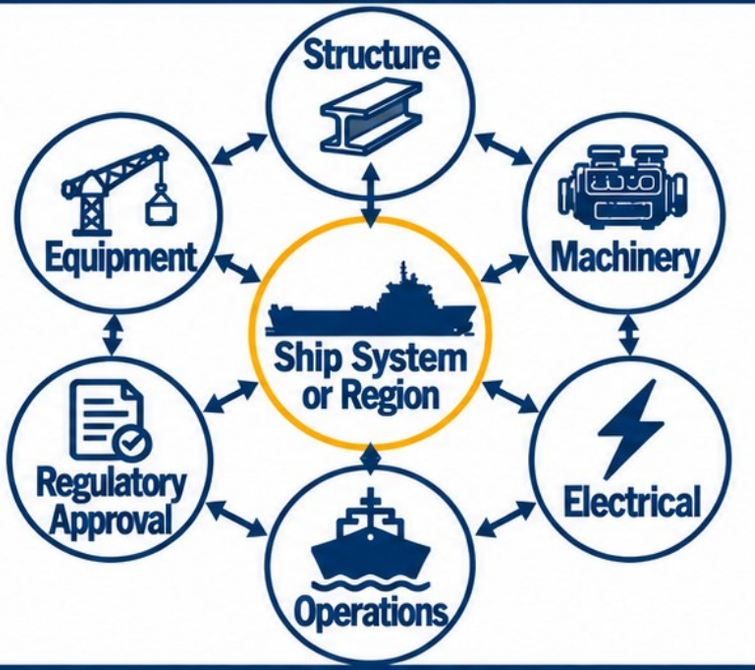
Decision need	Suitable early approach	Validation provided	What it does not establish
Concept viability	Bounding calculation or screening study	Whether a credible solution appears possible	Final compliance
Governing behavior	Regional or topical analysis	Likely controlling mode or region	Complete integrated response
Input sensitivity	Sensitivity or range study	Which assumptions matter most	A definitive single value
Configuration comparison	Consistent comparative model	Relative strengths and weaknesses	Final production design
Criteria applicability	Rule-intent review plus focused analysis	Whether inherited assumptions remain credible	Automatic regulatory acceptance
Final validation	Integrated higher-fidelity analysis	Detailed response and required cases	Requires mature inputs

How do we Focus the Analysis?

1. Ship Regions and Key Features



2. Cross-Disciplinary Interfaces



A Focused Analysis Can Be:

Geographic



Analyze a specific region (e.g., large opening)

Topical



Analyze a specific topic (e.g., machinery, structure)

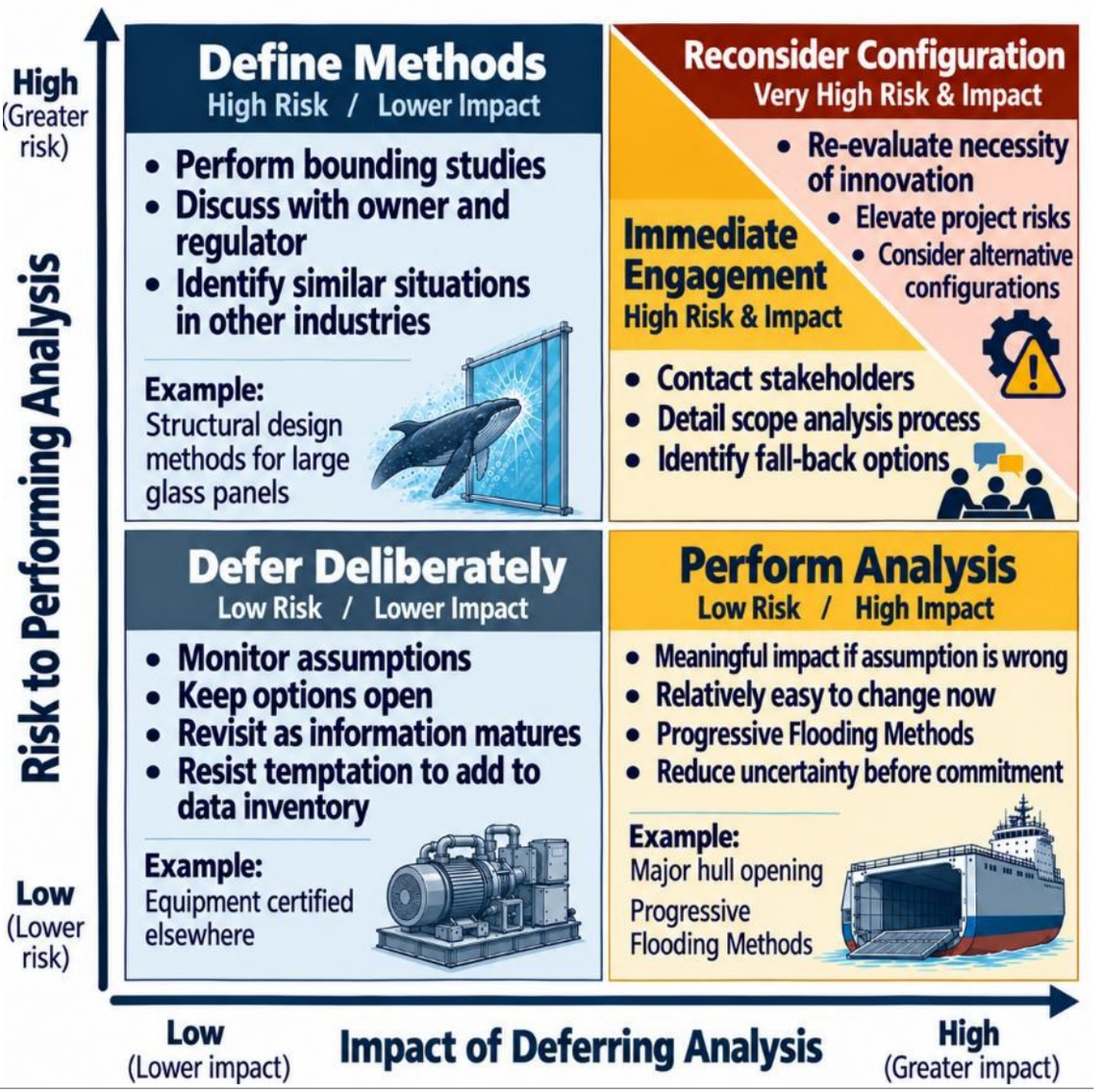
Cross-Disciplinary



Analyze interfaces across disciplines

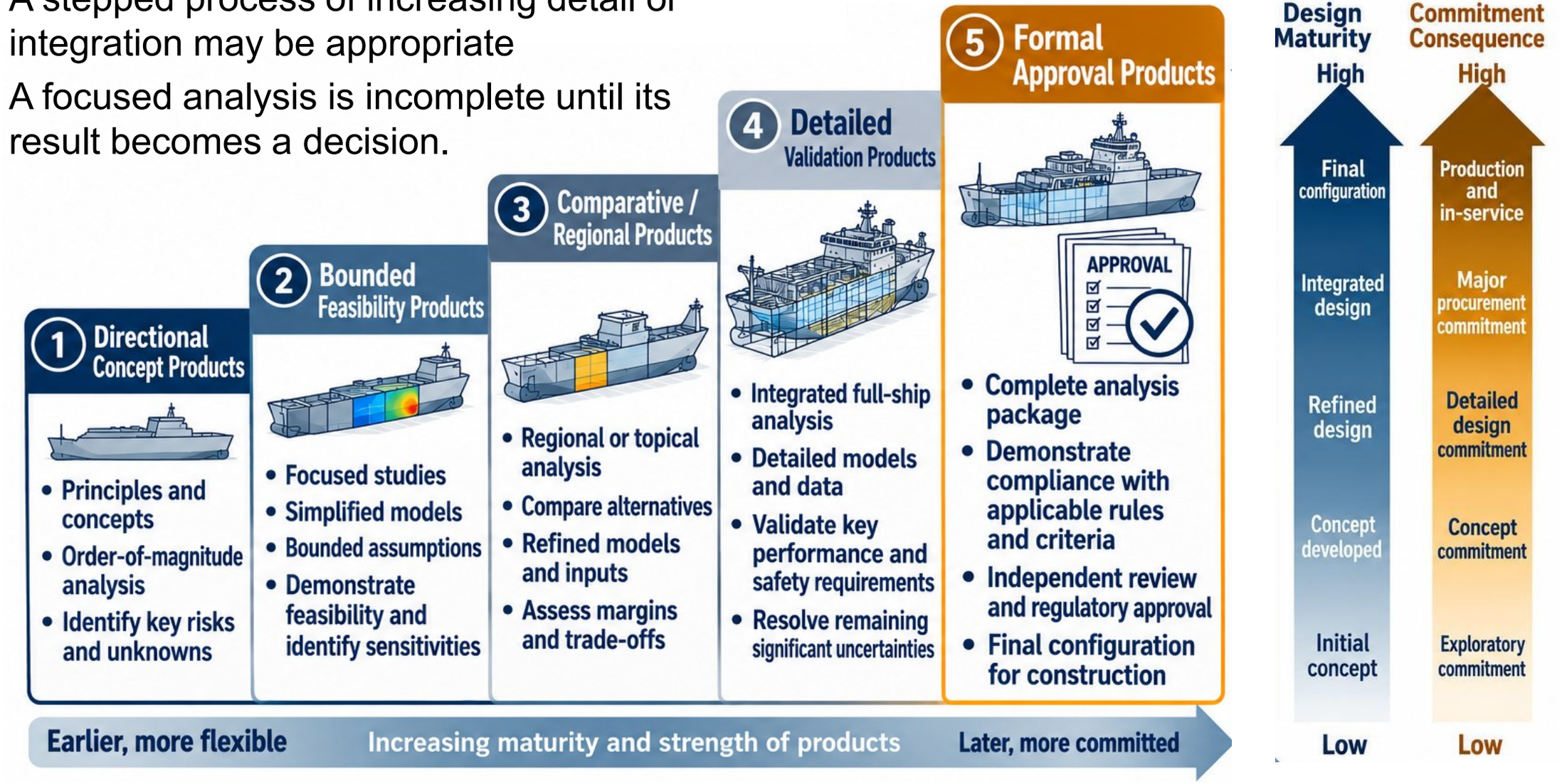
What to Analyze? Configuration Triage

- **Risk to performing the analysis:** How difficult is it to obtain and interpret a reliable answer?
  - Higher risk means more effort to establish method
- **Impact of deferring the analysis:** What decisions or future work could be affected?
  - High impact makes taking action early much more important.
- Also consider the consequence, confidence in the information, ease of later change, and cost of delay.
- If an issue is deferred, record why, what information is needed, and when it will be revisited.
- New analysis needs will emerge as the design, assumptions, and interfaces mature.



A Maturity Ladder for Focused Analysis

- A stepped process of increasing detail or integration may be appropriate
- A focused analysis is incomplete until its result becomes a decision.



Mission-Driven Stability and Damage Stability

Loading Condition

- Cargo deck significantly submerged
- Ballasted down for cargo transfer
- Reduced freeboard

Cargo Transfer

- Float-on / float-off
- Heavy lift cargo between pontoons
- Ballasted to operating draft



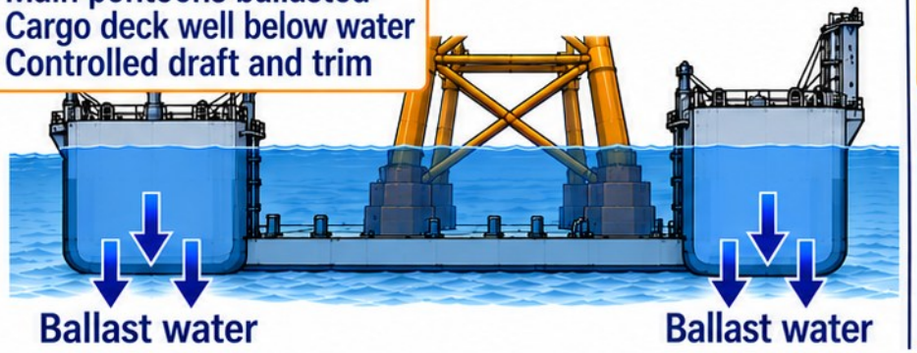
Controlled Operating Area

- Sheltered or restricted location
- Limited sea-state exposure
- Tug support
- Operating restrictions on wind, waves, current, and traffic



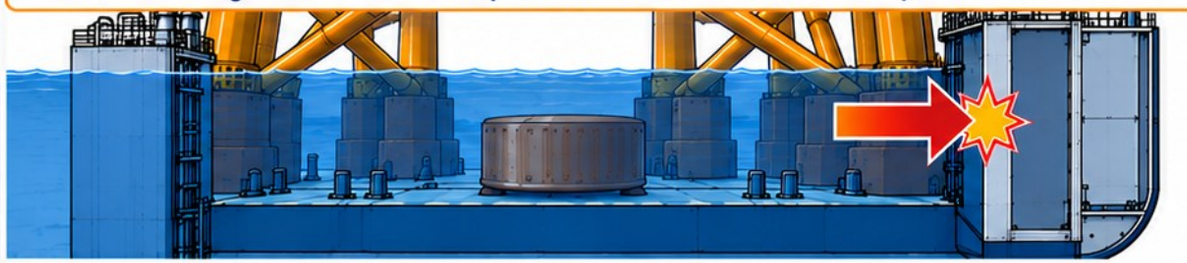
Ballast Condition

- Main pontoons ballasted
- Cargo deck well below water
- Controlled draft and trim

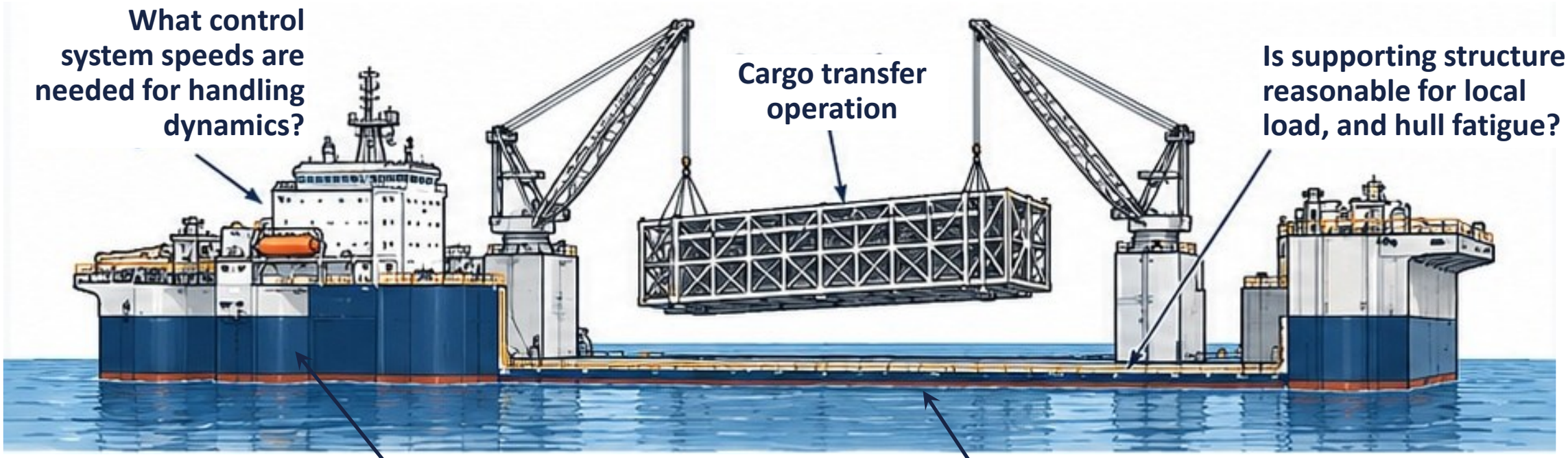


Horizontal Cargo Impact on Pontoon and Double-Hull Protection

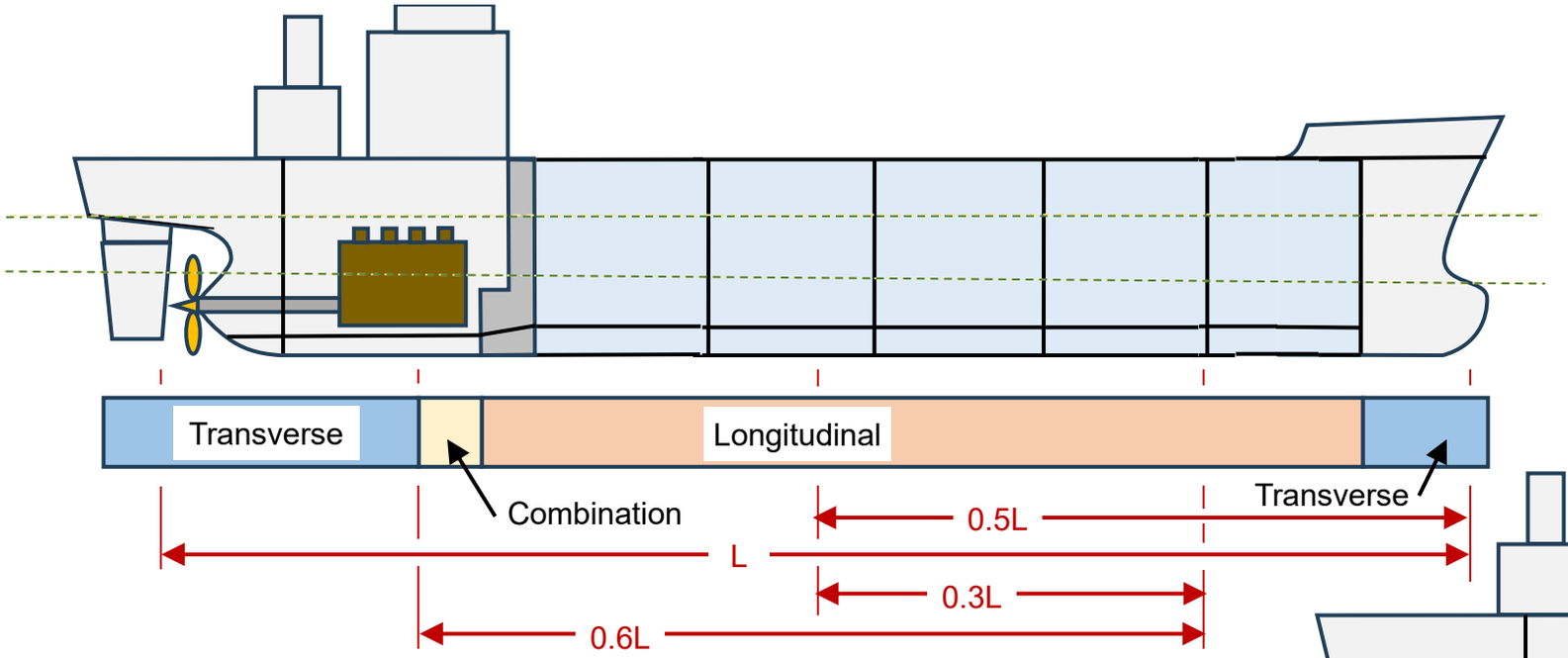
- Cargo between pontoons can move during transfer or an accident
- Double hull (outer and inner hull) provides full-height protection from cargo impact and breach
- Limits flooding to the double-hull space and reduces risk to critical spaces

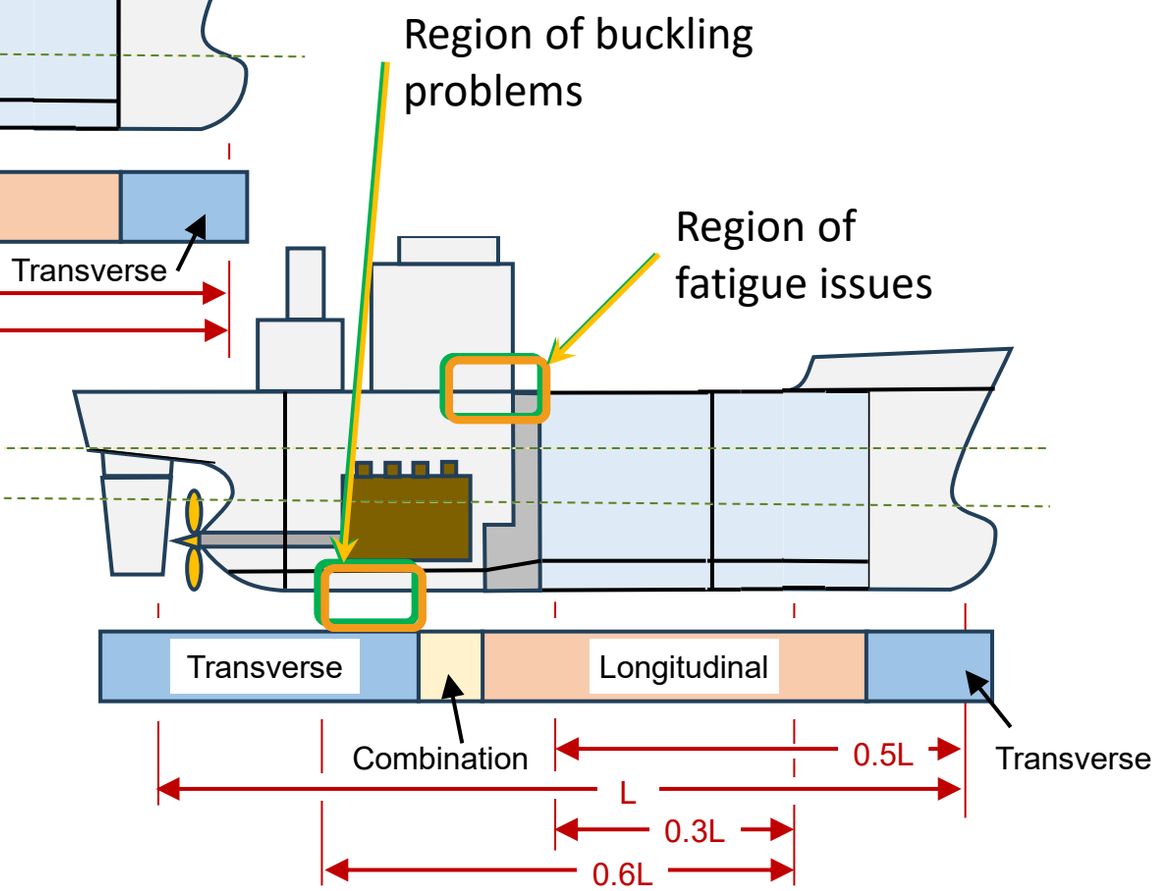


May Need Multiple Analyses For a Single Activity



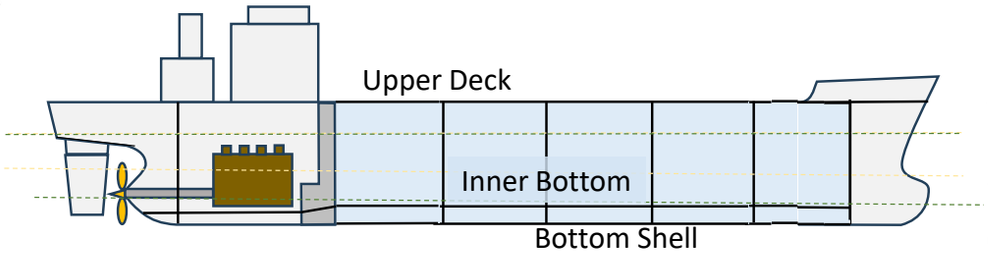
Simple Differences Can Prompt Early Focused Analysis



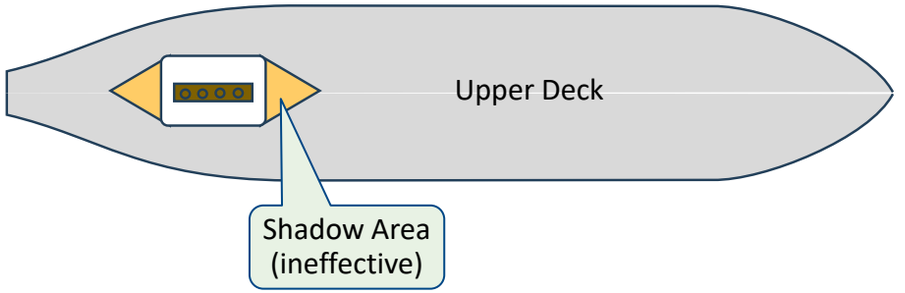


- Taking all the parallel midbody out of a tanker but leaving the scantlings may seem simple and low risk
- Early focused analysis can reveal problems caused by initial assumptions

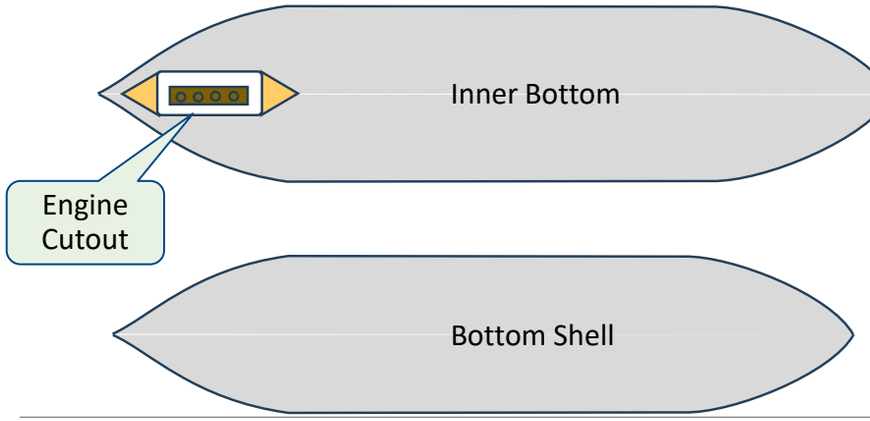
Conversion Arrangements can Prompt Early Focused Analysis



Upper Hull Girder



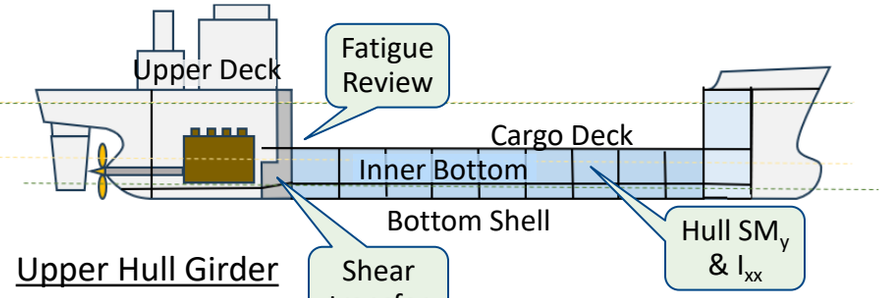
Lower Hull Girder



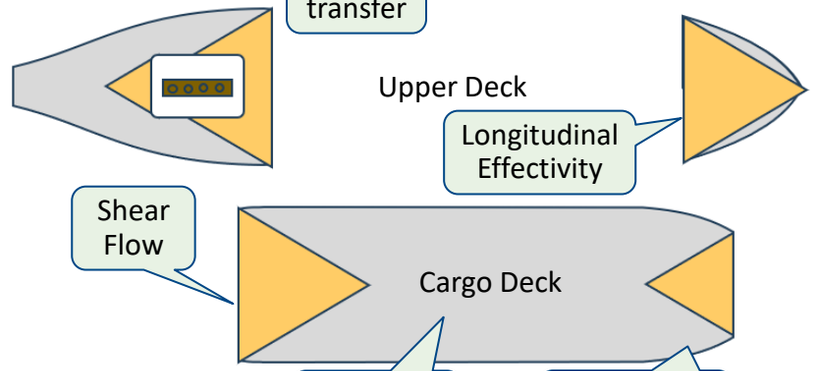
Conversion of a tanker to a heavy lift ship forces relocation of the upper strength deck.

Traditional regulations apply shadow areas of ineffective structure, nearly detaching the ends of the hull.

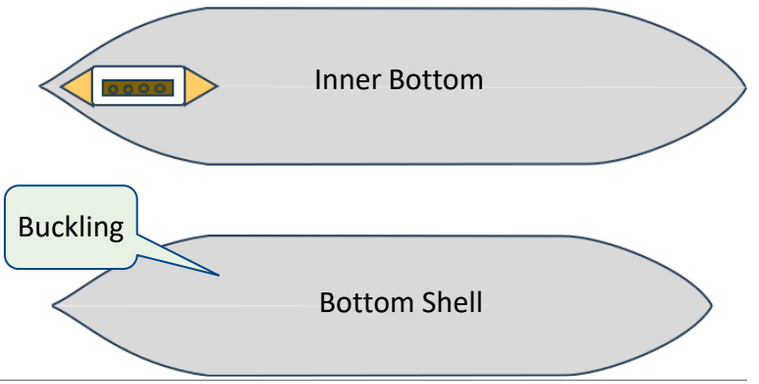
Early Focused Analysis helps to investigate all of these issues and more.



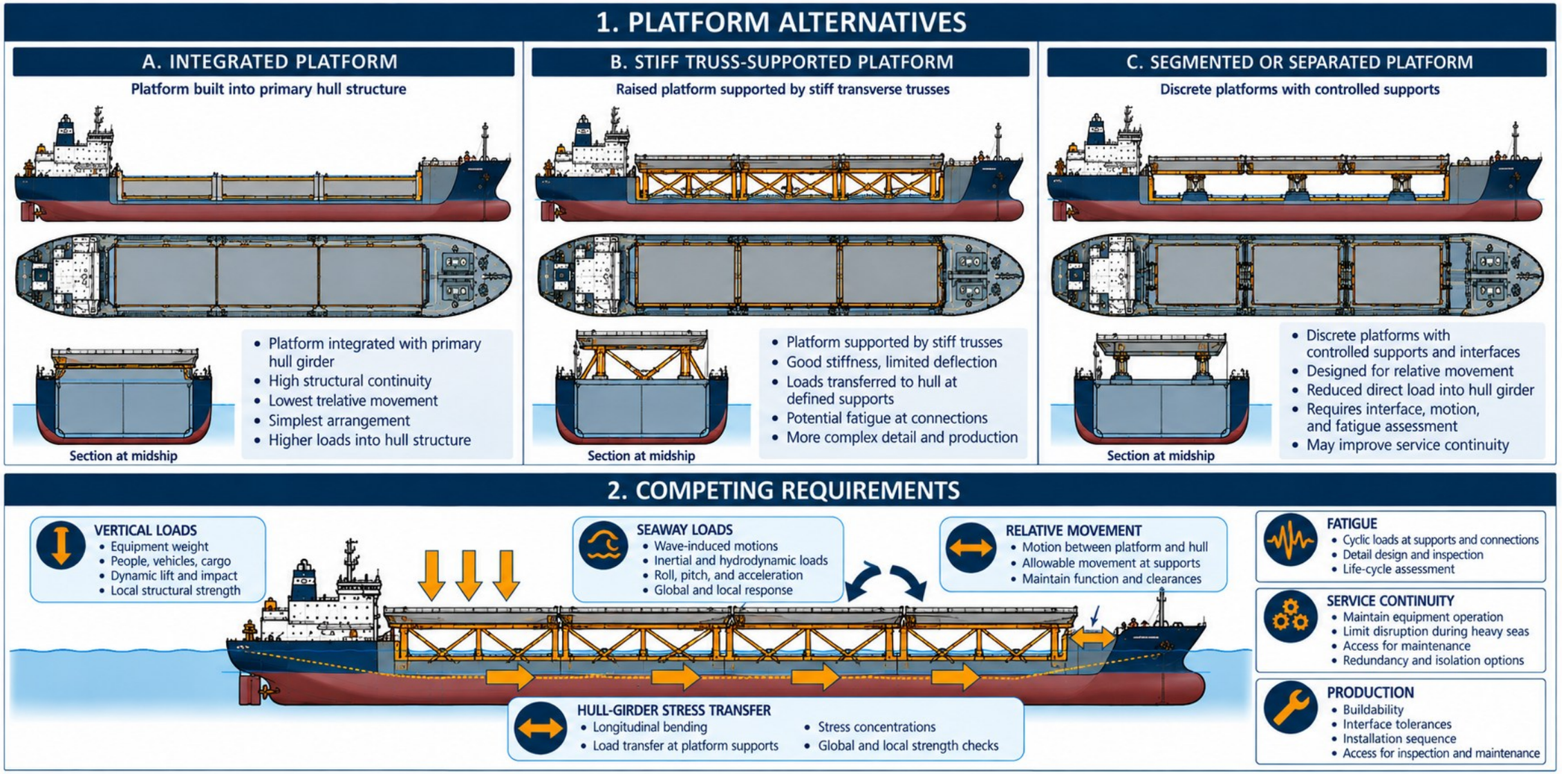
Upper Hull Girder



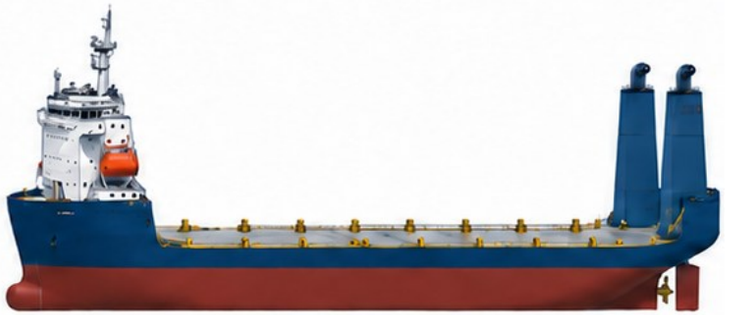
Lower Hull Girder



Added Platforms, Buckling, Fatigue, and Vibration



Same Ship, Different Missions, New Focused Analysis

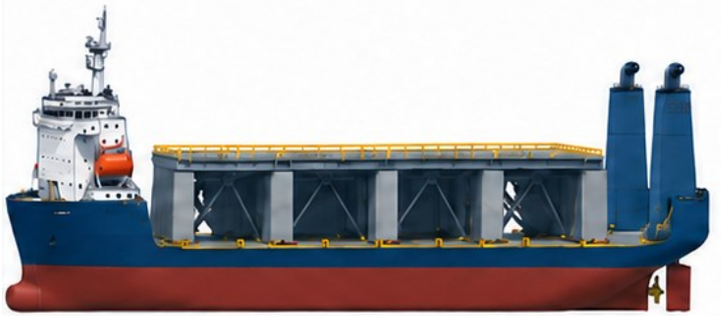






As a semi-submersible heavy lift ship, it must carry both distributed loads and a wide variety of moderate point loads. Both of these could be Early Focused Analyses.

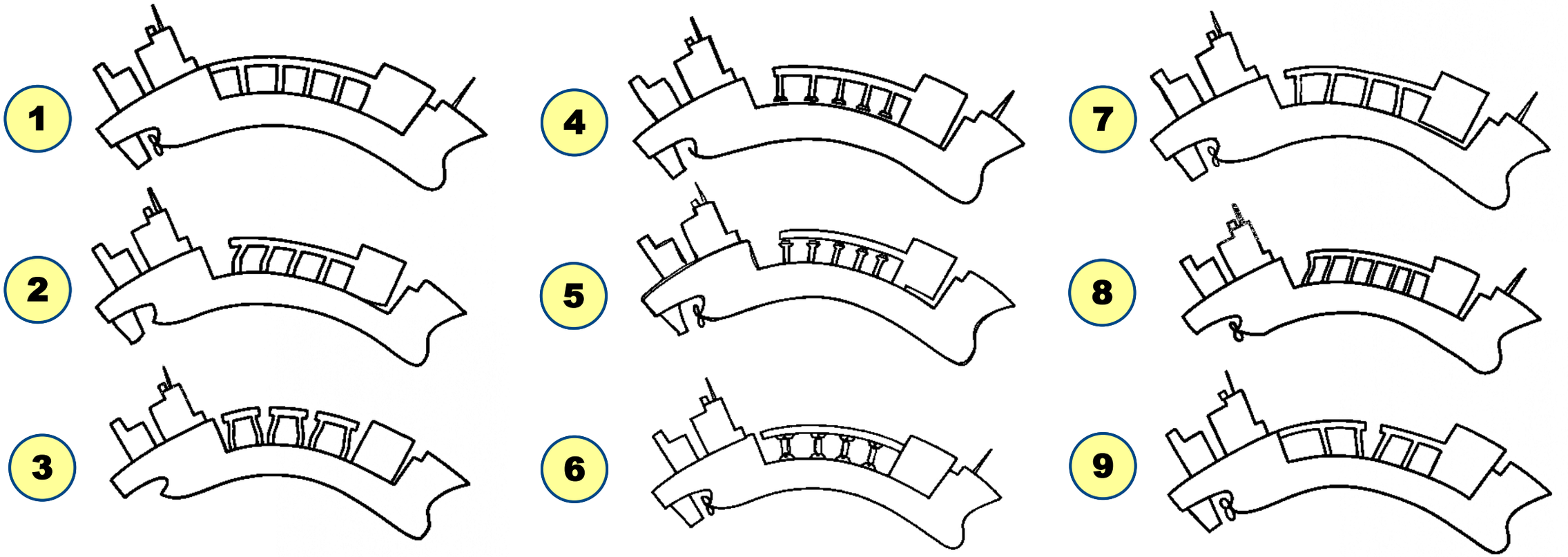
Conversion to an Offshore Support Vessel with raised platforms could mean a variety of different load paths depending on the internal strength and attachment of the platforms







Early Analyses May Shape How to Apply Rules

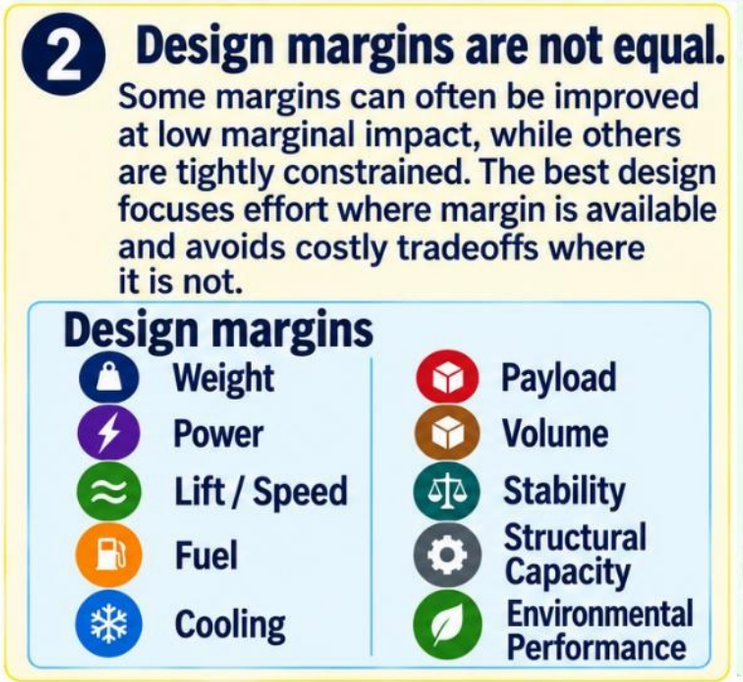


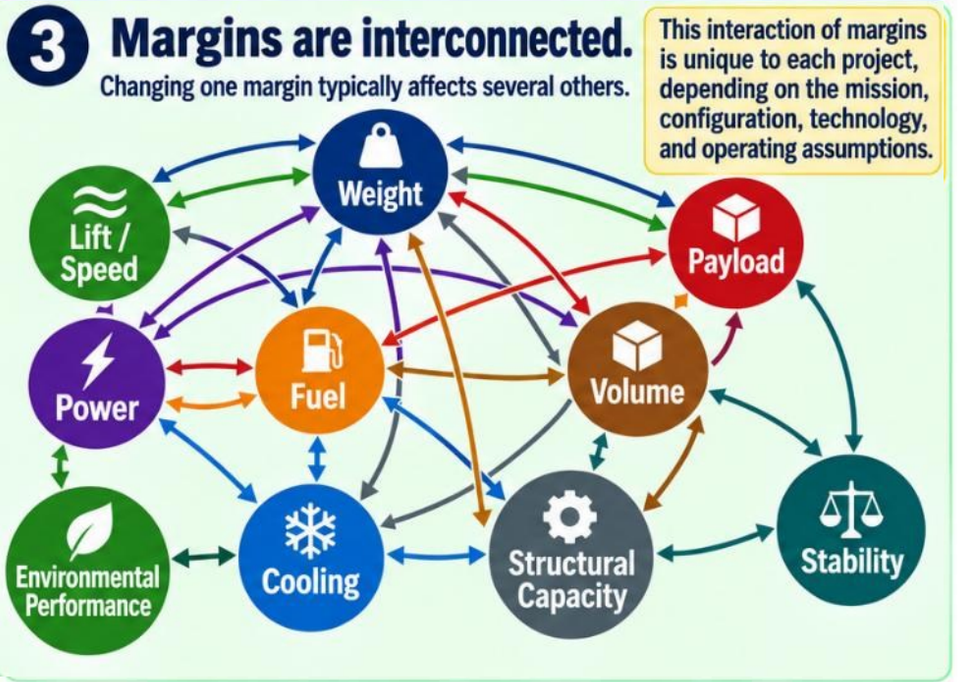
Early Focused analysis can find a way to resolve which configuration is ideal, and provide the data to satisfy the review authority with how to apply the rules. It can also tell which pill is too much to swallow.

Robust Solutions and Working for Margins

- Novel designs may be close to important limits; large margins everywhere may not be practical.
- Look for margin that is cheap to add without harming mission, schedule or other performance.
- Understand system exchanges: weight, power, volume, stability, fuel, and cooling can support one another.
- Hold available margin during analysis and validation; do not spend it too early.
- Remaining margin becomes useful capacity for the owner and operator

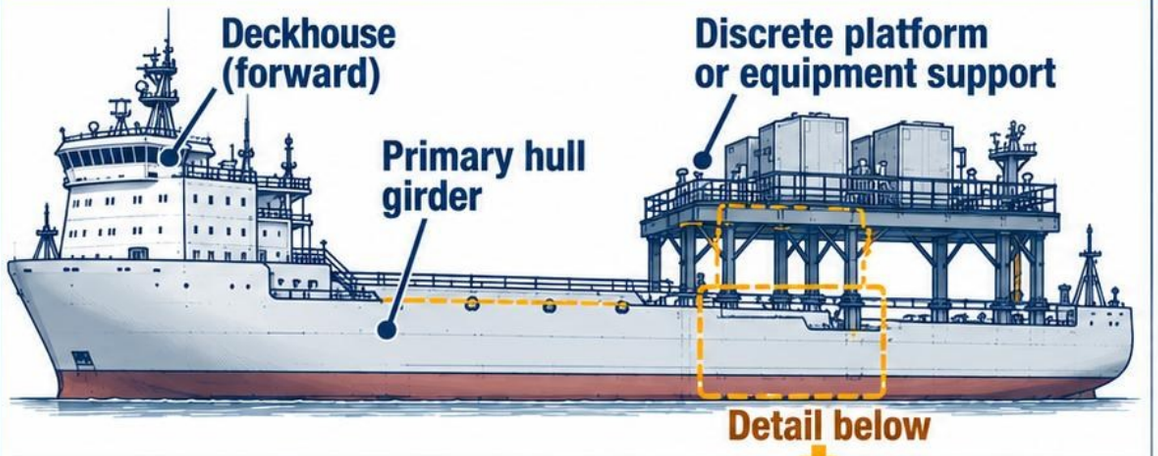




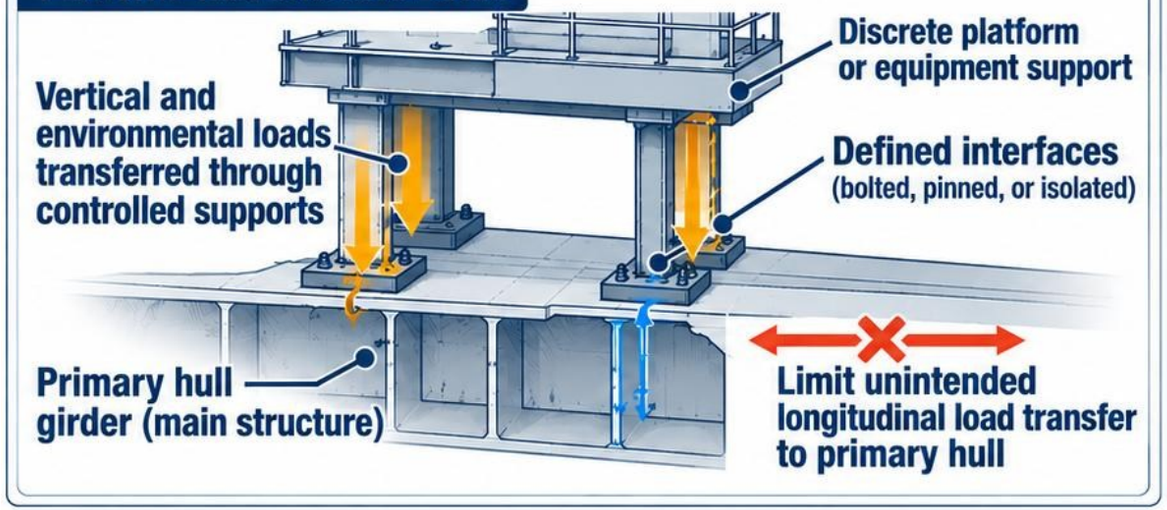


Strategic Separation

1 Separated Feature – Discrete Platform with Controlled Interfaces



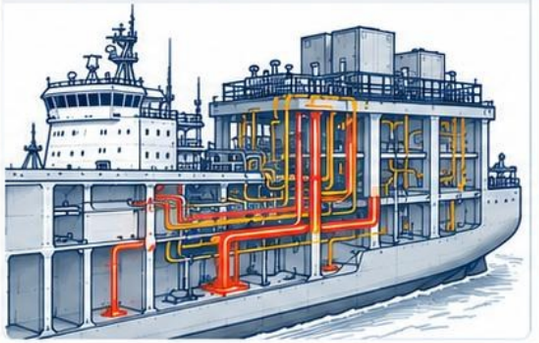
Platform–Hull Interface Detail



2 Change Propagation – Integrated vs. Separated Feature

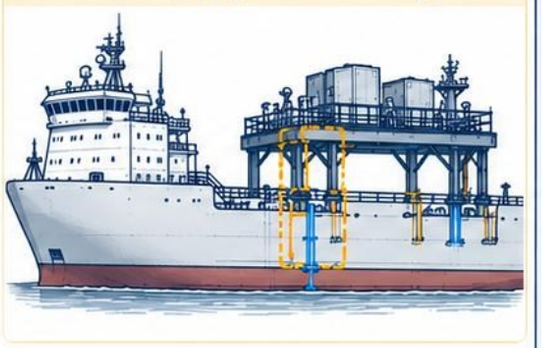
Integrated Feature

A change can propagate through many systems and production activities.

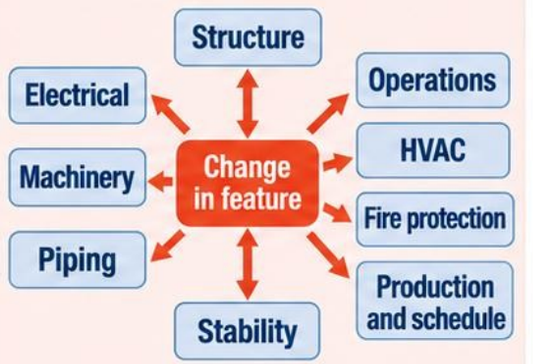


Separated Feature

A change is contained at defined interfaces with limited propagation to other systems.



Many systems affected

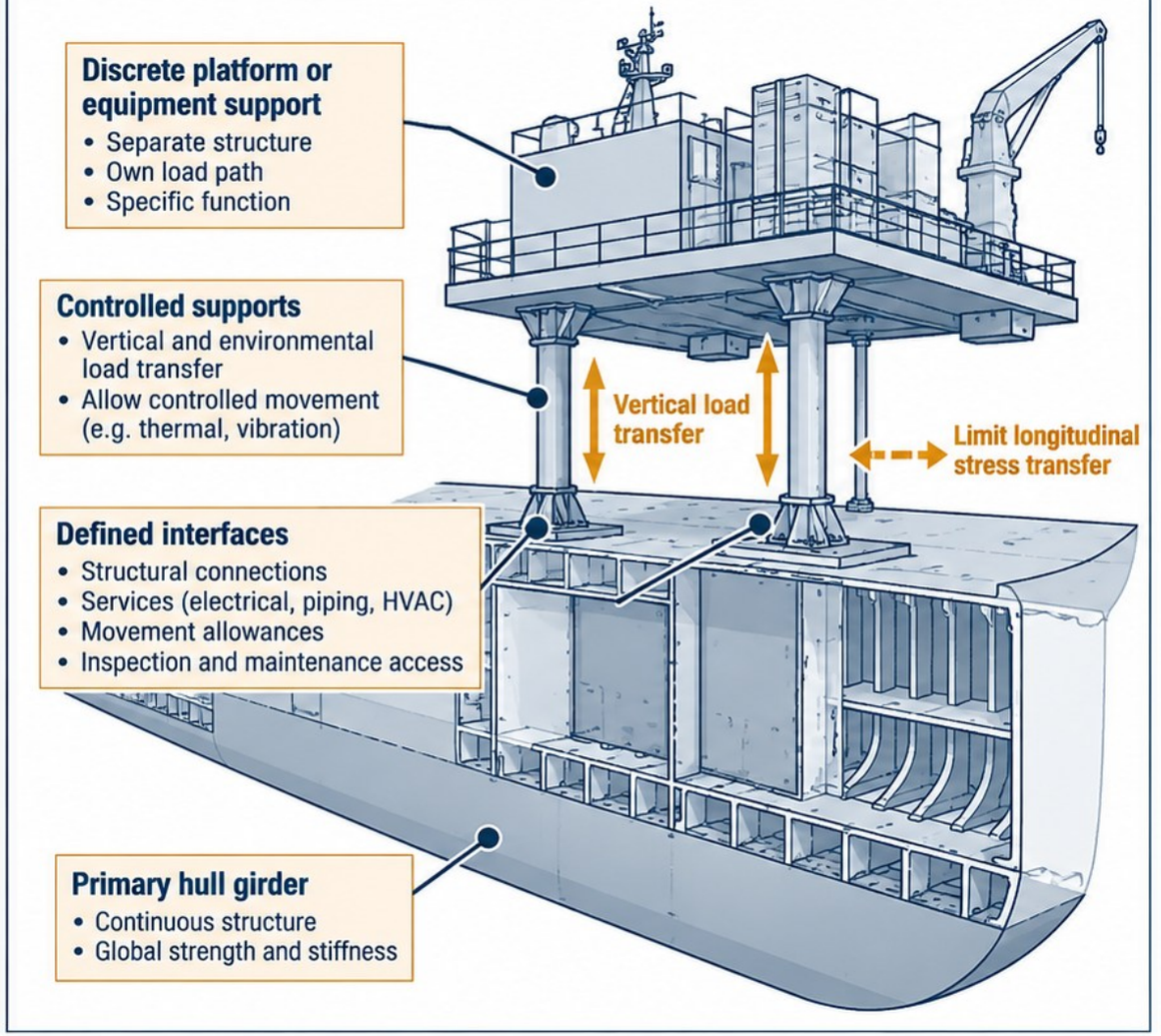


Change contained at interfaces



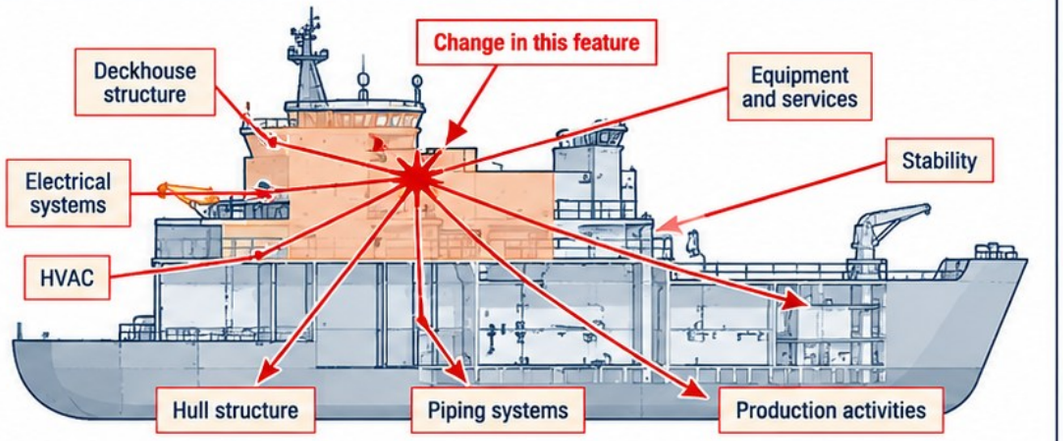
Another View of Strategic Separation

1. Separated Feature – Discrete Platform or Equipment Support

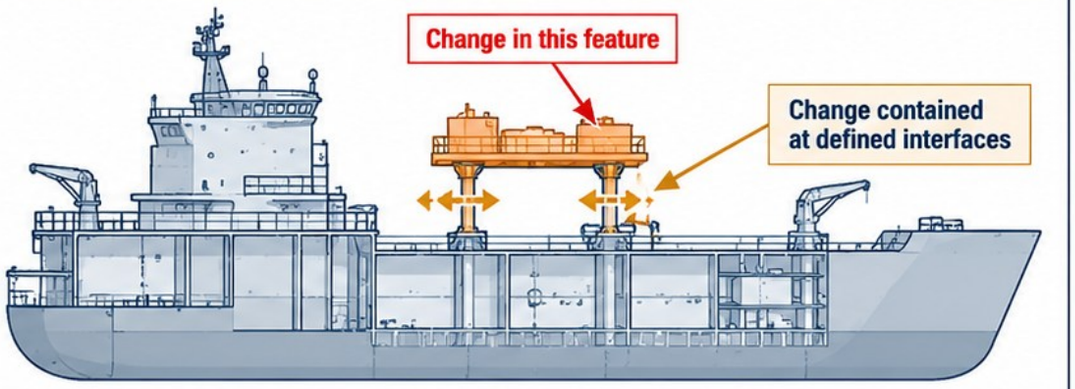


2. Change Propagation – Integrated vs. Separated Feature

Integrated Feature – Change Spreads Through Many Systems

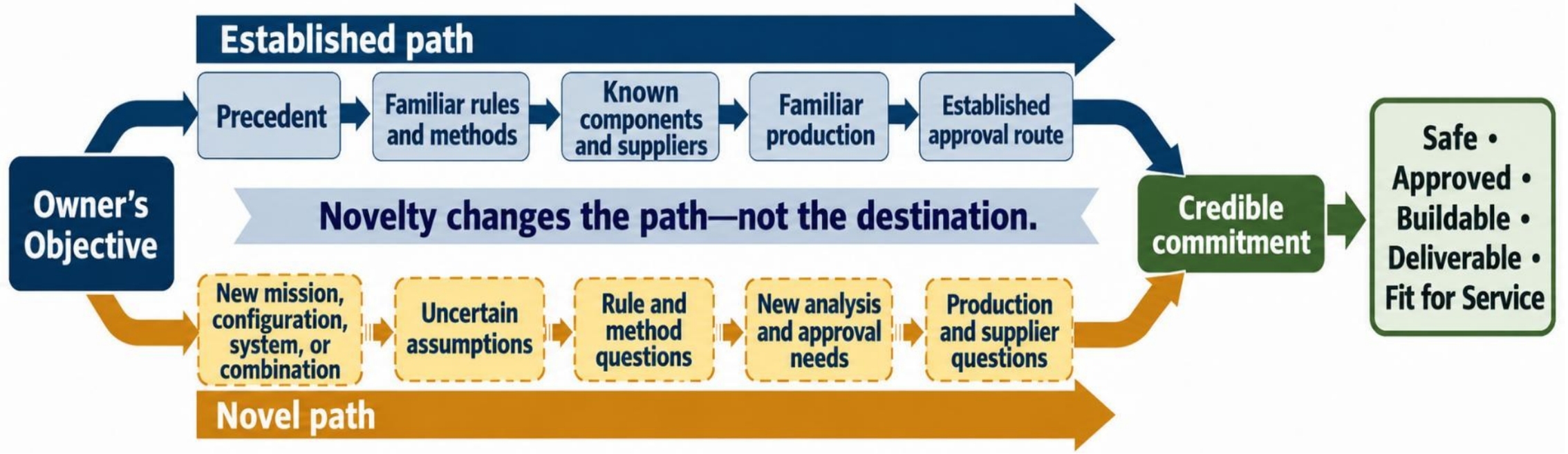


Separated Feature – Change Contained at Defined Interfaces



What Novelty Changes

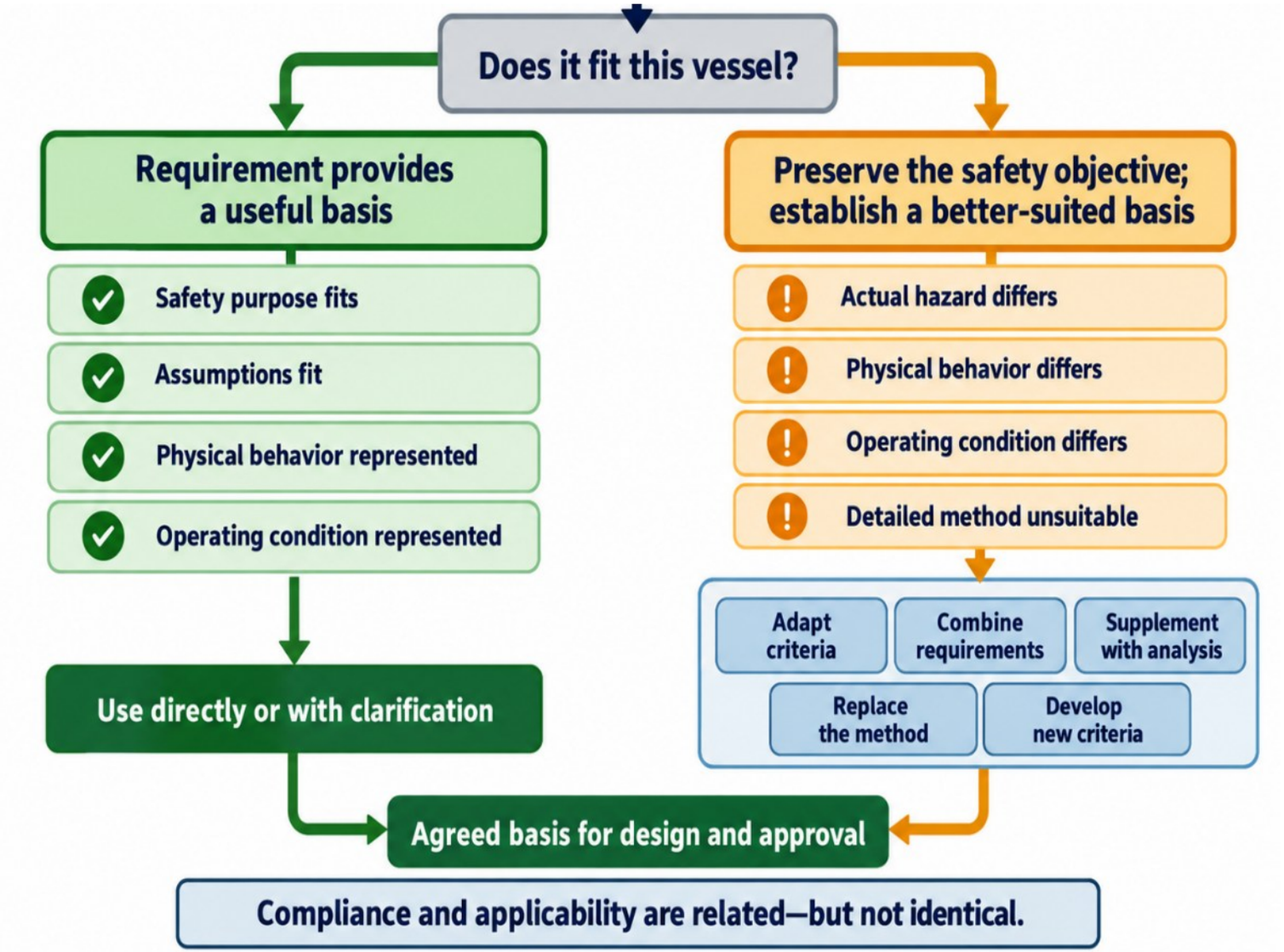
- Conventional ships often benefit from established rules, methods, components, and production experience.
- Novel ships may challenge the assumptions behind those established paths.
- The ship still must be safe, approvable, buildable, deliverable, and fit for service.
- The project must establish the uncertain parts of the path before making firm commitments.



- Innovation is not the problem; unmanaged novelty is.

Use the Inherited Basis Deliberately

- Established rules and standards remain the starting point for most ships—and much of many novel ships.
- Compliance with a requirement does not prove that the requirement represents the actua vessel.
- Test the safety purpose, assumptions, physical behavior, and operating condition.
- Keep the safety objective; adapt the technical basis when the inherited method does not fit.
- Use the simplest suitable combination of standards, criteria, analysis, and approval approach.



Establish the Path Before Commitment



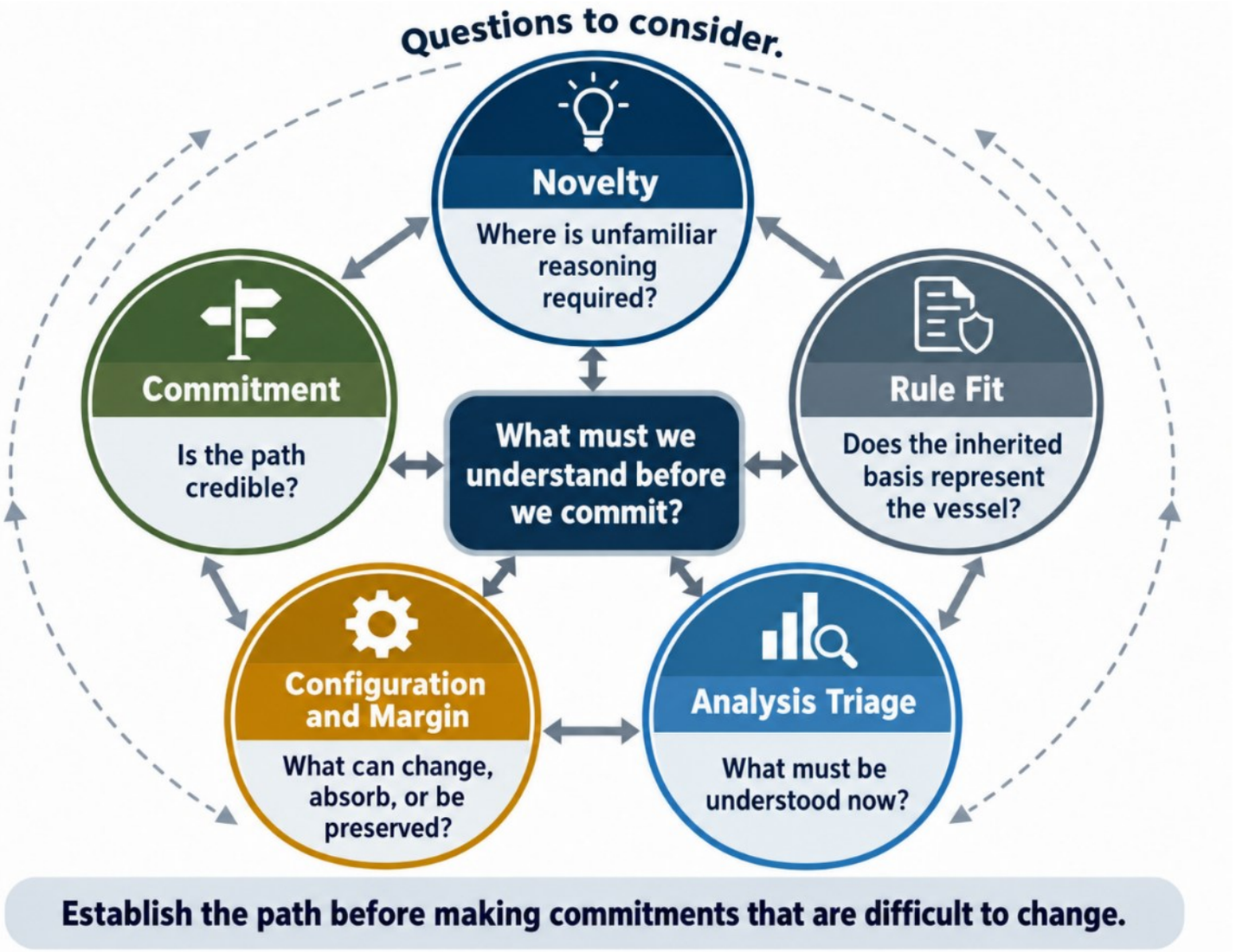
- Identify the uncertainties that could change the configuration, approval path, production plan, cost, schedule, or mission.
- Use focused analysis and early engagement to resolve the questions that matter most.
- Preserve alternatives while the technical basis is still developing.
- Match the strength of the commitment to the maturity of the design and approval path.
- Commit more firmly as confidence increases.

Do not begin a major voyage of discovery after fixing the delivery promise.

Judgment Under Pressure

- Tools should improve judgment, not replace it.
- **Novelty prompt:** Where does the design require unfamiliar reasoning?
- **Applicability check:** Does the inherited basis represent this vessel?
- **Focused-analysis triage:** What must be analyzed now, and what can wait?
- **Commitment check:** Is the price, schedule, approval path, and production basis credible?

If the path is not understood, preserve options and do the work that can change the decision.



A Bright Future for Your Innovative and Novel Design!



Moderately Large Cetacean Carrier (MLCC)



contact@airglide.ai

Our Company

AirGlide AI is a maritime technology company applying artificial intelligence, computational fluid dynamics (CFD), and naval architecture expertise to improve vessel performance, utilizing its revolutionary patented Air Layer Drag Reduction System (ALDR). This 21st century technology is far superior to legacy Air Lubrication Systems (ALS) of the 20th century. AirGlide AI, in collaboration with multiple leading research institutions, utilized its own Boundary Layer Testing Lab to recreate real-world hydrodynamic conditions to test and refine proprietary patented new air delivery unit designs utilizing ALDR principles.

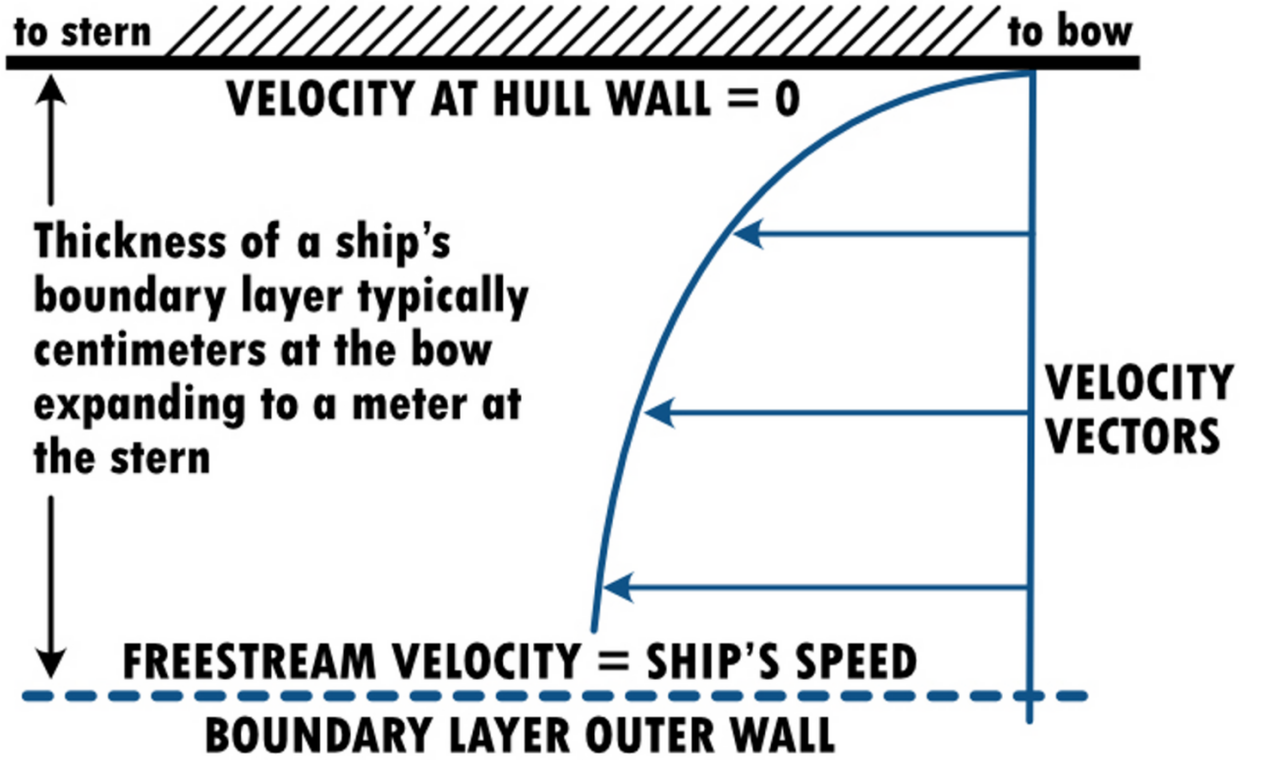
Our intellectual property portfolio is comprised of a robust mix of U.S. and international patent protections across three core pillars. More than 100 unique patent applications have been filed, with multiple patents granted and others pending worldwide, covering hydrodynamic testing methods, advanced software and artificial intelligence systems, and proprietary hydrodynamically efficient hardware, including specialized air-release technologies.

www.airglide.ai



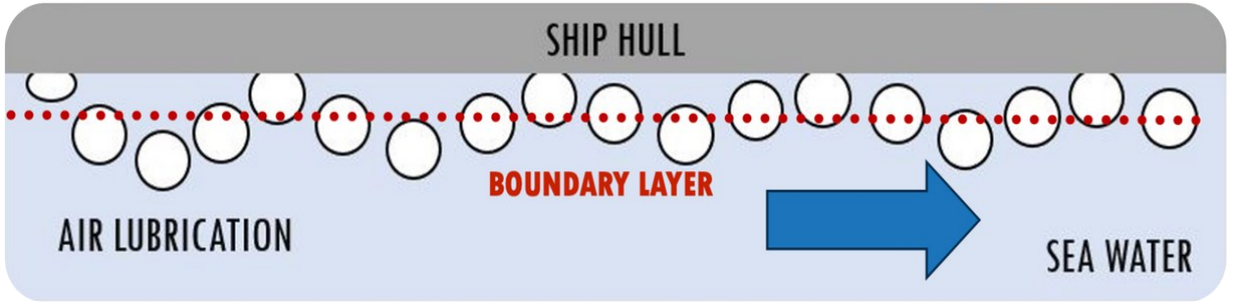
SHIP HULL BOUNDARY LAYER THICKNESS

ALS reduces frictional drag only while the air resides in the thin boundary layer

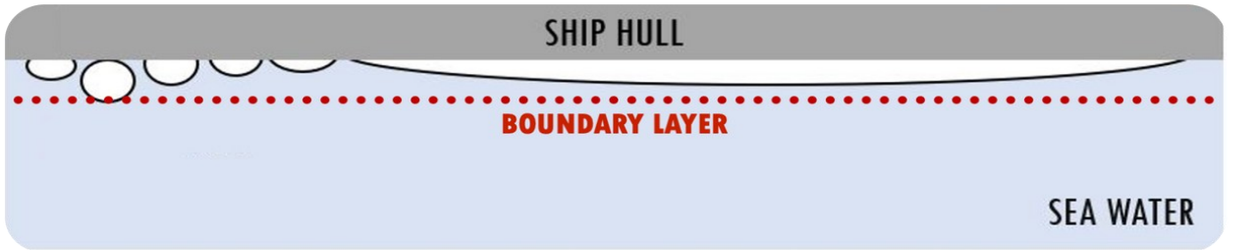


AirGlideAi

AIRGLIDE Ai's ENHANCED ALDR



Turbulent flows generate significantly greater drag than laminar flows



Air Layer Drag Reduction has much higher frictional drag reduction potential than Bubble Layer Drag Reduction according to numerous scientific studies

AirGlideAI

Kelvin-Helmholtz Instability

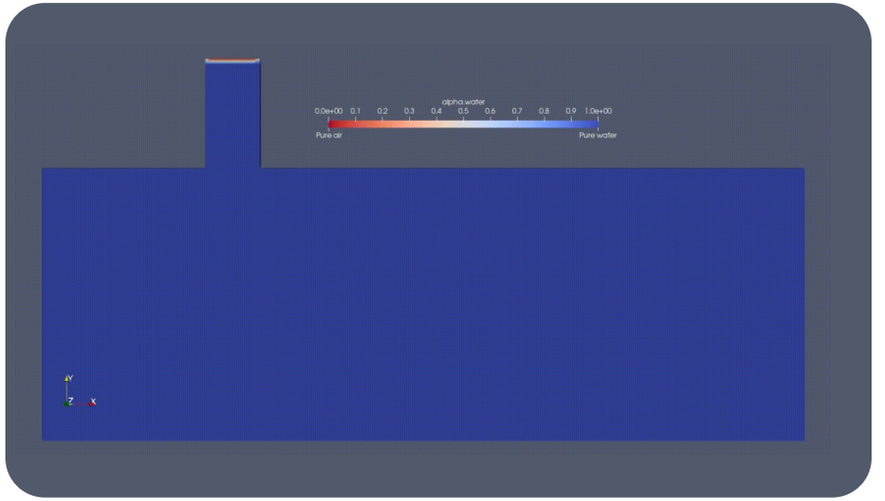


AirGlideAI

contact@airglide.ai

Boundary Layer Testing Lab Confirms Computational Fluid Dynamics (CFD) Simulations

KELVIN–HELMHOTZ INSTABILITY LEGACY DESIGNED ALS SYSTEMS NOZZLE DESIGN (LESS EFFICIENT, CREATES TURBULENCE DRAG) DEPLOYED ON OVER 200 SHIPS



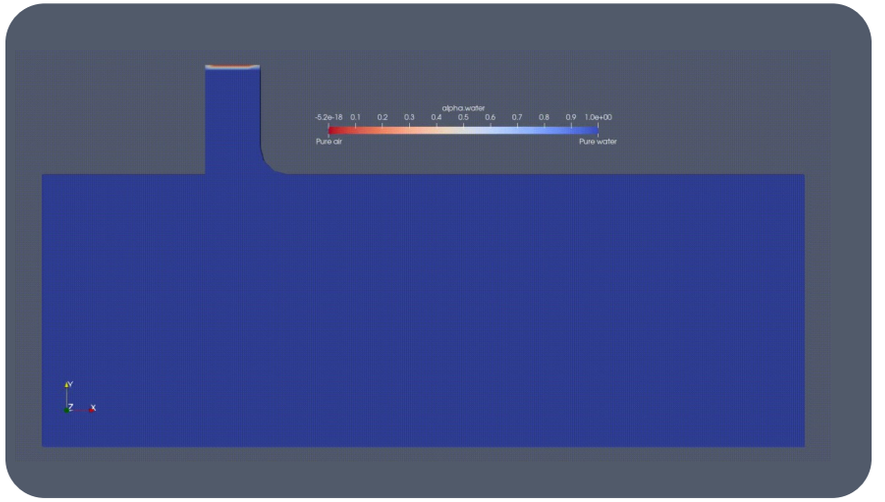
Kelvin-Helmholtz Instability

AIR LAYER DRAG REDUCTION (MOST EFFICIENT, NEAR–LAMINAR FLOW)

ENHANCEMENT OF LEGACY ALS TO ALDR

DEPLOYED ON LARGEST CRUISE SHIP IN THE WORLD

INCREASED EFFICIENCIES OVER 2X



AirGlide AI Air Layer Near-Laminar Flow

PATENT No: US 12,263,914 B2



BOUNDARY LAYER TESTING LAB (BLT)

contact@airglide.ai

BOUNDARY LAYER TESTING LAB

AirGlide AI has the only industry Boundary Layer Testing Lab, where different hull conditions can be replicated and analyzed to optimize nozzle design and air flow rate.

ROLE

Empirical Data Collection: Using various nozzle designs, the BLT Lab measures shear stress reduction to provide accurate data under controlled conditions.
Model Refinement: The empirical data are integrated back into CFD models to refine predictions and improve reliability.

AirGlideAI

Boundary Layer Testing Lab has Produced Several Significant Patents

contact@airglide.ai

US012263914B2

(12) **United States Patent**
Poe et al.

(10) **Patent No.: US 12,263,914 B2**
(45) **Date of Patent: Apr. 1, 2025**

(54) **SYSTEM AND METHOD FOR DELIVERING AIR TO A SUBMERGED SHIP SURFACE**

(71) Applicant: **John Dixon**, Fort Lauderdale, FL (US)

(72) Inventors: **Richard Poe,** Ft. Lauderdale, FL (US); **John Dixon,** Ft. Lauderdale, FL (US)

(73) Assignee: **Airglide, AI. Inc**, Tulsa, OK (US)

(*) Notice: Subject to any disclaimer, the term of this patent is extended or adjusted under 35 U.S.C. 154(b) by 0 days.

(21) Appl. No.: **18/219,375**

(22) Filed: **Jul. 7, 2023**

(65) **Prior Publication Data**

US 2024/0166306 A1 May 23, 2024

Related U.S. Application Data

(63) Continuation of application No. 18/119,324, filed on Mar. 9, 2023.

(60) Provisional application No. 63/427,144, filed on Nov. 22, 2022, provisional application No. 63/439,306, filed on Jan. 17, 2023, provisional application No. 63/454,549, filed on Mar. 24, 2023.

(51) **Int. Cl.**
B63B 1/38 (2006.01)
B63B 59/04 (2006.01)

(52) **U.S. Cl.**
CPC ***B63B 1/38*** (2013.01); ***B63B 59/04*** (2013.01); *B63B 2001/387* (2013.01)

(58) **Field of Classification Search**
CPC B63B 1/38; B63B 2001/382; B63B 2001/385; B63B 2001/387; B63B 59/04
See application file for complete search history.

(56) **References Cited**

U.S. PATENT DOCUMENTS

725,137	A *	4/1903	Quannone	B63B 1/38 114/67 A
900,296	A *	10/1908	Motheral	B63B 1/38 114/67 A
1,254,892	A *	1/1918	Elniff	B63B 1/38 114/67 A
1,408,178	A *	2/1922	Downing	B63H 19/06 114/67 A
2,849,941	A *	9/1958	Negoro	B60H 1/249 454/120
3,680,517	A *	8/1972	Morrison	B63B 1/38 114/67 A
5,389,022	A *	2/1995	Kobayashi	B63H 21/32 440/89 R

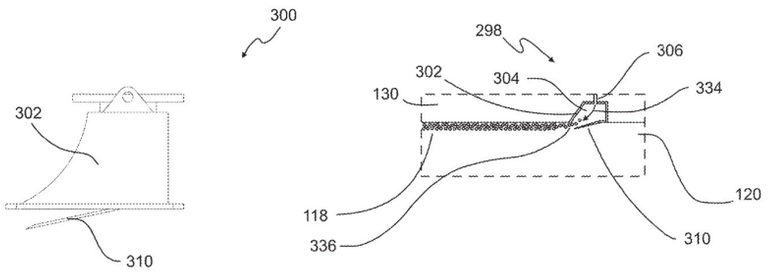
(Continued)

Primary Examiner — Ajay Vasudeva
(74) *Attorney, Agent, or Firm* — Origins Law, LLC; Nicholas Spatola

(57) **ABSTRACT**

This invention introduces a unique two-piece nozzle used to provide air to the hull bottom of a ship, reducing the drag of water friction while in motion. The unique base assembly will mount flush in the bottom portion of a hull of a ship, creating no additional drag when closed. The unique interchangeable and modular nozzle design will allow for maintenance and or development of various designs in the water, without requiring a drydock visit. A flap portion of the nozzle insert will open when air is supplied, releasing small air bubbles to a ship's hull. The flap portion of the nozzle insert may incorporate various materials and passive closing schemes to adjust the air plastron. The present invention creates and maintains an air curtain, called plastron, delivering air underneath a ship hull through an array of nozzles.

26 Claims, 22 Drawing Sheets



AirGlideAI

BOUNDARY LAYER TESTING SYSTEM WITH ENHANCED ENTRY REGION FOR ANGULATED SURFACES

contact@airglide.ai

US012680907B2

(12) **United States Patent**
Bell et al.

(10) **Patent No.: US 12,680,907 B2**
(45) **Date of Patent: Jul. 14, 2026**

(54) **BOUNDARY LAYER TESTING SYSTEM WITH ENHANCED ENTRY REGION FOR ANGULATED SURFACES**

(71) Applicant: **Airglide AI, Inc.**, Fort Lauderdale, FL (US)

(72) Inventors: **David Bell**, Naples, FL (US); **John Dixon**, Fort Lauderdale, FL (US)

(73) Assignee: **Airglide AI, Inc.**, Fort Lauderdale, FL (US)

(*) Notice: Subject to any disclaimer, the term of this patent is extended or adjusted under 35 U.S.C. 154(b) by 0 days.

(21) Appl. No.: **19/262,396**

(22) Filed: **Jul. 8, 2025**

(65) **Prior Publication Data**

US 2025/0334479 A1 Oct. 30, 2025

Related U.S. Application Data

(63) Continuation-in-part of application No. 18/642,696, filed on Apr. 22, 2024, now Pat. No. 12,377,941, (Continued)

(51) **Int. Cl.**
G01M 10/00 (2006.01)
B63B 1/38 (2006.01)
B63B 71/20 (2020.01)

(52) **U.S. Cl.**
CPC ***G01M 10/00*** (2013.01); ***B63B 1/38*** (2013.01); ***B63B 71/20*** (2020.01); *B63B 2001/387* (2013.01)

(58) **Field of Classification Search**
CPC G01M 10/00; B63B 1/38; B63B 2001/387; B63B 1/36; B63B 71/20
See application file for complete search history.

(56) **References Cited**

U.S. PATENT DOCUMENTS

H56 H * 5/1986 Chandler 73/198

FOREIGN PATENT DOCUMENTS

CN 107063629 A * 8/2017 ..... G01M 10/00
CN 110672302 A * 1/2020 ..... G01M 10/00

OTHER PUBLICATIONS

Lecoffre, Yves et al. "Bubbles and microbubbles for hydrodynamic test facilities", La Houille Blanche, 104:4, 43-55, Oct. 24, 2018. (Year: 2018).*

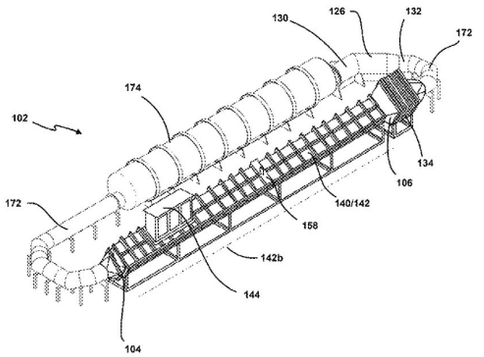
* cited by examiner

Primary Examiner — Paul M. West
(74) *Attorney, Agent, or Firm* — Origins Law, LLC; Nicholas Spatola

(57) **ABSTRACT**

The invention provides a solution for inadequate boundary layer testing methods. The invention includes a uniquely configured multi-module concentric loop cycling water past a testing module to obtain real-time values and variables to use in CFD calculations. The invention is comprised of various sections, specifically designed to support the entire system. The system includes: one or more water reservoirs/degassing tanks, high-capacity water pumps, water stream straightener(s), angulated entrance region including stable flow section, air induction ports, viewing ports, test modules containing test surfaces designed to measure friction and pressure of a passing water or air/water stream. The present invention includes one or more sensors on the test surface(s) that convey conditions to one or more computers that may receive, store, process and send interpretations to one or more visual monitors on or near the invention in real time.

25 Claims, 18 Drawing Sheets



ENGINEERING PROCEDURE

VESSEL SUITABILITY

- Speed
- Hull Form
- Fuel Consumption

CFD STUDY

- Air Flow Optimization
- Resistance Prediction

CALCULATIONS

- Airflow, Pipe Sizing, Nozzle and Compressor Quantity, Electrical Load
- Material Specification
- Air Ingress Consideration

CONCEPTUAL DESIGN

- General arrangement and P&ID
- Nozzle Location and Typical Nozzle Assembly (Valves and Instruments)
- Signal Cable Diagram

TECHNICAL DOCUMENTATION

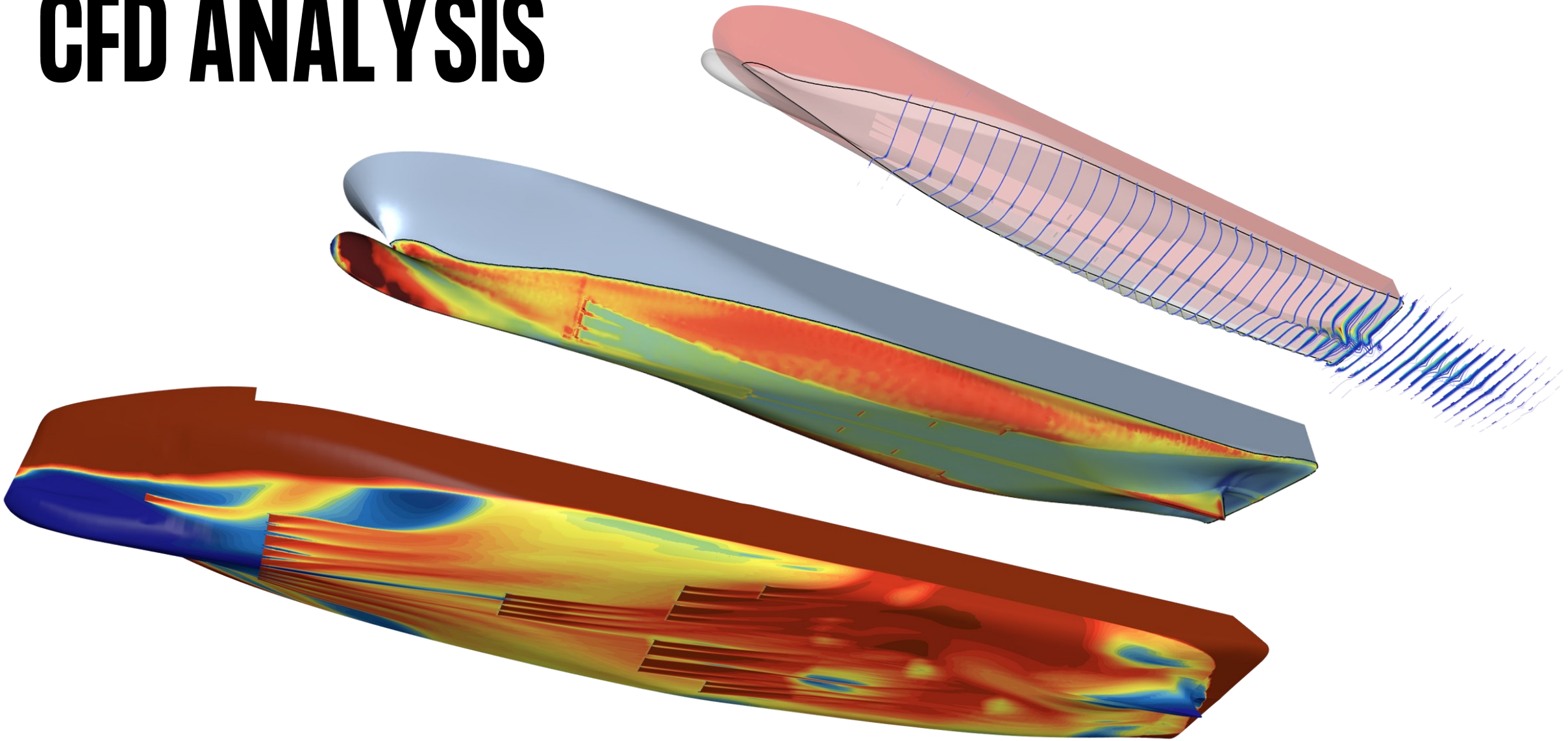
- Installation Procedures and Operational Manuals
- Project Planning
- Class Approvals

INSTALLATION AND COMMISSIONING

- New build Installation Support
- Software Implementation
- Commissioning and Sea Trials

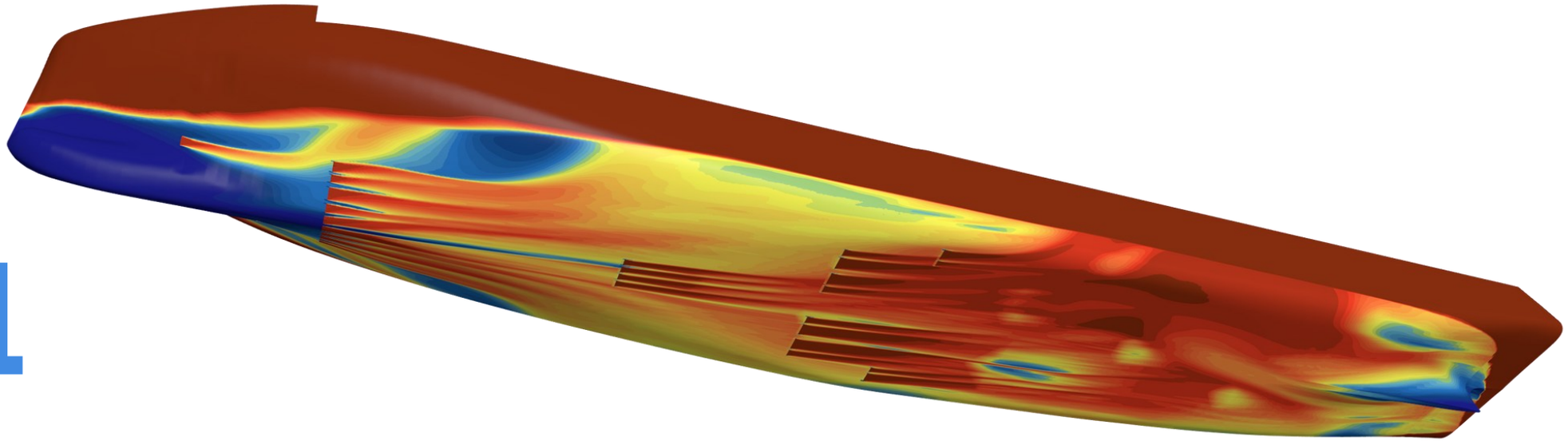
contact@airglide.ai

CFD ANALYSIS



contact@airglide.ai

CFD ANALYSIS

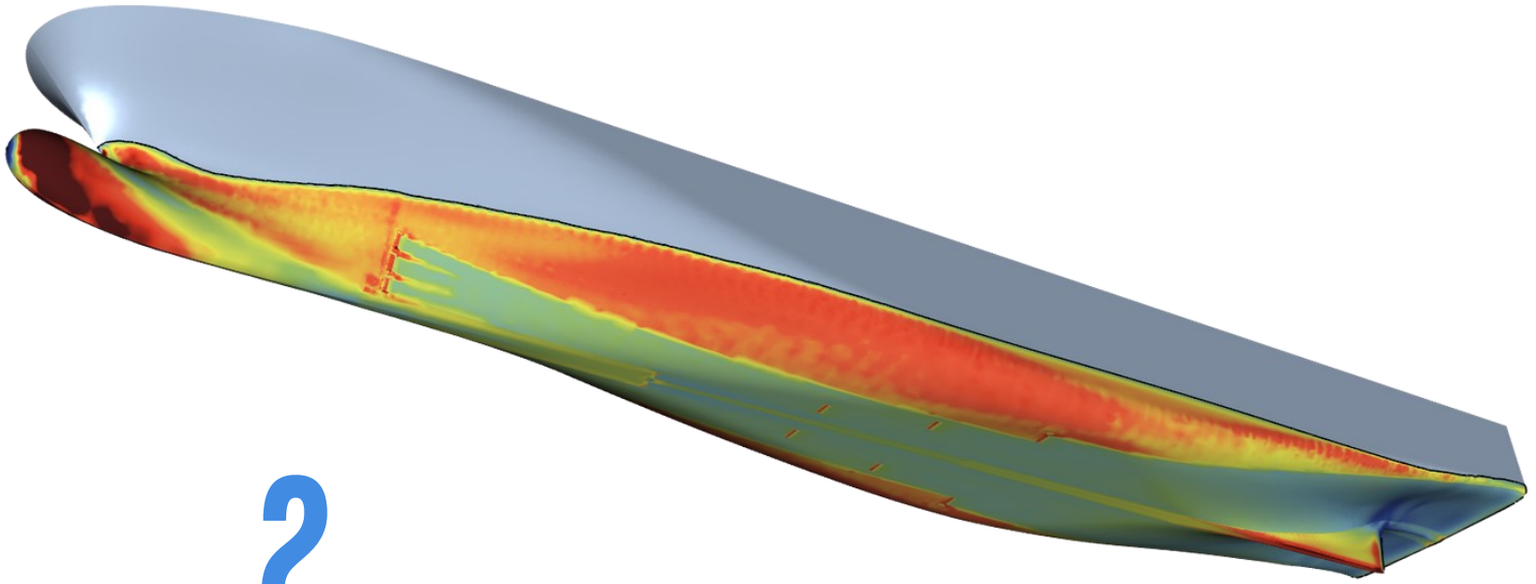


1

AIR COVERAGE OPTIMIZATION

contact@airglide.ai

CFD ANALYSIS



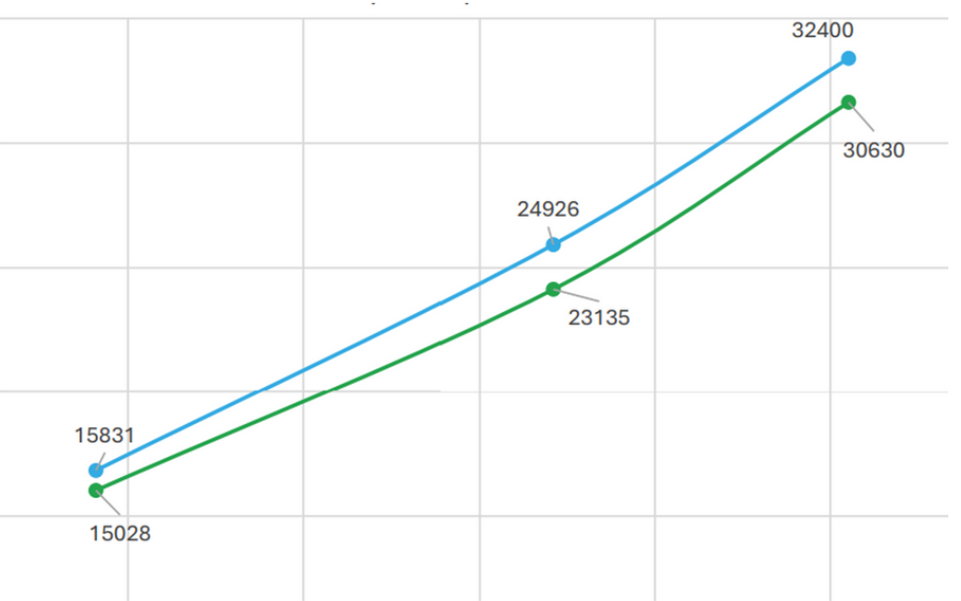
1

AIR COVERAGE OPTIMIZATION

2

PREDICT NET DRAG REDUCTION

CFD ANALYSIS



1

AIR COVERAGE OPTIMIZATION

2

PREDICT NET DRAG REDUCTION

3

PRODUCE SPEED POWER CURVE

Air Layer Drag Reduction is Scientifically Proven to have the Greatest Efficiencies for Air Delivery Systems

Technology Summary

Air Layer Drag Reduction (ALDR) is a method of reducing skin-friction resistance in marine vessels by introducing sufficient air beneath a hull to form a continuous or near-continuous air layer between the hull surface and the surrounding water flow. Air Layer Drag Reduction is understood to be the most effective way of reducing drag by introduction of air beneath a ship.

History

The U.S. Navy were the first to experiment with pumping air beneath the hull of a ship in the 1950s. However, their goal was to reduce the noise of their vessels by creating a carpet of bubbles to isolate the ships from surrounding water, making them harder to detect with sonar. Then, in the 1980s, researchers began investigating the use of air beneath a ship to increase fuel efficiency, calling it an air lubrication system (ALS). The typical method for air lubrication is micro-bubble drag reduction (MBDR)





Modern Technology

There are currently a few providers of air lubrication systems but only one provider of an air layer drag reduction system (AirGlide AI). With the consistent tightening of green house gas regulations across the world, the business case for air layer drag reduction systems becomes more compelling and many ship owners are turning to this fuel-agnostic drag reducing technology.

Air Layer Drag Reduction is Scientifically Proven to have the Greatest Efficiencies for Air Delivery Systems

STUDIES ON AIR LAYER DRAG REDUCTION

"Comparing MBDR with ALDR, Elbing [5] found that the significant drag reduction of MBDR (>25%) is limited to the first few meters downstream of the injection point, whereas the drag reduction of ALDR can extend further. The drag reduction rates of both the slot injection and the porous plate injection using ALDR can maintain more than 80% at 10 m downstream of the injection point, whereas the two injection methods of MBDR both decrease significantly at 2 m, and can only maintain a drag reduction rate below 20% after 4 m." - An, H., Pan, H., & Yang, P. (2022). *Research Progress of Air Lubrication Drag Reduction Technology for Ships. Fluids, 7*(10), 319.

"In this paper, the objective is to identify the optimum type of air lubrication using microbubble drag reduction (MBDR) and air layer drag reduction (ALDR) techniques ... The results show that the ship model using the air layer had the highest drag reduction up to a maximum of 90%. Based on the characteristics of the SPB, which operates at low speed, the optimum air lubrication type to reduce resistance in this instance is ALDR." - Yanuar, W., Waskito, K. T., Pratama, S. Y., Candra, B. D., & Rahmat, B. A. (2018). *Comparison of microbubble and air layer injection with porous media for drag reduction on a self-propelled barge ship model. Journal of Marine Science and Application, 17*, 165–172

"As observed in BDR [Bubble Drag Reduction], for the lower-range of gas injection rates, drag reduction rate is less than 20%. However, above a critical gas injection rate, the ALDR with volumetric air flux being approximately 50 percent greater than BDR gives rise to drag reduction rate over 80 percent. The net energy saving rate expected for ALDR in Fig. 1 becomes higher than that for BDR. " - Park, S. H. & Lee, I. (2018). *Optimization of drag reduction effect of air lubrication for a tanker model. International Journal of Naval Architecture and Ocean Engineering, 10*(4), 427–438.

"Results from the BDR experiments indicate that: significant drag reduction (>25%) is limited to the first few metres downstream of injection ... once ALDR was established: friction drag reduction in excess of 80% was observed over the entire smooth model" - Elbing, B. R., Winkel, E. S., Lay, K. A., Ceccio, S. L., Dowling, D. R., & Perlin, M. (2008). *Bubble-induced skin-friction drag reduction and the abrupt transition to air-layer drag reduction.* Journal of Fluid Mechanics, 612, 201–236.

AIRGLIDE AI STEALTH PROJECT ALDR BETA 2.0 YEAR 2023





DNV CERTIFIED RESULTS STEALTH SHIP 60m DATED 6 MARCH 2024

Summary

- The **objective of this study** is to assess the net power savings achieved by shipGlide Air Lubrication System (ALS) installed on [redacted]
- The assessment is done on the basis of measurements provided by shipGlide with the ALS “on” and “off”. Measurements have been performed during February 2024.
- Measurements affected by shallow water effects and outliers as per Chauvenet‘s Criterion have been disregarded.
- The measurements provided have been evaluated in two different ways. The evaluation as per “on/off” pairs is expected to be the more realistic one, as this procedure minimizes potential weather effects on the results.
- **The average net power savings <u>including</u> the parasitic load of the mechanically coupled compressors at speeds through water approximately between 8.5 knots and 10.5 knots have identified to be between 3.5% and 6%, depending on the evaluation approach.**

2 DNV © 6 MARCH 2024

DNV

Royal Caribbean Group *Icon of the Seas* Stealth Project
Air Layer Drag Reduction (ALDR) Enhancement



AirGlideAI

Flaps Installation
Patent No: US 12,263,914 B2

ICON OF THE SEAS
IMO No: 9829930
LOA: 364m
B: 48.47 m
DRAUGHT: 9.25 m
Tonnage: 248,663 GT
CAPACITY: 7,600 PAX



contact@airglide.ai

AirGlideAI

contact@airglide.ai

Flaps Installation

Icon of the Seas Stealth (ALDR)

US012263914B2

(12) **United States Patent**
Poe et al.

(10) **Patent No.: US 12,263,914 B2**
(45) **Date of Patent: Apr. 1, 2025**

(54) **SYSTEM AND METHOD FOR DELIVERING AIR TO A SUBMERGED SHIP SURFACE**

(71) Applicant: **John Dixon**, Fort Lauderdale, FL (US)

(72) Inventors: **Richard Poe,** Ft. Lauderdale, FL (US); **John Dixon,** Ft. Lauderdale, FL (US)

(73) Assignee: **Airglide, AI. Inc**, Tulsa, OK (US)

(*) Notice: Subject to any disclaimer, the term of this patent is extended or adjusted under 35 U.S.C. 154(b) by 0 days.

(21) Appl. No.: **18/219,375**

(22) Filed: **Jul. 7, 2023**

(65) **Prior Publication Data**

US 2024/0166306 A1 May 23, 2024

Related U.S. Application Data

(63) Continuation of application No. 18/119,324, filed on Mar. 9, 2023.

(60) Provisional application No. 63/427,144, filed on Nov. 22, 2022, provisional application No. 63/439,306, filed on Jan. 17, 2023, provisional application No. 63/454,549, filed on Mar. 24, 2023.

(51) **Int. Cl.**
B63B 1/38 (2006.01)
B63B 59/04 (2006.01)

(52) **U.S. Cl.**
CPC ***B63B 1/38*** (2013.01); ***B63B 59/04*** (2013.01); *B63B 2001/387* (2013.01)

(58) **Field of Classification Search**
CPC B63B 1/38; B63B 2001/382; B63B 2001/385; B63B 2001/387; B63B 59/04
See application file for complete search history.

(56) **References Cited**

U.S. PATENT DOCUMENTS

725,137	A *	4/1903	Quannone	B63B 1/38 114/67 A
900,296	A *	10/1908	Motheral	B63B 1/38 114/67 A
1,254,892	A *	1/1918	Elniff	B63B 1/38 114/67 A
1,408,178	A *	2/1922	Downing	B63H 19/06 114/67 A
2,849,941	A *	9/1958	Negoro	B60H 1/249 454/120
3,680,517	A *	8/1972	Morrison	B63B 1/38 114/67 A
5,389,022	A *	2/1995	Kobayashi	B63H 21/32 440/89 R

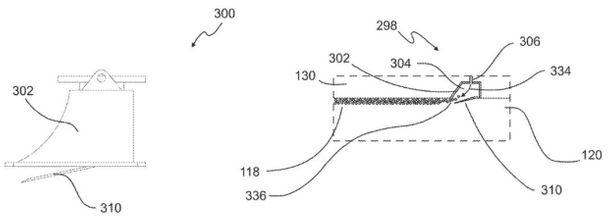
(Continued)

Primary Examiner — Ajay Vasudeva
(74) *Attorney, Agent, or Firm* — Origins Law, LLC; Nicholas Spatola

(57) **ABSTRACT**

This invention introduces a unique two-piece nozzle used to provide air to the hull bottom of a ship, reducing the drag of water friction while in motion. The unique base assembly will mount flush in the bottom portion of a hull of a ship, creating no additional drag when closed. The unique interchangeable and modular nozzle design will allow for maintenance and or development of various designs in the water, without requiring a drydock visit. A flap portion of the nozzle insert will open when air is supplied, releasing small air bubbles to a ship's hull. The flap portion of the nozzle insert may incorporate various materials and passive closing schemes to adjust the air plastron. The present invention creates and maintains an air curtain, called plastron, delivering air underneath a ship hull through an array of nozzles.

26 Claims, 22 Drawing Sheets











AirGlideAI

Icon of the Seas Stealth (ALDR) Server Rack Configuration & Integration

contact@airglide.ai



NVIDIA® Jetson AGX Thor™



NVIDIA

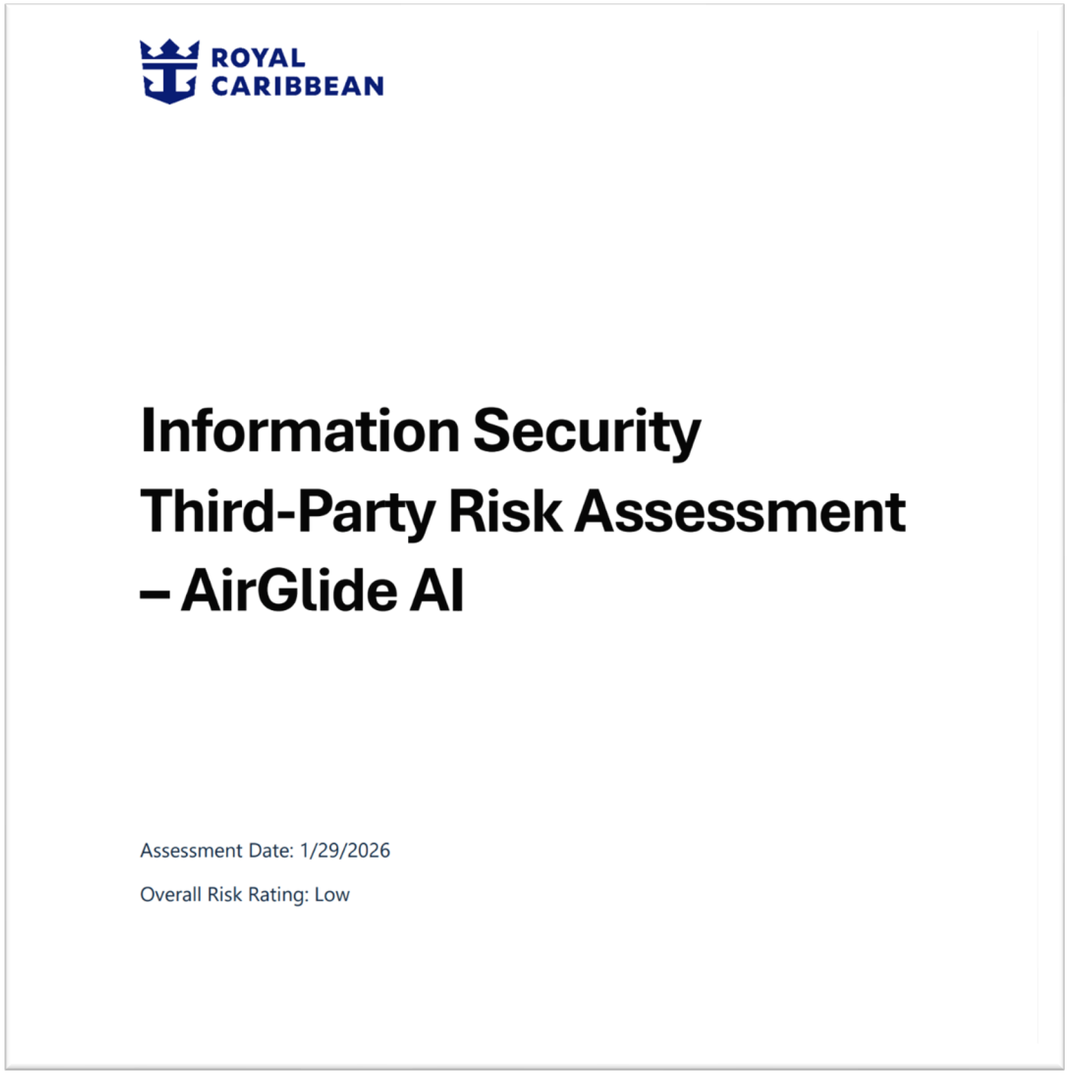
Icon of the Seas Stealth (ALDR) Fleet Training with NVIDIA Installation

contact@airglide.ai





Royal Cyber Risk Assessment


ROYAL CARIBBEAN

Information Security
Third-Party Risk Assessment
– AirGlide AI

Assessment Date: 1/29/2026

Overall Risk Rating: Low

AirGlideAI

Technical Memo 10599025-m01: Verification of Performance and Benchmarking of AirGlide AI Analysis Methodology

DNV

TECHNICAL MEMO

Verification of ALS Performance and Benchmarking of AirGlide Ai Analysis Methodology

Project No: 10599025
Memo No: 10599025-m01
Date of issue: 2026-02-20

To:	AirGlide Ai	**From:**	M-DP-H
		Prepared by:	Shuai Li
Attn:	Alex Taber <ataber@airglide.ai>	**Verified by:**	Fanny Berstad, Jaeouk Sun
Copied to:	Shafiul Mintu	**Approved by:**	Olav Rognebakke

Copyright © DNV 2026. All rights reserved. Unless otherwise agreed in writing: (i) This publication or parts thereof may not be copied, reproduced or transmitted in any form, or by any means, whether digitally or otherwise; (ii) The content of this publication shall be kept confidential by the customer; (iii) No third party may rely on its contents; and (iv) DNV undertakes no duty of care toward any third party. Reference to part of this publication which may lead to misinterpretation is prohibited.

1 EXECUTIVE SUMMARY

DNV has benchmarked the method applied by AirGlide Ai for ALS (Air Lubrication System) performance assessment in accordance with DNV-RP-0695 [1]. The report summarizes the methodological deviations introduced by AirGlide Ai and evaluates the differences against independently verified DNV results.

It was confirmed that AirGlide Ai's approach provided acceptable results for the studied dataset, as the results were consistent and fell within the allowable tolerance limits.

2 INTRODUCTION

AirGlide Ai approached DNV for assurance of analysis methodology to quantify ALS impact on vessel performance. Based on mutual agreement, AirGlide Ai provided a representative dataset of ALS on/off testing. DNV executed an independent analysis following DNV-RP-0695 requirements. AirGlide Ai's methodology was reviewed, and the results obtained for the specific dataset were compared.

3 BASIS FOR WORK

- The vessel's characteristics used for benchmarking are provided below. However, details such as the vessel type, principal dimensions, and comprehensive hydrostatic data were not made available to DNV for this study

Parameter	Value
Frontal Projected Area at current draft	3,325.24 m²
Propeller Diameter	6.3 m
Number of Propellers	3
Displacement (dens. 1.025 ton/m3) Tmld = 9.4m	114291 ton

Technical Memo 10625809-m02: Performance Verification of an Air Lubrication System

DNV

Table 5-2 and Table 5-3 present the corresponding results obtained using speed-power curves derived from CFD analyses with polynomial-fit and power-law-fit formulations. The results are broadly consistent with those obtained using the speed-power curves from the previous study, indicating only minor differences among the three curve-generation approaches.

The results show a consistent positive pattern, with mean savings between 3.5% and 5.3%. The average savings vary slightly depending on the speed vs. power curve applied but quite limited impact, the overall outcome remains broadly consistent. The confidence intervals remain high thus DNV is unable to draw a definitive conclusion based on the submitted dataset due to the high level of uncertainty indicated by the confidence interval analysis. It is therefore recommended that additional datasets be submitted following an internal investigation by the client, in line with the recommendations outlined in the previous report.

Table 5-1 ALS performance based on different speed application using **the curve from previous project**

Speed type	Total tests	Valid tests	Mean saving	90% Confidence interval (total)	Confidence interval _switching on	Confidence interval _switching off
STW	34	15	**4.42%**	[3.7, 5.2] %	[3.9, 5.6] %	[2.8, 5.5] %
Virtual Speed from STW	34	15	**3.54%**	[2.4, 4.6] %	[2.5, 5.8] %	[1.3, 4.8] %
Virtual Speed from SOG	34	15	**5.10%**	[4.0, 6.2] %	[4.1, 7.3] %	[2.9, 6.3] %

Table 5-2 ALS performance with different speed application using **polynomial curve generated from CFD results**

Speed type	Total tests	Valid tests	Mean saving	90% Confidence interval (total)	Confidence interval _switching on	Confidence interval _switching off
STW	34	15	4.56%	[3.8, 5.4] %	[4.1, 5.8] %	[2.8, 5.7] %
Virtual Speed from STW	34	15	3.65%	[2.5, 4.8] %	[2.6, 6.0] %	[1.2, 5.0] %
Virtual Speed from SOG	34	15	5.27%	[4.1, 6.4] %	[4.2, 7.6] %	[2.9, 6.6] %

Table 5-3 ALS performance with different speed application using **power law curve generated from CFD results**

Speed type	Total tests	Valid tests	Mean saving	90% Confidence interval (total)	Confidence interval _switching on	Confidence interval _switching off
STW	34	15	**4.44%**	[3.7, 5.2] %	[3.8, 5.7] %	[2.8, 5.5] %
Virtual Speed from STW	34	15	**3.63%**	[2.5, 4.8] %	[2.4, 6.0] %	[1.3, 5.0] %
Virtual Speed from SOG	34	15	**5.14%**	[4.0, 6.3] %	[3.9, 7.5] %	[2.9, 6.5] %

AirGlideAI

contact@airglide.ai

Airglide AI Bow Thruster Cover Patent





US012630261B2

(12) **United States Patent**
Poe et al.

(10) **Patent No.: US 12,630,261 B2**
(45) **Date of Patent: *May 19, 2026**

(54) **SYSTEM AND METHOD FOR ENHANCED MARINE VESSEL EFFICIENCY USING INTEGRATED HULL OPTIMIZATIONS**

(71) Applicant: **Shipglide, Inc.**, Fort Lauderdale, FL (US)

(72) Inventors: **Richard Poe**, Vail, CO (US); **John Dixon**, Fort Lauderdale, FL (US); **David Bell**, Naples, FL (US); **Danilo Contreras**, Davie, FL (US)

(73) Assignee: **Airglide AI, Inc**, Fort Lauderdale, FL (US)

(*) Notice: Subject to any disclaimer, the term of this patent is extended or adjusted under 35 U.S.C. 154(b) by 0 days.

This patent is subject to a terminal disclaimer.

(21) Appl. No.: **18/948,969**

(22) Filed: **Nov. 15, 2024**

(65) **Prior Publication Data**

US 2025/0074547 A1 Mar. 6, 2025

Related U.S. Application Data

(63) Continuation-in-part of application No. 18/219,375, filed on Jul. 7, 2023, now Pat. No. 12,263,914, which (Continued)

(51) **Int. Cl.**
B63B 1/38 (2006.01)
B63B 19/00 (2006.01)
(Continued)

(52) **U.S. Cl.**
CPC ***B63B 1/38*** (2013.01); ***B63B 19/00*** (2013.01); ***B63B 49/00*** (2013.01); ***B63H 25/42*** (2013.01);
(Continued)

(58) **Field of Classification Search**
CPC B63B 1/38; B63B 2001/382; B63B 2001/385; B63B 2001/387; B63B 19/00; B63B 59/04; B63H 25/42; B63H 25/46
See application file for complete search history.

(56) **References Cited**

U.S. PATENT DOCUMENTS

280,913 A * 7/1883 Laval ..... B63B 1/38 114/67 R
661,303 A * 11/1900 Briggs ..... B63B 1/38 114/67 A
(Continued)

FOREIGN PATENT DOCUMENTS

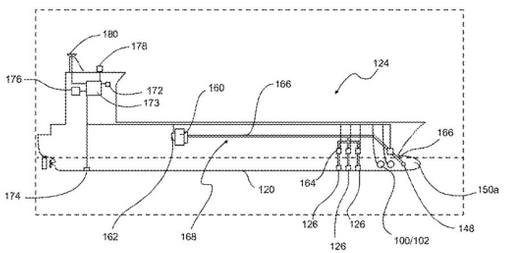
JP 2010083412 A * 4/2010 ..... B63B 1/32
KR 20130000054 A * 1/2013

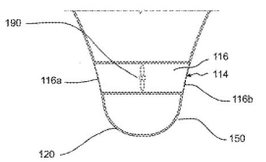
Primary Examiner — Ajay Vasudeva
(74) *Attorney, Agent, or Firm* — Origins Law, LLC; Nicholas Spatola

(57) **ABSTRACT**

A system and method for enhancing marine vessel efficiency through integrated hull optimizations is disclosed. The system includes automated bow thruster covers that reduce hull drag and condition water flow, coupled with strategically positioned air lubrication nozzles that create and maintain an air layer under the vessel. The bow thruster covers may be configured as circular doors or parallel panels, optionally incorporating air discharge ports or working in conjunction with dedicated air jets. An intelligent control system optimizes the integrated components using real-time sensor data and computational fluid dynamic analysis. The system modulates air distribution and cover positions based on sea conditions and vessel speed, maintaining optimal efficiency during operation. External surfaces may incorporate superaerophilic structures to enhance air retention and reduce drag. The comprehensive integration of these components provides improved hydrodynamic efficiency while maintaining full bow thruster functionality when required.

15 Claims, 22 Drawing Sheets





Airglide AI System Patents

US 20260062096A1

(19) **United States**

(12) **Patent Application Publication**

Barry et al.

(10) **Pub. No.: US 2026/0062096 A1**

(43) **Pub. Date: Mar. 5, 2026**

(54) **DEEP LEARNING PREDICTIVE AUTOMATION AND CONTROL SYSTEM FOR AN AIR DISTRIBUTION SYSTEM**

(71) Applicant: **AIRGLIDE AI, INC**, Fort Lauderdale, FL (US)

(72) Inventors: **Iyaan Barry**, Boca Raton, FL (US); **David Bell**, Naples, FL (US)

(73) Assignee: **AIRGLIDE AI, INC**, Fort Lauderdale, FL (US)

(21) Appl. No.: **19/386,111**

(22) Filed: **Nov. 11, 2025**

Related U.S. Application Data

(63) Continuation-in-part of application No. 18/948,969, filed on Nov. 15, 2024, which is a continuation-in-part of application No. 18/219,375, filed on Jul. 7, 2023, now Pat. No. 12,263,914, which is a continuation-in-part of application No. 18/119,324, filed on Mar. 9, 2023, now Pat. No. 12,097,932. Continuation-in-part of application No. 19/075,734, filed on Mar. 10, 2025.

(60) Provisional application No. 63/427,144, filed on Nov. 22, 2022, provisional application No. 63/439,306, filed on Jan. 17, 2023, provisional application No. 63/454,549, filed on Mar. 24, 2023, provisional application No. 63/733,841, filed on Dec. 13, 2024.

Publication Classification

(51) **Int. Cl.**

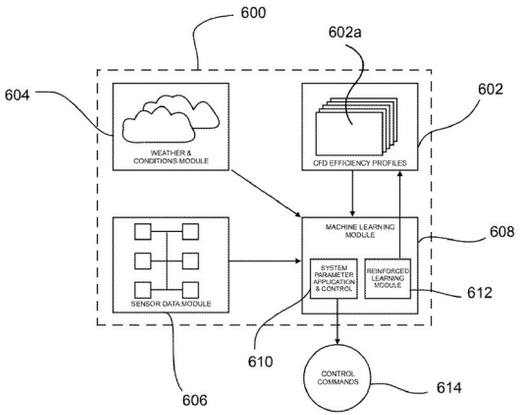
B63B 1/38	(2006.01)
B63B 13/00	(2006.01)
B63B 79/10	(2020.01)
B63B 79/30	(2020.01)
B63B 79/40	(2020.01)

(52) **U.S. Cl.**

CPC ***B63B 1/38*** (2013.01); ***B63B 13/00*** (2013.01); ***B63B 79/10*** (2020.01); ***B63B 79/30*** (2020.01); ***B63B 79/40*** (2020.01); *B63B 2013/005* (2013.01)

(57) **ABSTRACT**

A computer-implemented control system and method for dynamically managing airflow in an air lubrication system of a vessel are disclosed. Real-time sensor data including vessel motion, acceleration, and speed-through-water are processed by a controller executing a machine learning model to predict near-future sea-state conditions. The controller accesses and interpolates computational fluid dynamics (CFD) efficiency profiles to determine target airflow values and generate valve and compressor commands that modulate airflow to multiple outlets beneath the hull. Feedback from hull and pressure sensors is used to stabilize the air layer, while a learning-based prediction engine continuously refines CFD profiles to improve operational efficiency and reduce parasitic load. The system enhances vessel hydrodynamic performance and fuel economy under varying environmental conditions.



DEEP LEARNING PREDICTIVE AUTOMATION AND CONTROL SYSTEM FOR AN AIR DISTRIBUTION SYSTEM

CROSS-REFERENCE TO RELATED APPLICATIONS

[0001] This application is a continuation-in-part of co-pending U.S. patent application Ser. No. 18/948,969, entitled "System and Method for Enhanced Marine Vessel Efficiency Using Integrated Hull Optimizations", filed Nov. 15, 2024. U.S. patent application Ser. No. 18/948,969 is a continuation-in-part of U.S. patent application Ser. No. 18/219,375, now granted U.S. Pat. No. 12,263,914, entitled "A System and Method for Delivering Air to a Submerged Ship Surface", filed Jul. 7, 2023. U.S. patent application Ser. No. 18/219,375 is a continuation-in-part of U.S. patent application Ser. No. 18/119,324, entitled "A System and Method for Reducing Drag on Hulls of Marine Crafts Thereby Increasing Fluid Dynamic Efficiencies", filed Mar. 9, 2023, now U.S. Pat. No. 12,097,932, which claims the benefit of priority pursuant to 35 U.S.C. § 119 (e) to U.S. Provisional Patent Application Ser. No. 63/439,306, filed Jan. 17, 2023, and U.S. Provisional Patent Application Ser. No. 63/427,144, filed Nov. 22, 2022. U.S. patent application Ser. No. 18/219,375 also claims priority pursuant to 35 U.S.C. § 119 (e) to U.S. Provisional Application Ser. No. 63/454,549, entitled "A System and Method for Delivering Air to a Submerged Ship Surface", filed Mar. 24, 2023. All of which are hereby incorporated by reference in their entireties for all purposes. This application is also continuation-in-part of co-pending U.S. patent application Ser. No. 19/075,734, entitled "Aerodynamically Enhanced Air Lubrication Nozzle and Flap", filed Mar. 10, 2025. This application also claims the benefit of priority pursuant to 35 U.S.C. § 119 (e) to U.S. Provisional Patent Application Ser. No. 63/733,841, entitled "Airflow Throttling Based on Ship Motion Dynamic for an Air Lubrication System", filed Dec. 13, 2024. All of which are hereby incorporated by reference in their entireties for all purposes.

FIELD OF THE INVENTION

[0002] The present invention relates generally to marine automation systems, and more particularly to computer-implemented control systems for managing air lubrication operational processes.

BACKGROUND

[0003] Modern maritime transport faces increasing pressure to comply with international emission reduction mandates, such as those set forth by the International Maritime Organization (IMO), which require progressive decreases in greenhouse gas (GHG) emissions from ocean-going vessels. As fuel costs and regulatory compliance continue to drive operational expenses, ship owners and naval architects are motivated to explore technologies that enhance hydrodynamic efficiency and reduce energy consumption. The correlation between fuel consumption and CO_2 output means that improving propulsion efficiency directly contributes to both environmental and economic goals.

[0004] Various strategies have emerged to address these challenges. Some involve exhaust aftertreatment solutions such as scrubbers, which remove sulfur oxides (SO_x) and particulate matter from the exhaust gases to meet emissions standards. While such systems effectively mitigate airborne pollutants, they do not address the underlying issue of energy loss through hydrodynamic drag. Other innovations, such as rotor sails utilizing the Magnus effect to generate auxiliary propulsion, or hybrid and nuclear propulsion systems aiming to eliminate or supplement fossil fuel burn, seek to improve energy utilization at the propulsion stage. However, these technologies typically operate independently of hull-fluid interactions and therefore provide limited benefit to overall vessel hydrodynamic efficiency.

[0005] A significant portion of a ship's fuel consumption is expended in overcoming hull resistance, particularly viscous drag at the hull-water interface. For this reason, advances in hull design and surface treatments have been critical to improving efficiency. Developments such as optimized hull geometries, antifouling coatings, and enhanced propulsion components have each contributed incremental gains. Yet, as vessel designs approach hydrodynamic optimization limits, further substantial efficiency improvements require new approaches that manipulate the flow dynamics surrounding the hull itself.

[0006] Air lubrication systems represent one such approach. By introducing a layer of air bubbles between the hull and the surrounding water, these systems reduce the effective wetted surface area and frictional resistance, thereby lowering fuel consumption. However, legacy methods simply flood the area with air bubbles, many of which are wasted because they are too far away from the hull of the surface, and thus, the energy savings are often completely offset by the energy required to run the system. This leads to ship engineers turning the systems off because the use of these systems leads to more maintenance required without an efficiency benefit.

[0007] To produce a viable air lubrication system, the system must be able to account for various sources of drag and environmental variability. U.S. patent application Ser. No. 18/119,324, entitled "A System and Method for Reducing Drag on Hulls of Marine Crafts Thereby Increasing Fluid Dynamic Efficiencies," discloses a superaerophilic bottom hull surface configured to maintain an air plastron by encouraging air adhesion. That disclosure also introduces an air distribution network from compressors to the hull surface. U.S. patent application Ser. No. 18/219,375 ("the '375 Application"), entitled "A System and Method for Delivering Air to a Submerged Ship Surface," introduces a nozzle system to take air from the distribution network and discharge it strategically below the hull of a ship, which is more readily deployable than a porous surface layer. Unlike legacy air lubrication systems that rely on shear forces from downward-facing nozzles, the '375 Application introduces a descendible flap that directs hydrodynamic flow below the air plastron, allowing greater air coverage and improved efficiency. Nonetheless, these systems still experience efficiency losses in unsteady or varying sea states.

[0008] Despite their promise, all air lubrication systems are often limited by inefficiencies in air distribution and management, particularly in dynamic sea conditions. While current air lubrication systems can be turned on and off by the user, it is not efficient in varying sea states. In such situations, air will dissipate towards the side it can rise fastest, leading to large swaths of areas of the ship hull which are then subjected to drag once again. Without adaptive control, much of the injected air fails to adhere to the hull where it provides the greatest benefit, leading to

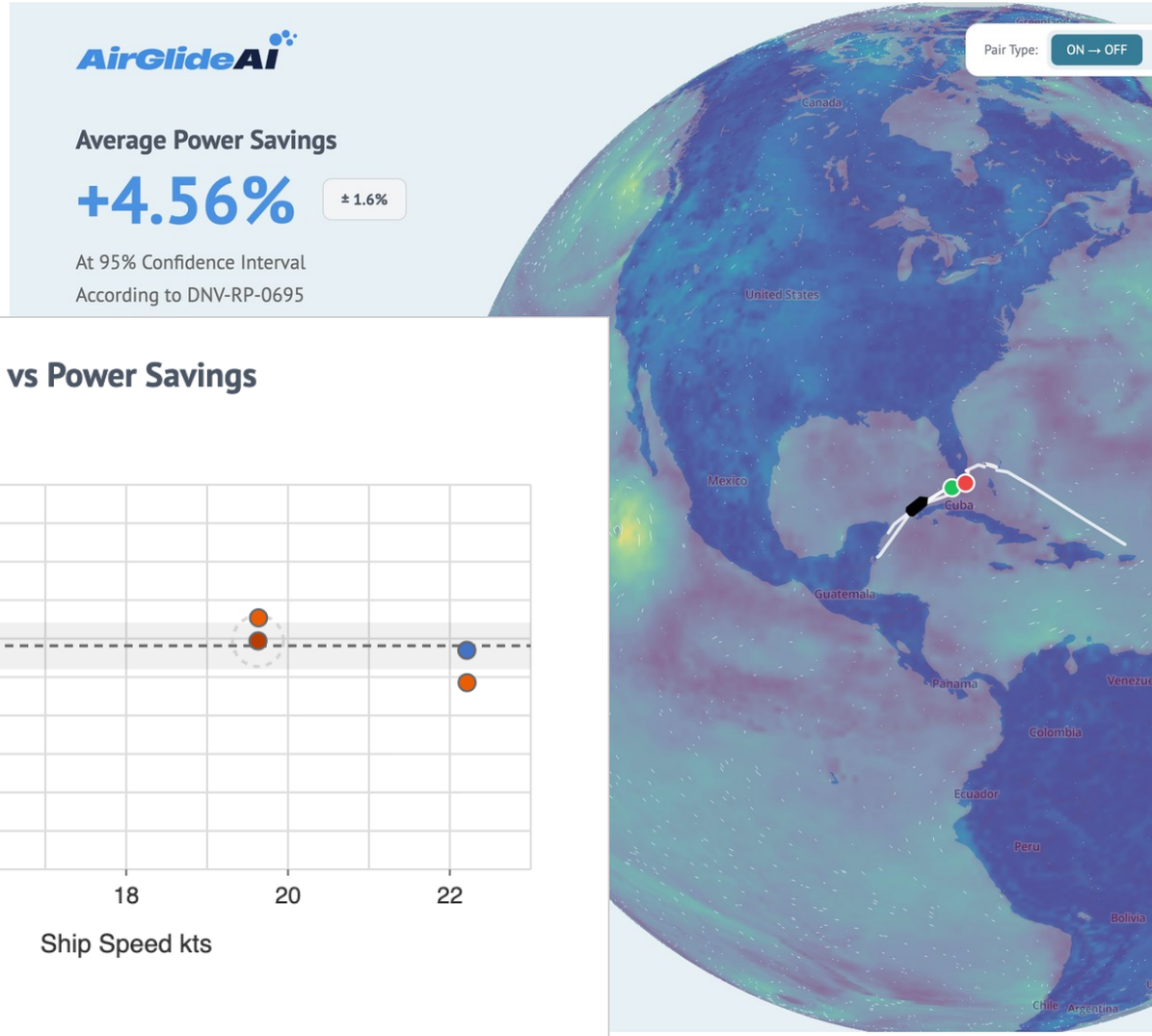


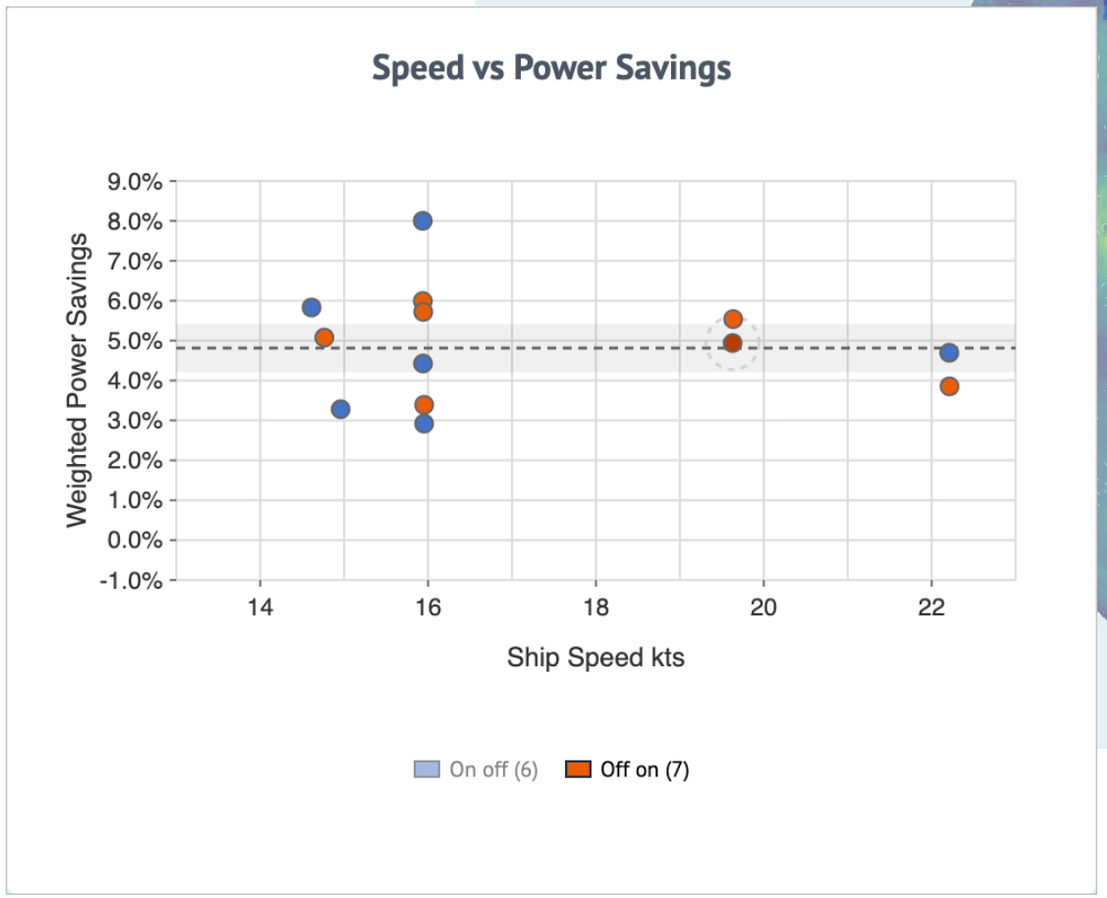
AirGlideAI

DNV

PERFORMANCE VERIFICATION

- Project No: 10625809
- Memo No: 10625809m02
- Date of issue: 2026-08-10

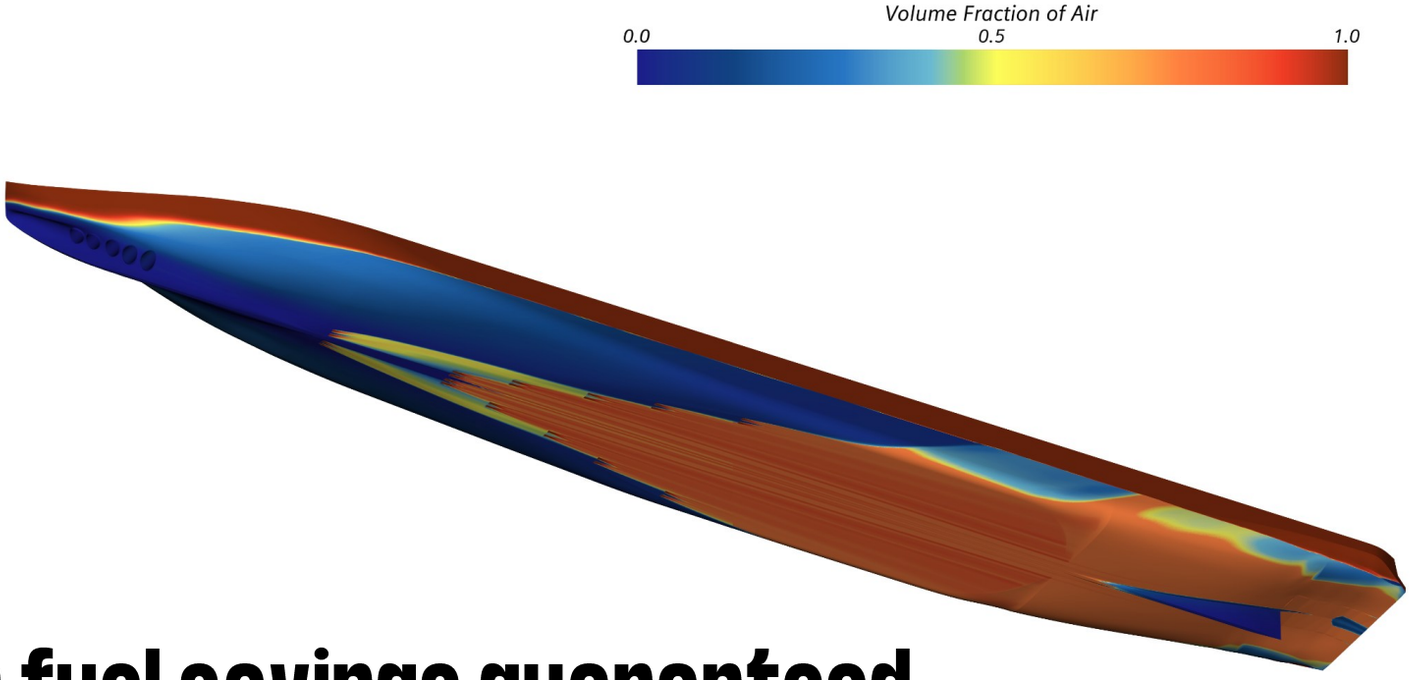




contact@airglide.ai

Air Delivery Unit Optimization with Placement of Air Delivery Boxes Optimum Design Standard

Airglide AI CFD Analysis of Optimized ADU Layout



6.5% propulsion fuel savings guaranteed Per contractual specifications

Our Company

AirGlide AI is a maritime technology company applying artificial intelligence, computational fluid dynamics (CFD), and naval architecture expertise to improve vessel performance, utilizing its revolutionary patented Air Layer Drag Reduction System (ALDR). This 21st century technology is far superior to legacy Air Lubrication Systems (ALS) of the 20th century. AirGlide AI, in collaboration with multiple leading research institutions, utilized its own Boundary Layer Testing Lab to recreate real-world hydrodynamic conditions to test and refine proprietary patented new air delivery unit designs utilizing ALDR principles.

Our intellectual property portfolio is comprised of a robust mix of U.S. and international patent protections across three core pillars. More than 100 unique patent applications have been filed, with multiple patents granted and others pending worldwide, covering hydrodynamic testing methods, advanced software and artificial intelligence systems, and proprietary hydrodynamically efficient hardware, including specialized air-release technologies.

www.airglide.ai

October, 2026

BAY STATE
— SAIL FREIGHT —

Bay State Sail Freight

(603) 276-9103

StevenW@baystatesailfreight.com



BAY STATE

— SAIL FREIGHT —

What is Bay State Sail Freight?

Conventional shipping is costly

$1,800,000 additional per day for the Cape Cod region

More than $114,191 for one pallet per day in 2025, using least-cost trucking option.

Nearly double the cost to go to Plymouth vs. Provincetown

2025 Average
$ 312.85

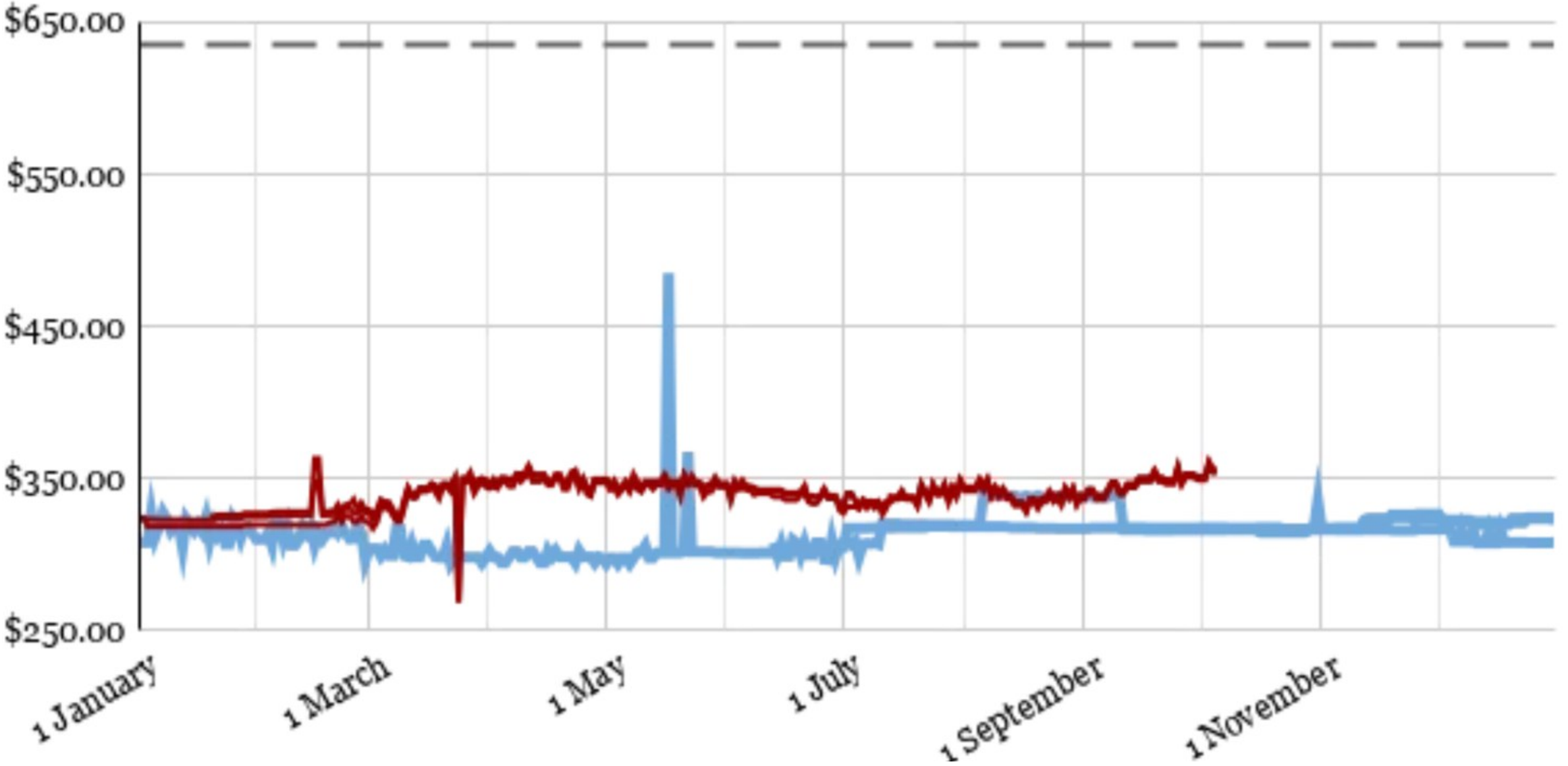
2026 YTD Average
$ 337.09

YoY Average Change
7.75%

Since Straight Closure, YoY
10.4%

Provincetown Inbound Freight Rates

2000 lb, 64 c.ft pallet carried LTL. Red Lines Indicate Current Year.



Solution



Avoid Bridges

Bridge congestion burns time on a driver's 12-hour limit, while burning more expensive fuel than free-flowing traffic due to stopping, starting, and idling

Avoid Fuels

Fuel Reduction
95%

Fixed Cost Structure

All costs for sail freight are effectively fixed and predictable, removing volatility entirely and allowing businesses to reliably plan around the future cost of products

Lowest Cost

Savings Rate
~15%+

BAY STATE
SAIL FREIGHT

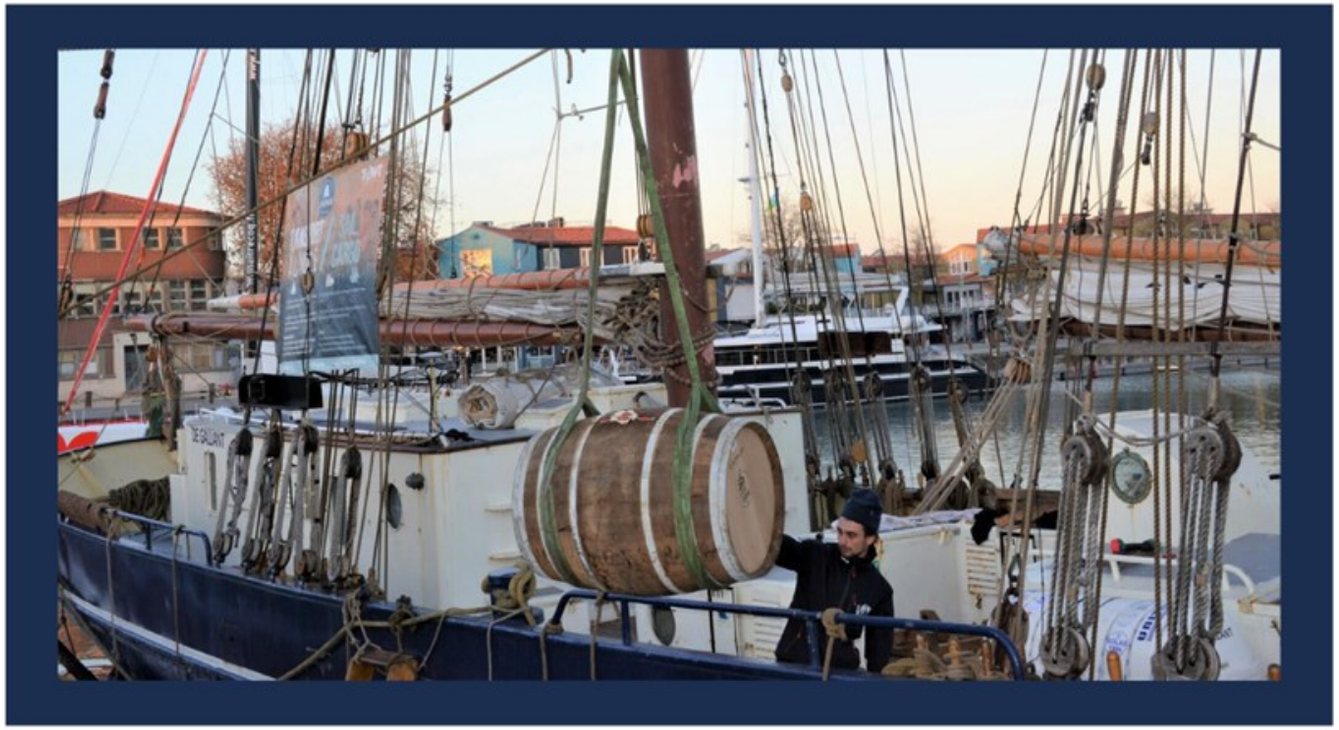

Marketing
Myopia

Competitive Advantage

Lower Cost —— We can offer a rate slightly under the lowest verage trcking cost for he past two years.

Fixed Cost —— Our freight quotes are good from January 1 to Dcember 31 each year, eliminating cost spikes and variability.

Marketing —— Sail freight allows customers to advertise the fact that they use sail freight which other shipping avenues may not gain that option



Target Customers



Offerings

- Less-than Truck Load
  - Pallet Rates
- Parcel Rates
  - Small-scale shippers
  - Subscription Services

Initial Customers

- Farm-To-Table
  - Restaurants
  - Farmers & Producers
- Small Producers
  - Coffee Roasters
  - Breweries
- Unique Regional Products

BAY STATE
SAIL FREIGHT

Why Bay State?



Bridge Work

$ 4.5 Billion

Up to 10 Years

MassPort Goals

Net Zero: 2031

Maritime Culture

150+ Marinas & Boat Clubs

HUB & SPOKE NETWORK



- Requires less capital equipment than fully connected network.
- Reduces Operating and Capital Expenses of Network.
- May slow progress of deliveries along multi-leg routes.
- Typical configuration of LTL/LCL transportation networks on land and sea.
- Reliable integration into existing logistics chain, replacing trucks on specific legs of transportation.
- Requires warehousing at larger scales and network complexity.

BAY STATE
SAIL FREIGHT

Bay State Sail Freight Business Model Canvas

Key Partners

Port Authorities/ Harbormasters

Longshore Labor & Unions

Drayage Providers

Seafarers

Coast Guard

Local/State Government

Cargo Brokers

*Tall Ships America

*Steamship Authority

N.B.: * Indicates low priority.

Key Activities

Sailing Vessel Operations

Logistics Coordination

Receiving Cargo Deliveries

Customer Communications

Key Resources

Sail Freight Vessel

Skilled/Credentialed Crew

Docking Space

Cargo Handling Gear

Warehousing Space

Value Propositions

Cost Stabilization

Cost Reduction

Product/Brand Differentiation

Climate Action Credentials

ESG Rating Enhancement

Product Co-Creation

BAY STATE
— SAIL FREIGHT —

Customer Relationship

Cargo Owners

Consignees

Co-Creators

Co-Branders

Channel

Journalism

Co-Advertisement

Website / Social Media

Direct Labeling/Contact

Schooner Festivals

Customer Segments

Business/Cargo Owners

- Restaurants & Breweries
- Farm-to-Table
- Local Producers
- Small-Mid Distributors
- 3rd Party Logistics Firms

Co-Creators

Co-Branders

Islands: Massachusetts Steamship Authority

N.B.: Bay State Sail Freight competes in the Less-than Truck Load (LTL) market segment, meaning most customers will be relatively small shippers initially.

Cost Structure

CAPITAL COSTS:	FIXED COSTS:	VOYAGE COSTS:
Ship Construction 5-Year Refits	Insurance Maintenance Port Fees*	Crew Wages Provisioning Longshore Fees Fuel Costs

N.B.: Port Fees for leased slips are a fixed cost for most Packet Service operations, which BSSF plans to operate. Future operations may change this.

Revenue Stream

Primary: Freight Revenue: Tonnage & Parcel Rates.

Secondary: Co-Branded & Co-Created Goods

Favor long-term contracts for cargo over spot-market cargo.

Rates will be provided for each direction of travel. All viability calculations are based on zero tons annually from Provincetown, which will be sold at a significant discount compared to trucking on the same leg.

Business Model Canvas template developed by Business Model Foundry, 2010. Used under Creative Commons Attribution-Share Alike 3.0 License.

TradeSailer project
www.tradesailer.com

The Center for
Post Carbon Logistics

Catran
NAVAL ARCHITECTS

BAY STATE
— SAIL FREIGHT —



There Are No Good Off-The-Shelf Plans Available For Sail Freighters... Until Now



Catran Galema

Catran Galema and his team at Catran Naval Architects is the mind behind the TradeSailer Project, which was initiated in 2023 to provide a standardized set of designs for sail cargo vessels through participation of interested parties. The Pacific was identified as the area with the biggest need due to the negative effect of global warming on these Island communities and the isolation of the island groups. Coupled with a high local fuel price having a self sustaining cargo vessel driven by wind in the small island developing states made the most sense.

Forming a partnership with the Bay State Sail Freight team in 2025, Catran and his team have been developing sailing cargo vessels for coastal trade worldwide, leading the way for an entire industry.

Catran
NAVAL ARCHITECTS

TradeSailer project
www.tradesailer.com

BAY STATE
SAIL FREIGHT



DESIGN CONSTRAINTS:

- Uninspected Cargo Vessel
- Onboard Crane - 250kg/550lb SWL
- Pallet-Capable hold and hatches
- Capacity for 10 Pallets, 7.5 tons
- No more than 2 Crew
- Under $500,000 target build cost
- Fits worldwide use requirements
- Designed for short distance, high frequency routes competing with Less-than Truck Load market

TradeSailer project
www.tradesailer.com

Rope Sling.

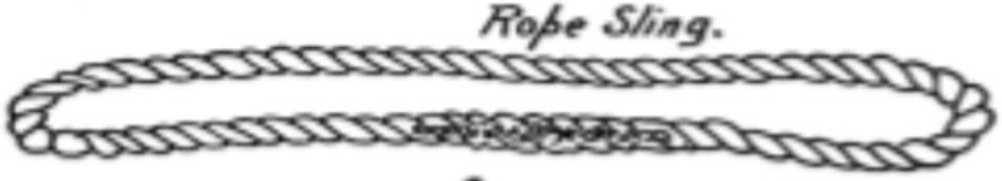




FIG. 46.—A WEB SLING FOR SOFT BAGS.



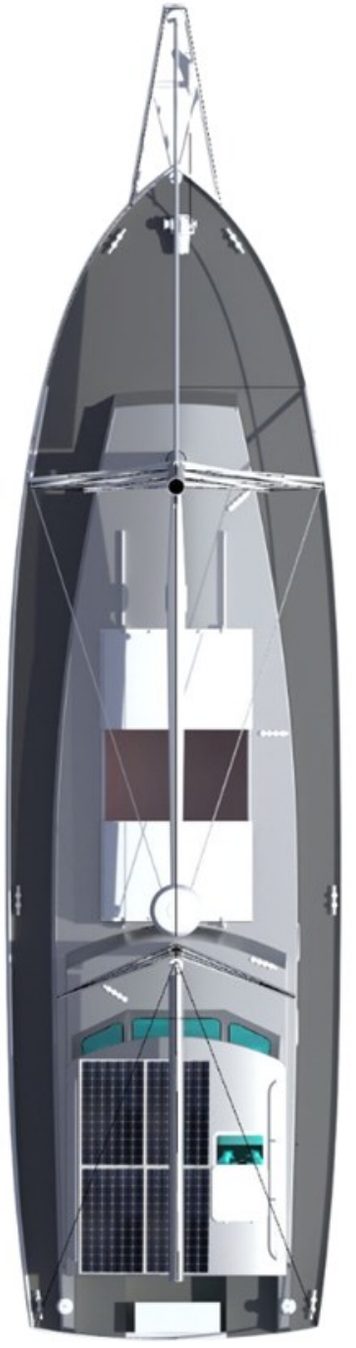
FIG. 45.







Length over all: 13.6 m
Length over deck: 11.9 m
Length waterline: 11.65 m
Beam moulded: 3.35 m
Draft: 1.90m
Displacement: 23 tonnes
Cargo Volume: 18 m3
9 US Pallets
CDWT: 7 tonnes
Sail Area: 80 m2





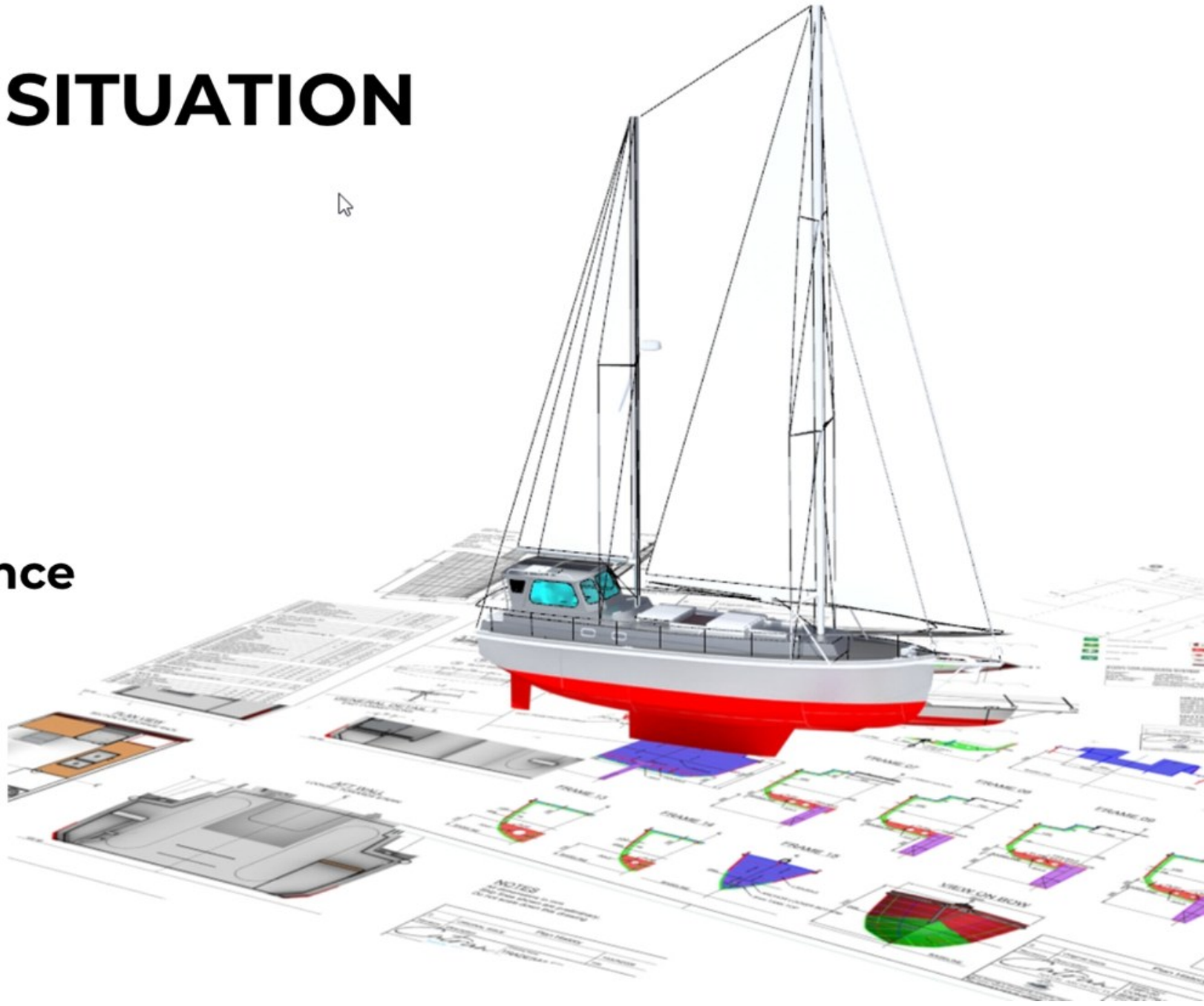
THE CURRENT SITUATION

What We Have:

- **Route**
- **Competitive Data**
- **Vessel Design**
- **Financial Analysis**
- **Real World Experience**

What We Need:

- **Customers & Cargo**
- **Investors**
- **Pilot Run**



Customer Acquisition

Challenges

- Distance from market area
- Uncertain Dates for Pilot Program
- Summer Tourist Season
- Transition Costs for participating in Pilot
- Cargo Network Mapping
- Definition of “Local” in regional organizations

Progress

- Well Recieved by Harbormasters
- Most people are receptive
- Identifying potential partners is easy in the market area
- Dissatisfaction with status quo is clearly present

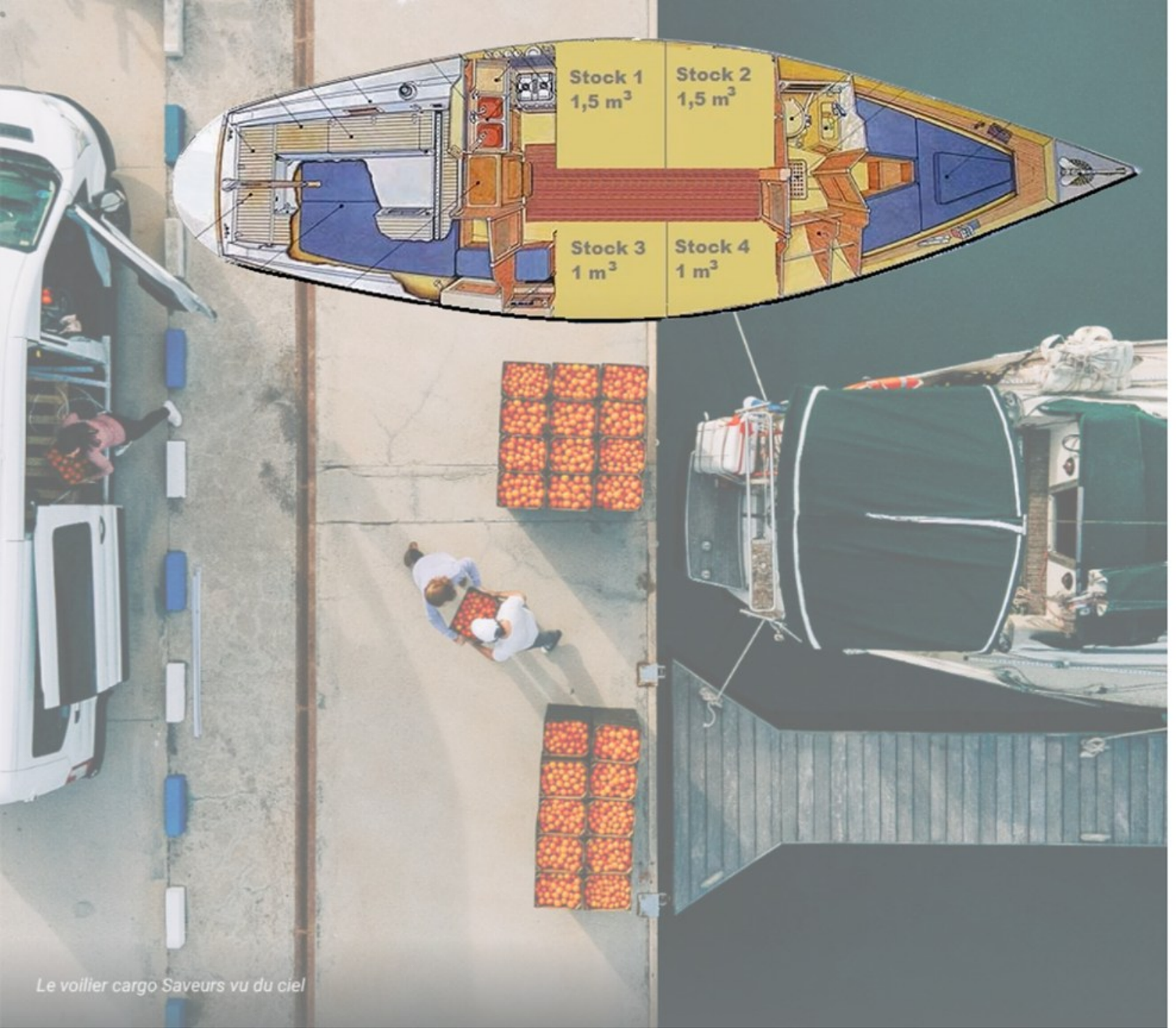
Investor Acquisition

Challenges

- Awaiting build estimates for TradeSailer 120
- Slow Returns
  - Poor fit for Venture Capitalist model
  - Requires patient capital
- Myth of Progress
- Minimum Scale
- Priority of Veblen Goods

Progress

- 3-Month Minimum Viable Product in development
  - Small, Short, Simple, Scalable, Safe, Sharable.
- Some interest is present
  - Impact Investors
  - Angel Investors
- Completed Blue Excellerator BX6 Cohort Accellerator



ÉOLIEN

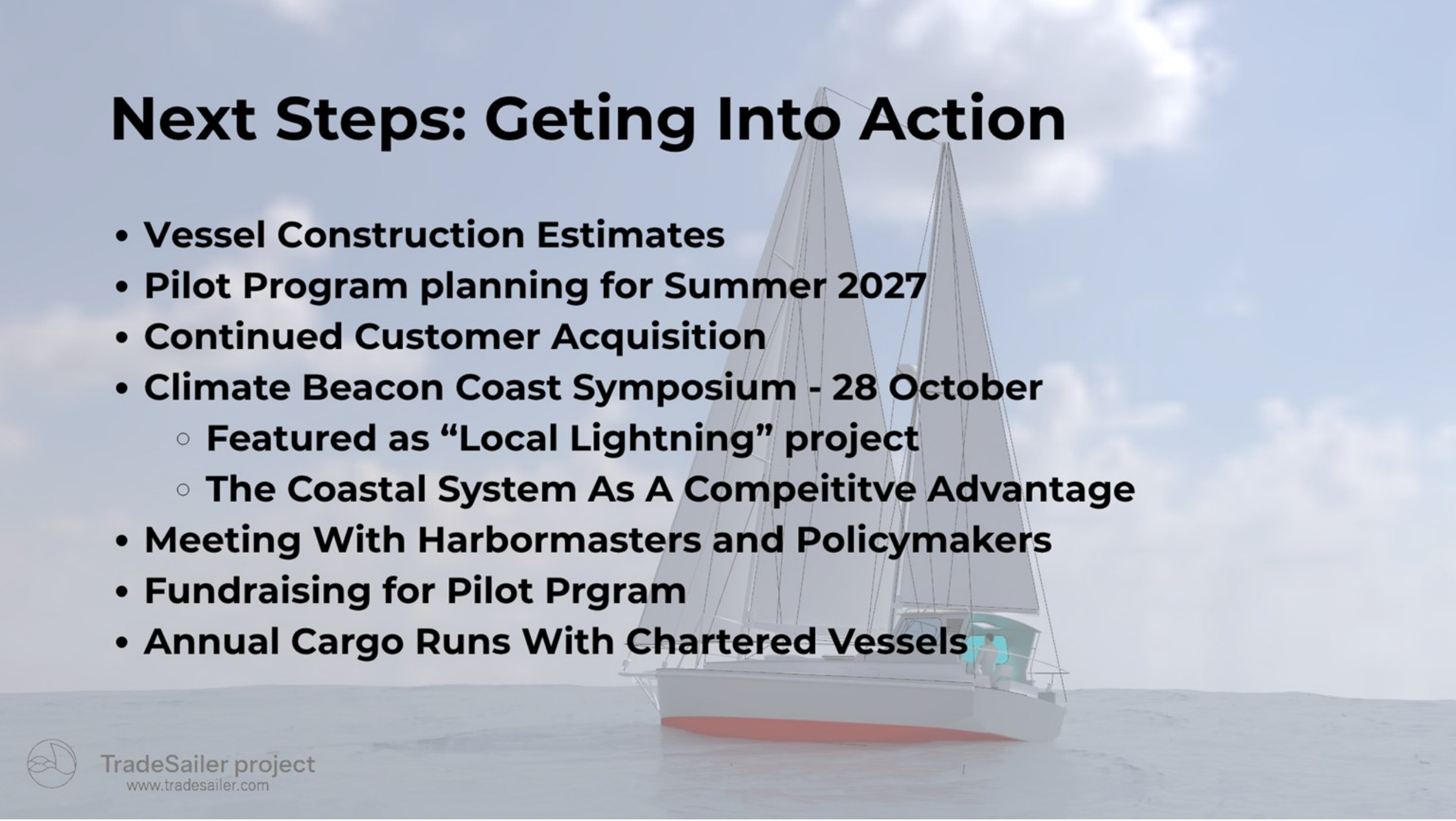
Le cabotage en Occitanie

Pilot Program:

- Summer 2027
- Commercial sailboat
- Proof Of Concept
- Customer List

Next Steps: Geting Into Action

- Vessel Construction Estimates
- Pilot Program planning for Summer 2027
- Continued Customer Acquisition
- Climate Beacon Coast Symposium - 28 October
  - Featured as “Local Lightning” project
  - The Coastal System As A Compeititve Advantage
- Meeting With Harbormasters and Policymakers
- Fundraising for Pilot Prgram
- Annual Cargo Runs With Chartered Vessels



TradeSailer project
www.tradesailer.com

Open Questions For The Future

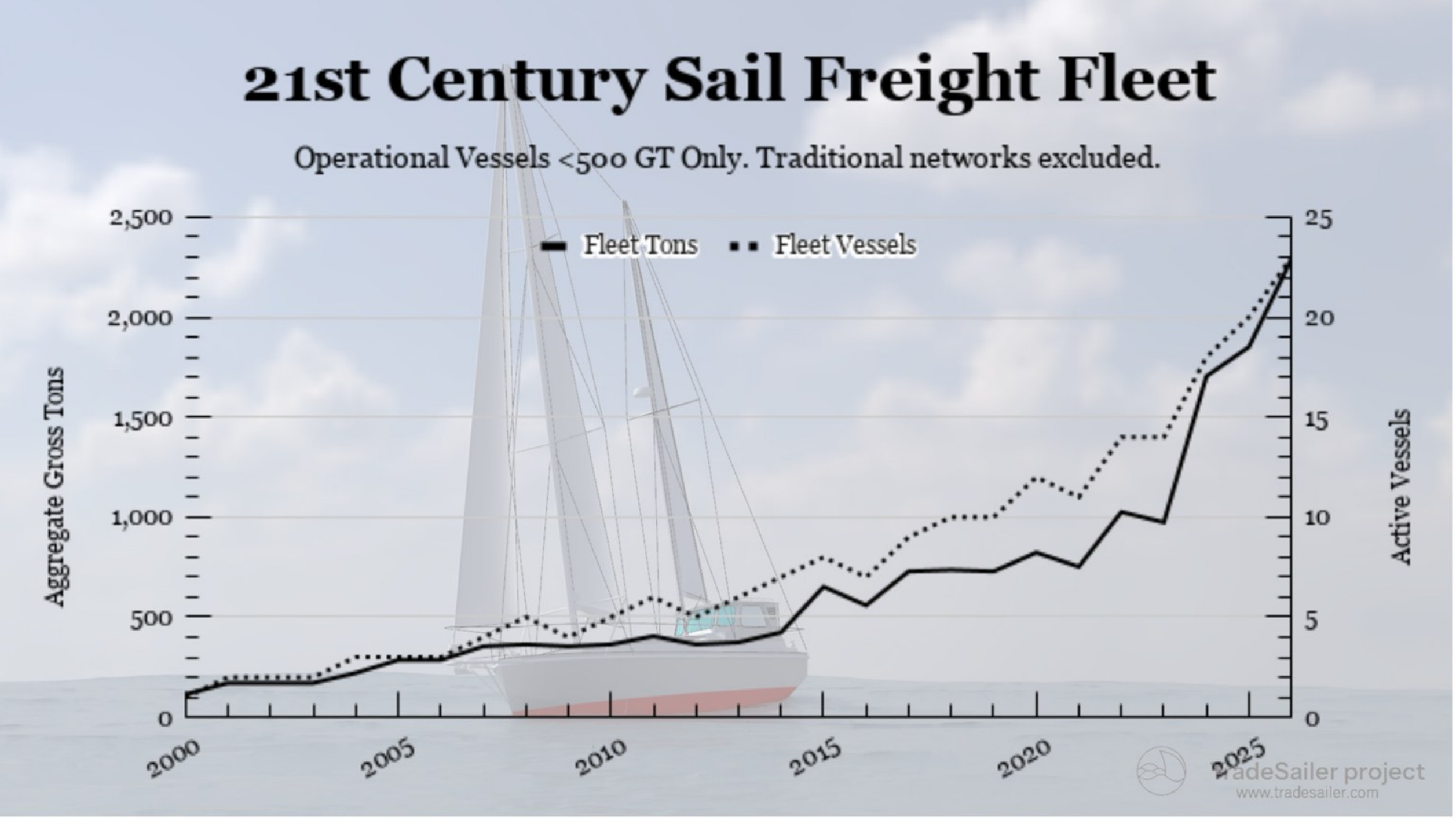
- Is there a big enough customer base?
- Does this route line up with the actual routing of cargo?
- What effects will the bridge construction actually have?
- How fast can this indutry grow?
- What will cause the next Oil/Fuel Crisis, and when?

THERE ARE NO TECHNICAL BARRIERS TO IMMEDIATE ADOPTION OF SAIL FREIGHT.

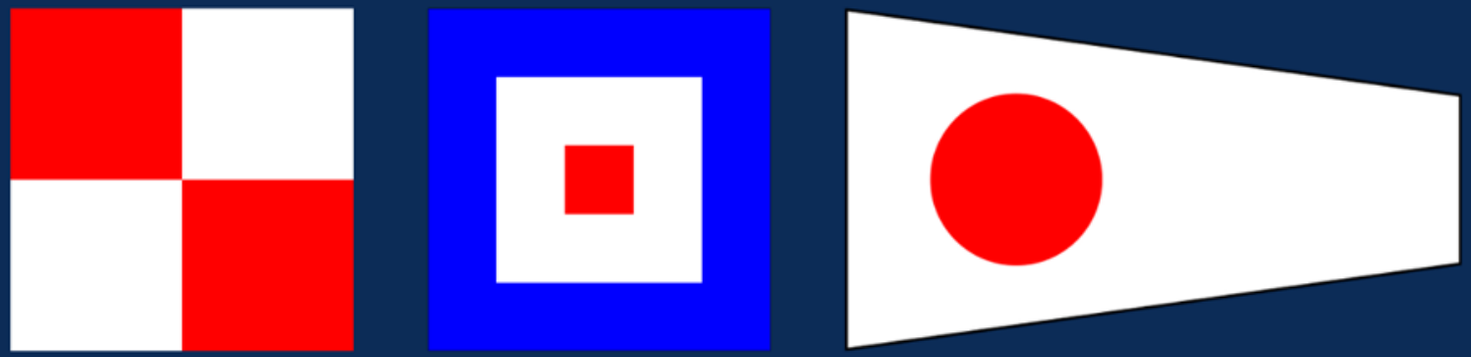
MONEY IS MADE UP, BUT CO2 IS REAL AND WILL KILL YOU.



TradeSailer project
www.tradesailer.com


21st Century Sail Freight Fleet
Operational Vessels <500 GT Only. Traditional networks excluded.
Fleet Tons
Fleet Vessels
Aggregate Gross Tons
Active Vessels
2,500
2,000
1,500
1,000
500
0
25
20
15
10
5
0
2000
2005
2010
2015
2020
2025
TradeSailer project
www.tradesailer.com

Thank You

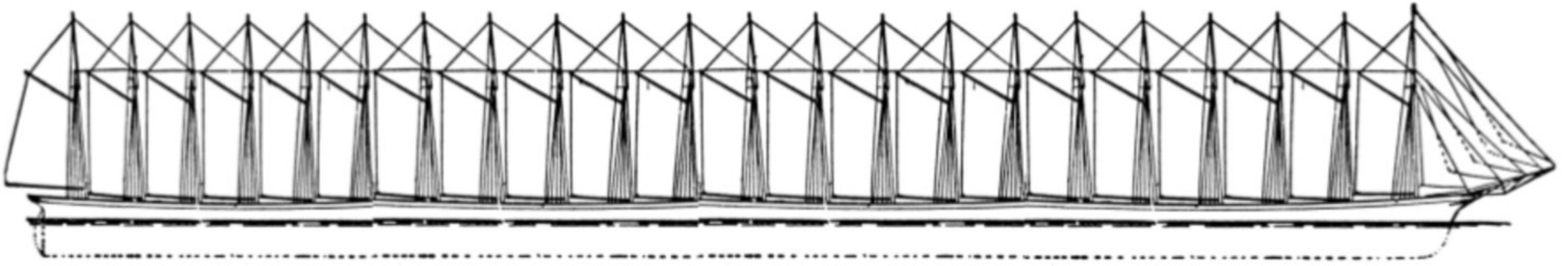


BAY STATE
— SAIL FREIGHT —

Decarbonize & Decongest
Coastal Transportation

Baystatesailfreight.com

603.276.9103



Questions?

StevenW@BayStateSailFreight.com

SUSTAINABILITY AND INNOVATION IN SHIP DESIGN AND OPERATIONS CONFERENCE SISDO 2026

GLEN COVE, NY

19 - 20 OCTOBER 2026

Improved Ship Engine Emissions Mitigation through Optimized Propeller Design for Reduced Cavitation

Dr. Lubomir A. Ribarov

Associate Professor
Department of Marine Engineering
United States Merchant Marine Academy
300 Steamboat Road
Kings Point, NY 11024
USA

Organization

- Introduction
- Ship Resistance – Brief Background
- Cavitation Theory and Inception – Brief Background
- Cavitation and Vessel Performance
- Propeller Basics and Cavitation
- Prototype Vessel
- 3-D Models of Propellers
- EasyCFD – Brief Background
- CFD Simulation Results (selected results)
  - Conventional Propeller
  - Straight Nozzle
  - Convergent Nozzle
  - Divergent Nozzle
- Ship Resistance Calculations
- Resistance Coefficients
- Emissions Factors
- Ship Emissions Calculations – Annual Emissions Reductions (AERs)
- Conclusions and Furute Work
- Acknowledgements
- References

Background

- The global shipping industry faces significant challenges towards reduction of its environmental impact. At the current rate, it is expected that carbon dioxide (CO_2) emissions are projected to increase 50–250% by 2050
- Modern advances in conventional marine power (i.e., 2-stroke/4-stroke diesel engines) and propulsion systems and energy management improvements, have already significantly contributed to reducing both CO_2 and nitrogen oxides (NO_x) emissions from marine diesel engines
- Despite these stringent regulations, the propulsion and power generation plants for future ships must significantly reduce fuel consumption and emissions over the coming years
- The use of advanced propeller designs for merchant shipping has seen an increased interest due to rising fuel costs, ever-stringent environmental protection requirements (especially stringent in specific emission control areas, ECAs**), and resulting increased operational costs, etc.
- The present research is focusing on the feasibility of the newly proposed propeller design incorporating a nozzle in its blades for reducing propeller cavitation on marine vessels
- If successful, the reduced propeller cavitation could reduce HC fuel consumption and exhaust emissions towards green (or "more-green") energy technologies to be implemented in ship propulsion systems of the future, consistent with IMO's global decarburization initiatives for marine vessels propulsion systems
- The current paper expands on prior related work*** where some of the initial CFD simulations were done



A containership emits a cloud of Diesel exhaust smoke when docking in the port of Hamburg*

*"CO_2- Emissionen der Schifffahrt bisher stark unterschätzt", ("CO_2 emisions from shipping have so far been greatly underestimated") Greenpeace Redaktion, 13.02.2008 (based on article in The Guardian)

**ECAs – emission control areas can be designated for SOx, PM, or NOx (or all three types of emissions combined)

*(Davis, A., Du., M.-H., Nilsson, K., & Ribarov, L.A., 2024)

Ship Resistance – Brief Background

- Determination of ship's resistance through water is influenced by ship's displacement, hull, form, and speed
- In order to determine the effectiveness of the proposed propeller improvement, one must first determine the total power to overcome the ship's resistance
- The effective required power is the total sum of all drag contributions to the ship's hull and other effects (e.g., hull fouling, strong weather (strong winds/high waves), roughness, appendages, etc.)
- In general, the ship's resistance can be subdivided into three main sub-groups*:
  - Frictional resisatnce, R_F
  - Residual resistance, R_R
  - Air resistance, R_A
- Next we consider the specific contributions (to the total ship's resistance) by each of these three main sub-groups
- Other (secondary) resistance contributions are mentioned (but not considered further)

SUSTAINABILITY AND INNOVATION IN SHIP DESIGN AND OPERATIONS CONFERENCE 2026

*(Guldhammer and Harvald, 1974; Harvald, 1983)

Ship Resistance – Brief Background (con't)

- **Frictional resisatnce, R_F** is the component of resistance due to integrating tangential stress over wetted surface area of submerged portion of the ship's hull in direction of motion:

$$R_F = C_F \left(\frac{1}{2}\rho V^2\right) S$$

- where:

  C_F is the specifc frictional resistance coefficient,
  V is the sped of the ship,
  S is the total wetted surface area of the submerged ship's hull, and ρ is the water density

- The total wetted surface area, S, of the submerged portion of the ship's hull can be calculated (within approx. 15%) using Denny-Mumford's formula*:

$$S = 1.025(L_{PP})[(C_B)(B) + 1.7(T)] = 1.025\left(\frac{\nabla}{T} + 1.7(L_{PP})(T)\right)$$

- where:

  L_{PP} is the hull length between the perpendiculars, C_B is the hull's block coefficient, B is the hull's width, T is the hull's draught, and ∇ is the displacement volume

SUSTAINABILITY AND INNOVATION IN SHIP DESIGN AND OPERATIONS CONFERENCE 2026

*(Bakker and van Vlaardingen, 2017)

Ship Resistance – Brief Background (con't)

- **Residuary resiatnce**, R_R, is obtained by subtracting from the total resistance of the ship's hull
- Most commonly this is the resistance due to wavemakeing, R_W, as the ship's hull is propelled through the water
- Other smaller contributions of resistance are due to viscous pressure resistance, R_{PV}, and the additioanl frictional resiatnce associated with the curvature of the hull, R_{CH}
- These latter two resistance contributons (R_{PV}, R_{CH}) are low, compared to R_W
- For relatively low ship hull speeds, wave resistance may not be considered as it is the practice in some towing tank and ship model laboratories*
- **Air resistance**, R_A, is due to the portion fo the hull which is not submerged in the water as well as any superstructures, deck cargo, auxiliary equipment, etc., which impede the ship's hull movement through the air.

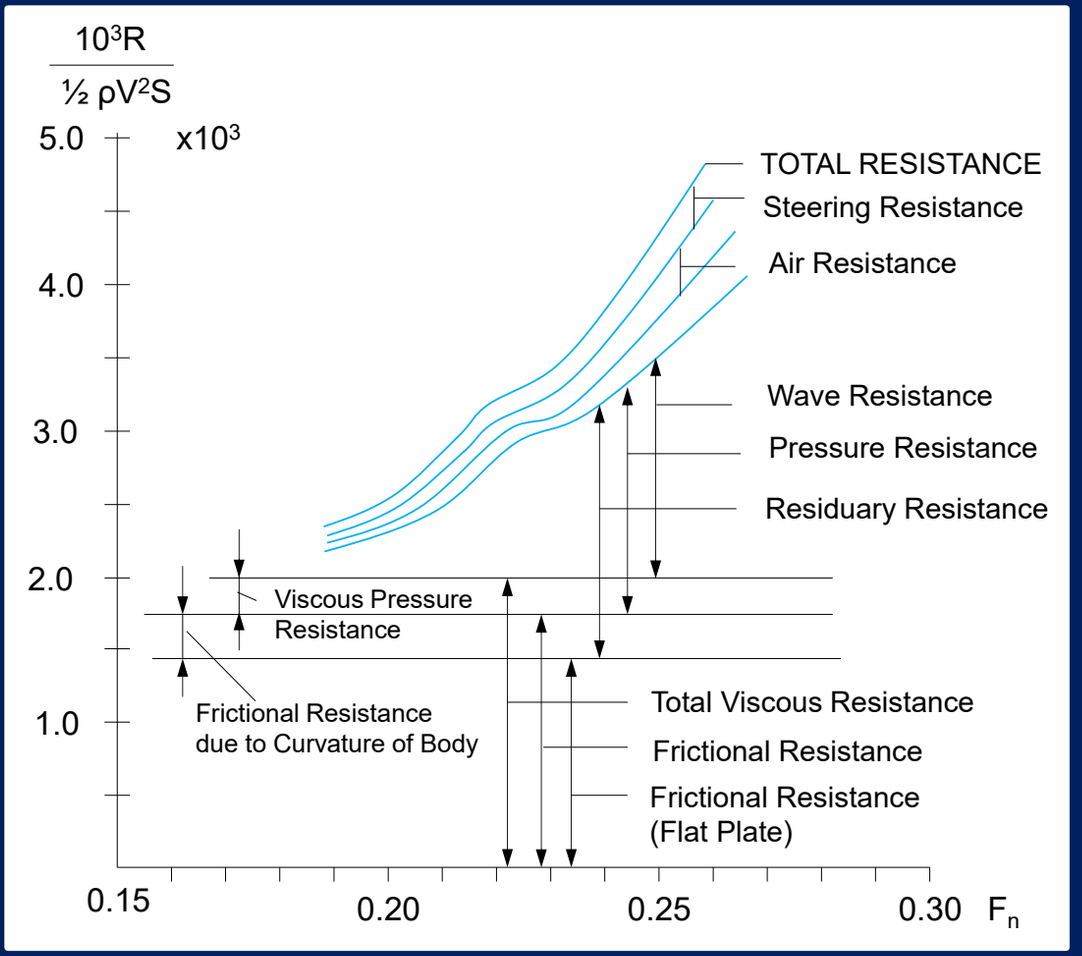
$$R_A = \frac{1}{2}\rho_{air} C_A A_{air} V^2$$

- Other secondary resiatnces, e.g., viscous resiatnce, R_V; pressure resistance, R_P; spray resistance, R_S; appendige resistance, roughness resisatnce, steering resistance, drift resistance (esp. in sailing vessels), etc. may be contributing to a lesser degree, are not being considered in this work

*(Harvald, 1983)

Ship Resistance – Brief Background (con't)

- A good visual representation of the different ship resistances is shown on the right (adapted from Harvald, 1983), where the specific ship resistance is given as function of Froude number (ratio of flow inertia to the external field), *Fr*. ($Fr = V/(gL)^{0.5}$), here $L = L_{WL}$
- The values on the ordinate are multiples of 10^3
- The significant contributions by R_F and R_R are clearly observed
- The contribution by R_A is somewhat smaller
- The remaining resistance contributions, while recognized, may be of diminishing values

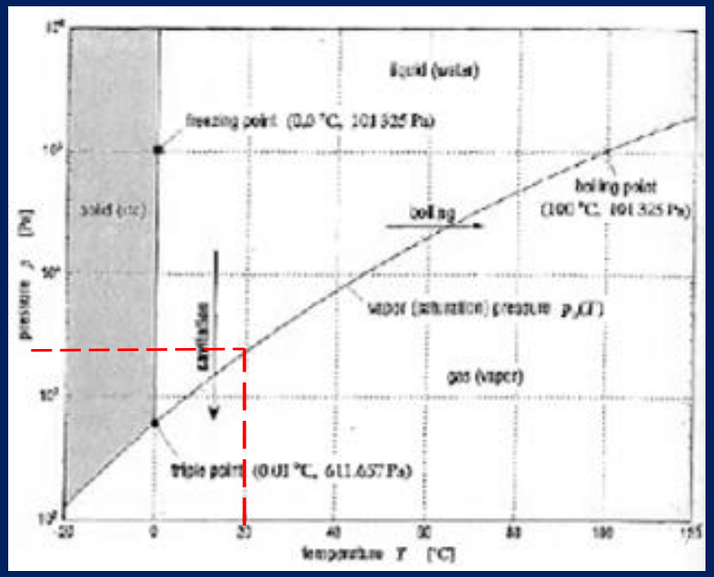


Parts of Total Specific Resistance of Ships as Function of Fr Number*

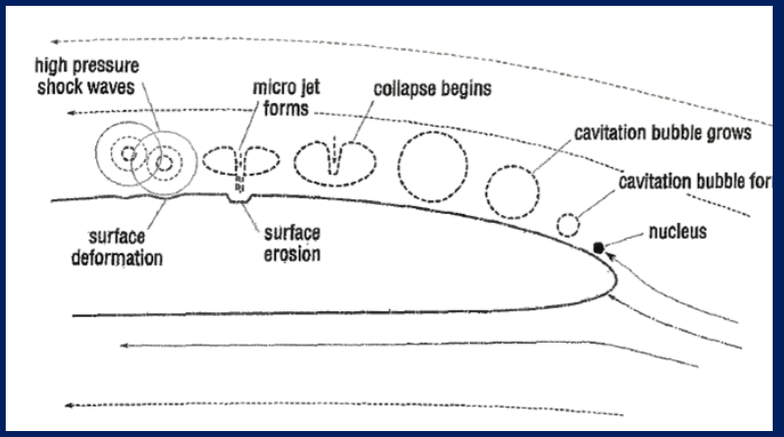
*(Harvald, 1983)

Cavitation Theory

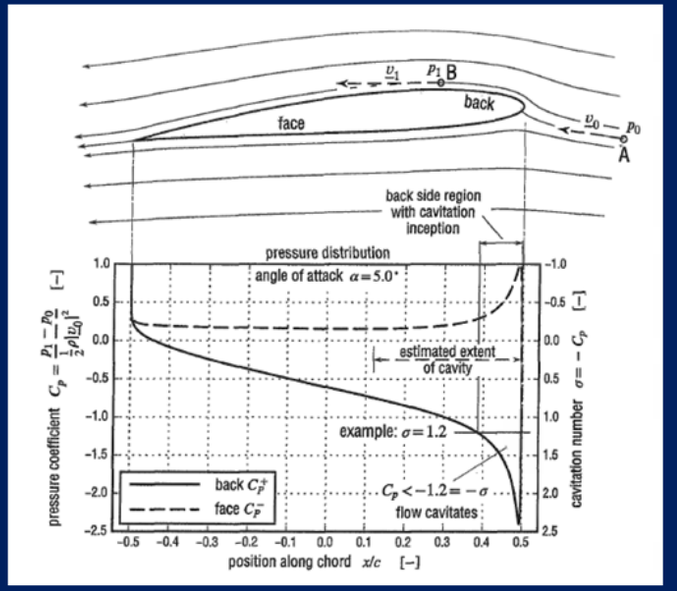
- What is cavitation? https://youtu.be/1DsidGXXW4A
- Plot (top right) shows regions of fresh water where for cavitation occurs based on the vapor pressure*; at 20°C, p_{vapor} = 2.339 kPa; (p_{vapor} =2.296 kPa (seawater**)
- A drop below the local vapor pressure can occur along the suction side of the propeller blade* (bottom right plot)
- Formation of cavitation bubbles is a gradual process* (bottom left sketch)
- Cavitation is caused by the collapse of vapor bubbles onto the propeller
- The vapor bubble implosion can cause surges of pressures up to 200 MPa which results in a high energy shock wave
- Other damage mechanisms are related to small micro-jets
- As a result of vapor bubble implosion, crater-shaped erosion is formed on the blade surface (center bottom sketch)
- Leading geometric causes of propeller cavitation are: uneven leading edge of the blade, excessive blade sharpness, poor finishing of blades, etc.
- Other factors: Rapid transients, operating beyond design limits, etc.



Simple phase diagram for fresh water



Evolution of a cavitation bubble

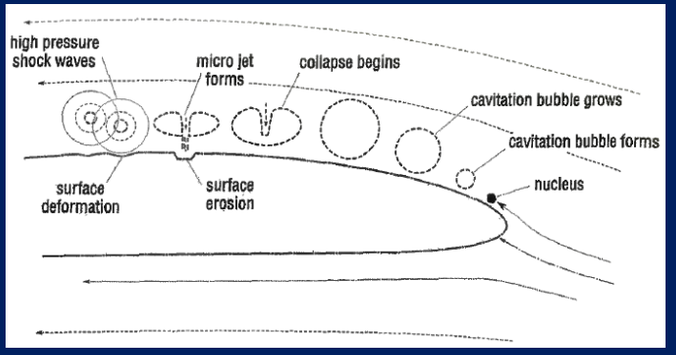


Flow around a cavitating foil and pressures

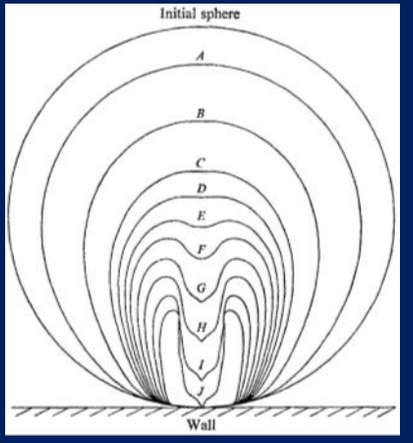
*(Birk, 2019)
**(Carlton, 2007)

Cavitation Theory (con't)

- A drop below the local vapor pressure can occur along the suction side of the propeller blade* (upper right plot)
- Formation of cavitation bubbles is a gradual process* (bottom right sketch)
- Cavitation is caused by the collapse of vapor bubbles onto the propeller
- The vapor bubble implosion can cause surges of pressures up to 200 MPa which results in a high energy shock wave
- Other damage mechanisms are related to small micro-jets
- As a result of vapor bubble implosion, crater-shaped erosion is formed on the blade surface (center bottom sketch)
- Leading geometric causes of propeller cavitation are: uneven leading edge of the
  blade, excessive blade sharpness, poor finishing of blades, etc.
- Other factors: Rapid transients, operating beyond design limits, etc.



Evolution of a cavitation bubble*



Computed collapsing sequence of a cavitation bubble near a wall**

*(Birk, 2019)
**(Carlton, 2007)

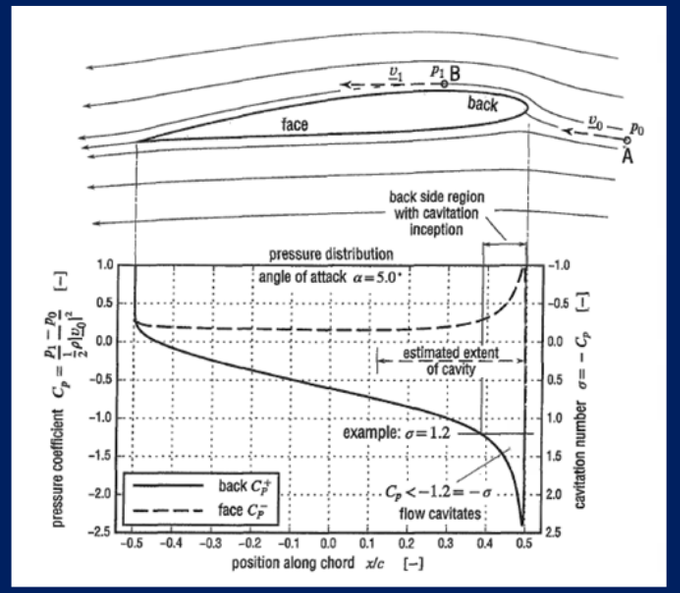
Cavitation Inception

- Likelihood of cavitation occurrence is shown by σ:

$$\sigma = \frac{p_o - p_v}{\frac{1}{2}\rho V^2}$$

where:

p_o – static pressure
p_v – vapor pressure
$q = 1/2\rho V^2$ – dynamic pressure



Flow around a cavitating foil and pressures*

- The larger σ is, the less likely cavitation to occur. High static pressure (p_o) lowers the propensity for cavitation (i.e., deeper submerging of the propeller blades). Higher speed operating propellers causing higher flow velocity (and hence higher q) increase the likelihood for cavitation to occur.
- Bernoulli's equation applied to an inviscid 2-D flow past a foil section (i.e., propeller blade) with two points on same streamline, A and B. Point A is upstream of the foil section, point B on the upper (suction) side of the foil. At point A the undisturbed fluid has local velocity v_0 and local static pressure p_0. According to Bernoulli's principle for steady flow, sum of static and dynamic pressure is constant, hence:

$$p_0 + \frac{1}{2}\rho V_0^2 = p_1 + \frac{1}{2}\rho V_1^2 = const.$$

*(Birk, 2019)

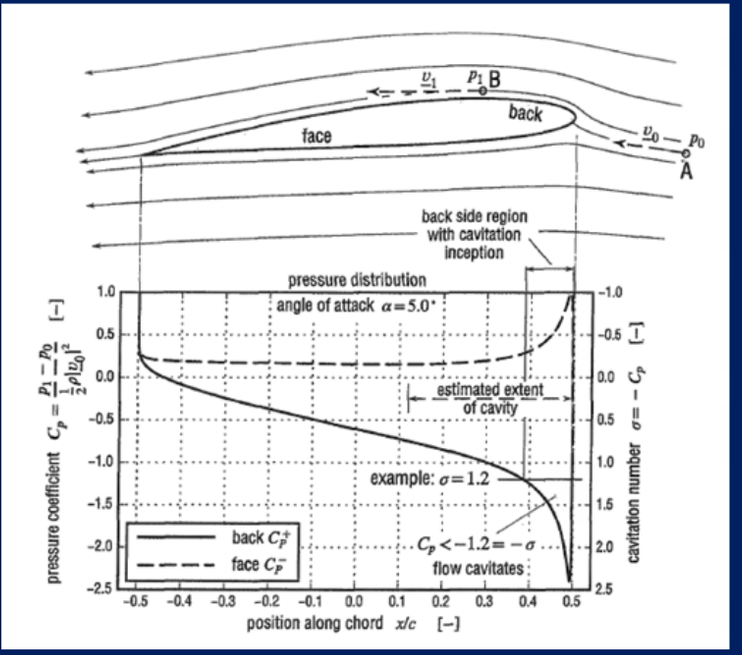
Cavitation Inception (con't)

- Since point B is on the suction side of the foil, where velocity is higher (than the pressure side), the corresponding pressure, p_1, is lower than the pressure p_0. This change in pressure, Δp, between point A and point B along the same streamline is simplified to:

$$\Delta p = p_1 - p_0 = \frac{1}{2}\rho(V_0^2 - V_1^2)$$

- Since the pressure drops at p_1, the resulting Δp is negative. Increasing the angle of attack, α, of the foil, further drops the pressure on the suction side at point B. The pressure at point B cannot drop below zero due to no surface tension support in the water. Hence the flow along the suction side breaks down leading to the formation of cavities. This happens also when the local conditions reach the vapor pressure (and drop below it). Cavitation inception is quantified as:

$$\Delta p = p_1 - p_0 = p_v - p_0 = -(p_0 - p_v)$$



Cavitation Inception*

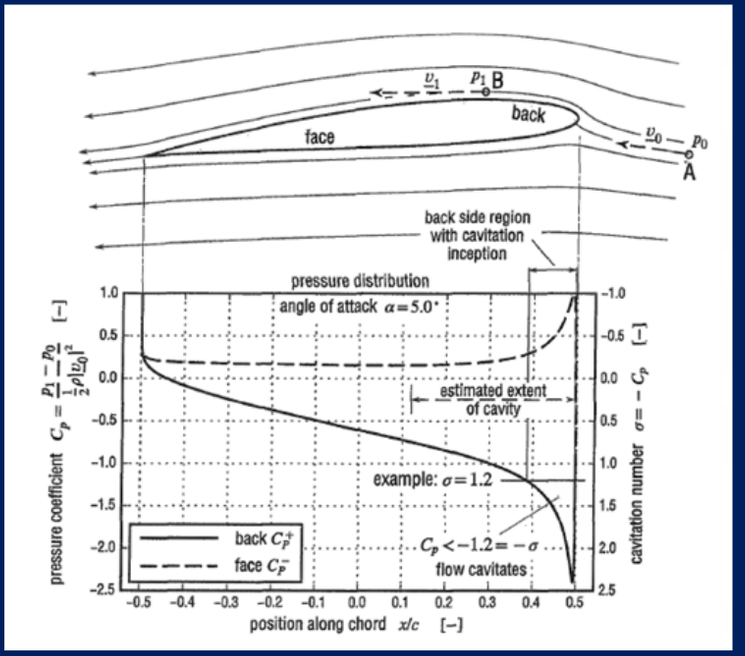
*(Birk, 2019)

Cavitation Inception (con't)

- Dividing both sides by the dynamic pressure, q, gives:

$$\frac{\Delta p}{q} = \frac{-(p_0 - p_v)}{q} = -\sigma \rightarrow -\frac{\Delta p}{q} > \sigma$$

- when this condition is reached, cavitation occurs. The figure shows the situation for σ = 1.2 when cavitation bubbles will occur and grow and further collapse due to increased pressure outside of the cavity. Further stretching of these cavities occurs, followed by subsequent collapsing of the cavitation bubbles.



Cavitation Inception*

*(Birk, 2019)

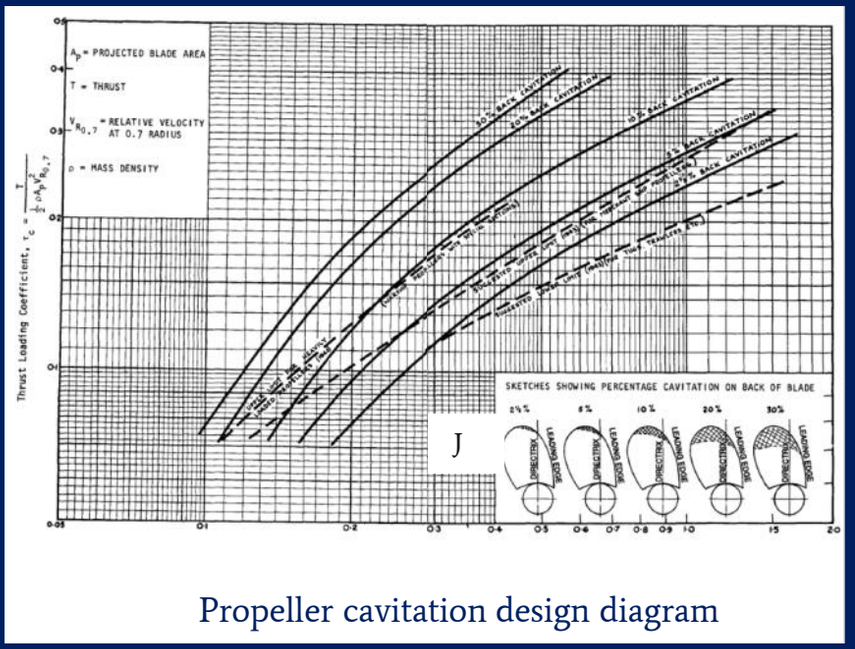
Cavitation and Vessel Performance

- Layers of bubbles on the propeller increases the overall thickness of the blade, which reduces the vessel performance.
- Cavitation number, $\sigma = (2gH) / V^2$, relating absolute static head at the place of cavitation minus the head due to vapor pressure of the liquid, H, and local velocity at the propeller, V (typically taken as the speed of advance of the propeller)

- Reduces thrust
- Increases noise and vibrations
- Decreases life expectancy of propeller blades
- Increases fuel consumption/operation costs

Cavitation and Vessel Performance (con't)

- Need to have low blade area for efficiency reasons (i.e., low drag, etc.)
- But blade must have sufficient area to prevent thrust breakdown
- Typical modern propellers tend to be highly loaded, hence, require large blade areas
- Experimental curves of optimal blade design is shown in the figure on the right*
- Suggested criteria for various designs and amount of back cavitation as function of thrust loading coefficient (at the 0.7R) and advance coefficient, $J = V_A/(nd)$

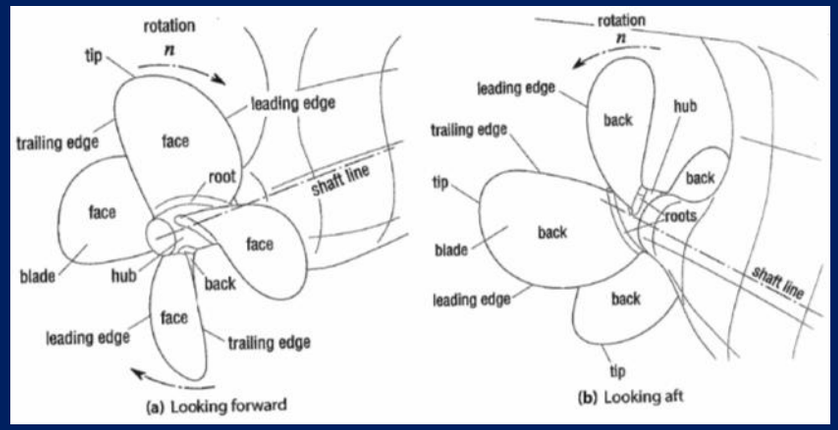


Propeller cavitation design diagram

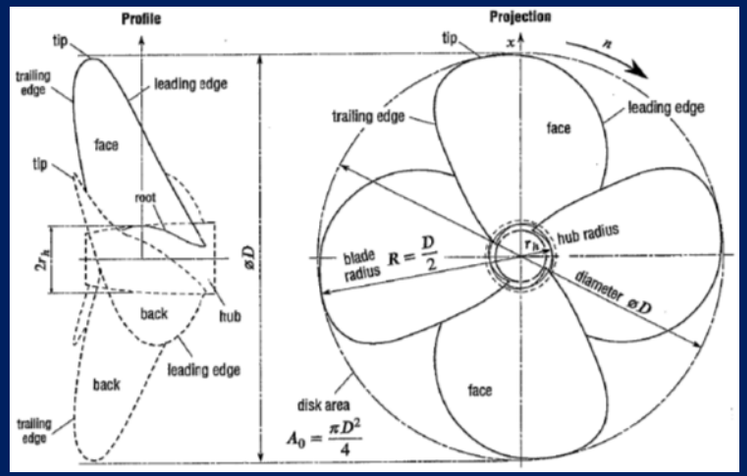
*(Hunt, Harbach and Rowen, Eds, 2002)

Propeller Basics

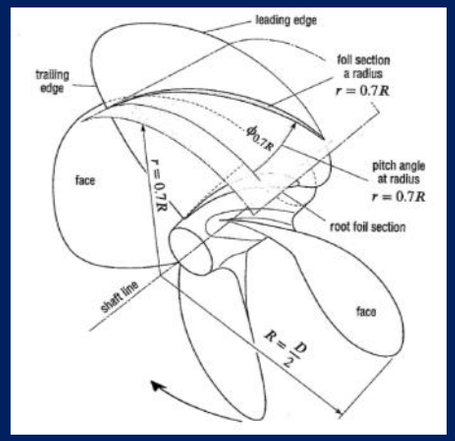
- Similar to aircraft wings (airfoils), propeller blades (hydrofoils) also generate lift force (with part of it parallel to the propeller shaft producing forward thrust)
- Looking forward the face of the blade is the high pressure side
- Looking aft, the back of the blade is the low pressure side
- Similar to airfoils, propeller blades have a leading edge (LE) and a trailing edge (TE)
- Single-screw ships have a right-hand turning blade (CW, ALF)
- Twin-screw ships have oppositely turning propellers
- All else the same, the larger the propeller face area (for a given D), the lower the possibility for cavitation
- However, this increases wetted area and drag
- Modern propellers, with minimal face area are highly stressed, and, hence prone to cavitation



Typical propeller parts*



Typical propeller geometry*

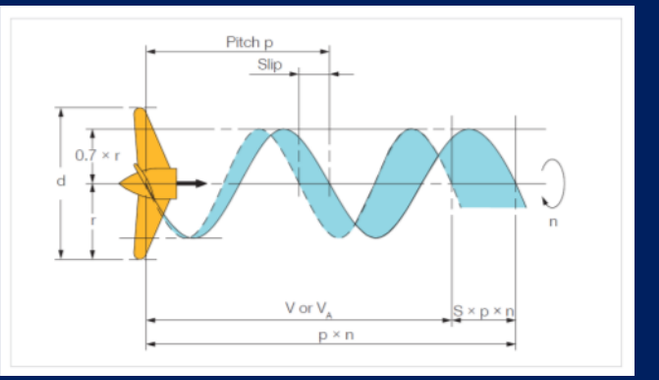


Typical propeller hydrofoil section (at 0.7R)*

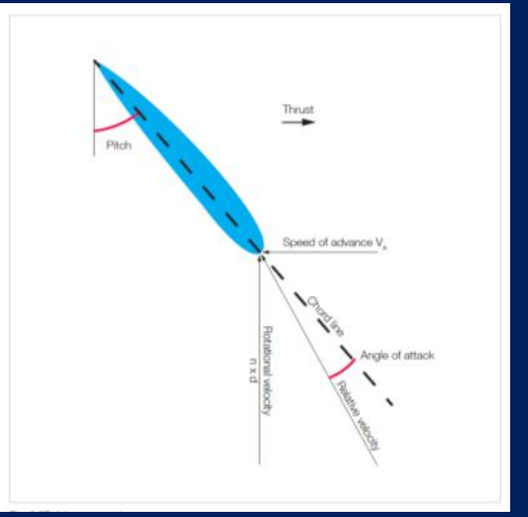
*(Birk, 2019)

Propeller Basics (con't)

- Largest possible propeller diameter, *d*, is desirable for optimal efficiency and lowest fuel consumption of the ship propulsion
- Size limitations due to bottom/keel clearance, top clearance with hull, in all operations propeller must be fully submerged
- This is especially critical to tankers (whose operational draft varies significantly), *d/T = 0.65*
- Pitch diameter ratio, *p/d*, is measured between propeller pitch angle and diameter, *d*
- Typical *p/d = 0.7r* (*r* = propeller radius = *d/2*) depending on propeller revolutions, *n* and propeller diameter, *d*
- Slip of propeller (like a screw) is difference in propeller forward speed drop (due to water "yielding" acceleration aft) and propeller speed in non-yielding medium
- This theoretical propeller forward speed is: *V = p * n*
- Typical propeller blade cross-section is similar to an airfoil (hydrofoil) shape with pressure and suction sides, and angle of attack



Typical propeller pitch and slip*

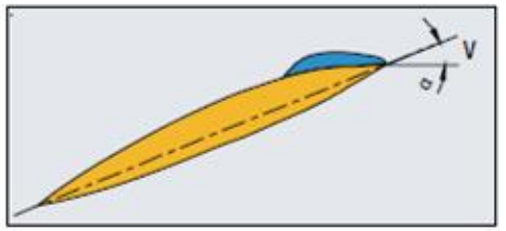


Propeller hydrofoil design*

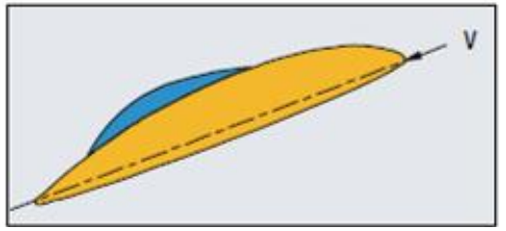
*(MAN Energy Solutions, 2018)

Propeller Cavitation

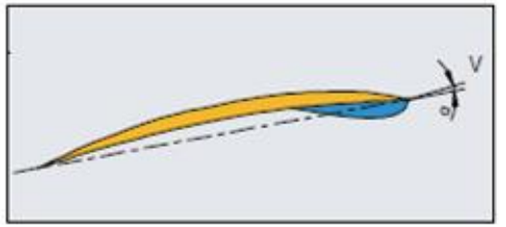
- Layers of bubbles appear when local pressure drops below the fluid's vapor (saturation) pressure
- Migration of bubbles along the propeller blades leads to collapsing of bubbles on the propeller blades' surfaces causing noise and vibrations und ultimately erosion
- Decreases life expectancy of propeller blades
- Increases fuel consumption/operation costs
- Three main types of cavitation* (based on the type- and relative position on the blades surfaces:
- **Sheet cavitation (suction side)** – by leading edge due to low pressure peak. Relatively benign unless extends further along (> 0.5 chord) of the blade – cloud cavitation
- **Sheet cavitation (pressure side)** - similar to other sheet cavitation, but bubbles collapse on the blade surface before leaving the trailing edge. Best blades designed with no pressure side cavitation
- **Bubble cavitation (suction side)** – in most modern high performance propellers, where blade area may be too small for the thrust required. Causes the blade mid-chord to cavitate on suction side. Strong cavitation, leading to large cloud cavitation and very erosive. Must be avoided (mitigated/minimized) at all conditions
- Our project investigated bubble (vaporous) cavitation on the suction side of the propeller blades



Sheet cavitation (on suction side)



Bubble cavitation (on suction side)



Sheet cavitation (on pressure side)

*(MAN Energy Solutions, 2018)

Prototype Vessel

MT-46 Veteran Class Tanker Propeller

- The MT-46 Veteran Class Tanker is based on an Athenian-class 46,000 dwt (design by Hyundai Mipo Dockyard, HMD) Jones Act product tanker built by Aker Philadelphia shipyard, USA*
- The MT-46 Veteran Class tanker has an overall length of 183.2 m, molded breadth of 32.2 m, and scantling draft of 12.2 m with a capacity of approx. 330,000 barrels.

Prototype Propeller (4-bladed FPP, pitch = 0.7R)

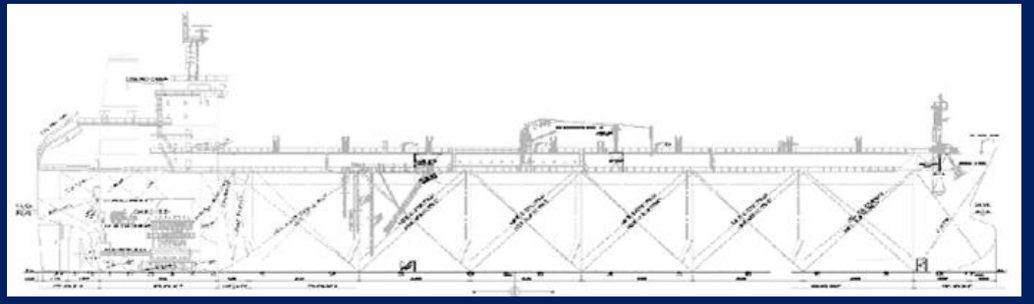
- Diameter = 5.82 m
- Normal Operation Speed: 100 RPM

3-D Model Propeller (4-bladed FPP, pitch = 0.7R)

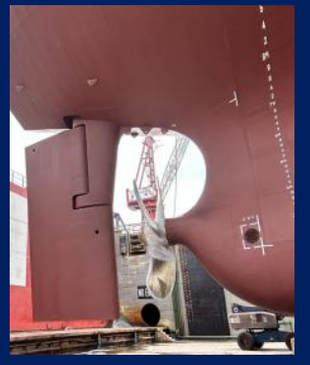
- Diameter = 202.87 mm
- Blade length = 100 mm
- Blade height = 67.55 mm
- Simulated Operation Speed: 100 RPM

*(Ship Technology, 2010)





MT-46 Veteran Class Tanker



MT-46 Veteran Class Tanker four-bladed FPP

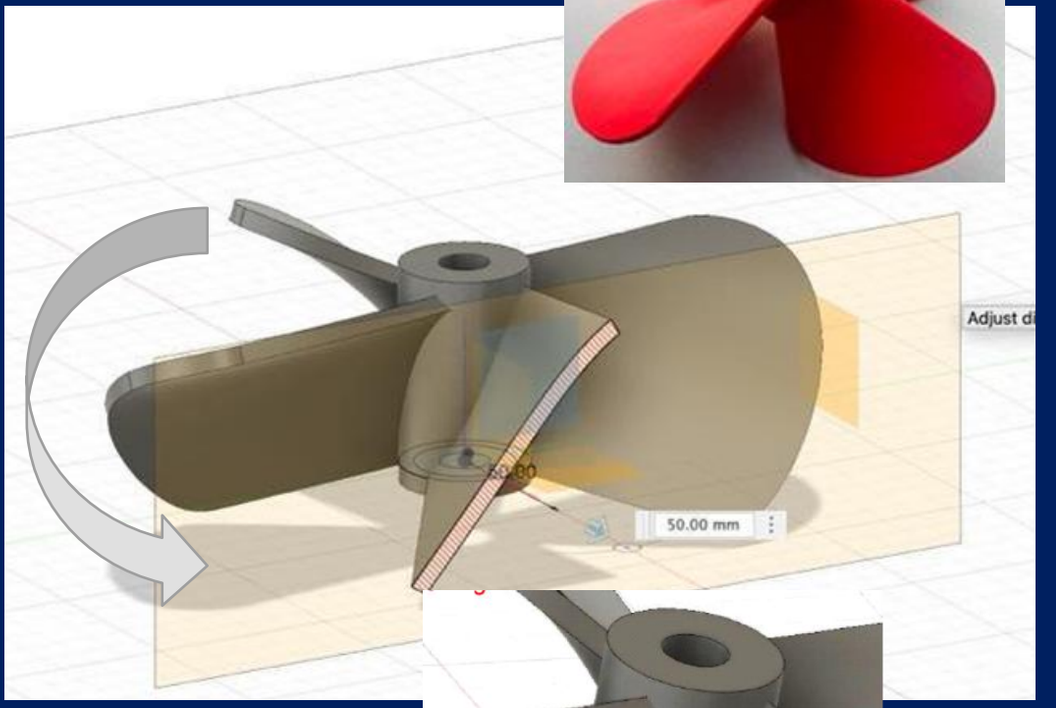
3D Model of a Conventional Propeller

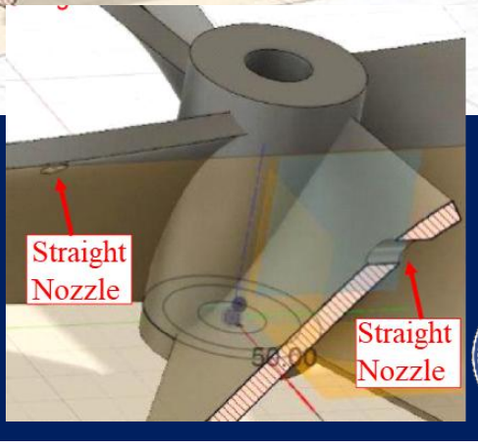
- 3D model by Fusion 360 (top right image in red)
- CFD simulation by EasyCFD
- Prototype Propeller: 4-bladed fixed pitch (0.7R)
- Prototype Propeller Dia. = approx. 5.8 m
- Model propeller Dia. = 202.87 mm
- Resulting scale = approx. 1:28.6
- Model Propeller Blade Length = 100 mm
- Blade Height = 67.55 mm
- Pitch = 0.7R = 0.35D
- Pitch length = D(P/D) = 202.87 mm (0.35D/D) = 71 mm
- Pitch angle, ϕ (at $x = 0.7R$) = 17.66°

$$\tan\phi = \frac{P_{length}}{\pi Dx} = \frac{PP_{length}}{\pi(0.35D)} = \frac{71\ mm}{\pi(0.35)(202.87\ mm)} = 0.318289$$

$$\phi = \tan^{-1} 0.318289 = 17.66°$$

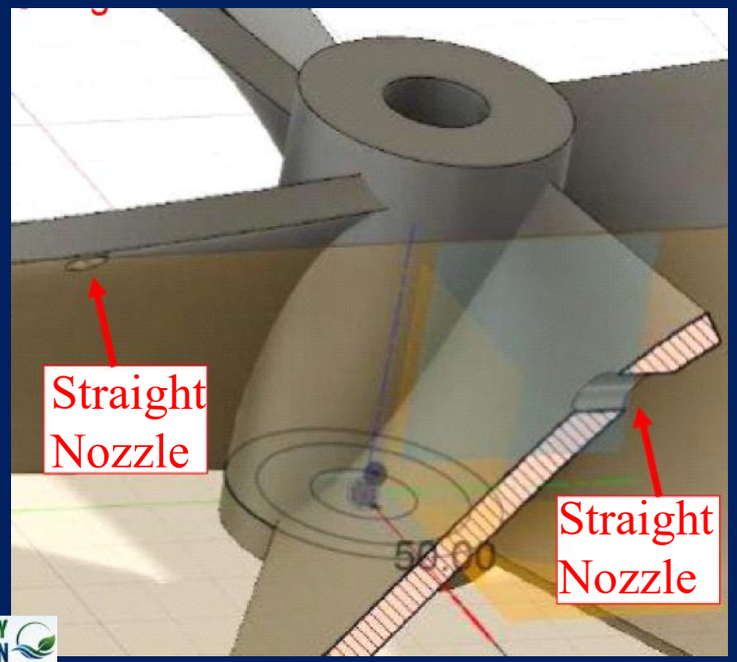


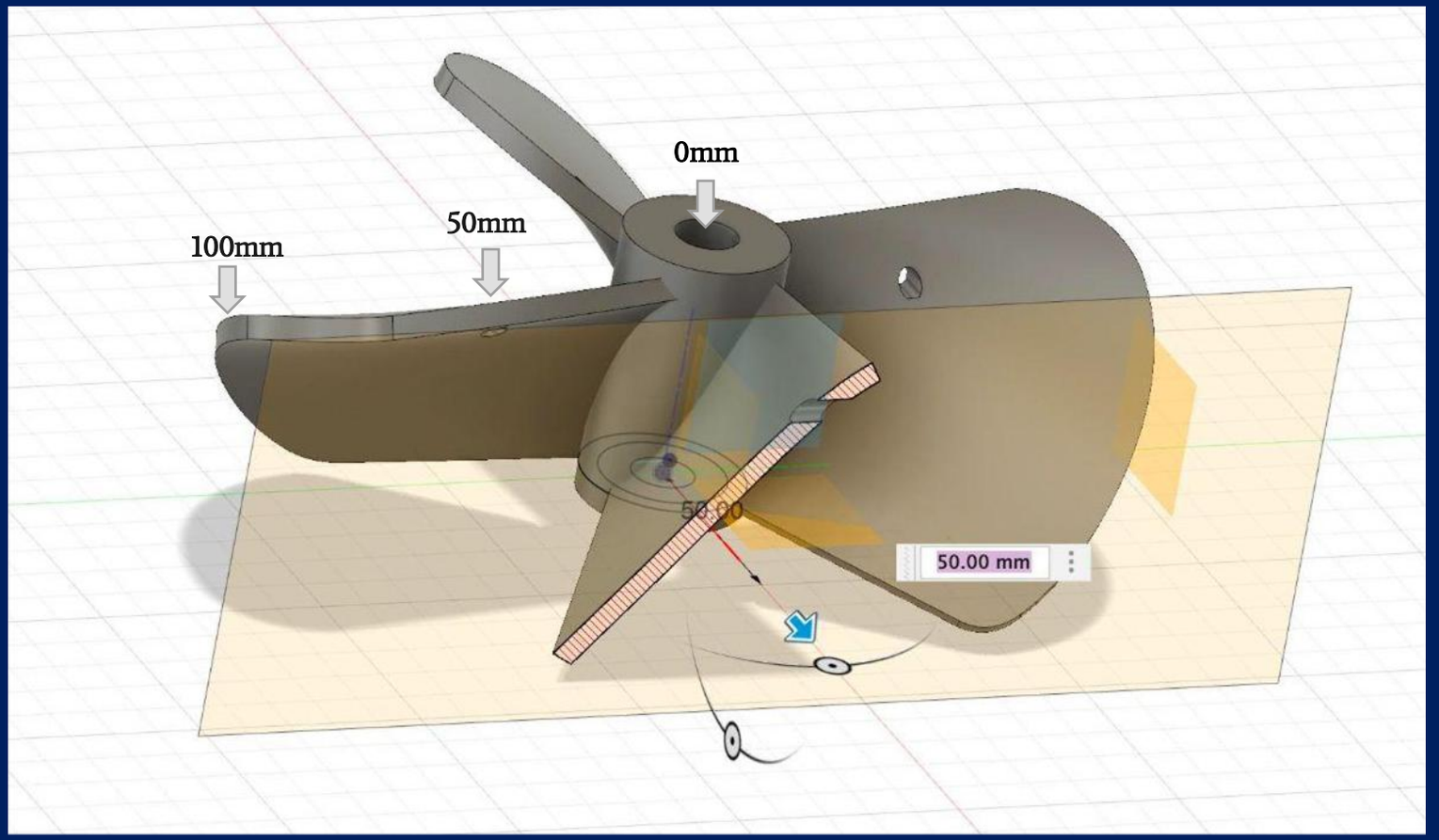




3D Model of a Propeller with Straight Nozzle

- Propeller with Nozzle at 50 mm from the hub
- Propeller was printed using an “Original Prusa i3 MK3S+ 3D printer”.





EasyCFD Brief Background

- EasyCFD* is a commercially available teaching tool for CFD designed to be simple to use
- EasyCFD can solve both fluid flow and heat transfer problems (but only in 2-D)
- During pre-processing of CFD model, one selects an appropriate turbulence model. The challenge is to accurately capture the many varying features of turbulent flow, i.e., turbulent eddies
- Also, as the *Re* number increases so do the *differences in the length scales* between the largest and the smallest turbulent eddies**
- In most CFD programs, turbulence is modeled by parametric fits to experimental results
- Traditionally, there are two broadly-defined families of CFD models: **Scale Resolving Simulations (SRS)** and **Reynolds Averaged Navier Stokes (RANS)**
- While **SRS** is very accurate (at the expense of resource intensive requirements, **RANS** is rather economical (but with lower accuracy)
- Alternative to RANS, **Unsteady RANS (URANS)** has been applied to simple eddy viscosity models with no attempts to resolve spatial and temporal scales

SUSTAINABILITY AND INNOVATION IN SHIP DESIGN AND OPERATIONS CONFERENCE 2026

*(Lopes, 2016a)
**(Tennekes and Lumley, 1972)

EasyCFD Brief Background (con't)

- EasyCFD offers two turbulence RANS models: κ-ε and **SST** κ-ω
- ***κ-ε model*** – a model which specifies in its calculation both κ (turbulent KE) and ε (turbulent dissipation rate), hence κ-ε* (one of the most popular turbulence models used in CFD)
- This "two-equation" model adds two more transport equations (to be solved simultaneously)with equations for mass and linear momentum)
- Also, two additional B.C.'s must be specified for the turbulence properties at the inlet and outlet**
- ***SST (Shear Stress Transport) κ-ε model*** – another two-equation turbulence model which also specifies both κ and ε
- This is a variation of the standard κ-ε *m* model, combining the standard κ-ε model for use near walls with the κ-ε model. This is robust for B.L. flows with pressure gradients and at near-wall conditions
- The CFD simulations for this work were done using Easy CFD with the ***SST*** model with a mesh size of approx. 3500-4700 cells. This varies based on geometric construction.

SUSTAINABILITY AND INNOVATION IN SHIP DESIGN AND OPERATIONS CONFERENCE 2026

*(Menter, 1993; 1994)
**(Launder and Spaulding, 1974)

CFD for a Propeller with Nozzle

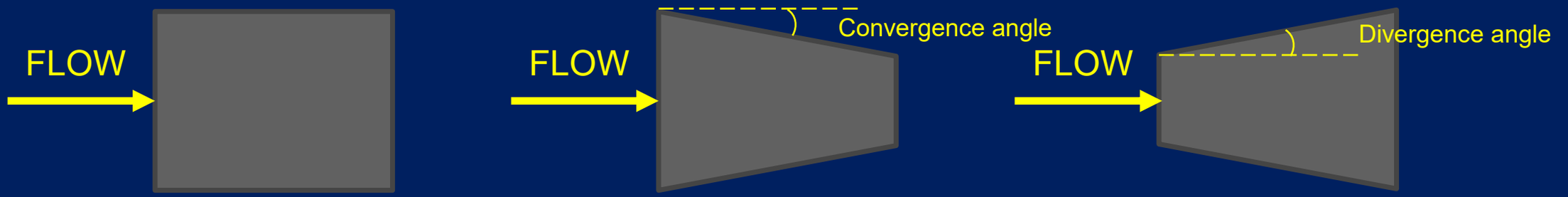
- Using a proopsed “nozzle” to convert the flow energy from the front (pressure) side (“P”) of the propeller into high pressure on the back (suction) side (“S”) of the propeller blade in an effort to mitigate local cavitation on suction side
- Three nozzle types were simulated:

- Straight – Direct Flow

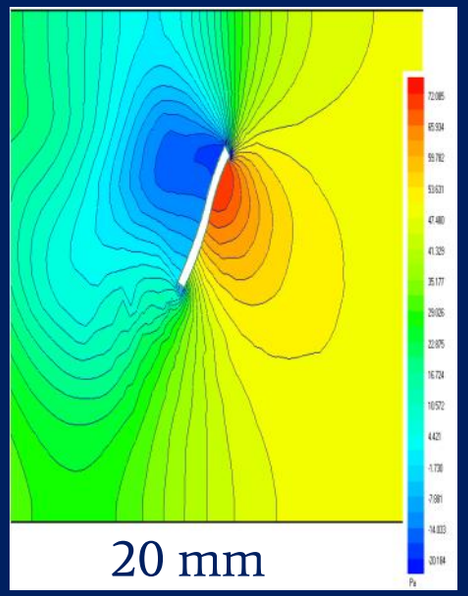
- Convergent – Velocity Increases, Pressure Decreases: 3.1-deg. **convergence** angle

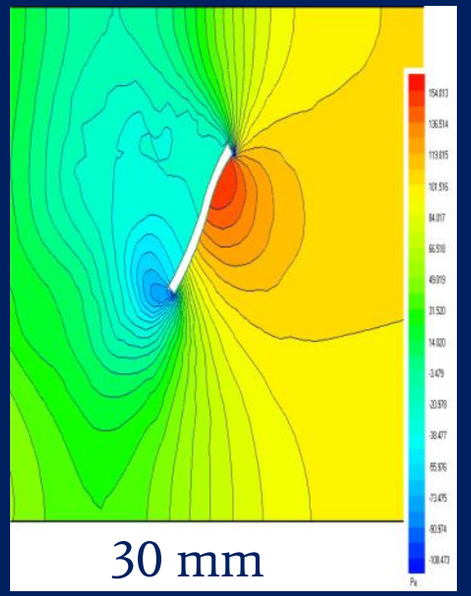
- Divergent – Velocity Decreases, Pressure **Increases**: 2.1-deg. **divergence** angle (initial)

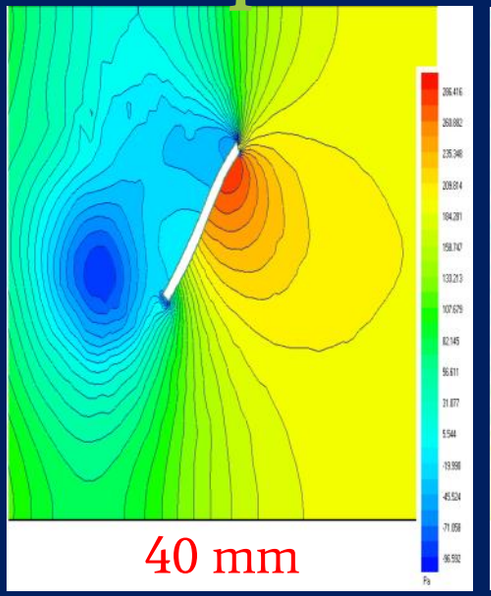
- Divergent – after initial success, other configurations were tested (5-, 10-, 15-, and 18-deg)

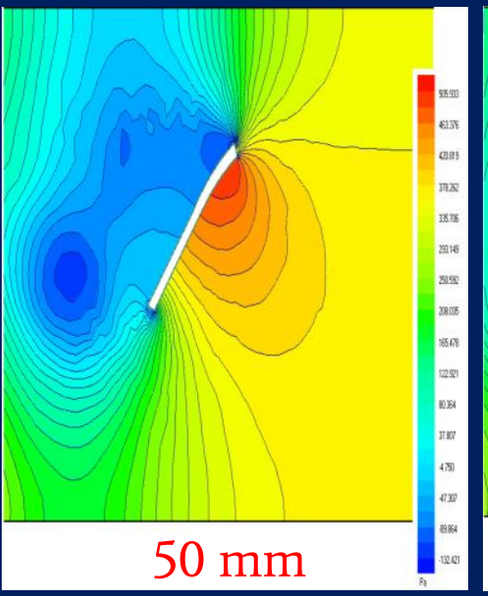


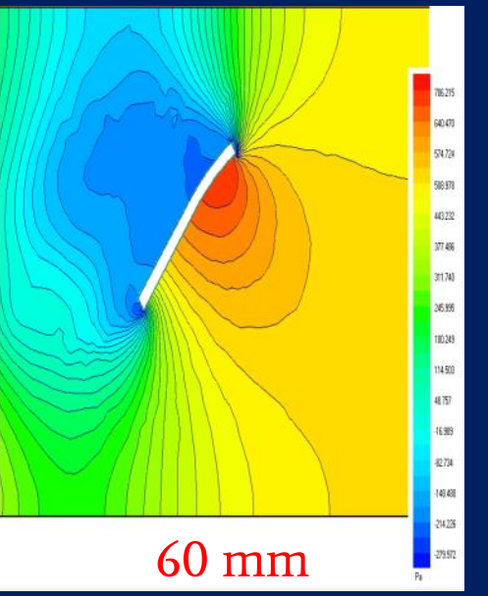
CFD for a Conventional Propeller – Cross Sectional View

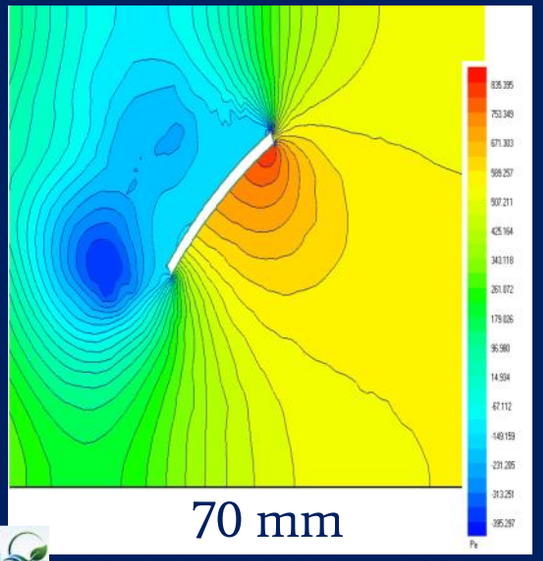

20 mm

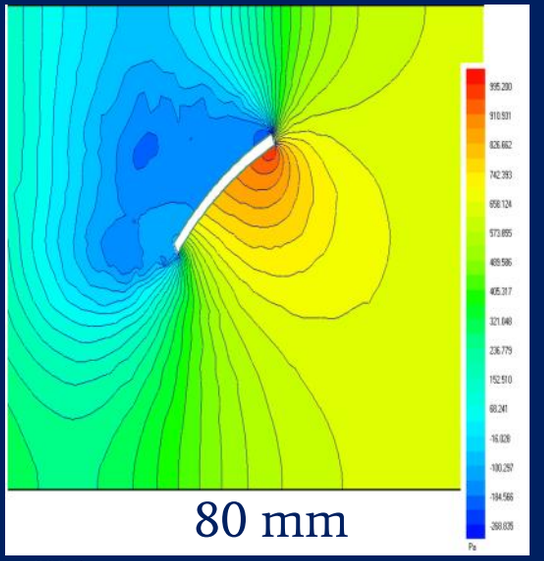

30 mm

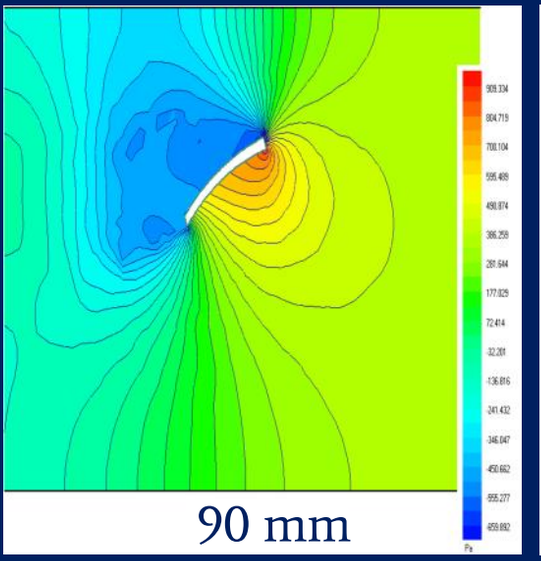

40 mm

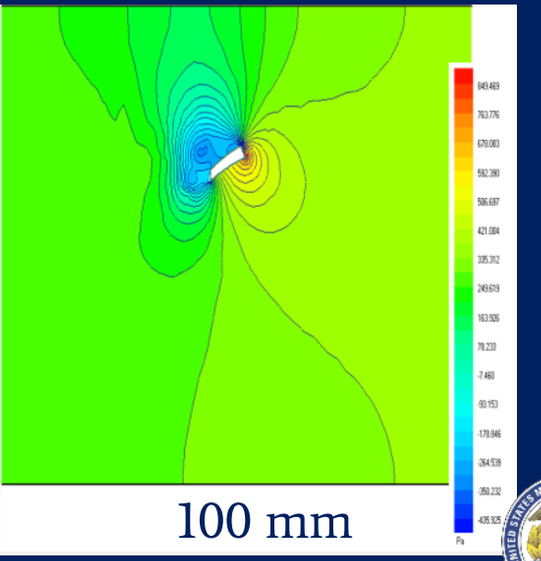

50 mm


60 mm


70 mm


80 mm


90 mm


100 mm

*(Davis, A., Du., M.-H., Nilsson, K., & Ribarov, L.A., 2024)

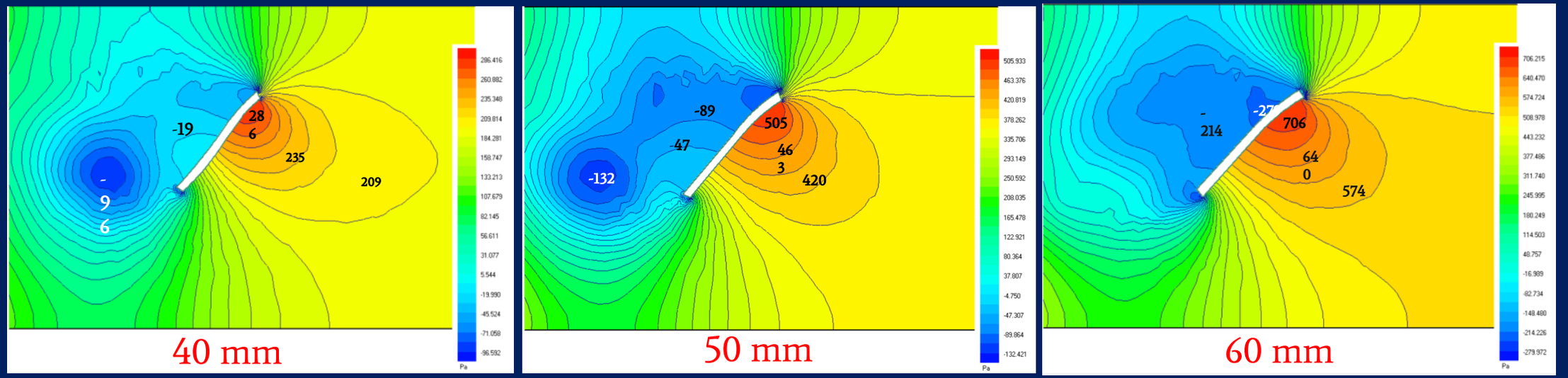
CFD for a Conventional Propeller

Critical Points of Discussion:

- Low pressure zones of interest on suction (“S”) side of blade
- These will cause a low enough pressure to form vapor cavitation bubbles

Note: All pressure measurements are in pascals (Pa) and are gauge pressure

(Relative pressures are depicted through the color scheme)

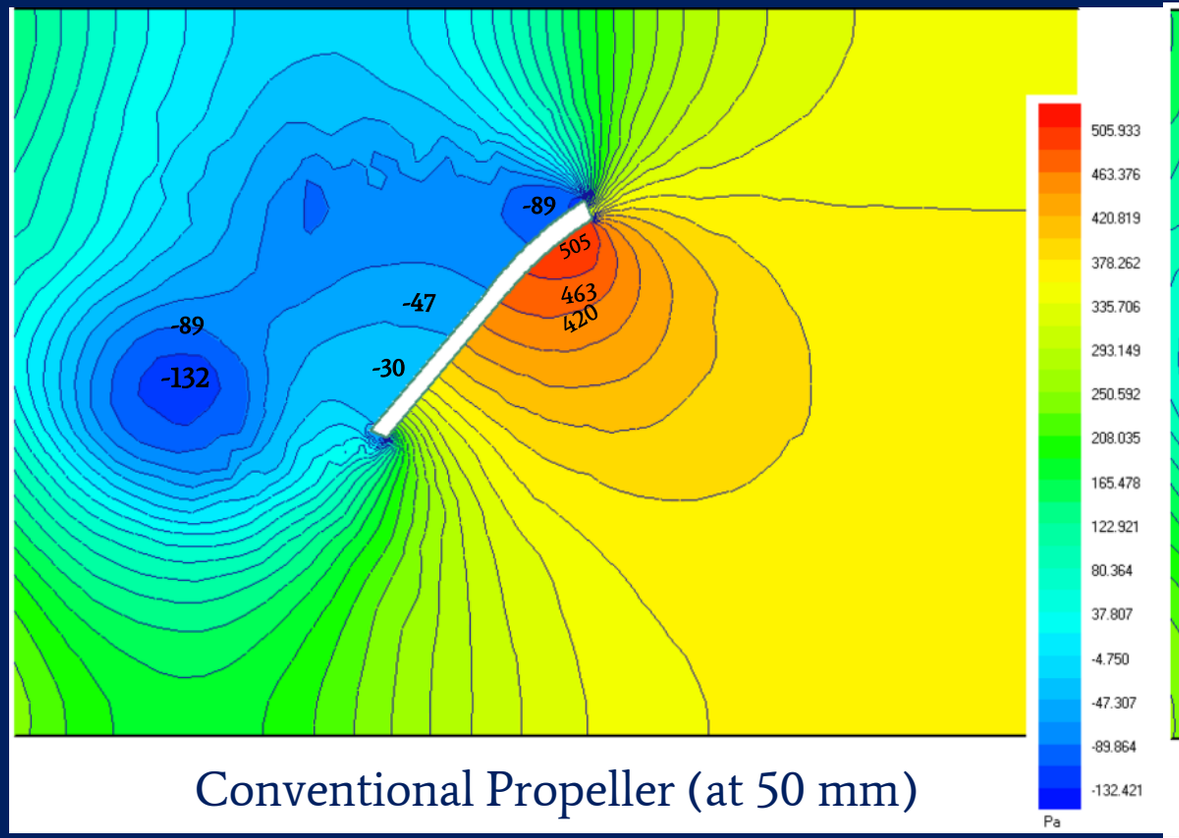


*(Davis, A., Du., M.-H., Nilsson, K., & Ribarov, L.A., 2024)

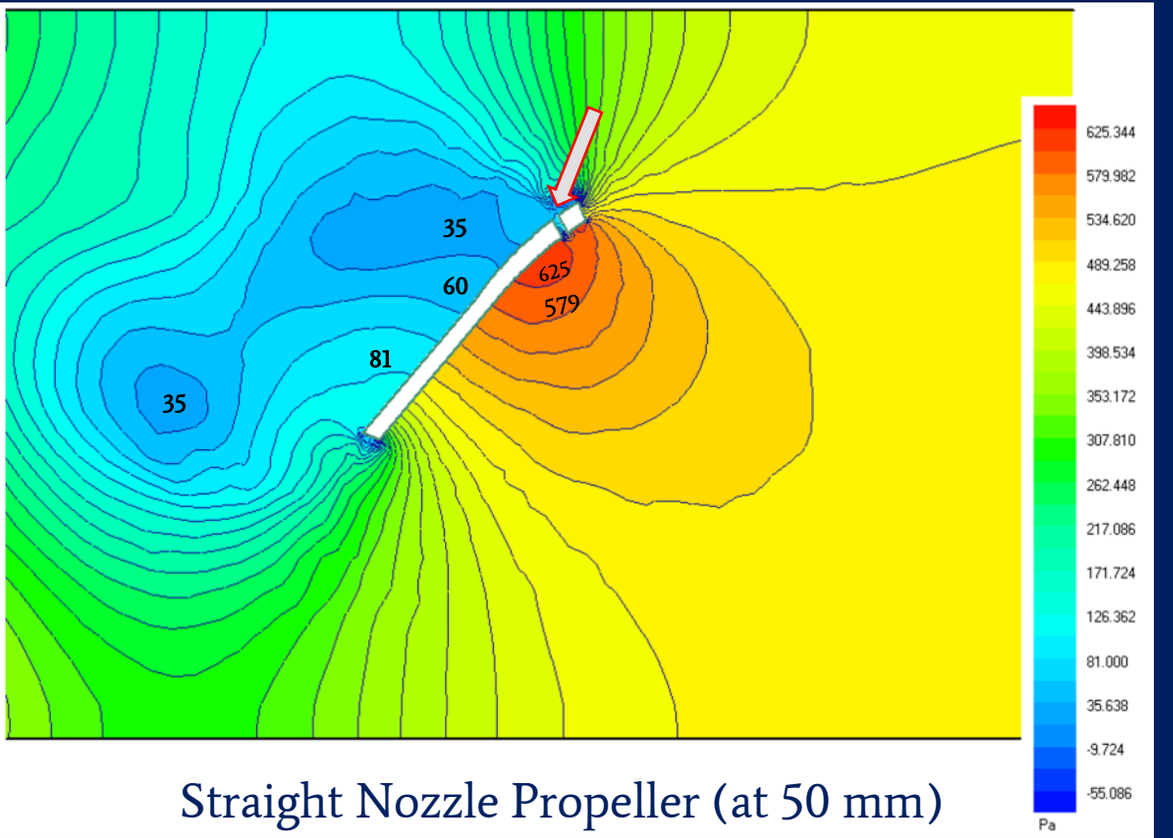
CFD for a Propeller with Straight Nozzle

CFD Results* Comparison of Conventional Propeller and Propeller with Straight Nozzle

- Improvement of the pressure field distribution on the **suction side** of the propeller blade



Conventional Propeller (at 50 mm)



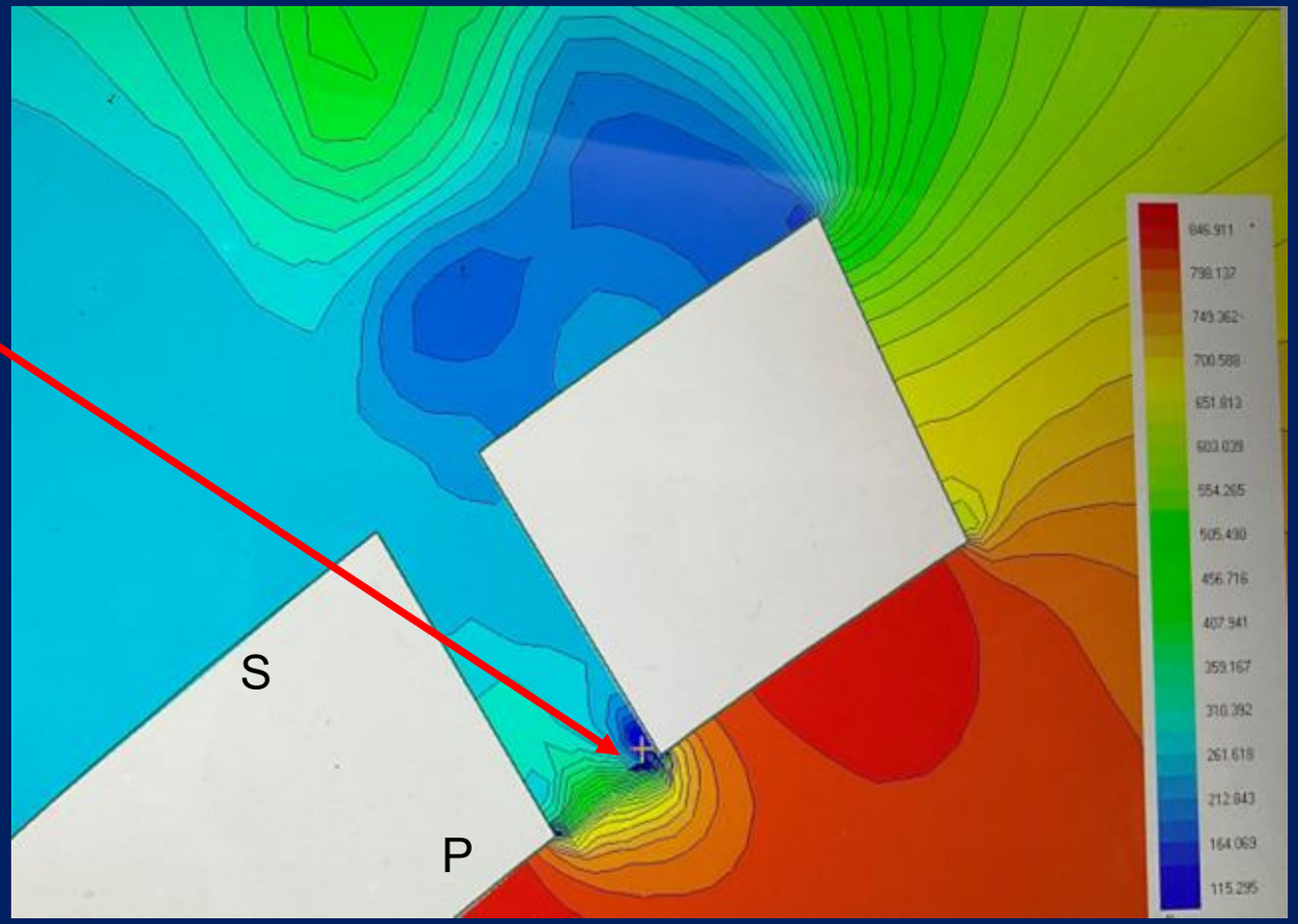
Straight Nozzle Propeller (at 50 mm)

*(Davis, A., Du., M.-H., Nilsson, K., & Ribarov, L.A., 2024)

CFD for a Propeller with Straight Nozzle

Closer Look* at Straight Nozzle

- Walls of straight nozzle are parallel
- There is still a low pressure zone at the entrance of the straight nozzle
- Overall, the low pressure zone is decreased compared to a conventional propeller design
- Leading towards a propeller improvement in **diminishing propensity for cavitation** on suction side of the blade

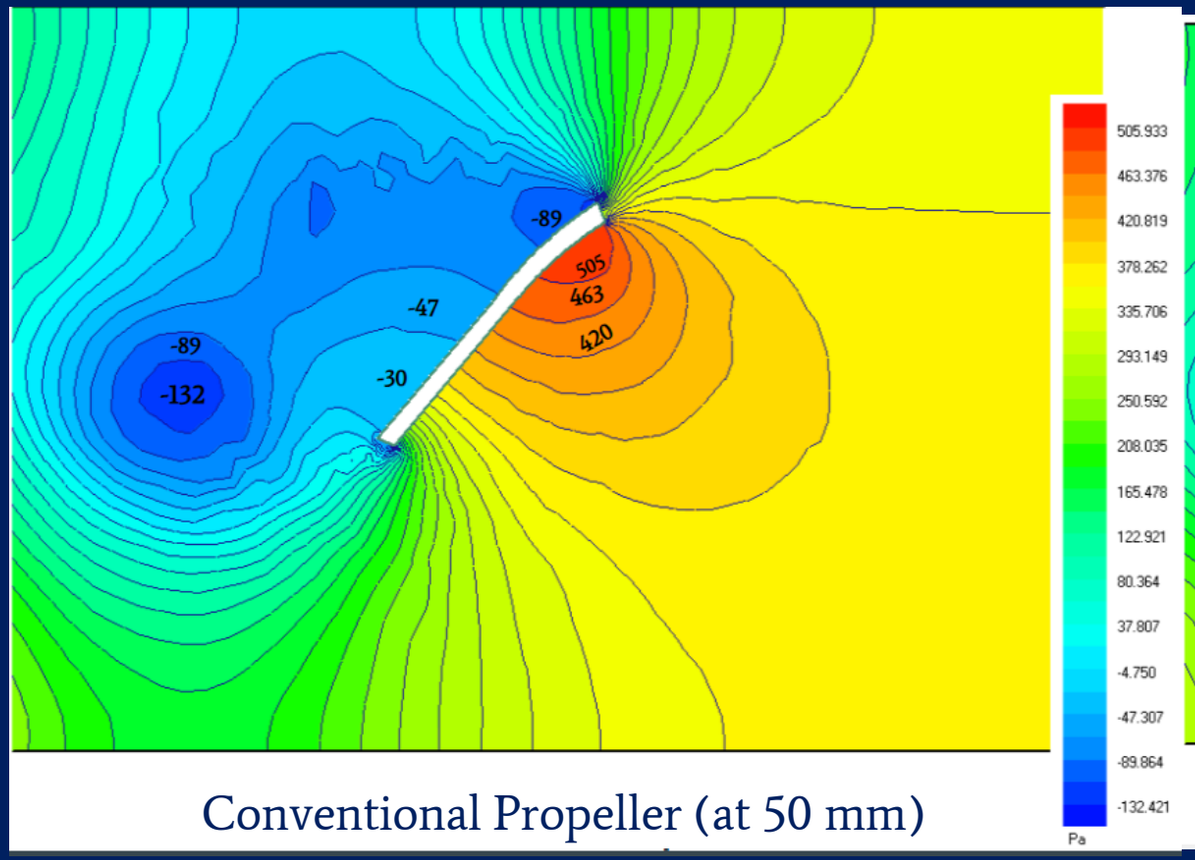


*(Davis, A., Du., M.-H., Nilsson, K., & Ribarov, L.A., 2024)

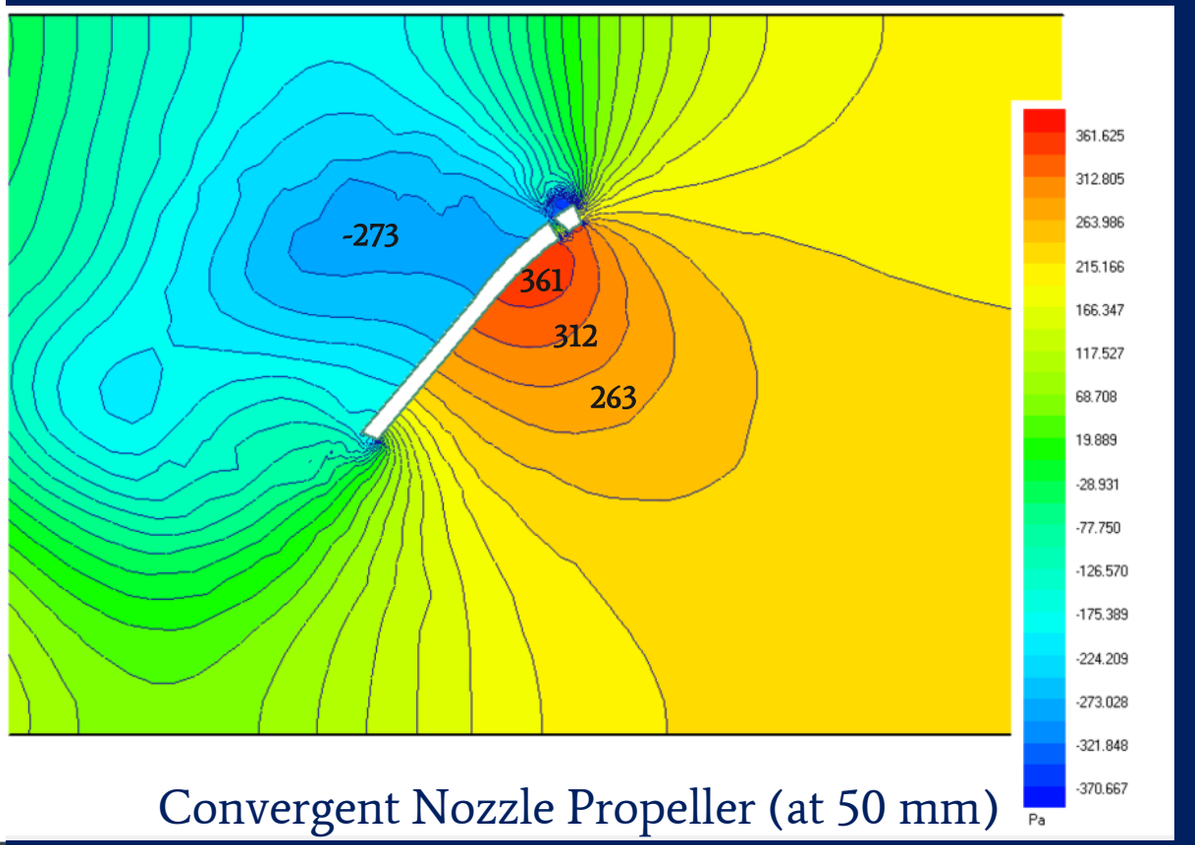
CFD for a Propeller with Convergent Nozzle

CFD Results* Comparison of Conventional Propeller and Propeller with Convergent Nozzle

- No improvement of the pressure field distribution on the **suction side** of the propeller blade



Conventional Propeller (at 50 mm)



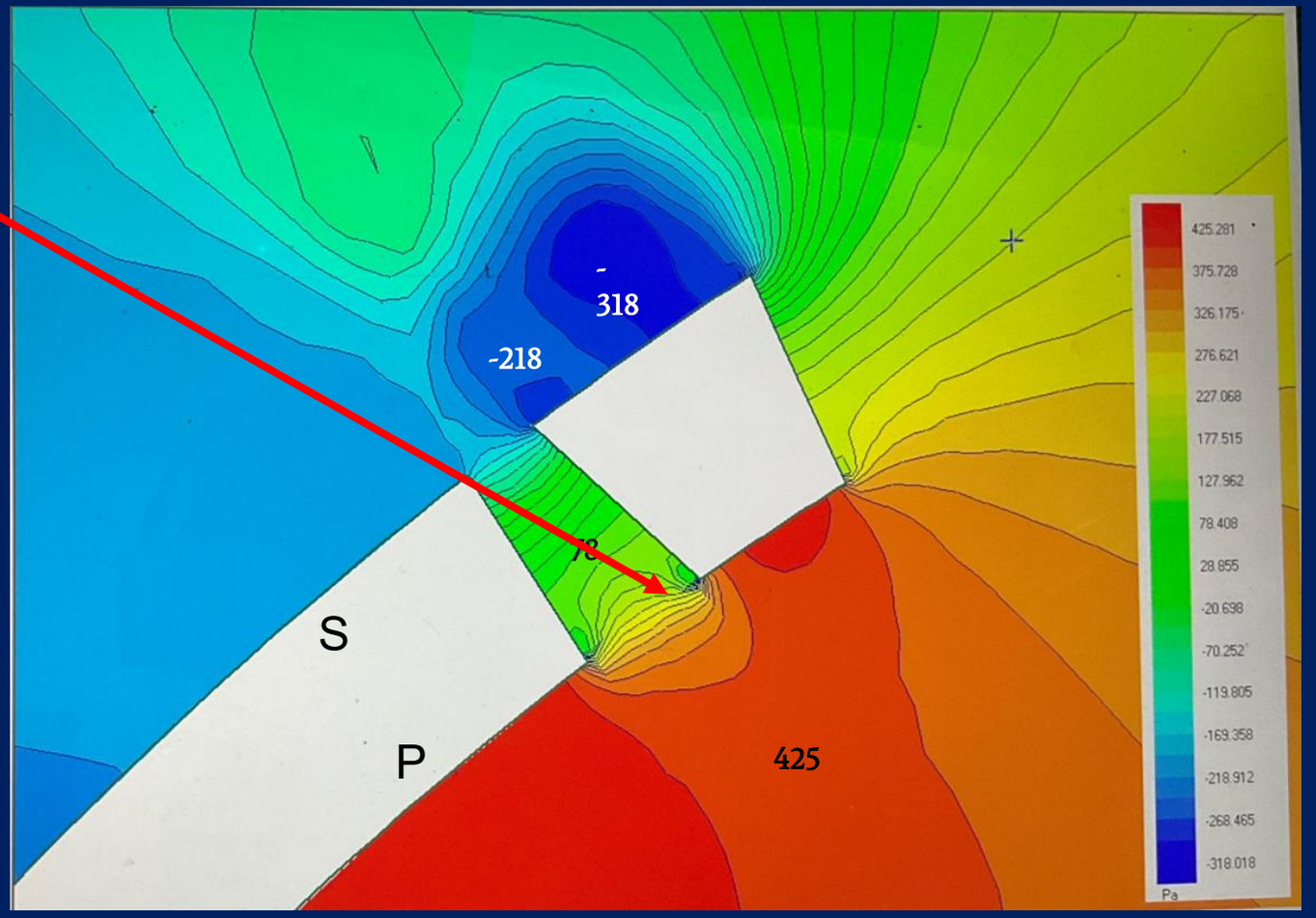
Convergent Nozzle Propeller (at 50 mm)

*(Davis, A., Du., M.-H., Nilsson, K., & Ribarov, L.A., 2024)

CFD for a Propeller with Convergent Nozzle

Closer Look* at Convergent Nozzle

- Elimination of the entire low-pressure zone within the nozzle entrance
- Position may need to be adjusted to be aligned with the low pressure zone that normally occurs
- Accelerated flow exiting the convergent nozzle creates even lower pressure zone on suction side
- 3.1-deg. convergent angle

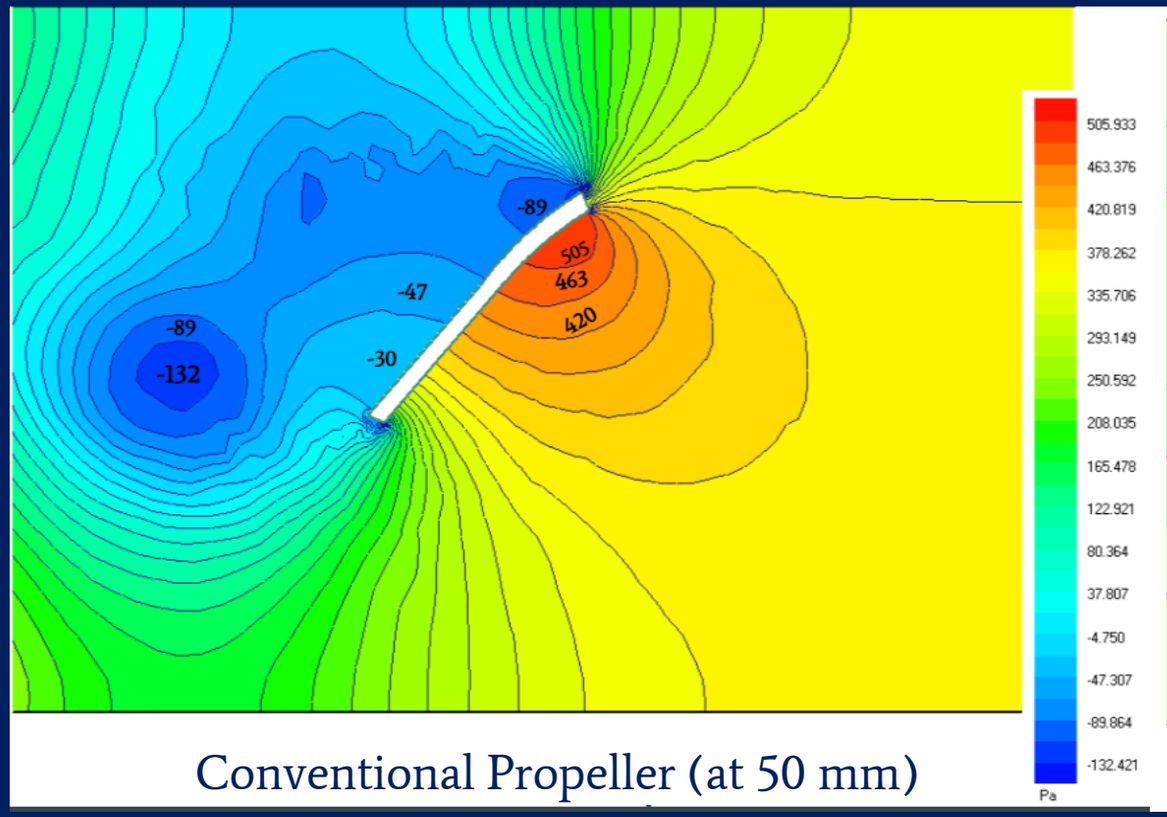


*(Davis, A., Du., M.-H., Nilsson, K., & Ribarov, L.A., 2024)

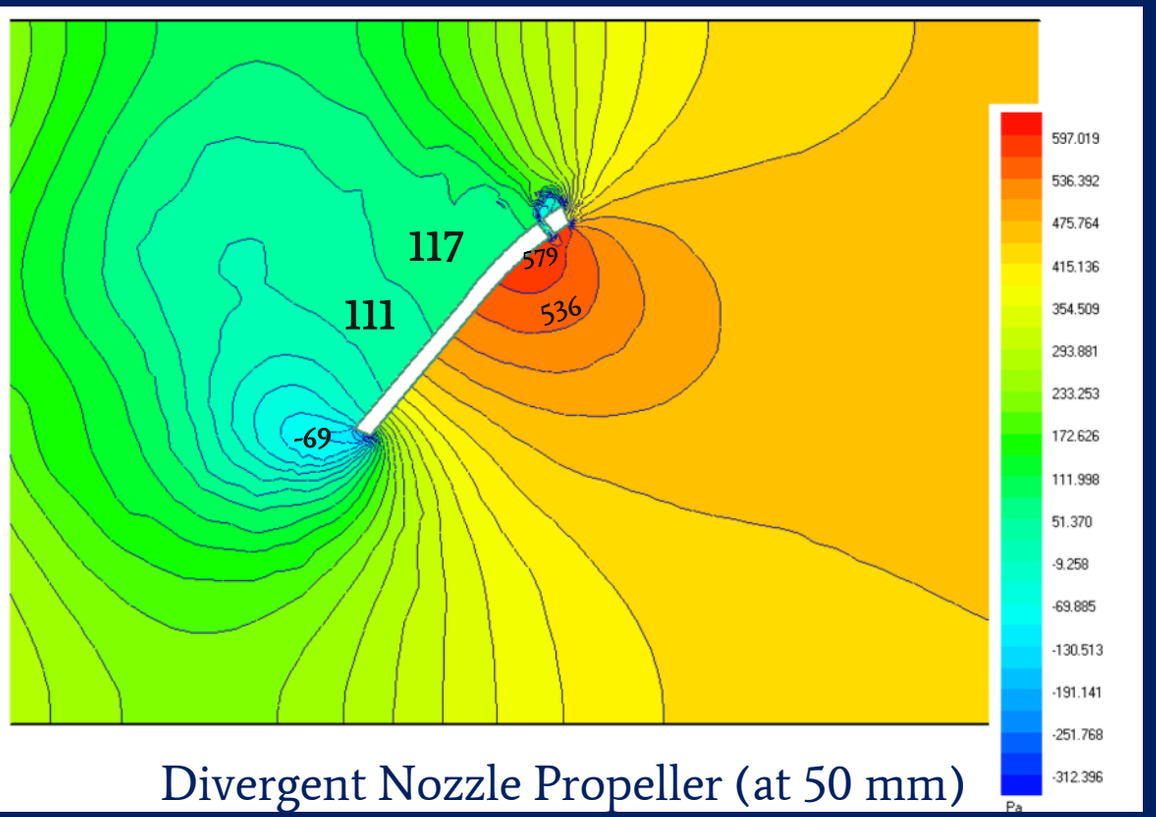
CFD for a Propeller with Divergent Nozzle

CFD Results* Comparison of Conventional Propeller and Propeller with Divergent Nozzle

- **Significant** improvement of the pressure field distribution on the **suction side** of the propeller blade



Conventional Propeller (at 50 mm)

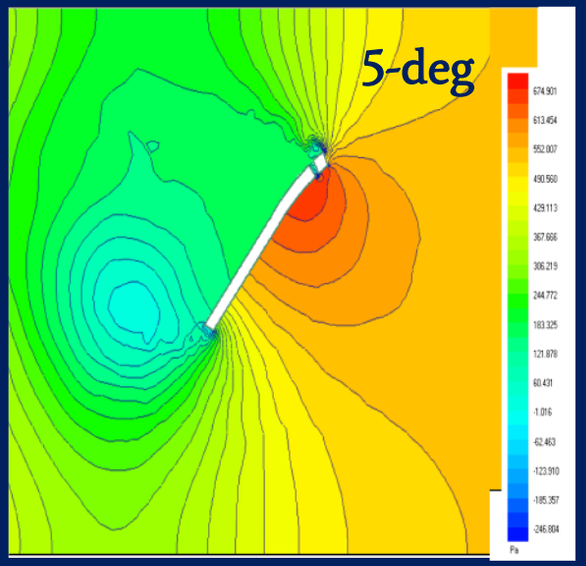


Divergent Nozzle Propeller (at 50 mm)

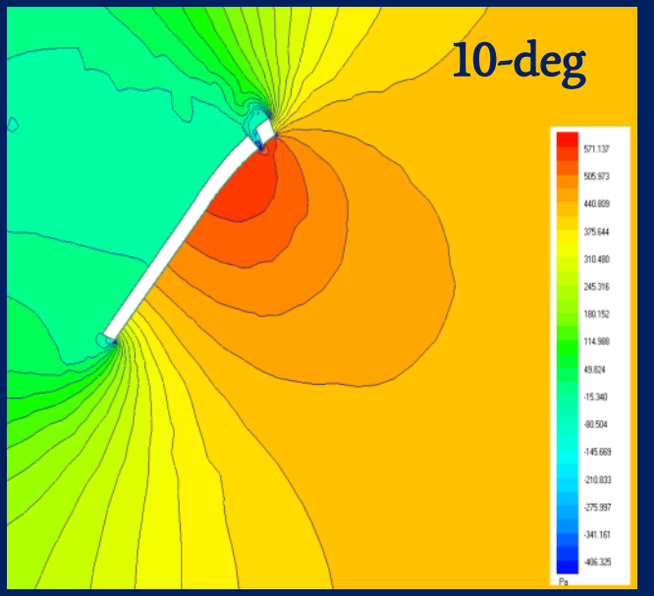
*(Davis, A., Du., M.-H., Nilsson, K., & Ribarov, L.A., 2024)

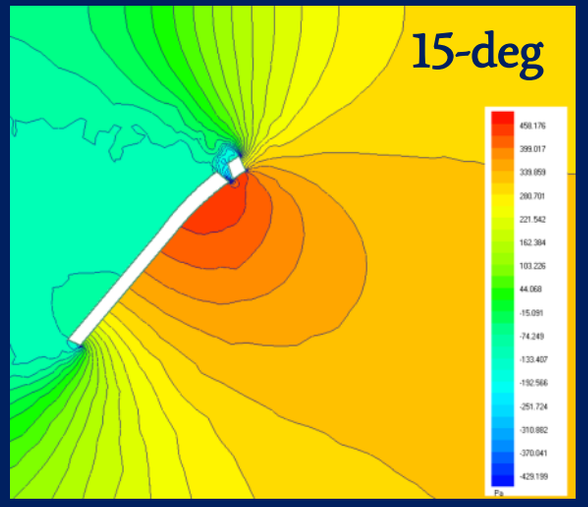
CFD for a Propeller with Divergent Nozzle

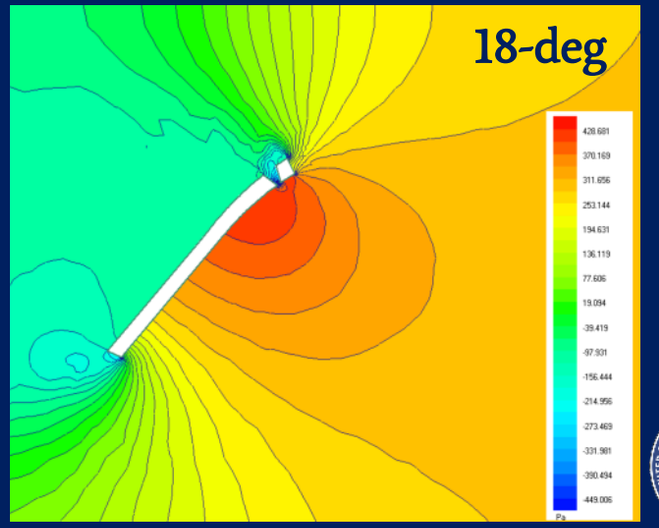
Pressure Results* Comparison of Propeller with Various Divergent Nozzles Angles (at 50 mm)



- Low pressure zone located at nozzle entrance (5-deg.)
- **Much higher** pressure at the nozzle exit
- There is a **significant reduction** in the **propensity for cavitation**
- Best results for smaller divergent angles



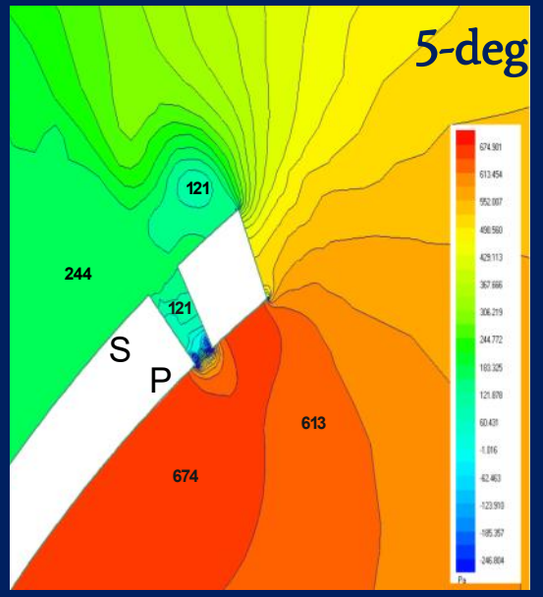


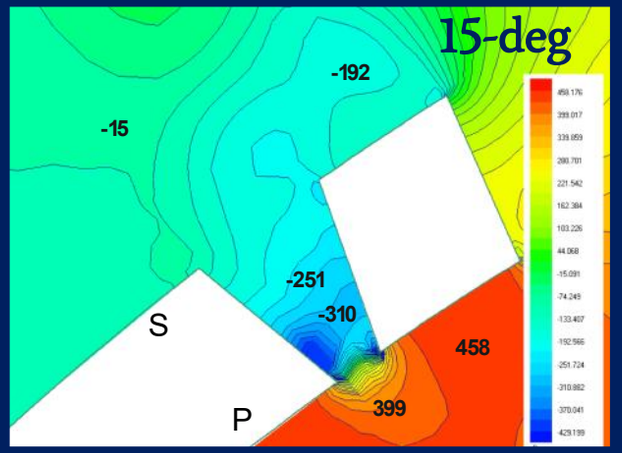


*(Davis, A., Du., M.-H., Nilsson, K., & Ribarov, L.A., 2024)

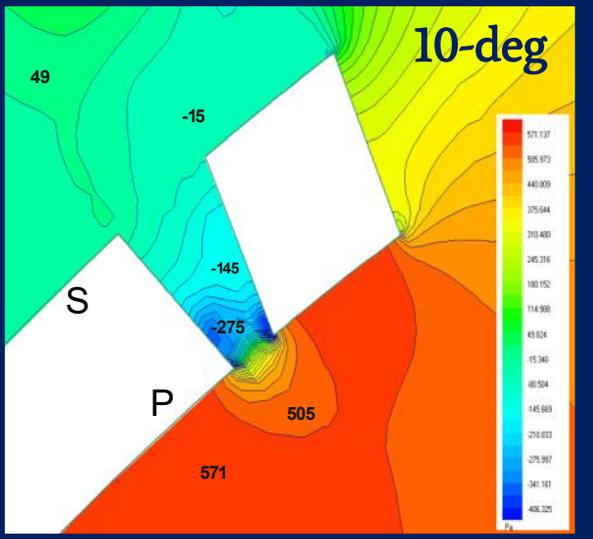
CFD for a Propeller with Divergent Nozzle

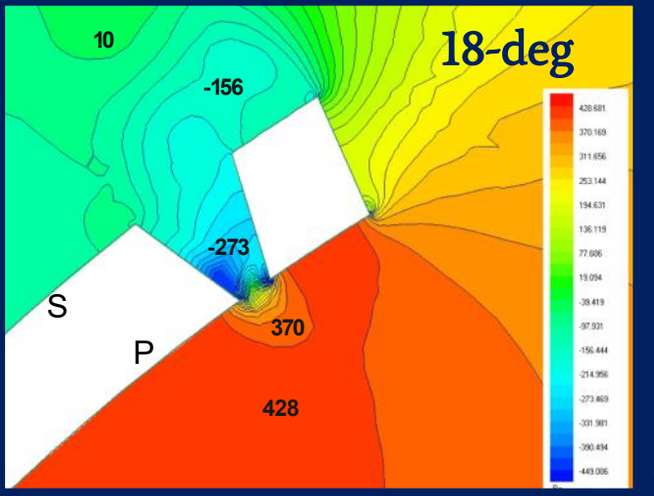
Pressure Results* Comparison of Propeller with Various Divergent Nozzles Angles





- Low pressure zone located at nozzle entrance
- <u>Much higher</u> pressure at the nozzle exit
- There is a **significant reduction** in the propensity for cavitation
- Higher divergence angles result again in lower pressures on suction side (due to recirculation (unwanted)
- <u>Best results occurred for 5-deg. divergent angle</u>

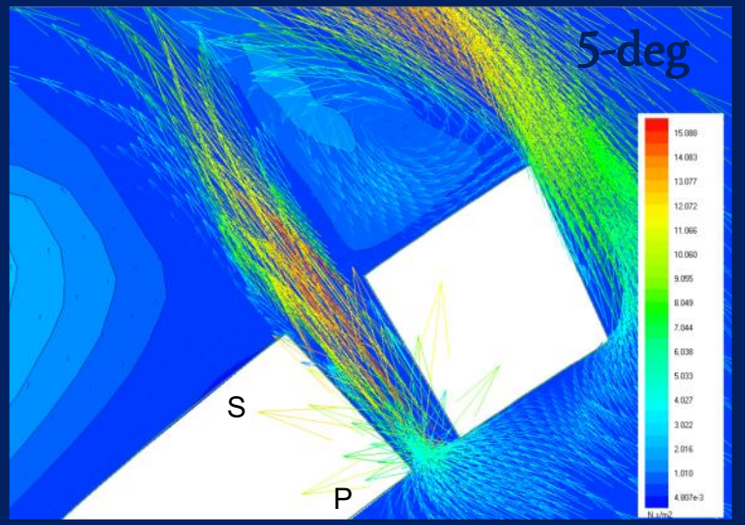


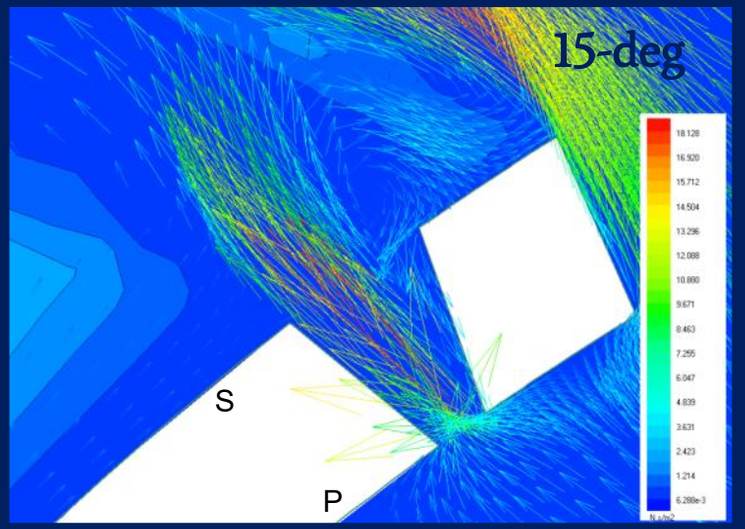


*(Davis, A., Du., M.-H., Nilsson, K., & Ribarov, L.A., 2024)

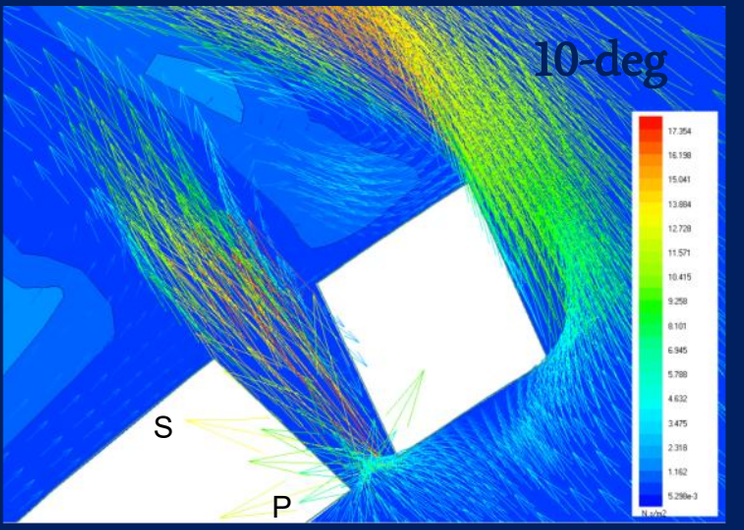
CFD for a Propeller with Divergent Nozzle

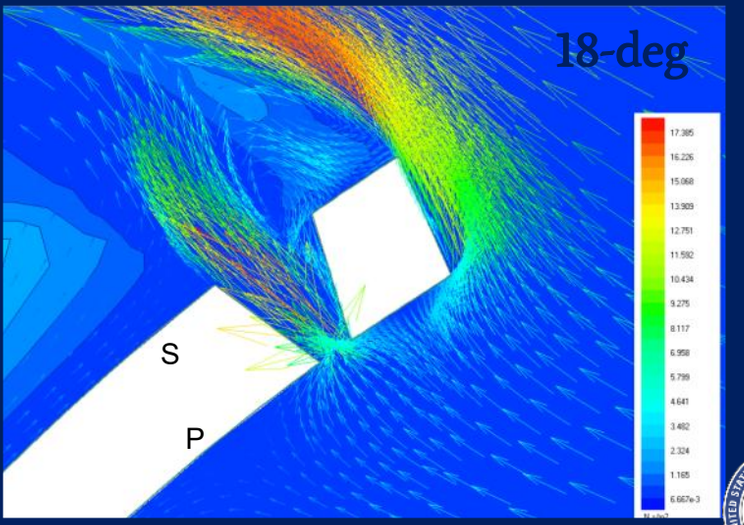
Velocity Field Results* Comparison of Propeller with Various Divergent Nozzles Angles





- No recirculation of fluid through the nozzle (some recirculation around the leading edge (of the blade)
- At the higher divergence angles (> 10-deg.) a slight recirculation beginning to occur at the exit of the nozzle
- At 18-deg. recirculation occurring at the exit of the nozzle (clearly visible)
- This recirculation is undesirable because it will increase the chance of cavitation





*(Davis, A., Du., M.-H., Nilsson, K., & Ribarov, L.A., 2024)

Ship Resistance Calculations

- To determine the total displacement, need to know the mass of the light ship, LWT
- For a product tanker, we used this relationship*: $0.15 < LWT/DWT < 0.30$
- Selected a value of 0.25 so that $LWT = 0.25$ x $DWT = 0.25$ x 40700 t = 10175 t
- Total displacement $\nabla = LWT + DWT = 40700$ t + 10175 t = 50875 t
- For s.w. density $\rho = 1026$ kg/m^3, we got $VOL = \nabla/\rho = 50875$t / (1.026 t/m^3) = 49586 m^3
- Next, the block coefficient, C_B, was calculated:

$$C_B = \frac{\nabla}{L_{WL}\ x\ B_{WL}\ x\ T} = \frac{49586\ m^3}{174\ m\ x\ 32.2\ m\ x\ 11\ m} = 0.804$$

- This compared well with the established range of values ($0.75 < C_B < 0.80$) for product tankers**
- Wetted hull surface, S, was calculated using the Mumford Formula:

$$S = 1.025\ L_{PP}\ (C_B * B + 1.7T) = 1.025\ (174\ m)(0.804 * 32.2\ m + 1.7 * 11\ m) = 7952\ m^2$$

*(MAN Energy Solutions, 2018)
**(MAN Energy Solutions, Table 1.01, p. 10, 2018)

Ship Resistance Calculations (con't)

- The ship's midship section area, A_M, was calculated by*:

$$A_M = B_{WL}\ x\ T = 32.2\ m\ x\ 11\ m = 354.2\ m^2$$

- And the midship section coefficient, C_M, was calculated by*:

$$C_M = \frac{A_M}{B_{WL}\ x\ T} = \frac{354\ m^2}{32.2\ m\ x\ 11\ m} = 1.0$$

- Next, we computed the prismatic coefficient, C_P:

$$C_P = \frac{\nabla}{A_M\ x\ L_{WL}} = \frac{VOL}{A_M\ x\ L_{WL}} = \frac{49586\ m^3}{354\ m^2\ x\ 174\ m} = 0.8$$

- As is the case with most modern straight hull tankers/product carriers, C_B and C_P are nearly identical
- The length-displacement ratio, M, for this ship was:

$$M = \frac{L}{VOL^{\frac{1}{3}}} = \frac{174\ m}{(49586\ m^3)^{\frac{1}{3}}} = 4.75$$

*(MAN Energy Solutions, 2018)

Ship Resistance Calculations (con't)

- Computing the Froude number, *Fr*, was important to determine the ship's resistance:

$$Fr = \frac{V}{\sqrt{g \; x \; L_{WL}}}$$

- It was noteworthy that at values of *Fr > 0.19*, the ship's wave making resistance was significant (as seen in Fig. 1, slide 6) while for *Fr < 0.19* the biggest contribution to ship resistance is due to friction
- In our case, for a ship speed of V = 15 kn (7.72 m/s) and L_{WL} = 177.48 m, we obtained *Fr* ~ 0.187
- The Reynolds number, *Re*, comparing inertial force to viscous force, was calculated by: $Re = \frac{\rho VL}{\mu} = \frac{VL}{\nu}$
- In our case, for V = 15 kn, and s.w. kinematic viscosity ν =1.189 x 10^{-6} m^2/s, we obtained *Re* ~ 1.13 x 10^9
- As this was well over the critical value turbulence onset for external flows (*Re* > 1 x 10^6), the flow past the ship's hull was considered fully turbulent (as expected)

Resistance Coefficients

- The total resistance coefficient, C_T, is simply the summation of all other resistance coefficients, namely:

  $$C_T = C_R + C_F + C_A + C_{AA} + C_{AS}$$

  where:

  C_R = residuary resistance coefficient
  C_F = frictional resistance coefficient
  C_A = combined correlation & roughness allowance coefficient
  C_{AA} = air resistance coefficient
  C_{AS} = steering resistance coefficient

- A summary of all relevant resistance coefficients, total resistance, and effective ship power*, P_E, for different ship speeds is summarized in Table 1**

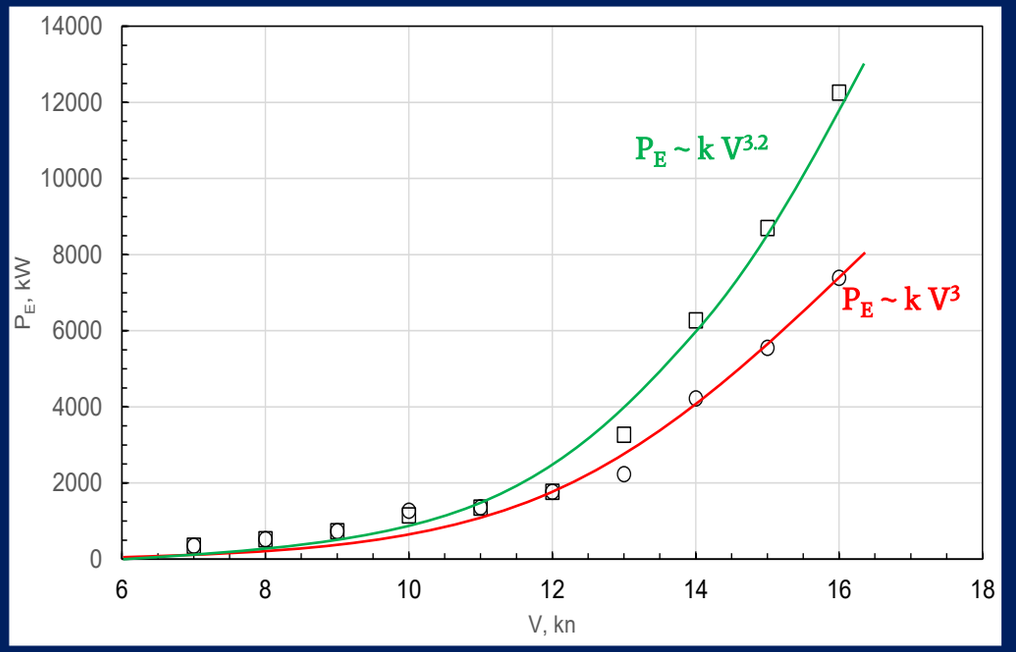
				x10^{-3}		x10^{-3}	x10^{-3}				$P_E \sim k V^3$	$P_E \sim k V^{3.2}$
V (kn)	V (m/s)	Fr	Re	C_R	C_F	C_A	C_{AA}	C_{AS}	C_T	R_T (kN)	P_E (kW)	P_E (kW)
7	3.601	0.087	5.27E+08		0.00166	0.14304	0.06	0	0.0019	98.55	354.9	354.9
8	4.116	0.100	6.02E+08		0.001632	0.14304	0.06	0	0.0018	126.77	521.7	521.7
9	4.630	0.112	6.77E+08		0.001607	0.14304	0.06	0	0.0018	158.31	733.0	733.0
10	5.144	0.125	7.53E+08	0.5	0.001586	0.14304	0.06	0	0.0023	247.13	1271.3	1149.1
11	5.659	0.137	8.28E+08	0.07	0.001567	0.14304	0.06	0	0.0018	240.38	1360.3	1352.9
12	6.173	0.149	9.03E+08	0.09	0.00155	0.14304	0.06	0	0.0018	286.54	1768.9	1768.9
13	6.688	0.162	9.79E+08	0.096	0.001535	0.14304	0.06	0	0.0018	334.58	2237.5	3272.1
14	7.202	0.174	1.05E+09	1.05	0.001521	0.14304	0.06	0	0.0028	586.92	4227.1	6273.9
15	7.717	0.187	1.13E+09	1.25	0.001508	0.14304	0.06	0	0.0030	719.22	5549.9	8699.9
16	8.231	0.199	1.20E+09	1.55	0.001496	0.14304	0.06	0	0.0032	897.93	7390.8	12257.5

** for detailed calculations please refer to the conference paper

* Corrected P_E calculation (MAN Energy Solutions, 2018)

Resistance Coefficients (con't)

- Figure below shows graphical comparison between the two power curves. i.e., "conventional" (circles) and "adjusted" (squares)
- For the "conventional" curve we used $P_E \sim kV^3$
- For the "adjusted" curve we used $P_E \sim kV^{3.2}$
- For V = 15 kn, the "corrected" power curve (8,688 kW) <u>matched very closely</u> the advertised ship power (8,700 kW)



Emission Factors, F_e

- The following emission factors (F_e) values (g/kW-h) were used*:
  - NOx = 18.1; SOx = 10.29; CO = 1.4; CO_2 = 620.62; HC = 0.6; PM = 1.42
- These compared to older F_e values**:
  - NOx = 17; SOx = 10; CO = 1.4; CO_2 = 655; HC = 0.6; PM = 1.25
- In above, the F_e values for SOx values were based on older assumption of average fuel-sulphur content of 2.5% for HFO
- However, consistent with IMO's latest fuel sulphur content of 0.5% for HFO, it is expected that the F_e values SOx will be further adjusted down (future work!)
- Compared to the above F_e values for NOx (rather dated at 18.1 g/kW-h), IMO's NOx limits have been dropping considerably from 17.0 g/kW-h (2000) to about 3.4 g/kW-h (2016), and with continued tendency for further restrictions
- At the same time, marine engine makers have been developing strategies for newly built ships (post-2000) to comply with IMO's stringent limits by introducing water in the combustion chamber, or by humidifying the intake air (approx. NOx = 4 g/kW-h)
- Further NOx reductions are achieved by applying Selective Catalytic Reactor (SCR) technologies*** to reach even lower emissions (< 2 g/kW-h)
- (Reporting these adjustments may be included in a future follow-up work)

*(Seddiek, I., Anmar, N.R., 2011)
**(Corbett, J.J., Kohler, H.W., 2003)
***(Kohler, H.W., 2003)

Reductions of Engine Emissions - Calculation

- Based on the proposed improved propeller design, diminished propulsive losses of approx. 7.5% was estimated
- Hence, the same amount of approx. 7.5% is assumed to lead to commensurate improvement in propulsive efficiency
- For the MT-46 Veteran Tanker prototype, for a typical cruise speed of 15 kn, a conservative approach to "slow steaming" (say, 15% speed reduction) yielded: $V_R = V - 0.15\ x\ V = 15\ kn. - 0.15\ x\ 15\ kn. = 12.75\ kn.$
- From the speed/power curve, for V = 12.75 kn, $P_E \sim 3080$ kW
- Applying the 7.5% engine output power reduction due to the improved propeller efficiency, the "reduced saved" engine power, P_{RS}, was estimated to be: $P_{RS} = 7.5\%\ of\ P_E = 0.075\ x\ 3080\ kW = 231\ kW$
- Annual Emission Reductions (AERs) for each of the emissions species, using the calculated P_{RS} =231 kW were:

$$AER_{PR} = P_{RS}F_eH = (231\ kW)\left(18.1\ \frac{g}{kW-h}\right)(4380\ h)\left(\frac{1\ ton}{1\ x\ 10^6\ g}\right) = 18.31\ tons \qquad \text{(NOx)}$$

$$AER_{PR} = P_{RS}F_eH = (231\ kW)\left(10.3\ \frac{g}{kW-h}\right)(4380\ h)\left(\frac{1\ ton}{1\ x\ 10^6\ g}\right) = 10.42\ tons \qquad \text{(SOx)}$$

$$AER_{PR} = P_{RS}F_eH = (231\ kW)\left(1.4\ \frac{g}{kW-h}\right)(4380\ h)\left(\frac{1\ ton}{1\ x\ 10^6\ g}\right) = 1.42\ tons \qquad \text{(CO)}$$

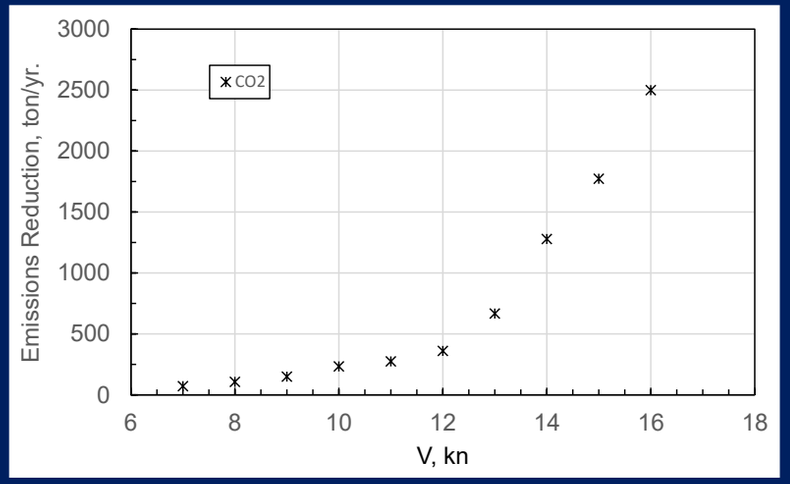
$$AER_{PR} = P_{RS}F_eH = (231\ kW)\left(620.62\ \frac{g}{kW-h}\right)(4380\ h)\left(\frac{1\ ton}{1\ x\ 10^6\ g}\right) = 627.9\ tons \qquad \text{(CO}_2\text{)}$$

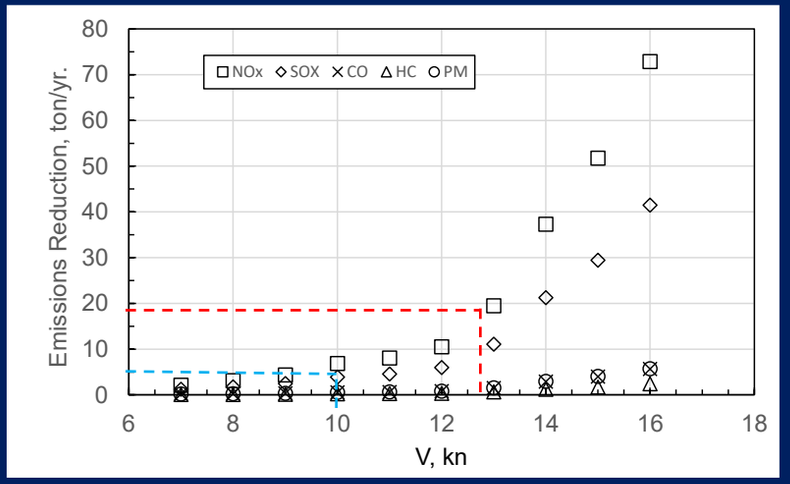
$$AER_{PR} = P_{RS}F_eH = (231\ kW)\left(0.6\ \frac{g}{kW-h}\right)(4380\ h)\left(\frac{1\ ton}{1\ x\ 10^6\ g}\right) = 0.61\ tons \qquad \text{(HC)}$$

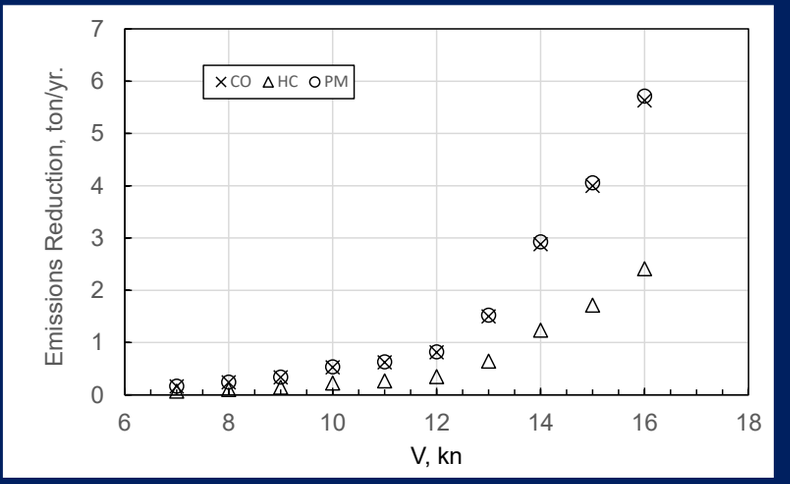
$$AER_{PR} = P_{RS}F_eH = (231\ kW)\left(1.42\ \frac{g}{kW-h}\right)(4380\ h)\left(\frac{1\ ton}{1\ x\ 10^6\ g}\right) = 1.44\ tons \qquad \text{(PM)}$$

Reductions of Engine Emissions - Graphs

- The effects of using the proposed propeller for the selected tanker ship at varying ship speeds (7 kn – 16 kn) on the estimated AERs are shown below
- As expected, the “slow steaming” approach (V = 12.75 kn) showed significantly lower emissions compared to the normal cruise sped (V = 15 kn)
- Notably, compared to their corresponding emissions at full speed (16 kn), both NOx and SOx, showed a drop of **2.7x** in the in the actual emissions (at 12.75 kn), and **10.7x** (at 10 kn)







Conclusions and Future Work

- The current paper expands on prior related work* where some of the initial CFD simulations were done
- The introduction of a divergent nozzle on the propeller blade significantly reduced propeller cavitation in comparison to the prototype conventional propeller
- With the use of a divergent nozzle, the low pressure zone on the suction side of the propeller blade was almost completely eliminated, thus decreasing cavitation
- The **divergent nozzle with a 5- deg. divergence angle was the best option** in terms of cavitation reduction
- Detailed analyses of ship resistance for the selected prototype ship hull were used to match the proposed propeller design
- An improvement of approx. 7.5% (due to propeller design improvement) resulted in commensurate reduced engine power
- This resulted in reduced fuel consumption by the main Diesel engine, which, in turn, showed reduced exhaust emissions
- Additional 15% reduction in ship speed ("slow steaming") led to overall emissions reductions
- Notably, NOx and SOx annual emissions reductions (AERs) values were significant
- Similar (commensurate) AERs were observed with the other exhaust gas species (CO, CO_2, HC, and PM)

*(Davis, A., Du., M.-H., Nilsson, K., & Ribarov, L.A., 2024)

Acknowledgements

- This work includes many resources and references of related past works form our colleagues in the broader global wind-assisted ship propulsion community – any inadvertent omission of relevant works is, therefore, non intentional. Any helpful reviews, advice, and suggestions offered by the co-authors' classmates and instructors are welcome and appreciated

- The author wishes to acknowledge:

- His collaborators on the prior related work: Alyssa Davis, MaoHai Du, and Kristy Nilsson (ex-USMMA Midshipmen)

- His institution, the U.S. Merchant Marine Academy, and specifically:

- Dr. Susan Comilang, Assistant Dean for Academic Affairs – for continued encouragement and guidance

- Capt. Anthony Nigro, Chair, Department of Marine Engineering – for the opportunity to work on this project

- Dr. Sergio Perez (Ret.), Department of Marine Engineering – for guidance and help with the EasyCFD software

ANV!

References

Bakker, J., and van Vlaardingen, P.L.A. (2017). Wetted Surface Area of Recreational Boats, EIVM Report 2017-0016, National Institute for Public Health and the Envornmnet, Ministry of Health, Welfare and Sport, Bilthoven, The Netherlands.

Basic Principles of Ship Propulsion - Optimisation of hull, propeller, and engine interactions for maximum efficiency. (2018) MAN Energy Solutions, Copenhagen.

Birk, L. (2019). Fundamentals of Ship Hydrodynamics. John Wiley & Sons Ltd, West Sussex, UK.

Brown, I.N., Aldridge, M.F. "Power Models and Average Ship Parameter Effects on Marine Emissions Inventories." *J. Air Waste Manag. Assoc.* 69(6):752-763. doi:10.1080/10962247.2019.1580229, 2019.

Corbett, J.J., & Koehler, H.W. "Updated Emissions from Ocean Shipping." *J. of Geophys. Res.*, 108(D20):4650, doi:10.1029/2003JD003751, 2003.

Corbett, J.J., & Koehler, H.W. "Considering Alternative Input Parameters in an Activity-Based Ship Fuel Consumption and Emission Model: Reply to Comment by Ø yvind Endersen et al on "Updated Emissions from Ocean Shipping."" *J. of Geophys. Res.*, 109(D23303):4650, doi:10.1029/2004JD005030, 2004.

Davis, A., Du, M., Nilsson, K., & Ribarov, L.A. "Numerical Investigation into Propeller Cavitation Reduction." *World Maritime Technology Conference (WMTC 2024)*, 310-316, Chennai, India, Dec. 2024.

Endresen, Ø, Søgård, E., Sundet, J.K., Dalsøren, S.B., Isaksen, I.S.A., Berglen, T.F., & Gravir, G. "Emission from International Sea Transportation and Environmental Impact." *Journal of Geophysical Research*, 108(D17), 4560. doi:10.1029/2002JD002898, 2003.

Endresen, Ø, Søgård, E., Bakke, J., & Isaksen, I.S.A. "Substantiation of a Lower Estimate for the Bunker Inventory: Comment on "Updated Emissions from Ocean Shipping" by J. J. Corbett and H.W. Koehler." *J. of Geophys. Res.*, 109(D23302), 4560. doi:10.1029/2004JD004853, 2004.

EPA. *United States Environmental Protection Agency. Overview of Greenhouse Gases* https://www.epa.gov/ghgemissions/overview-greenhouse-gases, 2026, April 27.

Fiber, J. et al., *Fourth IMO GHG Study 2020*– Executive Summary and Final Report, London, UK, 2021.

Guldhammer, H.E., and Harvald, S.A. (1974). Ship Resistance: Effect of Form and Principal Diemnsions, Akademisk Forlag, Copenhagen, Denmark.

Harvald, S.A. (1983). Resistance and Propulsion of Ships, John Wiley & Sons, Inc., New York, NY, USA.

Hunt, E.C., Harbach, J.A., Rowen, A.L., (eds). (2002). Modern Marine Engineer's Manual, vol. 2. Cornell Maritime Press, A Division of Schiffer Publishing. Ltd, 3rd ed., Atglen, PA.

References (con't)

IMO Nitrogen Oxides (NOx) – Regulation 13 (https://www.imo.org/en/OurWork/Environment/Pages/Nitrogen-oxides-(NOx)-%E2%80%93-Regulation-13.aspx).

Janes Sea Module Global Shipping Database. https://customer.janes.com/portal/Account/PreAuthenticate?callingurl=https%3A%2F%2Fcustomer.janes.com%2, (2024, May 13).

Koehler, H.W. "NOx Emissions from Merchant Ships." *Marine Reporter & Eng. News*, 68-70, Jun. 2003

Kristensen, H.O., Lützen, M. "Prediction of Resistance and Propulsion Power of Ships." Project no. 2010-56, Emissionsbeslutningsstøttesystem Work Package 2, Report no. 4. Technical University of Denmark (DTU), 2013.

Kristiansen, H.O. Ship-DESMO. Calculation Tool. Technical University of Denmark (DTU), 2017a.

Kristiansen, H.O. "Energy Demand and Exhaust Gas Emissions of Marine Engines. Project no. 2016-108: Update of Decision Support System for Exhaust Gas Emissions Calculations." Report no.5. Technical University of Denmark (DTU), 2017b.

MARPOL Annex VI. IMO, London, 1997.

Molland, A.F., Turnock, S. R., and Hudson, D. A. Ship Resistance and Propulsion. Cambridge, UK: Cambridge University Press, 2011.

Plesset, M.S., Chapman, R.B. "Collapse of an Initially Spherical Vapor Cavity in Neighbourhood of a Solid Boundary." *J. Fluid Mech.*, 47(2):283-290, 1971.

Radojčić, D., Simić, A., Momčilović, N., Motok, M., Friedhoff, B. "Technologies for Improvements of Energy Efficiency and Environmental Performance." In: Design of Contemporary Inland Waterway Vessels. Springer, Cham. https://doi.org/10.1007/978-3-030-77325-0_9, 2021.

Seddiek, I., & Ammar, N.R. "Harnessing Wind Energy on Merchant Ships: Case Study Flettner Rotors onboard Bulk Carriers." *Env. Sci. and Pollution Res.,* (28), 32695-32707, 2021.

Ship Technology. "Veteran Class MT-46 Product Tanker." Apr. 29, 2010.

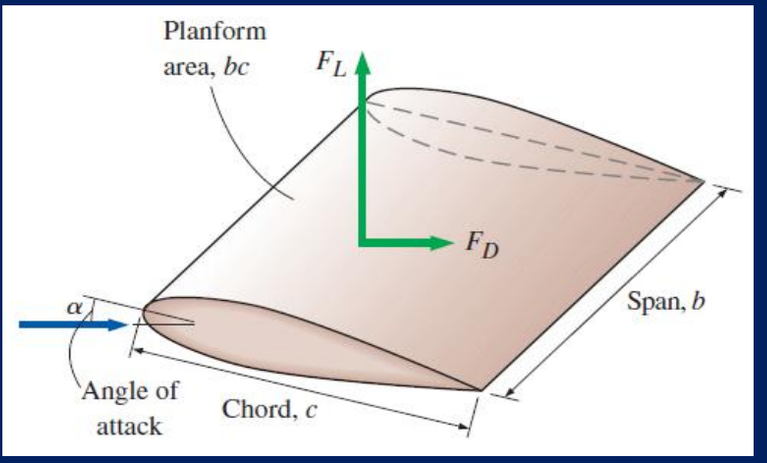
Smith, T.W.P., et al. Third IMO Greenhouse Gas Study 2014 – Executive Summary and Final Report, London, 2015.

Questions?

Appendix

Airfoil Theory for Lift and Drag

- A rotating rotor (such as the Flettner Rotor) is similar to an airfoil in producing lift, *L*, and drag, *D* while monitoring the value of L/D
- The lift, drag, and pitching moments of airfoils, described by their respective section coefficients, C_L, C_D, and C_M, are functions of the angle of attack (AOA), α, and the operational speed of the airfoil (i.e., the Reynolds number, *Re*).
- For a given α and *Re*, a typical airfoil reaches its maximum lift at a point beyond whcih it is assumed to be stalled (where lift is rapidly lost, while drag is increasing).
- Fundamental airfoil theory* indicates that different airfoil shapes (cross-sectional profiles) offer different lift-to-drag (L/D) ratios.
- The Aspect Ratio, *AR* (i.e., span/chord = *b/c*) is an important wing performance characteristic relating lift and drag. Typcially, higher *AR*s lead to higher *L/D* ratios but with more structural challenges (i.e., wing bending, wing tip dflection, wing root stresses, etc.).
- Lift Force: $L = \frac{1}{2}\rho A V_a^2 C_L$ C_L = 12.5**
- Drag Force: $D = \frac{1}{2}\rho A V_a^2 C_D$ C_D = 0.2**

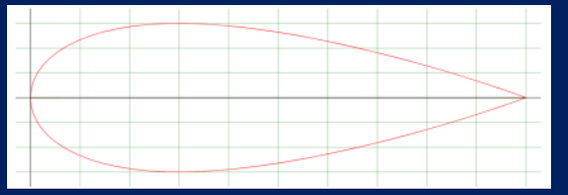


Definition of iterms of an airfoil***

*(Anderson, 2017)
**(Iacovides, et al., 2012)
***(Çengel and Cimbala, 2014)

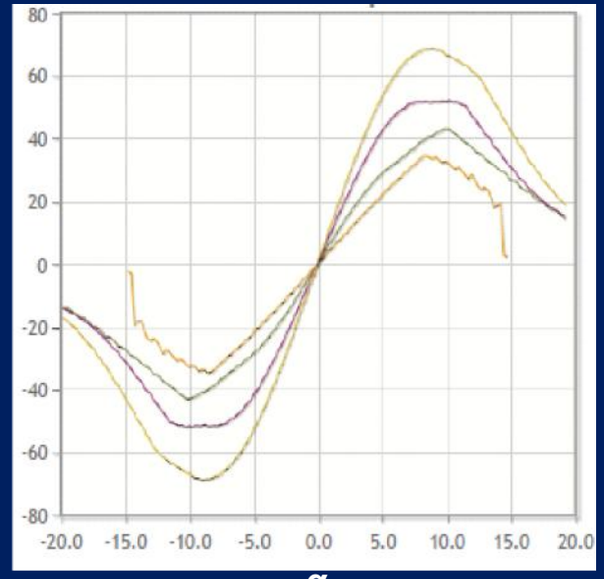
(Air) Foil Theory for Lift and Drag

- A rotating propeller blade foil is similar to an airfoil in producing lift, L, and drag, D while monitoring the value of L/D
- A typical symmetric airfoil is the NACA 0030 wing profile (a symmetric airfoil produces no lift at $\alpha = 0$ deg.)
- The corresponding maximum value for $C_L/C_D = 68.8$ at $Re = 1{,}000{,}000$ occurs at $\alpha = 9$ deg. Values for C_L/C_D are lower for the lower Re values, respectively.
- In our work, the modelled propeller blade foils were at fixed pitch, P, but due to its helical shape, the created complex camber curvature varies its pitch angle ϕ (similar to α for airfoils) along the radius of the blade.
- At $x = 0.7R$, the calculated** ϕ was approx. 17.6 deg., and then gradually decreasing to approx. 13.1 deg. towards the blade tips (at x = $0.96R$).

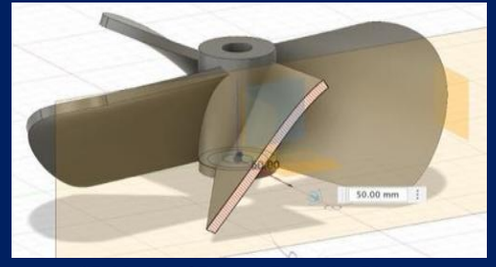


NACA 0030 Symmetric Airfoil

http://airfoiltools.com/airfoil/details?airfoil=naca0024-il



C_L/C_D vs. α for NACA 0024 symmetric airfoil profile for four different values of Re (100,000; 200,000; 500,000; 1,000,000)



3D Model of Printed Propeller Blade

*(Anderson, 2017)
** see slide 30

Airfoil Theory for Lift and Drag

- The total lift coefficient, C_L, for a finite wing is defined*:

$$C_L = \frac{(c_l)^2}{1 + \frac{c_l}{\pi\,(AR)}}$$

- Similarly, for modest values of α, the induced drag coefficient, $C_{D,\,i}$, and the total drag coefficient, C_D, are defined as:

$$C_{D,i} = \frac{(C_L)^2}{\pi\, e\, AR}$$

$$C_D = c_d + C_{D,i}$$

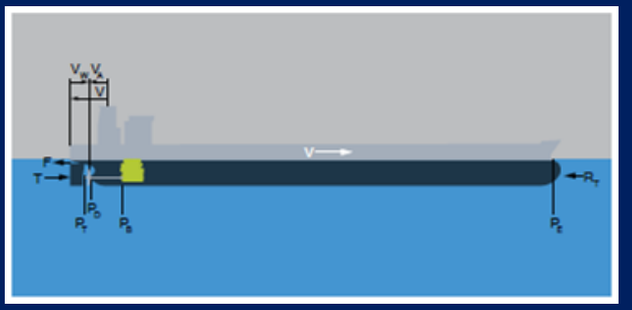
- According to Prandlt Lifting Line Theory**, an eliptical oval represents an *ideal wing planform* (which minimizes induced drag through reduced wing downwash). In the equation above, e is the span efficiency factor, which is an index of how ideal a wing planform is, compared to the ideal eliptical oval shape

SUSTAINABILITY AND INNOVATION IN SHIP DESIGN AND OPERATIONS CONFERENCE 2026

*(Houghton and Carpenter, 2003)
**(Anderson, 2005)

Propeller Basics

- **Wake fraction coefficient,** $w = V_w/V = (V - V_A)/V = 1 - V_A/V$, where V_W is the speed of the wake, V is the speed of the hull, V_A is the propeller's speed of advance
- Due to boundary layer around the hull, the water arriving at the propeller (aft of hull) has a decreased velocity, V_w (effective wake velocity)
- The propeller's efficiency is affected by w, which, in turn is proportional to the hull's block coefficient, $C_B = (\nabla) / (L_{WL} * B_{WL} * T)$
- Typical values are given by: $w = 0.5 * C_B - 0.05$
- **Thrust deduction coefficient,** $t = F/T$ is a measure of increased drag of propeller behind the hull, where the thrust deduction fraction, $F = T - R_T$
- Typically, t is measured as: $(T - R_T) /T = 1 - R_T/T$, (relating hull's towing resistance, R_T, and thrust force, T) and it is approx. estimated as: $t = 0.27 * C_B = 0.6 * w$
- **Propeller Thrust coefficient,** $K_T = (T) / (\rho * n^2 * d^4)$, relating propeller's thrust torque, T, to the propeller's geometry and water density
- **Propeller Torque coefficient,** $K_Q = (Q) / (\rho * n^2 * d^5)$, relating propeller's torque, $Q = P_D/(2\pi n)$ to the propeller's geometry, water density, and power delivered to the propeller, P_D
- **Propeller Thrust Loading coefficient** $C_n = p_{propeller} / p_{dynamic}$ is a measure of the loading degree onto the propeller due to the dynamic pressure of the arriving water flow to the propeller
- Typically, C_n is measuring the thrust divided by the propeller's speed of advance, V_A, and its diameter squared, d^2, $C_n = (T/A_{propeller}) / (0.5 \rho V_A^2)$



Ship propulsion forces*

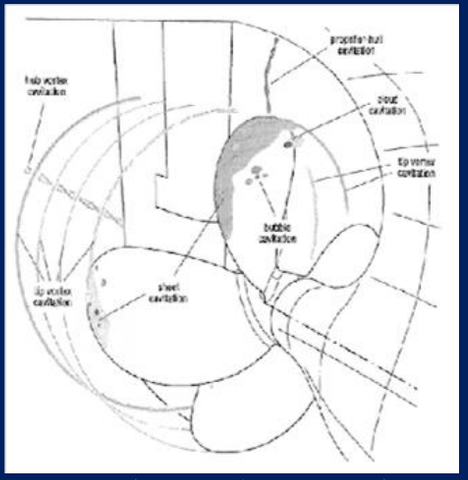
Typical propulsion coefficients*

Propeller arrangement	Wake fraction coefficient, w	Thrust deduction coefficient, t	Hull efficiency, η_H
Single-screw	0.20-0.45	0.10-0.30	1.1-1.3
Twin-screw, single skeg	0.10-0.25	0.05-0.15	0.95-1.15
Twin-screw, twin skeg	0.15-0.35	0.05-0.25	1.05-1.25

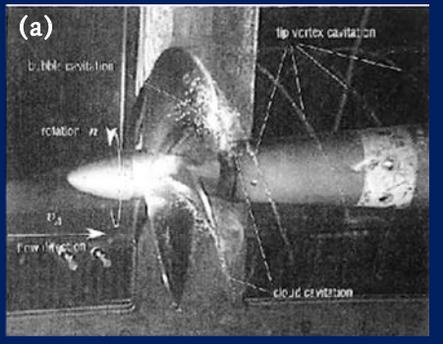
*(MAN Energy Solutions, 2018)

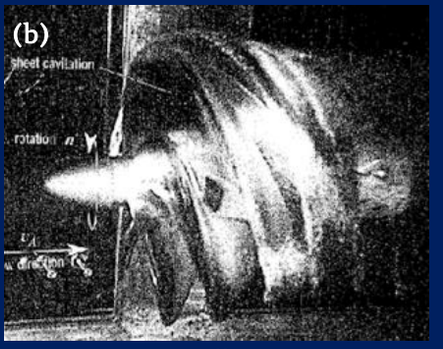
Propeller Cavitation Basics

- Typical cavitation forms and their relative locations on a four-bladed propeller are shown on the top right image
- The propeller blade tips move at the highest velocity, hence, initial bubbles may start appearing there first forming **p vortex cavitation** – top right image
- Further increase in the flow speed past the propeller creates the propeller hub vortex – top right image
- A further pressure drop on the back (suction) side of the propeller blades forms **bubble cavitation** – right middle image
- Further growth and migration of these cavitation bubbles (along the suction side) form a **cloud cavitation** – right middle image
- When the pressure drops below the vapor pressure over the entire blade's leading edge, then a thick layer forms a sheet cavitation – right bottom image
- Small clearances between the propeller's blade tips and the vessel's hull may cause propeller-hull cavitation**
- Other types of cavitation (e.g., face cavitation, streak cavitation, etc.) are known but were not be considered further in this work



Locations for typical cavitation forms



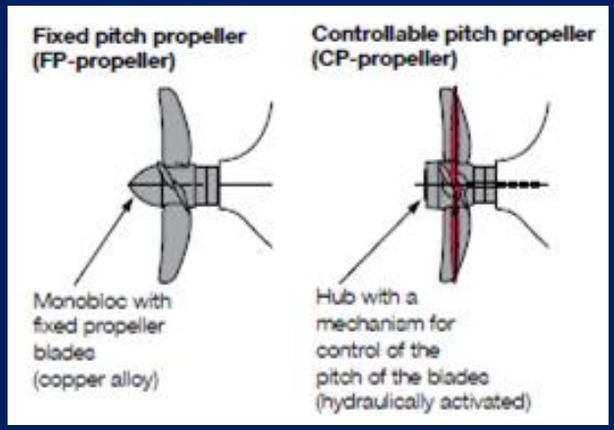


Open water test propeller cavitation:
(a) bubble; (b) sheet

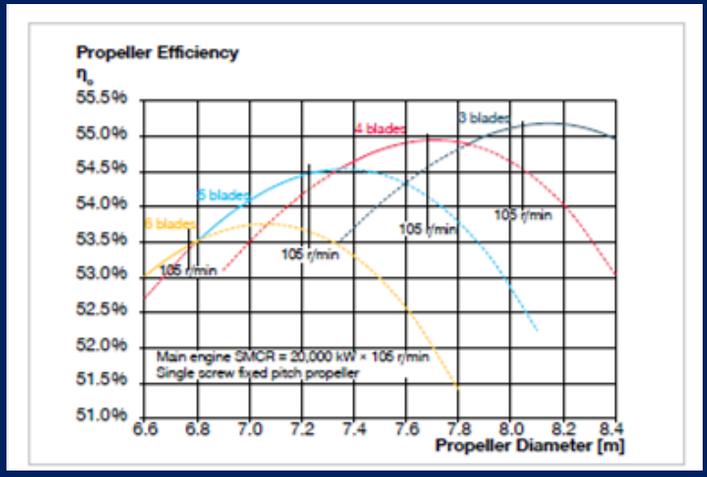
*(Birk, 2019)
**(Franc, J.-P. and Michel, J.;M., 2004)

Propeller Basics

- **Disk area coefficient** – ratio of swept surface area by propeller relative to the relative disk area
- Typically, this ratio is about 0.5 – 0.6 for most 4-bladed propellers with normal blade loading
- **Blade number** – typical propellers have 2 – 7 blades with higher number of blades leading to higher efficiency
- The higher the blade number, the lower the propeller optimal speed
- Certain specific blade numbers must be avoided to prevent natural frequency excitations with ship's hull and machinery
- Due to strength and vibration requirements, 4-bladed propellers tend to be most common in large merchant ships
- **Fixed Pitch Propellers (FPP)** – monolithic build (cast) with fixed number- and positions of blades (at a fixed pitch)
- Simpler design, highest number of blades and blade area ratio – our work investigated an FPP model
- **Controllable Pitch Propellers (CPP)** – relatively large hub area (containing all gearing mechanisms, etc.)
- CPP provide greater maneuverability (at a more complex construction)
- Slightly lower propeller efficiency compared to FPP



FPP vs CPP*

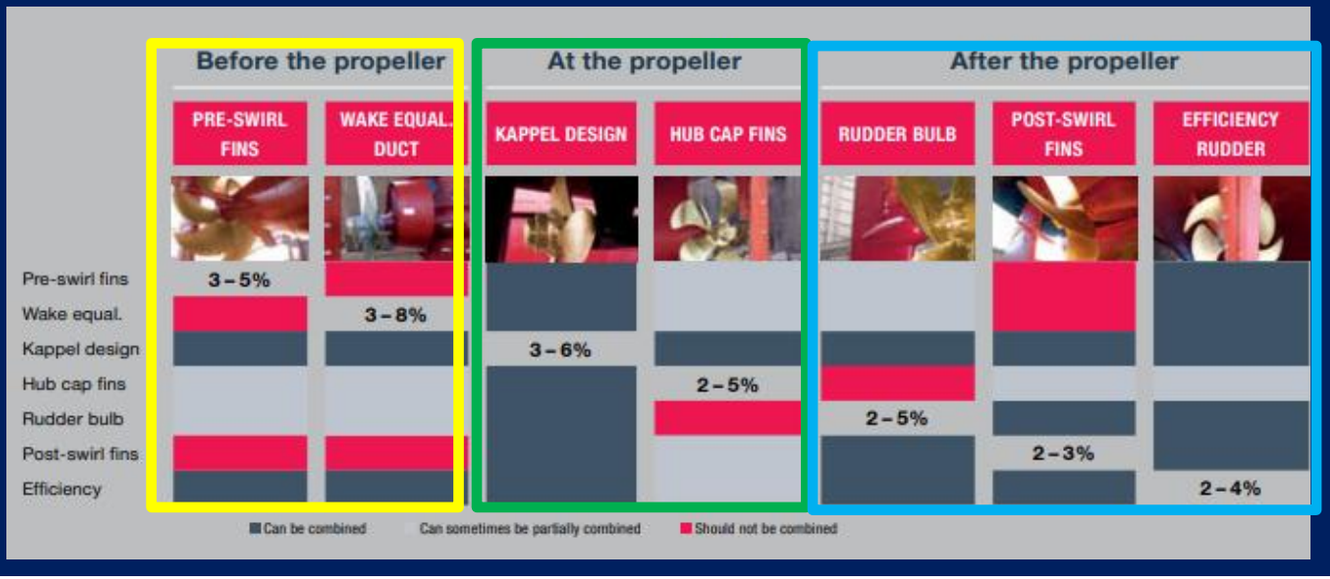


Propeller efficiency vs propeller blade number*

*(MAN Energy Solutions, 2018)

Energy Saving Devices (ESDs) - Prior Work

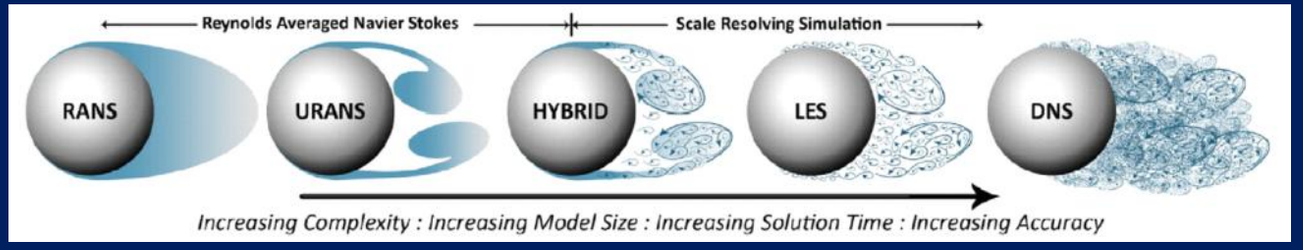
- Many propeller ESDs, yielding savings of 2% — 8%, have been developed falling into three main categories* (based on their location relative to the propeller):
- Before the Propeller:
  - Pre-swirl Vanes (PrSV): attempting to minimize rotational losses of water flow into the propeller
  - Wake Equalizing Duct (WED): attempting to minimize rotational losses of water into propeller AND separation in aft hull
- At the Propeller:
  - Kappel Design (KD): attempting to minimize tip vortex losses from the propeller blades
  - Hub Cap Fins (HCF): attempting to minimize propeller hub vortex losses
- After the Propeller:
  - Ruder Bulb (RD): minimize propeller hub vortex losses
  - Post Swirl Vanes (PoSV): similar to above
  - Efficiency Rudder (ED); similar to above
- For all ESDs must consider expected benefits vs. added wetted surface area, weight, cost, and complexity
- Possibilities for combining ESDs (i.e. PrSV and RD, etc.) can improve efficiencies (at cost of higher complexity)



*(MAN Energy Solutions, 2018)

Models for Turbulence Spatial Scales

- **SRS** CFD Models – accuracy is highest in the **Direct Numerical Simulation (DNS)** model, where unsteady motion in turbulent flow in *all scales* is resolved (very costly in CPU and time)
- **Large Eddy Simulation (LES)** models are a step below DNS as they resolve *only large scale eddies*, while small-scale eddies are modeled
- **RANS** CFD Models are the next step below LES, where *all the turbulent eddies* are modeled using time-averaged turbulence properties with satisfactory accuracy (most of the time)
- **URANS** is also part of the RANS CFD models, albeit a more accurate model (than RANS) for *near-wall flows* (as already explained on previous slide)
- **Hybrid SRS/URANS** models have been used recently where **Scale Adaptive Simulations (SASA)** and **Detached Eddy Simulations (DES)** combine LES and URANS near the wall
- **Hybrid SRS/URANS** are bridging the gap between RANS and SRS models
- Further fine-tuning can be done for specialized applications with **Delayed Detached Eddy Simulations (DDES) and Wall-Adapting Local-Eddy (WALE)** viscosity models



(Adapted from (Hart, 2016))

SUSTAINABILITY AND INNOVATION IN SHIP DESIGN AND OPERATIONS CONFERENCE 2026

oes, 2016a)
ennekes and Lumley, 1972)

3D-Printing System

- Benefits of 3-D printing models for testing include its ease of access, the user-friendly program, and the ability to create and change experiment components as needed.
- .STL file created using Fusion 360 program, converted to Makerbot File for the printing process
- Printed using PLA filament on a MakerBot Method X 3-D printer
- PLA filament is relatively inexpensive for the amount of variability it provides





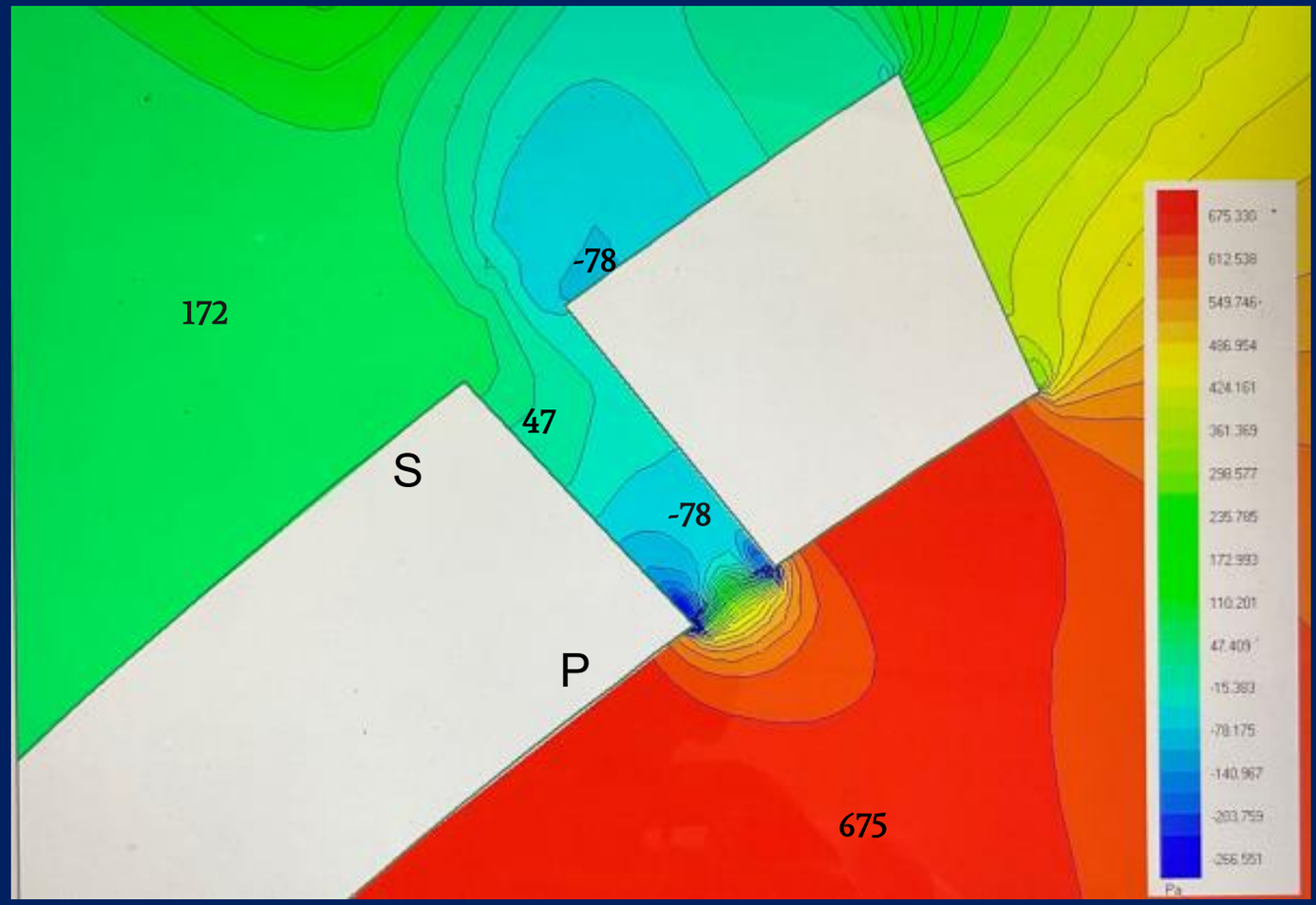


*METHOD X 3D Printer | MakerBot

CFD for a Propeller with Divergent Nozzle

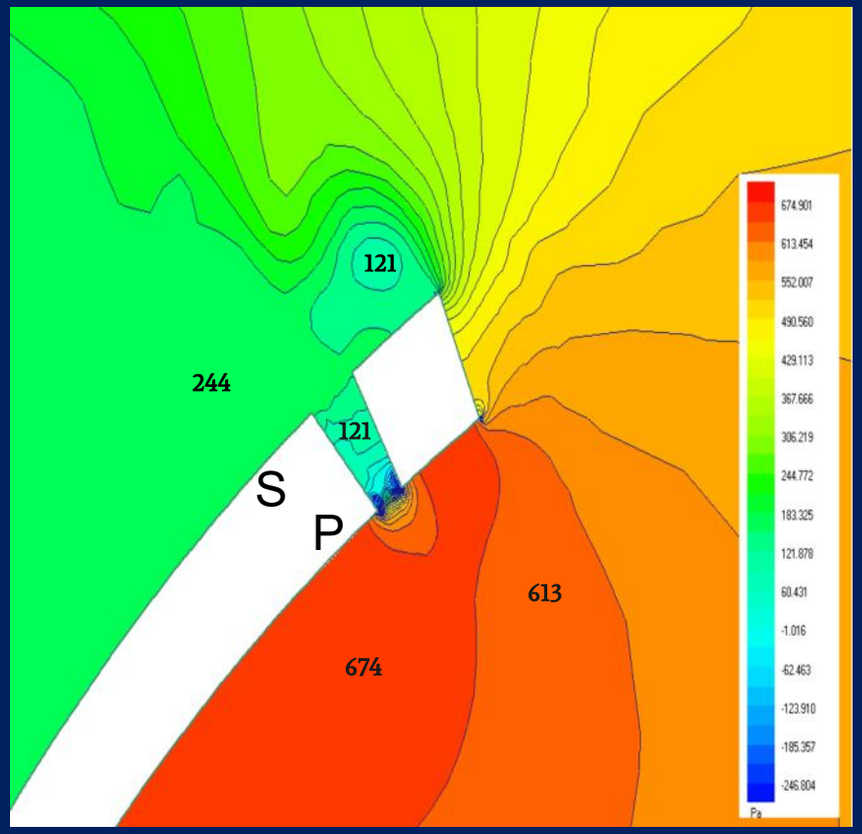
Closer Look at Divergent Nozzle

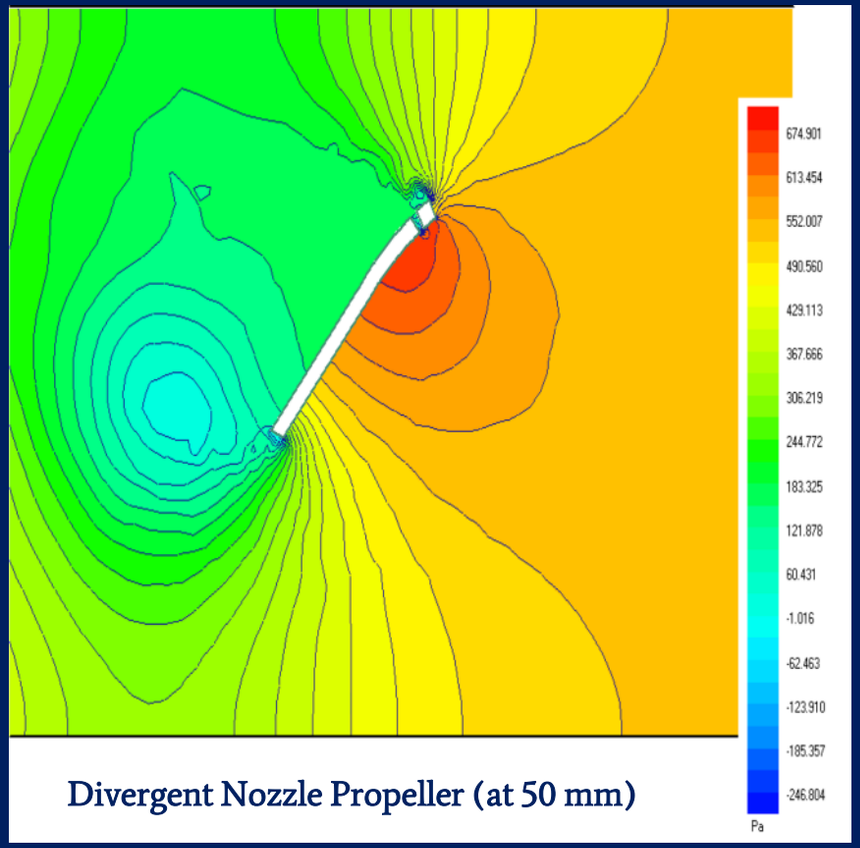
- Low pressure zone located at nozzle entrance
- **Much higher** pressure at the nozzle exit
- There is a **significant reduction** in the propensity for cavitation
- 2.1-deg. divergence angle



Propeller with Divergent Nozzle: 5-deg. Divergence angle
CFD Calculations of Pressure Fields

- At 5-deg. divergence angle, the low pressure zone was decreased throughout the nozzle
- A larger high pressure zone is formed in comparison to the original 2.1-deg. divergence angle

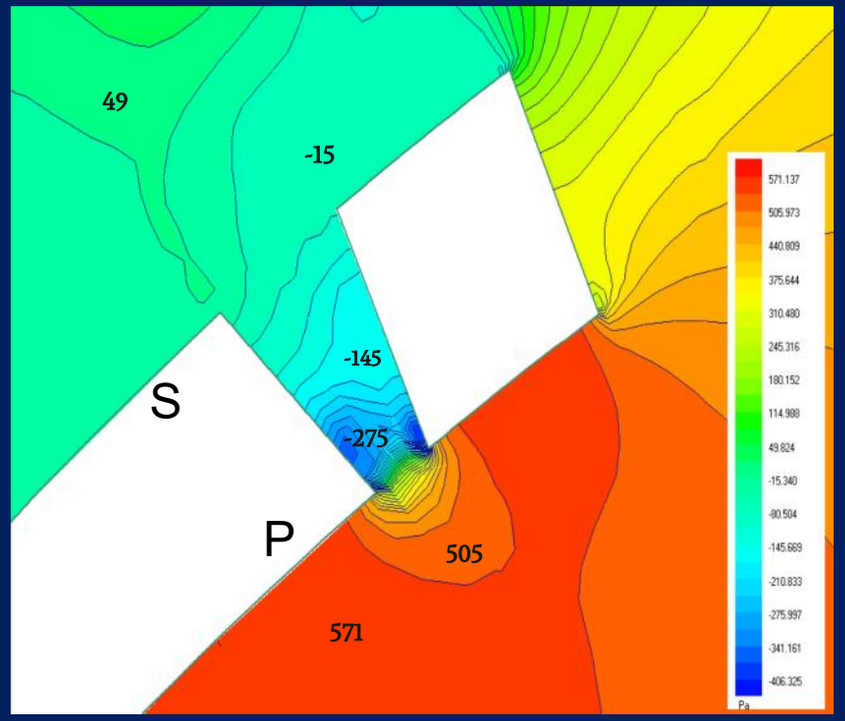


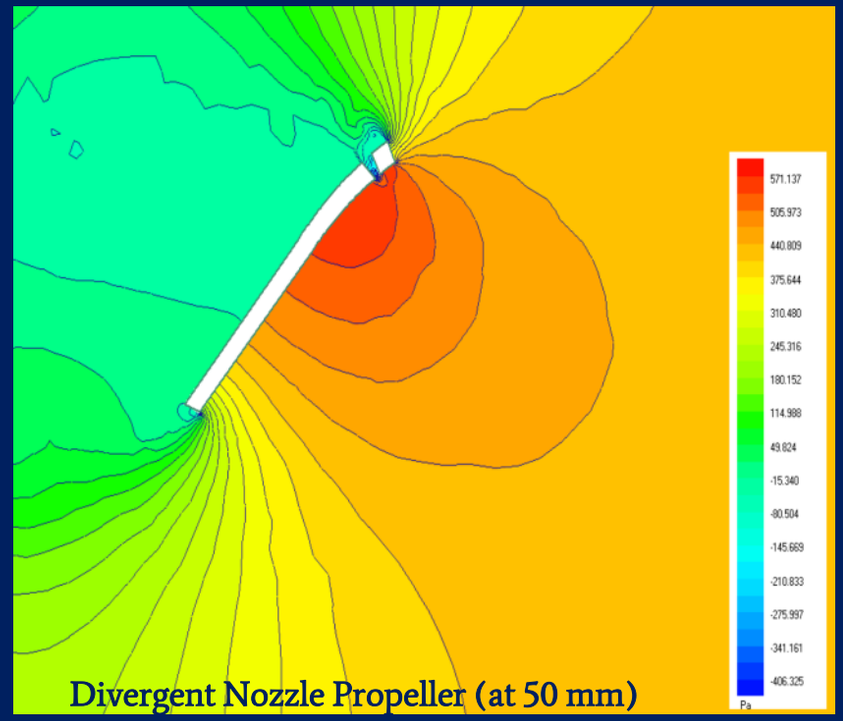


Divergent Nozzle Propeller (at 50 mm)

Propeller with Divergent Nozzle: 10-deg. divergence angle
CFD Calculations of Pressure Fields

- At a 10-deg. divergence angle the low pressure zone begins to increase
- In comparison to the 2.1-deg. and 5-deg. divergence angles, the 10-deg. divergence angle is not as effective in mitigating propensity for cavitation on suction side of the blade

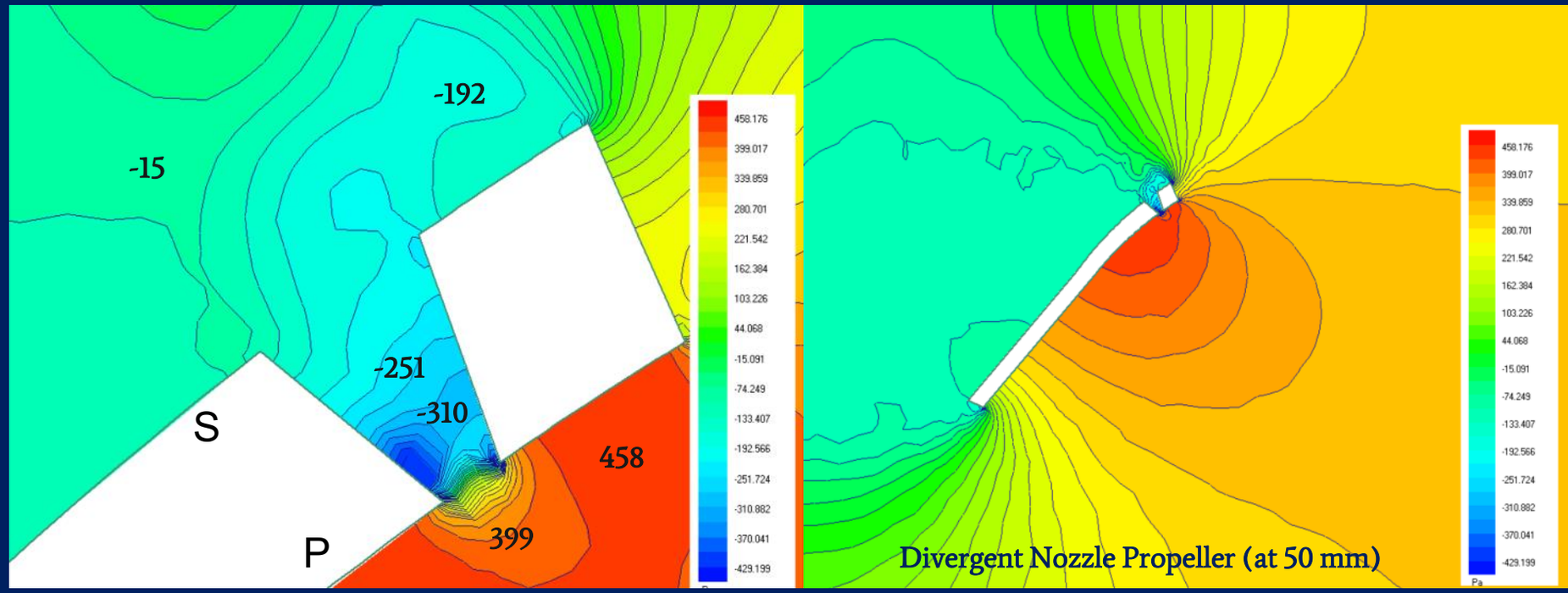




Propeller with Divergent Nozzle: 15-deg. divergence angle

CFD Calculations of Pressure Fields

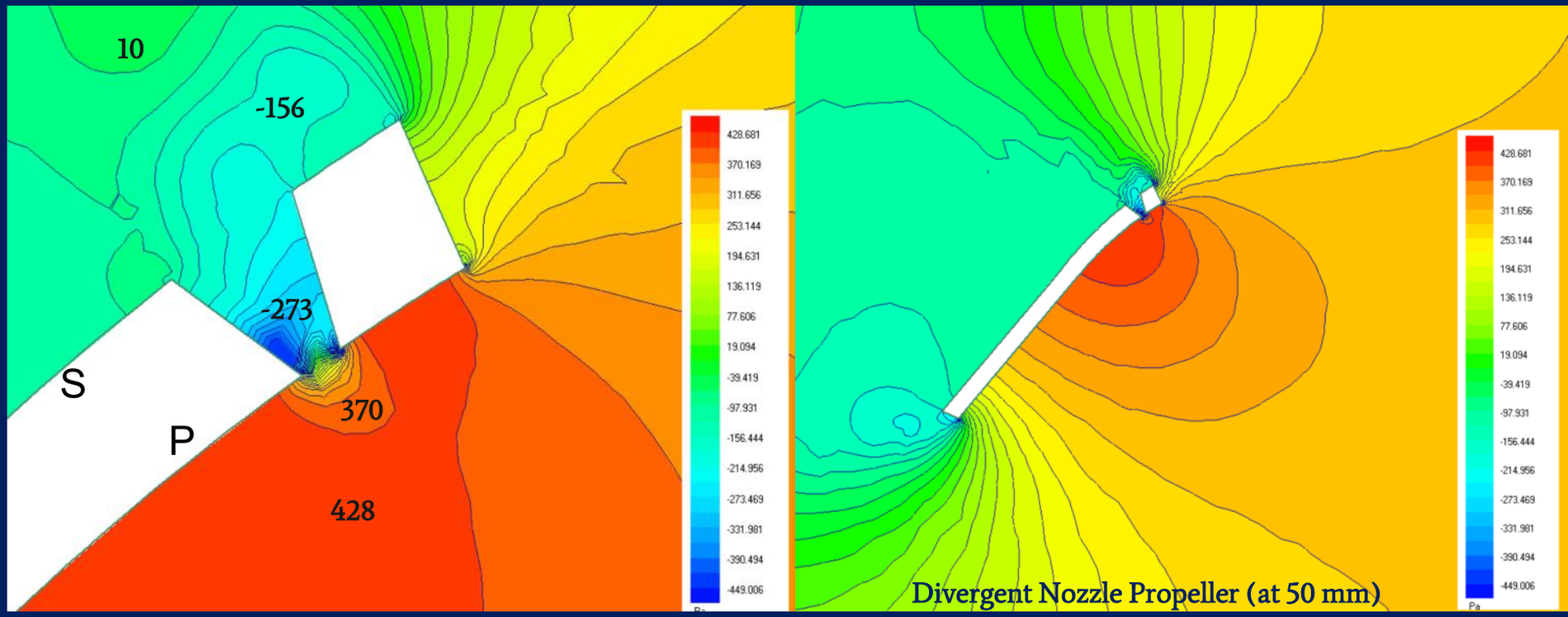
- At a 15-deg. nozzle divergence angle, there is a decrease in improvement from the conventional propeller



Propeller with Divergent Nozzle: 18-deg. divergence angle

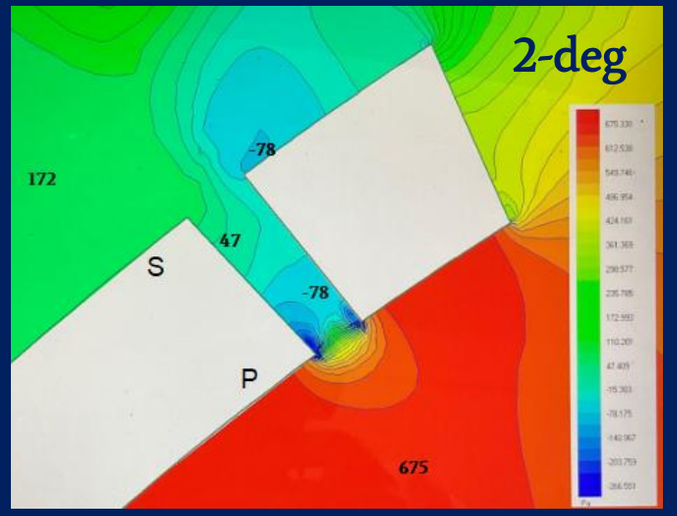
CFD Calculations of Pressure Fields

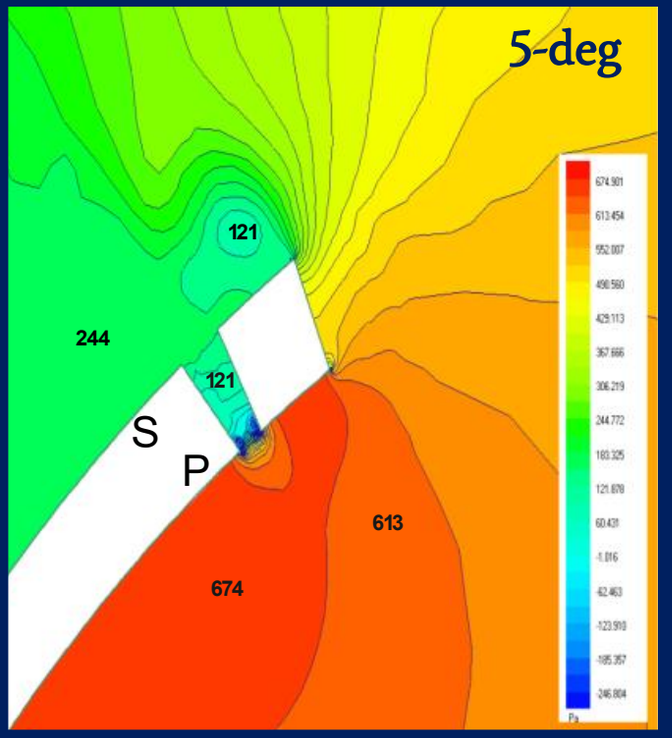
- At an 18-deg. divergence angle, there is a decrease in improvement from the conventional propeller
- Low pressure zone located at nozzle entrance
- **Much higher** pressure at the nozzle exit
- There is a **significant reduction** in pressure on the suction side of the blade (which can **increase** propensity for cavitation)

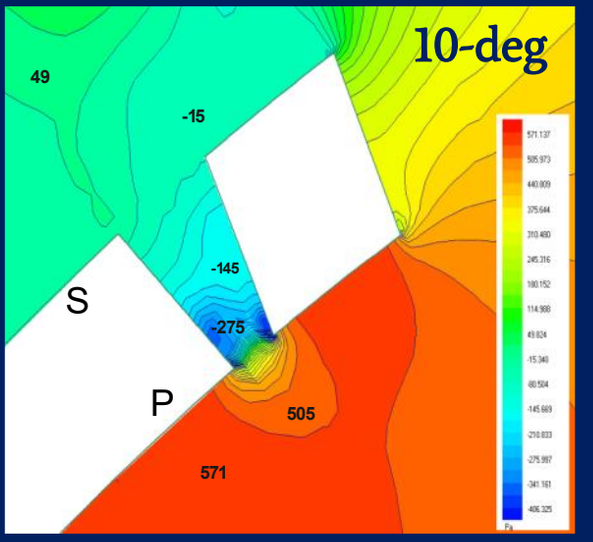


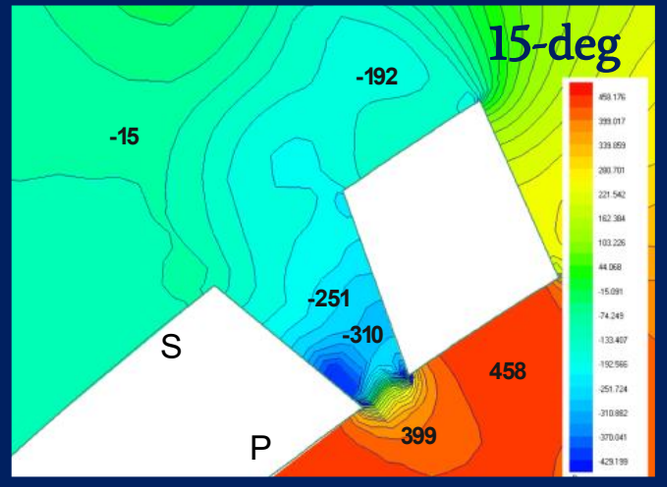
CFD for a Propeller with Divergent Nozzle

Pressure Results Comparison of Propeller with Various Divergent Nozzles Angles

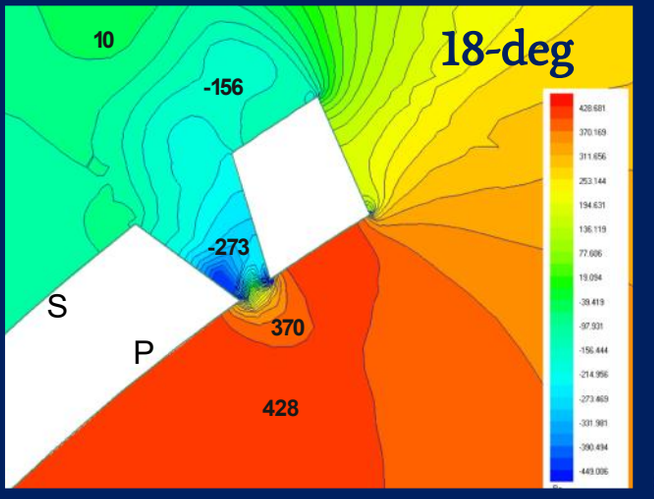








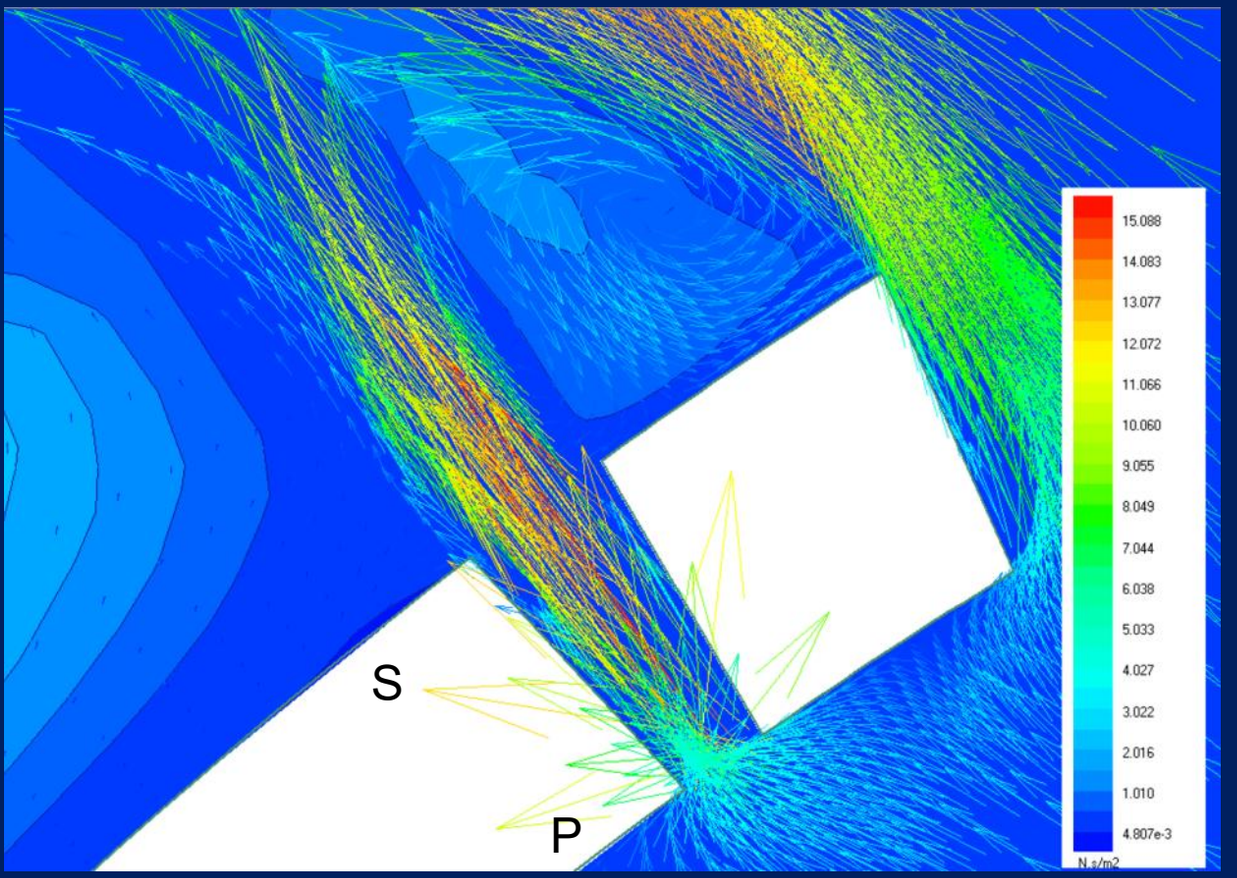
- Low pressure zone located at nozzle entrance
- **Much higher** pressure at the nozzle exit
- There is a **significant reduction** in the propensity for cavitation
- **Best results for 5-deg. divergent angle**



SUSTAINABILITY AND INNOVATION IN SHIP DESIGN AND OPERATIONS CONFERENCE 2026

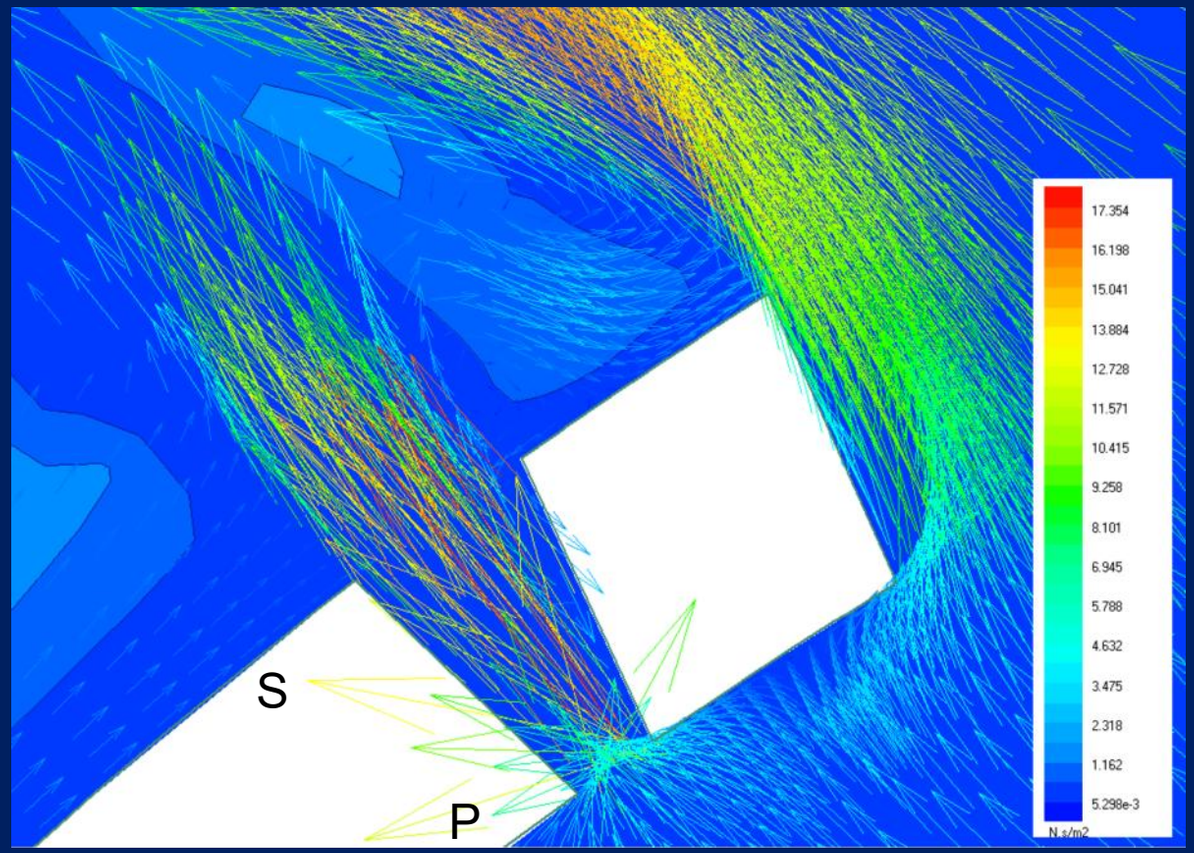
Propeller with Divergent Nozzle: 5-deg. divergence angle
CFD Calculations of Velocity Field

- No recirculation of fluid through the nozzle, however, there is recirculation around the leading edge (of the blade)
- Units are m/s (check!!)



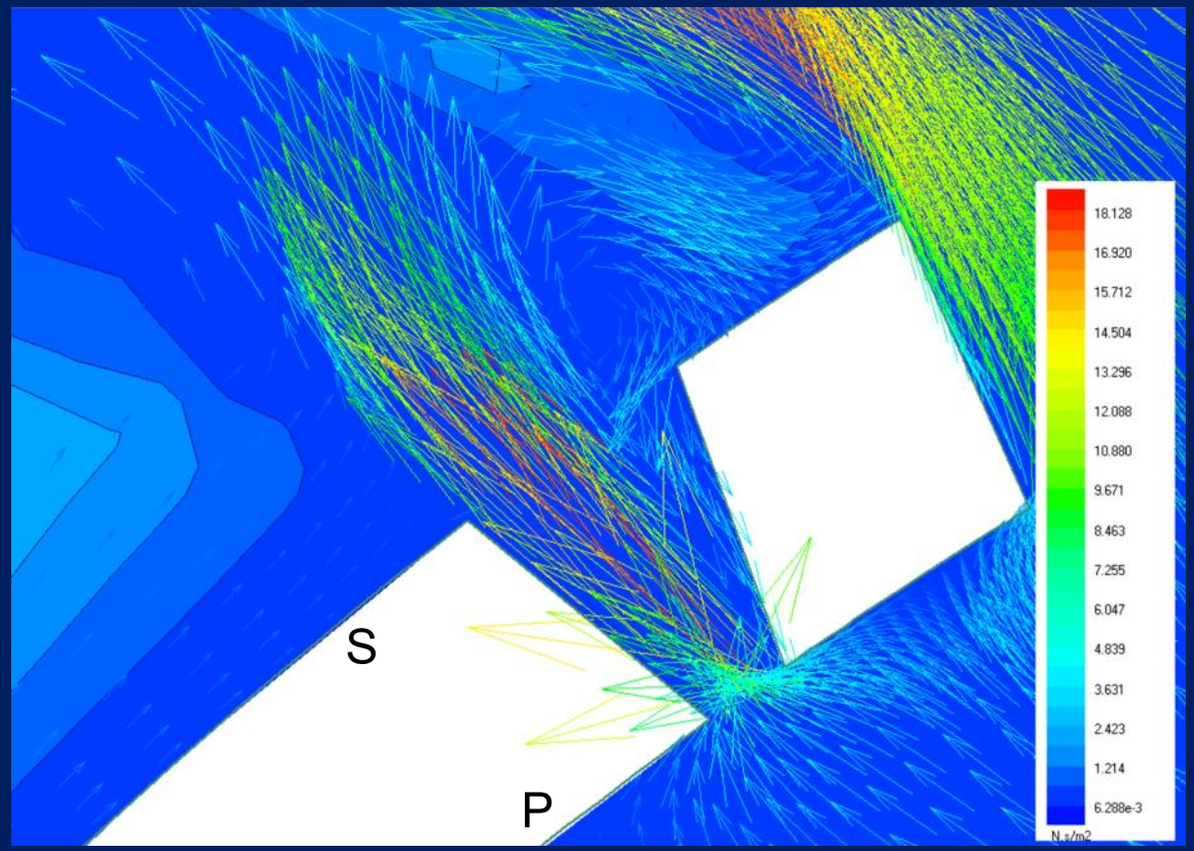
Propeller with Divergent Nozzle: 10-deg. divergence angle
CFD Calculations of Velocity Field

- At the 10-deg. nozzle divergence angle, we observed a slight recirculation beginning to occur at the exit of the nozzle
- There is still recirculation around the leading edge (of the blade)



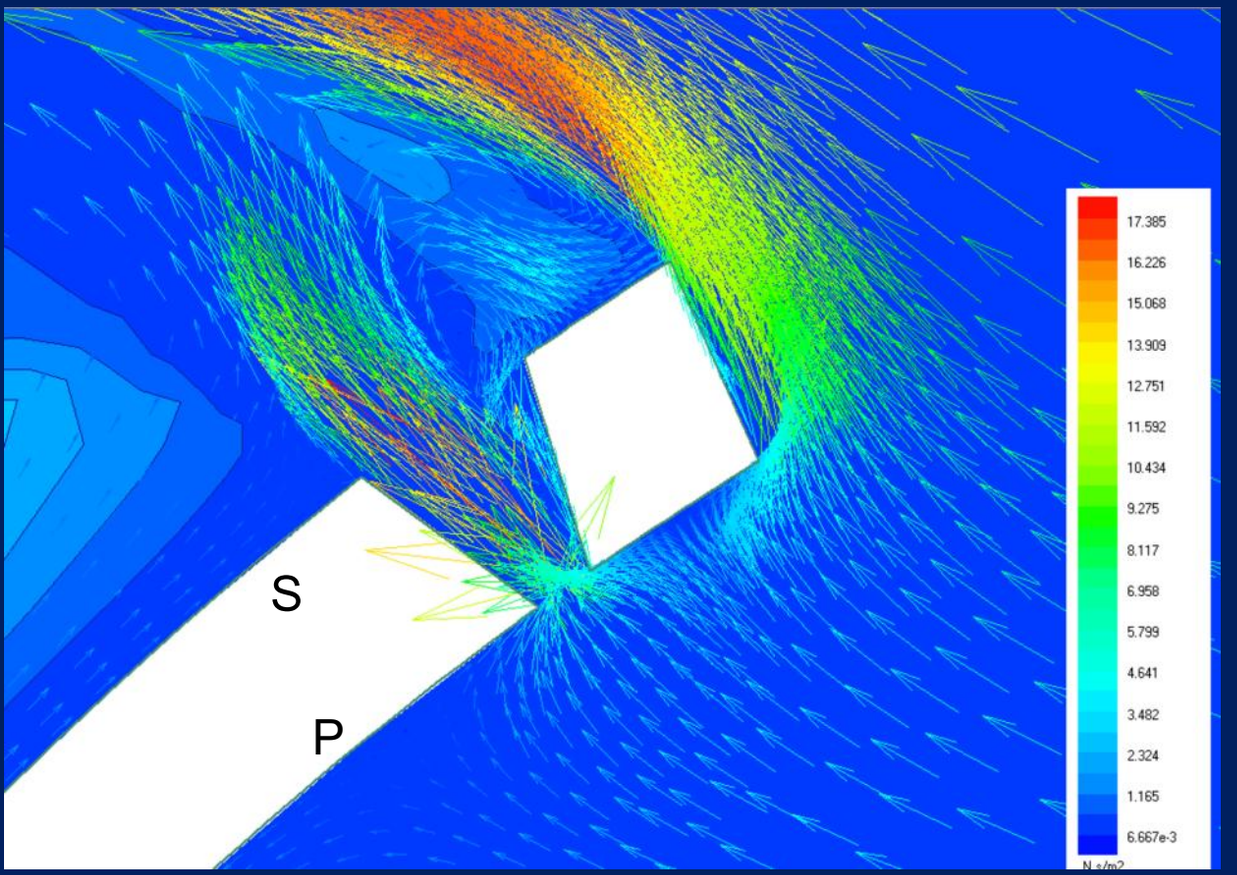
Propeller with Divergent Nozzle: 15-deg. divergence angle
CFD Calculations of Velocity Field

- For the 15-deg. nozzle divergence angle, flow separation was observed inside the nozzle (upper-back side)
- Indication that this may not be a suitable nozzle divergence angle for mitigating cavitation on suction side of the propeller blade



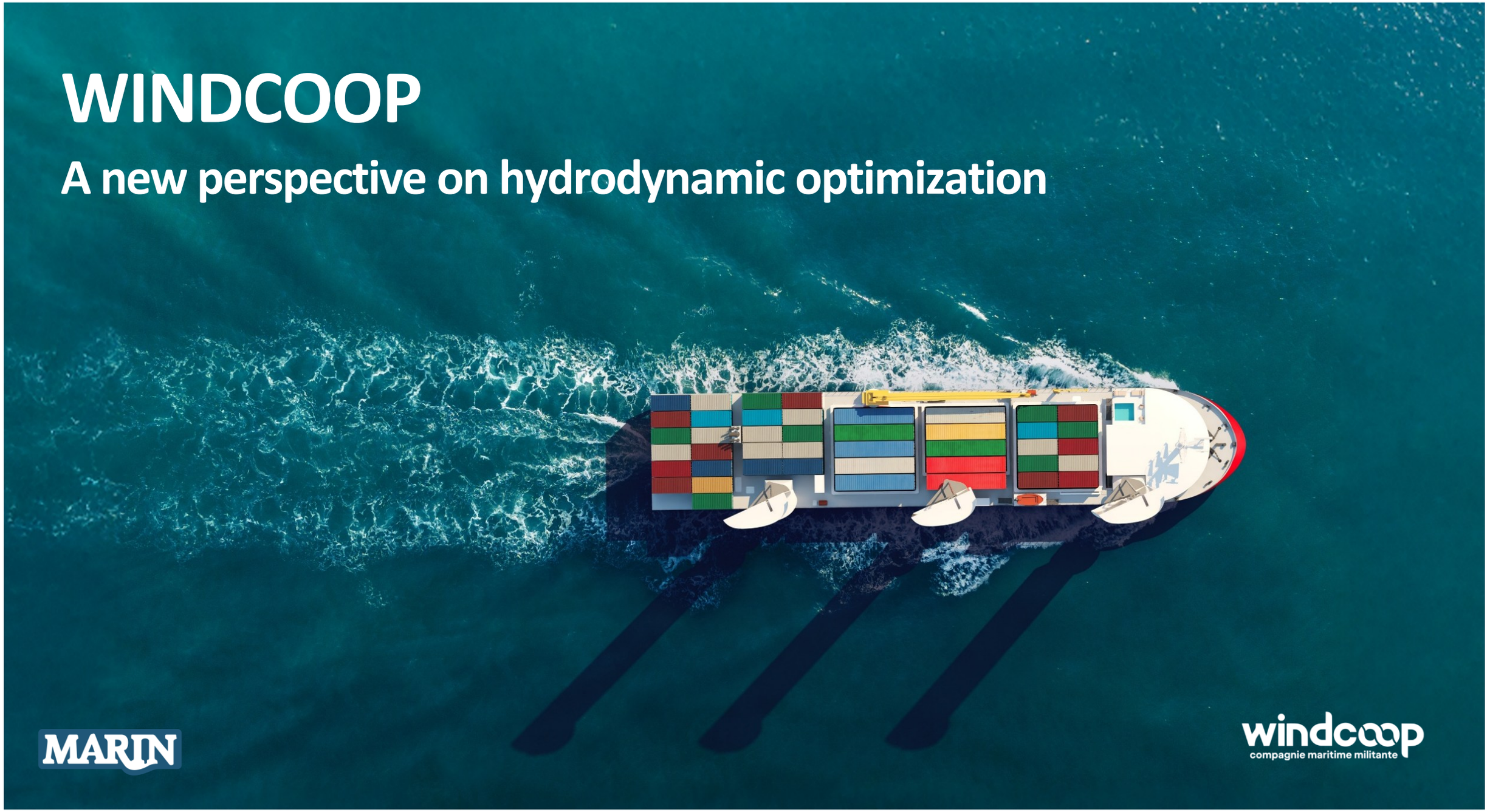
Propeller with Divergent Nozzle: 18-deg. divergence angle
CFD Calculations of Velocity Field

- Recirculation occurring at the exit of the nozzle (clearly visible)
- Recirculation is undesirable because it will increase the chance of cavitation
- There is still recirculation around the outer edge of the blade



WINDCOOP

A new perspective on hydrodynamic optimization



MARIN

windcoop
compagnie maritime militante

01 Context and project overview

WINDCOOP introduction

A wind-powered shipping initiative

- Founded in 2021 by Zéphyr & Borée, ARCADIE and enercoop
- Low-carbon shipping
- Cooperative business model

Marseille - Madagascar service

- Direct service between Marseille and Madagascar
- Regular liner operations

Strong environmental ambition

- Reduced carbon intensity (g CO_2 / TEU.km)
- Wind propulsion as a primary energy source



The development of the vessel MIARAKA

An iterative design process, from 67 TEUs to 220 TEUs











2021
Concept
67 TEUs

2023
Scaling up #1
100 TEUs

2024
Scaling up #2
200 TEUs

2025
Rig configuration
220 TEUs

2025
Final design
220 TEUs

Shipbuilding contract
(Main particulars defined)

RMK MARINE

03 Maximizing Wind Propulsion Benefits

A TWO –PHASES OPTIMIZATION PROCESS

I. MAIN PARTICULARS AND OPERATIONAL PROFILE

- CO_2 intensity (g CO_2/TEU.km)
- Transport cost
- Transit time

→ **SHIPBUILDING CONTRACT**

(Main particulars and operational profile defined)

RMK MARINE



Pure sailing vessel

II. HULL OPTIMIZATION PROCESS

→ **A new optimization method developed with MARIN …**

- Based on operational profile → variable conditions (Speed, pitch, RPM, …)
- Wind assists conditions (Leeway, Heel angle)
- Including route optimization (routing & speed)

→ **…and respecting contractual constraints**

- Cargo capacity (containers)
- Accommodation
- Bow thruster
- Contract speed (sea trials)
- …



Optimized hybrid vessel

The approach for the optimisation of the hull of a wind-powered vessel is different that for a classic motorized vessel

→ The hull optimisation of a classic motorized vessel targets minimal fuel consumption through minimal resistance and maximized propulsive efficiency
- Usually 1 condition (e.g. contractual speed, design draught) or relatively simple operational profile (2D matrix of draughts and speeds)
- Sailing in straight, upright condition
- Hull-propeller interaction, considering a relatively constant propeller loading (KT)

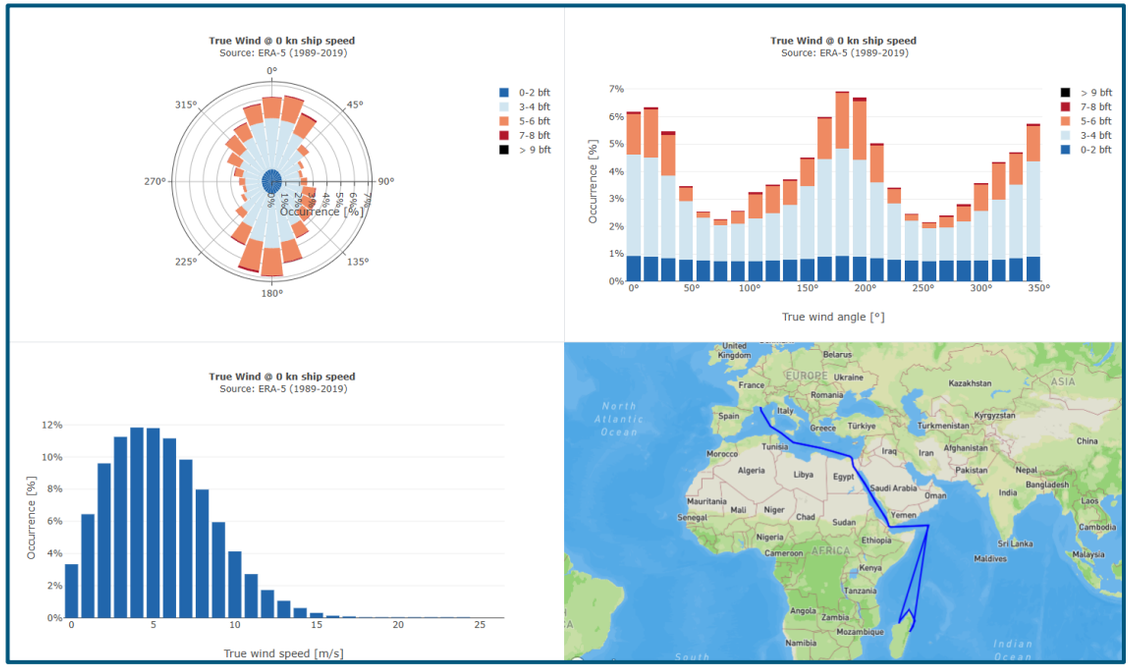
→ However, a wind-powered vessel takes a large part or the entireness of its propulsion from wind.
→ Therefore, the hull form will be determined from the route (and the associated wind conditions) the vessel will be sailing on.
- Objective becomes fuel consumption along the given route
- The operational profile extends to include wind (and wave) conditions (speeds, direction)
- Sailing in straight and upright condition, but also under drift and heel
- Large variations in propeller loading
- Trade-off between optimal resistance and sufficient course-stability

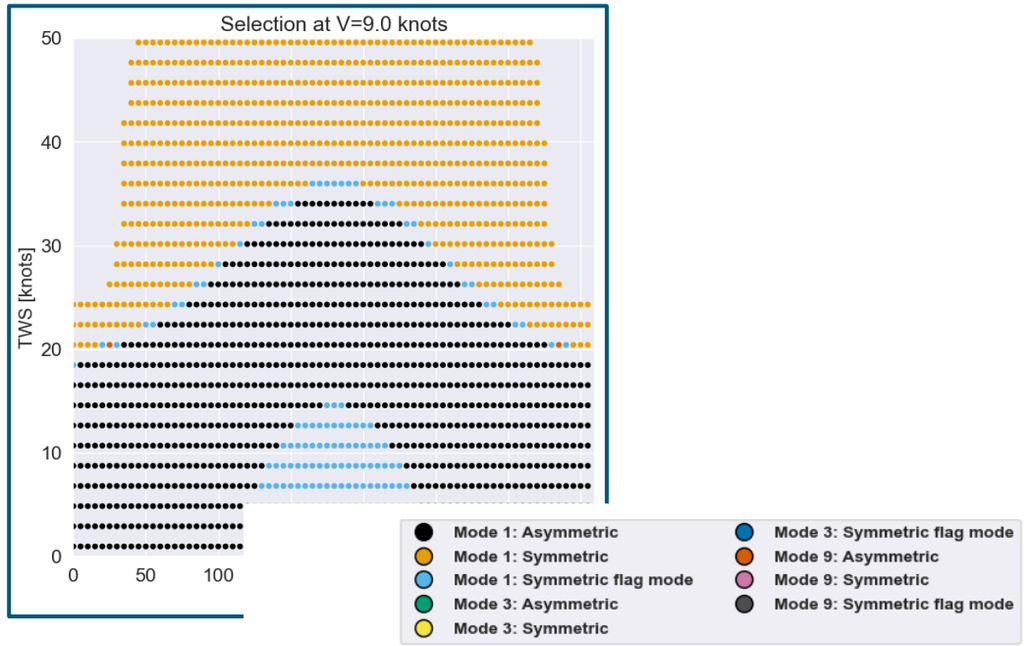
The different steps in the optimisation

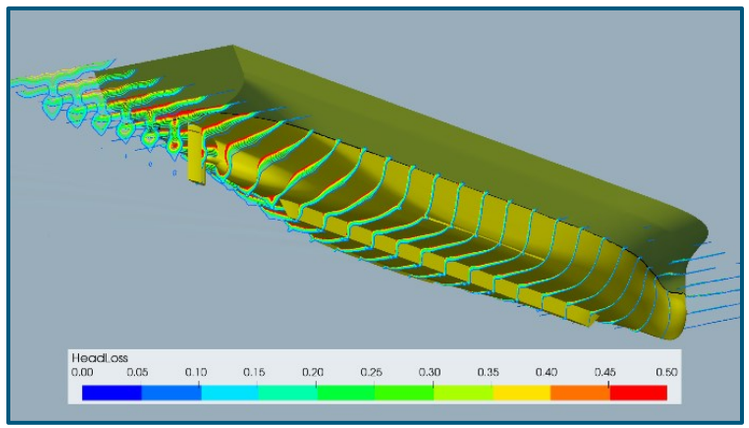
- Determination of the environmental conditions
  - BlueRoute (wind conditions)
- Determination of the sailing profile (initial PPP)
  - Using initial numerical models (hydro, aerodynamics, propulsion, etc…)
- Identification of the optimisation constraints (design restrictions due to cargo capacity, etc…) and operational constraints (heel angle, rudder angle, leeway angle)
- Initial hull form analysis, including wake field
- Hull form optimisation
  - Manual form exploration, search for improvements in most typically encountered sailing configurations
  - Innovative approach where:
    - every single variation is evaluated through CFD (sailing straight and under leeway) and a (simplified) PPP
    - The results from the weighted PPP simulations (based on the voyage simulations) are fed to an optimiser to optimise the fuel savings and CLR under 3 deg leeway

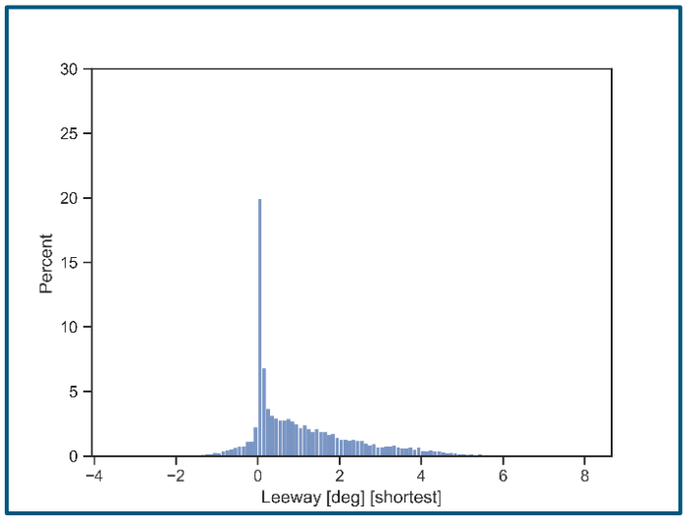


06 Initial conditions







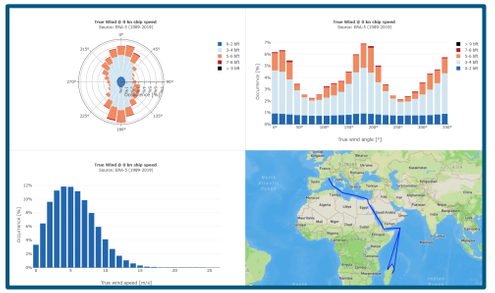


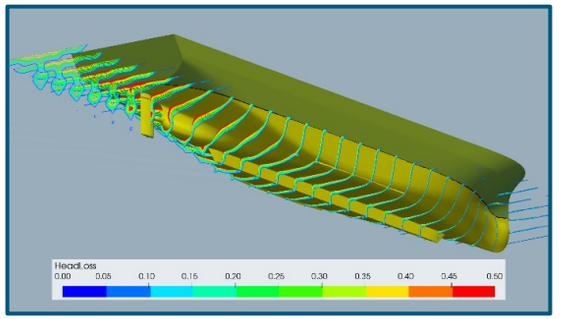
07 Initial conditions

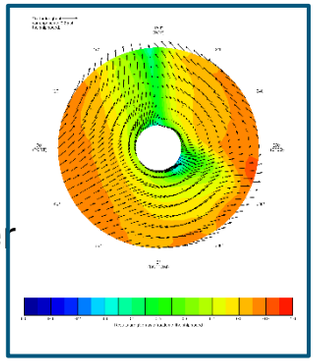
- Initial analysis of hull form and effective wave field
  - RANS-BEM calculations using MARIN's codes REFRESCO (RANS) and panel code PROCAL
  - Evaluation of wave systems, viscous losses and areas of reversed flow
  - Effective wake field → input for propeller design
  - Effective wake field → effect of skeg at drift angles 0°, 3°, 6° and 9°

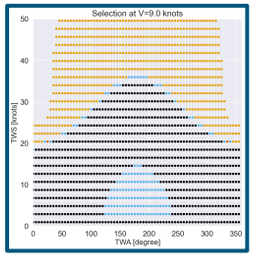
- Performance prediction program (PPP)
  - Sailing on fixed route (see above) at a fixed speed (9, 10, 11 and 12 knots)
  - Preferred propulsion modes as function of speed
  - Wind conditions (TWS, TWA)
  - Influence of sail protection curve (asymmetric, symmetric, symmetric feathered)

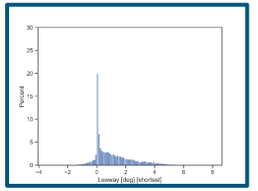
- Voyage simulations
  - Sailing on fixed route or sailing on route including weather routing
  - Prediction of CO2 emissions along the route
  - Insight in the operational profile of the vessel (speed, leeway, heel, rudder angle, propeller rotation rate (including 'smart' combinator curve)







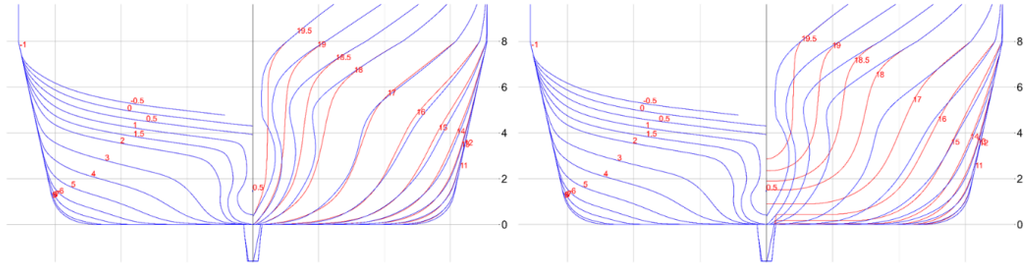


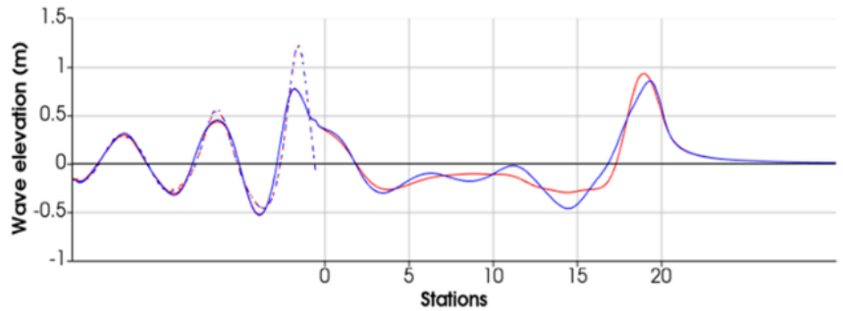


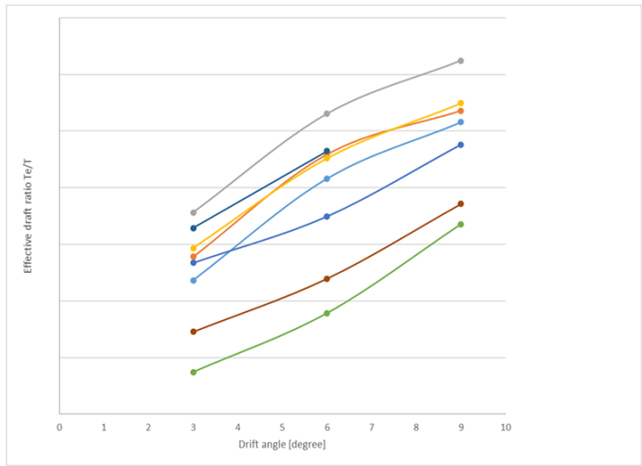
08 Hull form optimisation

- **First phase: manual hull form exploration (potential flow, RANS)**
  - Obtain a relatively good hull form for the second phase
  - Explore the effect of major changes in hull design
    - Removal of the bulb
    - Larger bulb
    - Fore shoulder variation
    - Lifted bow without bulb, inspired by classical sailing
    - Raising transom
    - Adding deadrise
    - Etc…
  - Drift keel kept unchanged

→ Benefit observed from raising transom
→ Variation with bow up valuable for the second phase (parametric optimization) due to performance under drift







09 Hull form optimisation

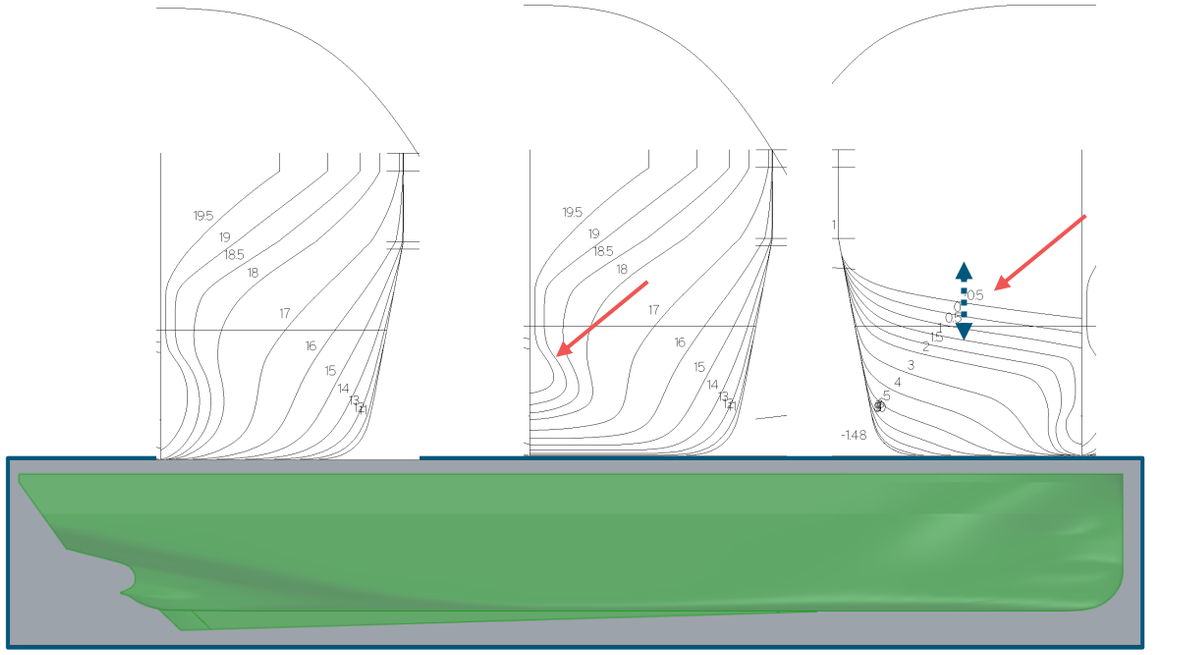
- **Second phase: parametric hull form variation (RANS, PPP)**
  - Use of the knowledge from previous phase
  - Intermediate hull form used as reference
  - Hull form variations
  - Drift keel (skeg) variations
    - Length
    - Position
    - Slope

  → <u>64 different combinations of hull form and drift keel</u>
    - DoE realized by a Latin Hypercube sample plan

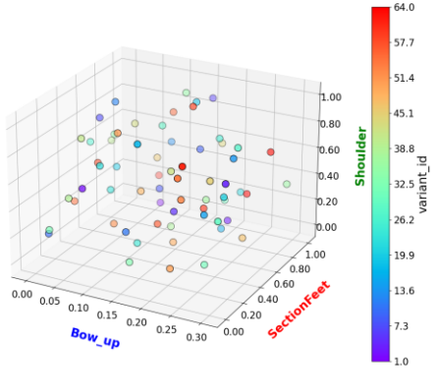
  - One propulsion mode
    (engine for propulsion, generator set for hotel loads)

  - One sail mode (asymmetric)

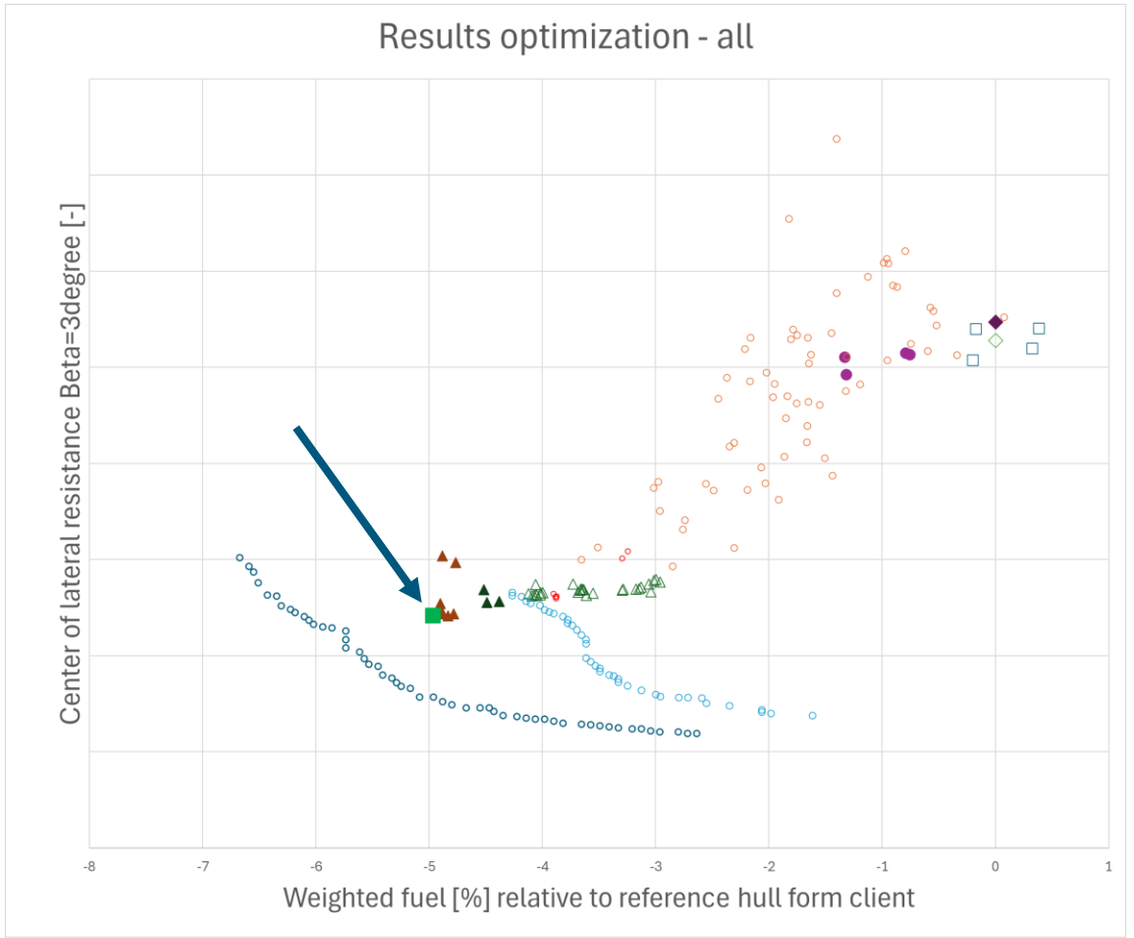
  - 4 speeds, covering the expected speed range







10 Results



- Reference hull client
- Reference hull client [fine]
- Corners points [hull form]
- Corners points [hull form- Fine grid]
- DOE [64 samples]
- Estimated pareto
- Evaluated pareto
- Estimated pareto iteration 1
- Evaluated pareto iteration 1
- Evaluated pareto [fine]
- Evaluated pareto [fine - No Bow up]
- Winning hull form [fine]

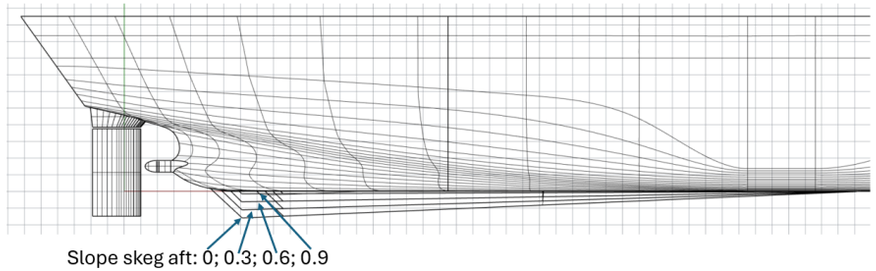
11 Further appendage refinement

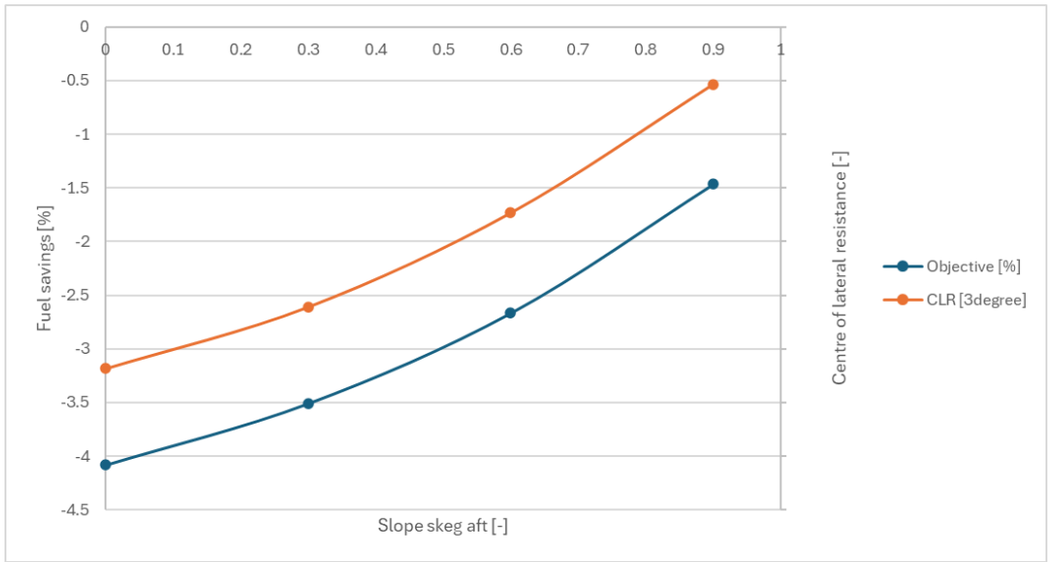
- **Third phase: a smaller parametric variation of appendages (RANS, PPP)**
  - Variation on drift keel height, width and shape
  - Variation on bilge keel position
  - Variation on rudder size

→ reducing the drift keel height is beneficial for resistance but **detrimental** for fuel savings

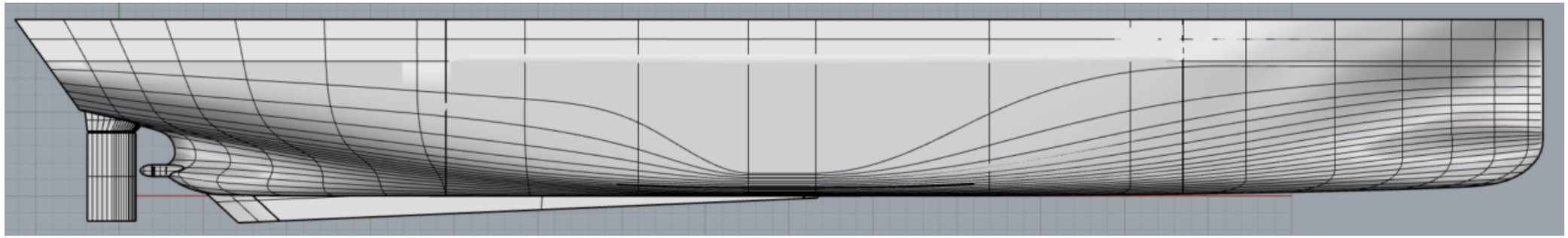
→ increasing the keel height moves the centre of lateral resistance backwards and reduces the drift angle

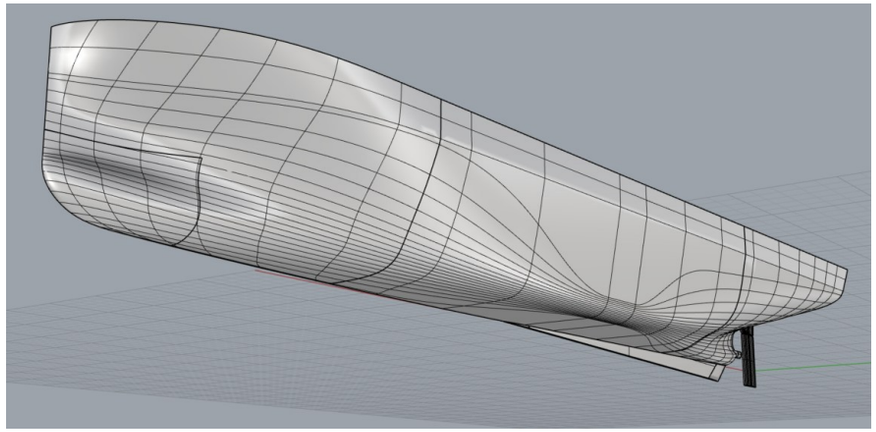
→ **highlights the fact that such ships need to be optimized in a broader range of conditions than pure straight sailing.**

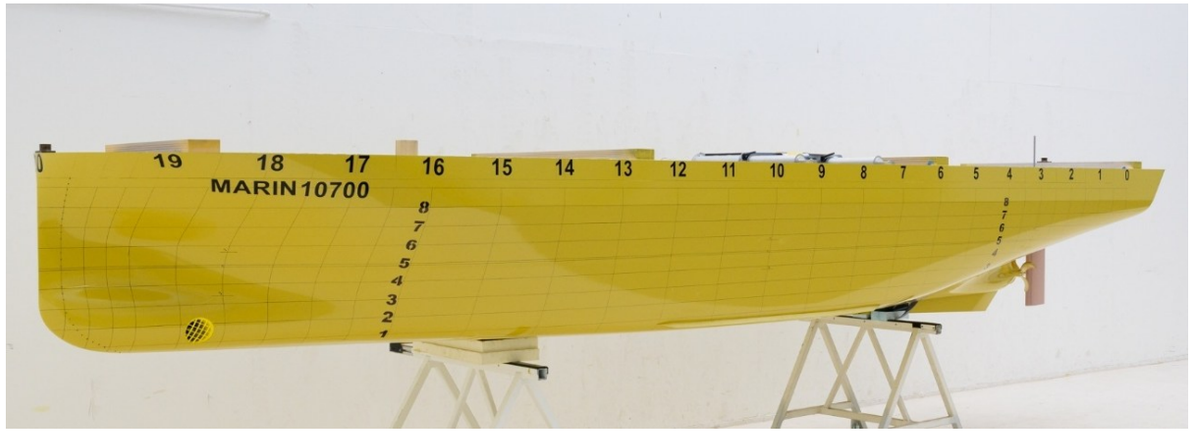




12 Results: optimal hull form and appendages

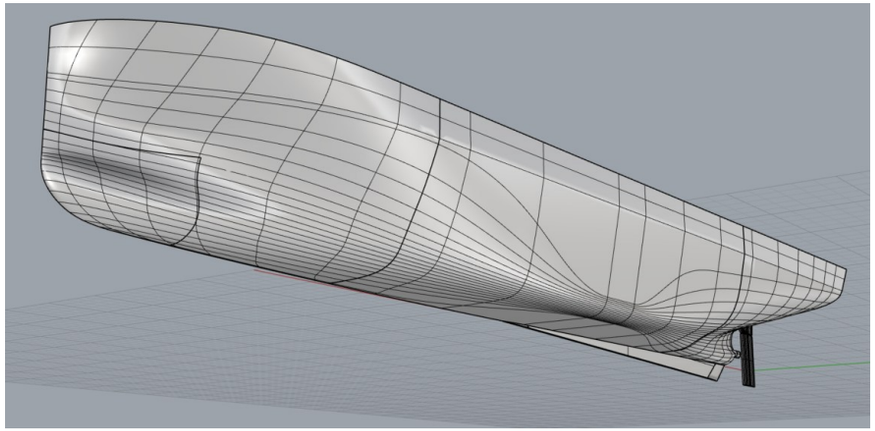




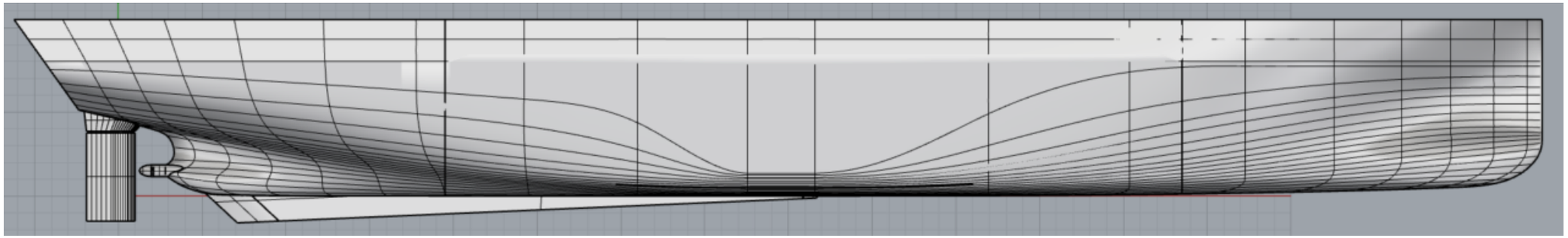


13 Assessment with final hull form

- **The selected optimum hull form features**
  - a sloped skeg moved aft of moderate length
  - a bow raised to the maximum allowable vertical position to accommodate the bow thruster
  - a raised transom.
  - the fore and aft sections are more rounded than those of the original hull form.
  - the skeg has a rounded leading edge and unchanged width compared to that of the original design.
  - the rudder remains identical to that of the reference hull form
  - the bilge keels are centred around midship

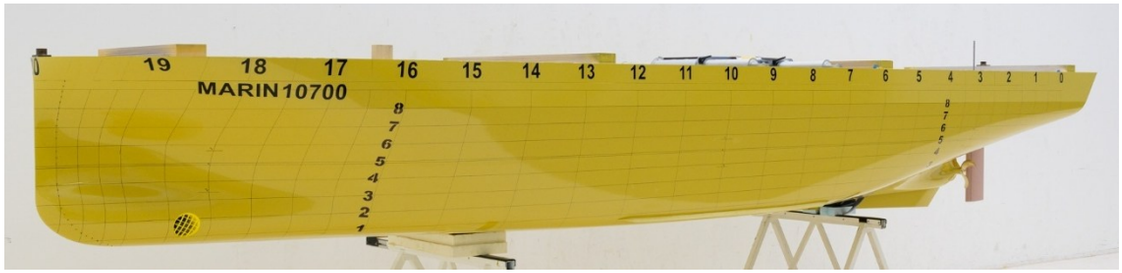


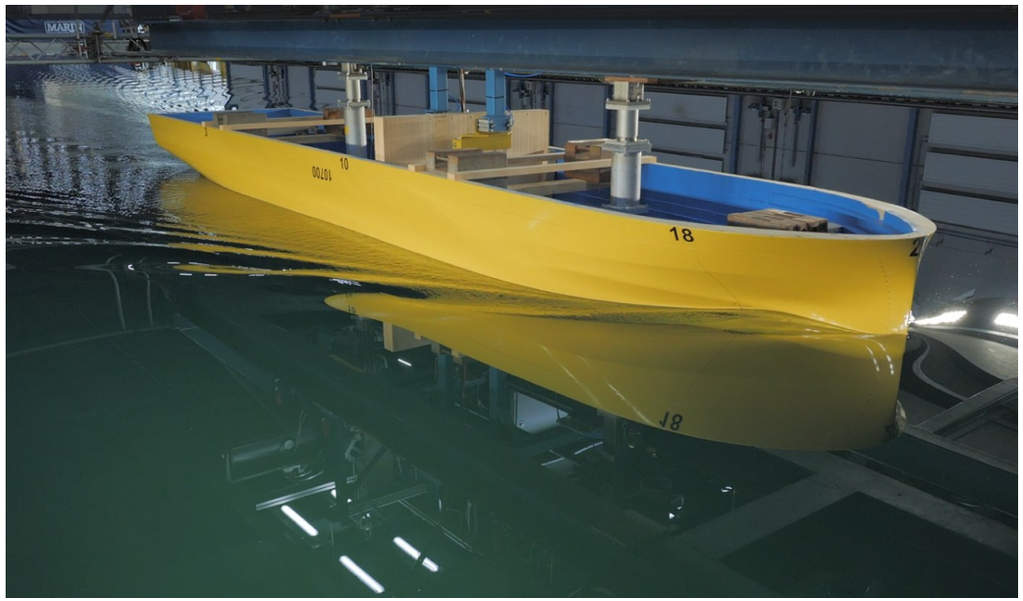
- The selected hull form is expected to deliver about 5 % fuel savings compared with the initial hull form

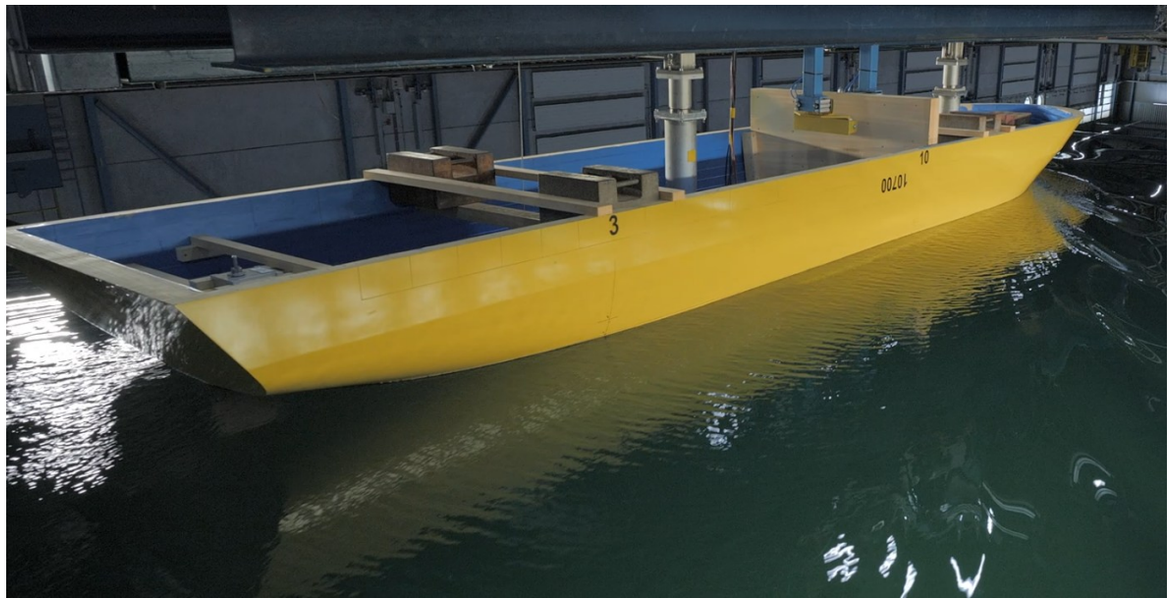


14 Model tests

- **Model tests performed with a semi-captive model**
  - Model scale 1:13.5, model length approx. 6.5 m
  - Objective: develop a hydrodynamic force database
    - Ship drag and lift forces and moment around vertical axis
    - Variation in drift angle, heel angle, speed, propeller thrust contribution



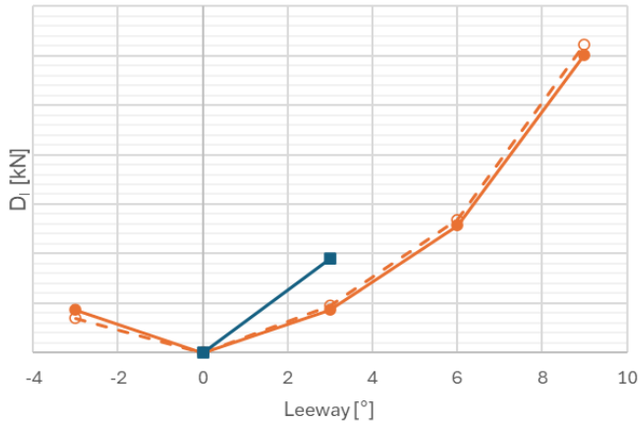


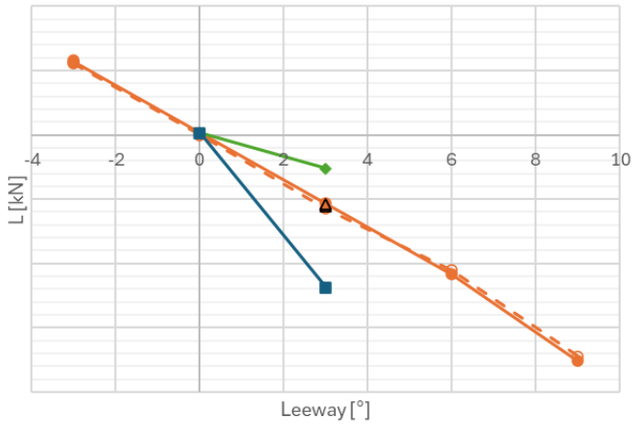


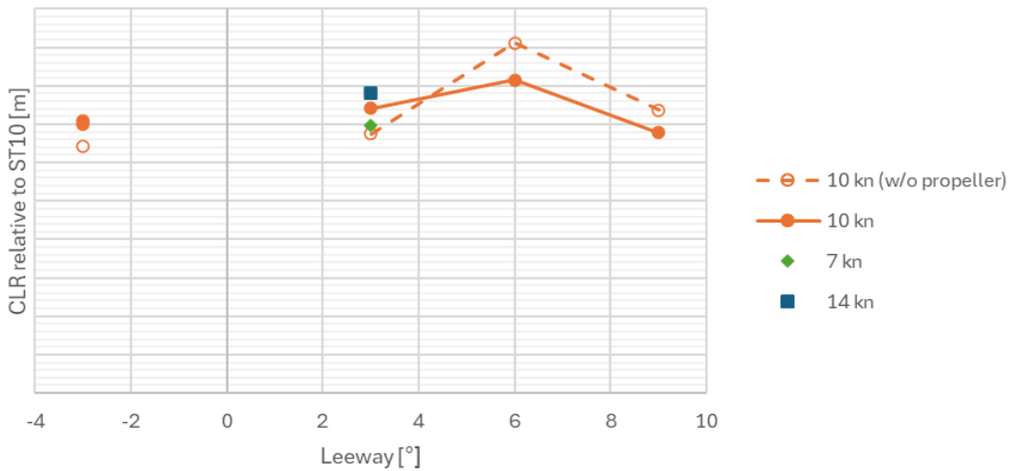
15 Model tests

- **Model tests performed with a semi-captive model**
  - Effect of appendages (with and w/o rudder, bilge keels)
  - Effect of trim



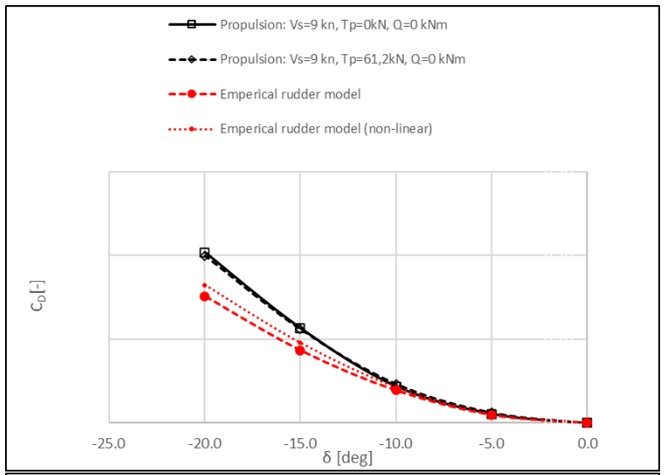


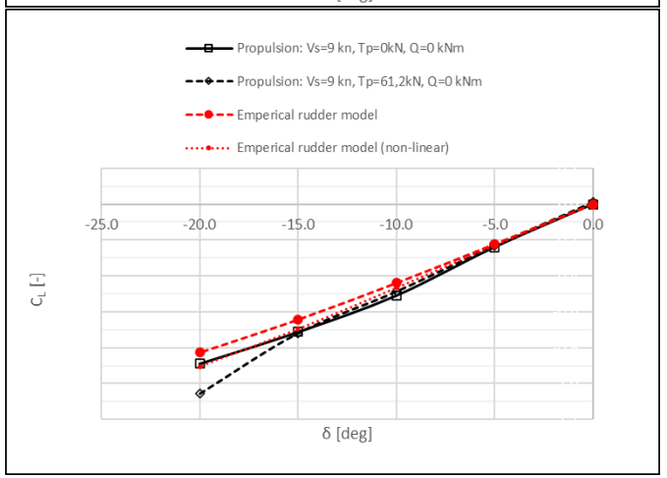


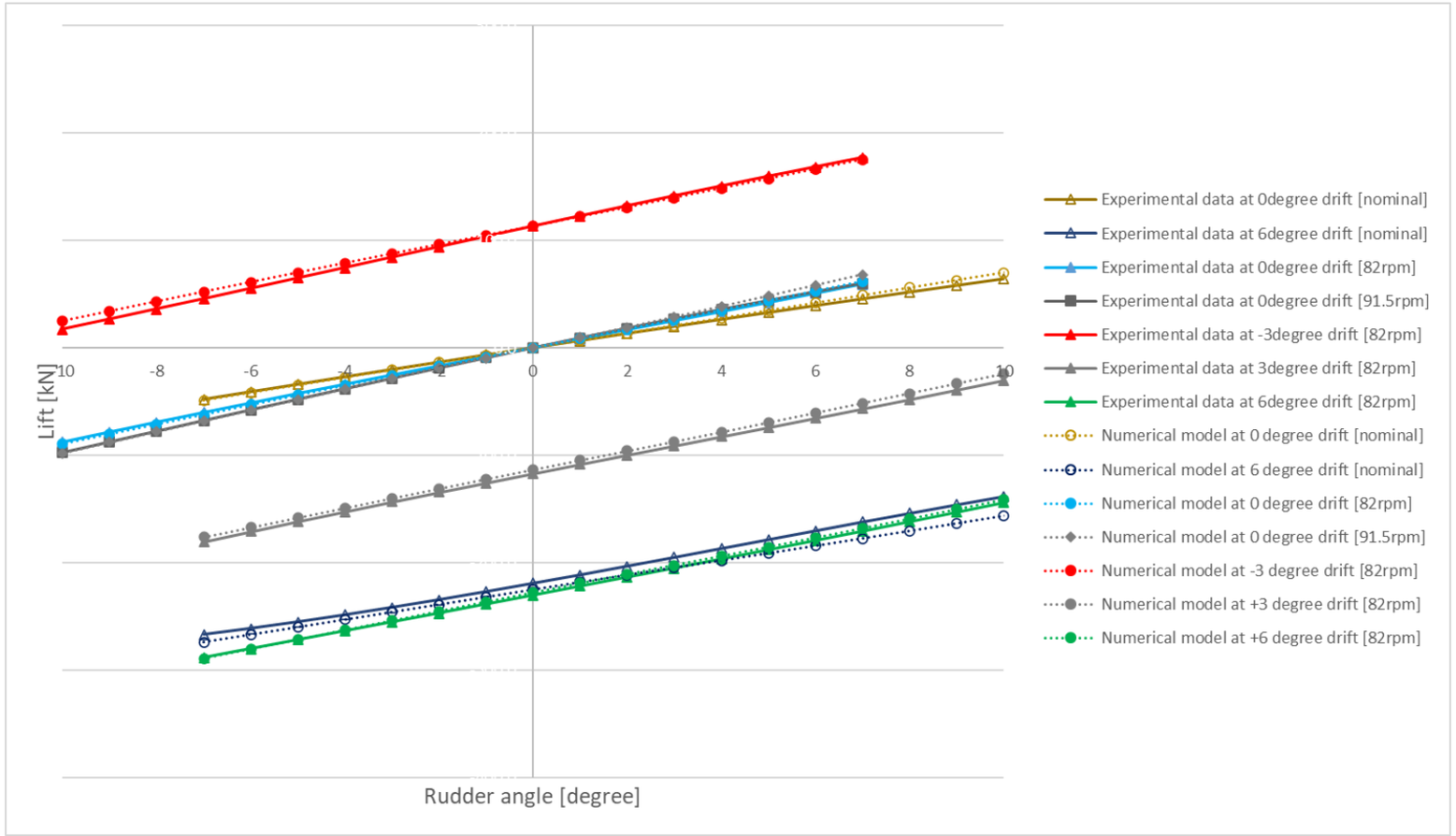


Tuning of numerical model

- **Tuning of the numerical model based on the results of the model tests**
  - CL / CD model of the hull
  - CL / CD model of the rudder

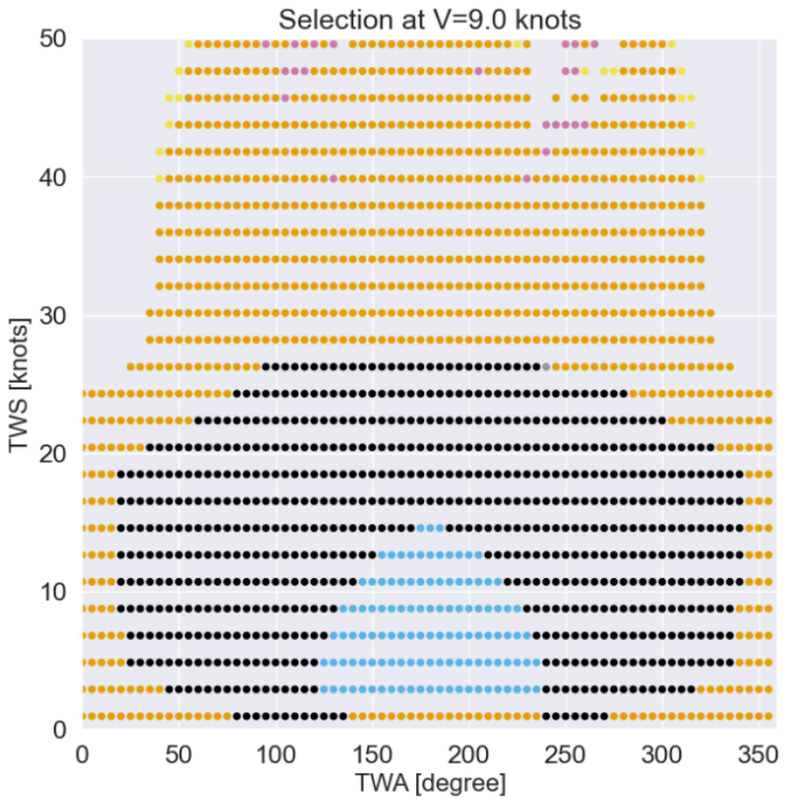


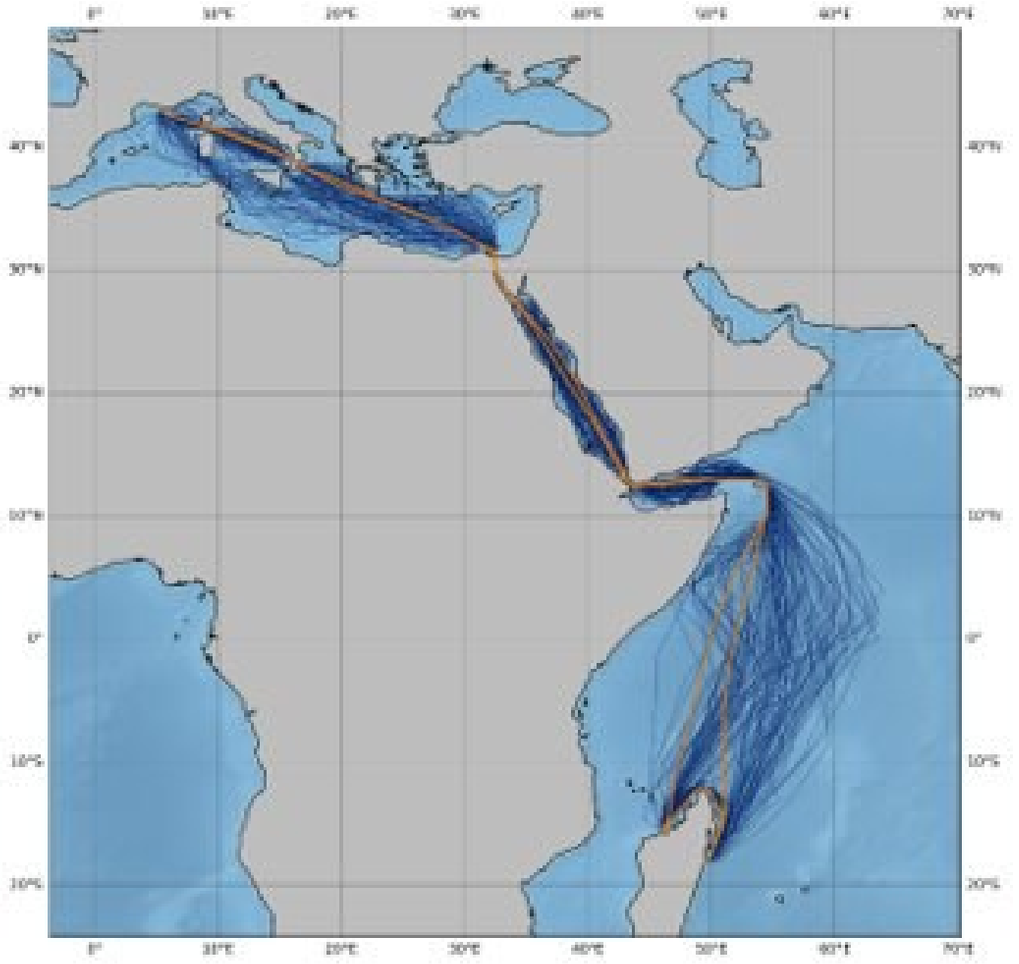




17 Final PPP and voyage simulations

- **After the numerical models have been tuned, the PPP and voyage simulations were executed once again**





18 Conclusions

- **The WINDCOOP project was subject to a new hydrodynamic optimization approach**

- In this approach the hull form was optimized considering the particular conditions encountered by a sailing ship:
  - Sailing straight and sailing under drift and heel
  - Importance of the route
  - Importance of good anti-drifting performance versus resistance

- Each hull form and appendage variation was subject to a separate PPP calculation

- Target was lowest CO2 emissions along route, with and without rerouting

- The optimal skeg was found to be the largest from all variations, highlighting the contribution of efficient anti-drifting measures (high lift, low drag) on the final CO2 emissions.

- Still some improvements in the process are needed:
  - Improve the streamlining process between numerical and experimental work
  - Extend the scope of the optimization to include propeller design

Thank you

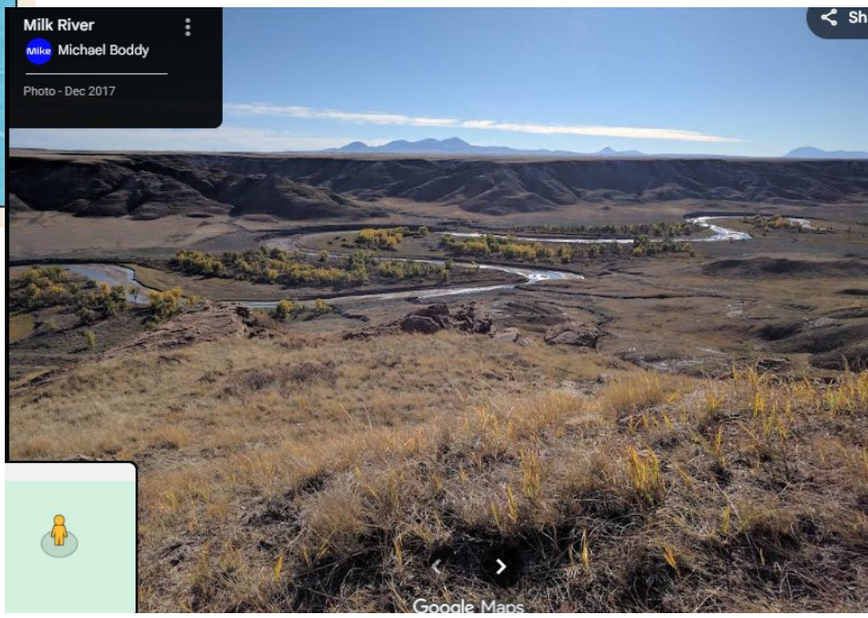


A Prototype Human-Powered Electric-Drive Small Boat for Long-Distance Cruising on Rivers and Lakes

Isaac Lee, Erik Lunn and Sergio Perez

The Inspiration: Bill Hayward's 18 month, 7000 mile journey

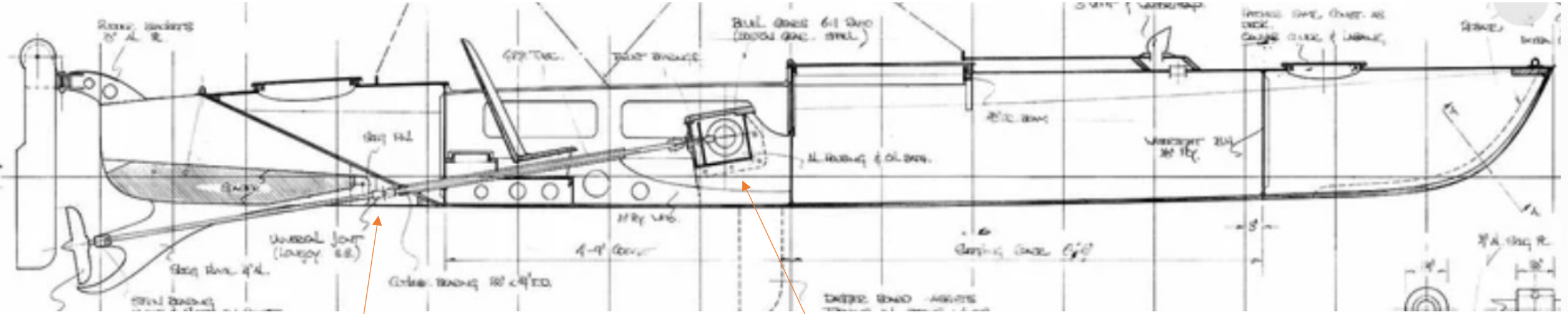




Mik River-Missouri River, Mississippi River, Gulf He traveled across Fla at lake Okeechobee, not down to miami. Up the Hudson to Troy to Champlain Canal system, to lake champlain to Richelieu River to St Lawrence river. Pedaled past Quebec sity, then got lift to dAlhouise.. About a hundred miles, across from Quebec city, to new Brunswick.



Hayward’s Vessel: Blue Skies, designed by Paul Gartside



Universal joint allows shaft to kick up if propeller hits bottom

Right angle drive converts pedaling rotation axis to propeller rotation axis

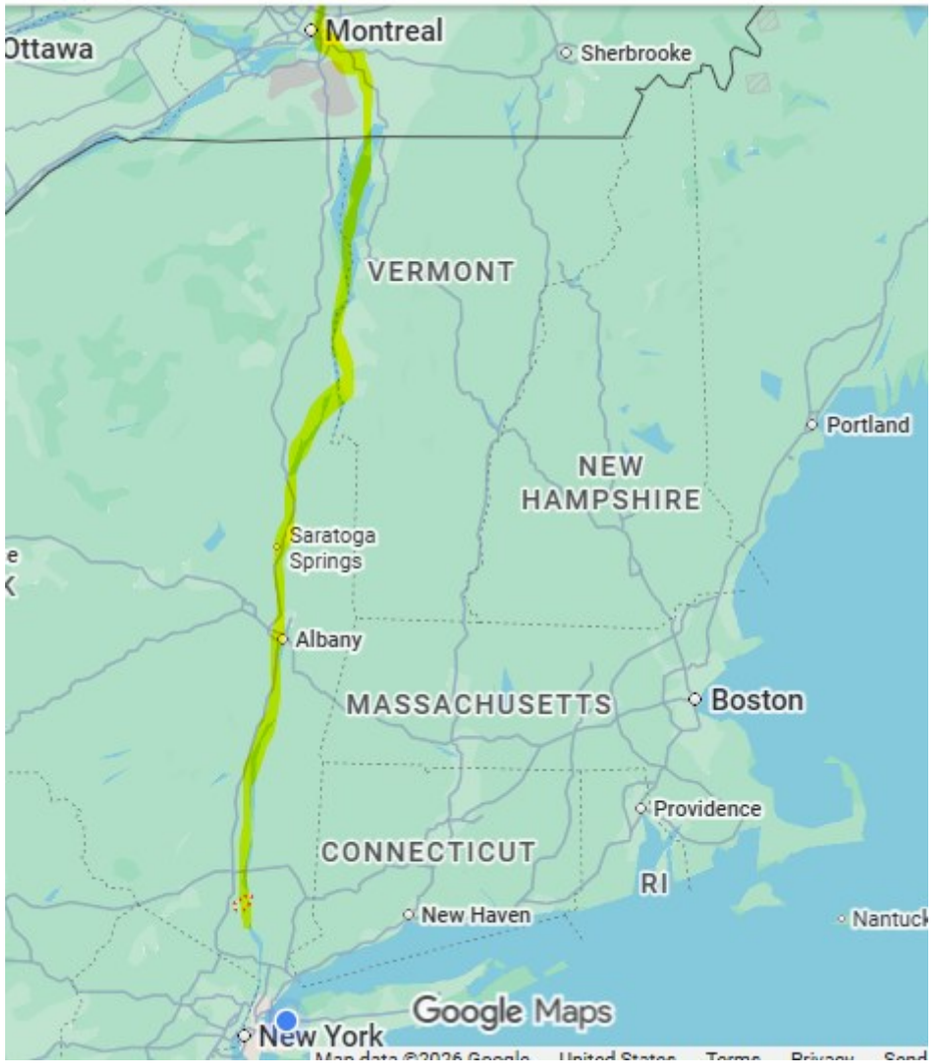
https://gartsideboats.com/

Proposal… a shorter, but no less exciting trip from West Point NY to Quebec City (about 500 miles)

The Hudson River from NYC to Troy NY (150 miles) is affected by tides.

- West Point, NY Hudson River to Troy, NY (~100 miles)
- Into Champlain Canal System (with locks) to Lake Champlain (~60 miles)
- Cruise north on Lake Champlain (~120 miles)
- North on Richelieu River, Canada to St Lawrence River (~80 miles)
- St. Lawrence River to Montreal (~45 miles)
- North to Quebec City on St. Lawrence River (~160 miles)

South of West Point may be too challenging

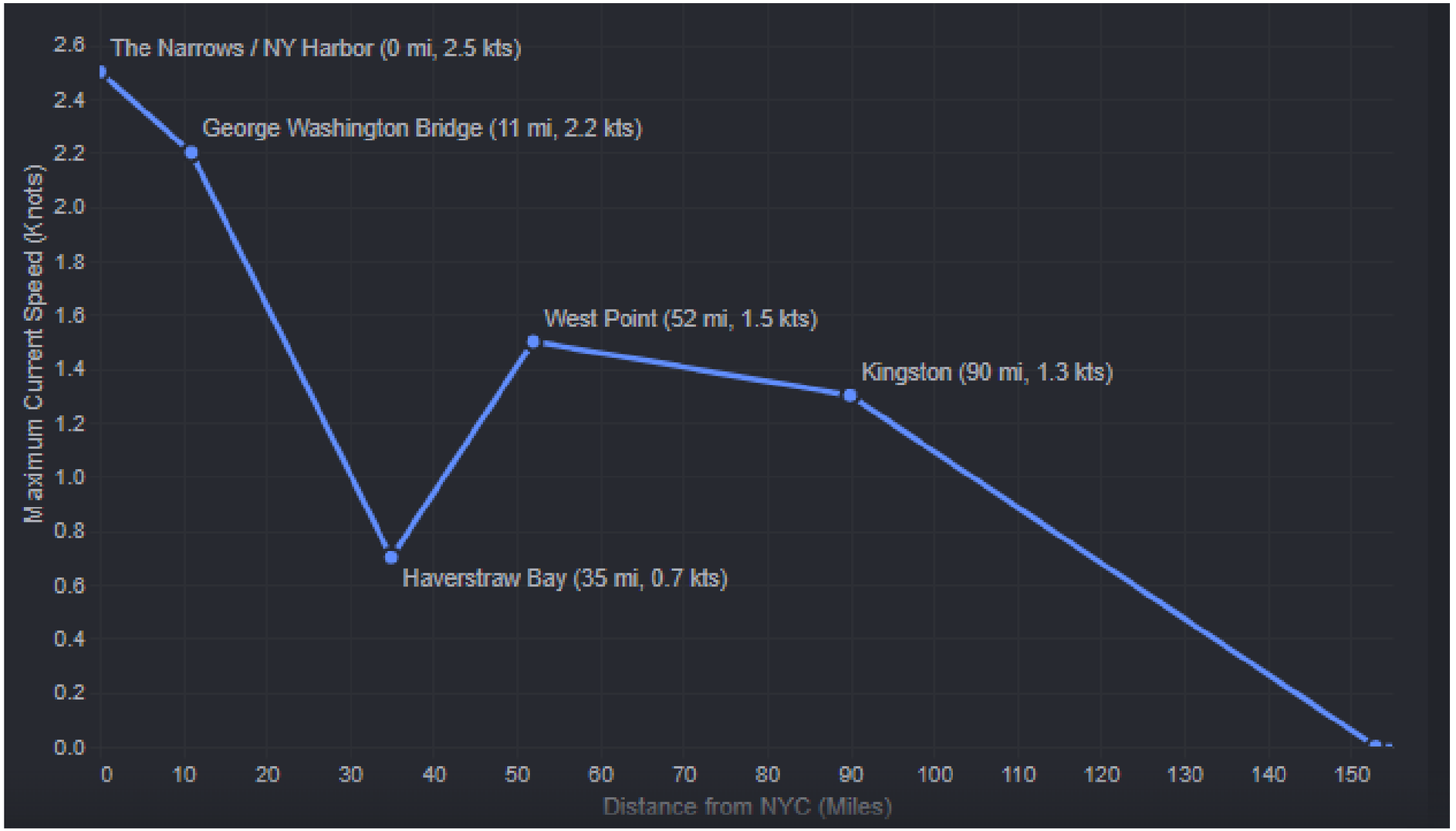




Troy, NY Lock and dam

Hudson River Maximum Currents at center-river

Tidal River with direction changing every six hours from NYC to Troy, NY (150 miles from NYC)



[1] https://dec.ny.gov

[2] https://www.instagram.com

[3] https://www.caryinstitute.org

[4] https://lamont.columbia.edu

[5] https://nycwatertrail.org

[6] https://www.waterwayguide.com

[7] https://hudsonriverestuary.pbworks.com

[8] https://tidesandcurrents.noaa.gov

[9] https://www.waterwayguide.com

[10] https://www.youtube.com

[11] https://en.wikipedia.org

Effect of distance from shore on current speed

https://bowman.com

Distance from Shore (Meters)	Typical Water Depth (Feet / Meters)	Current Speed (Knots)	Hydrodynamic Zone Description
0 m	0 ft / 0 m	0.00	Shoreline Boundary: Absolute zero velocity due to frictional drag against the bank.
25 m	6 ft / 1.8 m	0.45	Nearshore Shallows: Extreme shear zone; rapid speed changes over short distances.
50 m	12 ft / 3.6 m	0.90	Inner Littoral Shelf: Current begins to stabilize as depth drops off.
100 m	25 ft / 7.6 m	1.40	Channel Slope: Velocity scales up cleanly with increasing water depth.
200 m	40 ft / 12.2 m	1.85	Outer Channel: Core river flow begins to take over; friction decreases.
300 m	52 ft / 15.8 m	2.15	Main Channel Boundary: Approaching maximum kinetic energy.
400 m	58 ft / 17.7 m	2.32	Deep Channel: Flow is highly uniform and driven directly by tidal momentum.
500 m	60 ft / 18.3 m	2.40	The Thalweg (Center): Peak velocity zone where boundary friction is minimized.

But, what if large ships are passing?

Effects of commercial ship wake, as function of distance from ship at center-channel

https://www.coastalwiki.org/wiki/Wave_transformation

https://cosefm.cee.wisc.edu/CEE514_Coastal_Engineering/2003_Students_Web/Scott/Wave%20Height.htm

Distance from Ship Track	Water Depth	Wake Base Height	Wave Period / Length	Near-Shore Transformation & Impact on a 16-Foot Boat
0–100 meters *(Deep Channel)*	50–60 ft	**1.5 to 2.5 ft**	Long Period (4–6 seconds) / ~100 ft apart	**Gentle Roller:** In deep water, a 16-foot boat easily rides up and over these long, smooth swells with minimal slamming.
200–300 meters *(Channel Margin)*	25–30 ft	**2.0 to 3.0 ft**	Compressing	**Steepening Swell:** The waves begin to bunch closer together. The slope of the wave face steepens, causing a small boat to pitch sharply.
400 meters *(Shallows Edge)*	10–12 ft	**3.0 to 4.5 ft**	Very Compressed	**Shoaling Danger Zone:** The wake height spikes due to bottom friction. The waves become vertical "walls of water." A 16-foot boat will slam violently and take spray over the bow.
450–500 meters *(At Seawall/Shore)*	0–5 ft	**4.5 to 6.0+ ft**	Breaking / Shattered	**The Rebound / Breaker Zone:** The waves break violently like ocean surf or collide with steep seawalls, rebounding backward to create chaotic, unpredictable cross-chop capable of swamping a small hull.

Try to stay within about 100-200 m from ship

For maximum speed relative to land:

Adverse current: stay as close to shore as practical, but if large ship approaches move towards ship as much as fear and judgement will allow.

Favorable current: move towards center channel at your discretion (watch for collision with ships, wake from ships, loss of control from low relative speed to water).

Proposed Boat: Catamaran boat with Pedal-Power connected to Electric Generator, to electric outboard motor

Why an electric generator pedal-drive?:



- Propeller drive can be complex. Pilot typically near center of boat longitudinally, propeller is at stern, requiring a vulnerable shaft.
- Hobie style flapping systems usually work directly next to hull bottom – not easily applicable to catamaran design.
- Generator can be used to charge batteries on land if cruising not possible due to weather or strong currents (electric motor as generator could be complicated).
- With generator pedal drive there is more freedom to move the position of the pilot.
- Disadvantage: conversion from kinetic energy at legs, to electrical at generator and back to kinetic energy at propeller shaft results in losses

Power transmission comparison from human to propeller shaft (based on commercially available components)





Generator, 75-80% efficiency



Electric outboard motor 80-90% efficiency

Total efficiency
= 0.77* 0.85
= 0.65





Right-angle drive 90-99% efficiency

Shaft 95-98%

Total efficiency
= 0.95* 0.97
= 0.92

Generator option requires significantly more work than transmission option, but cost is lower.

PROTOTYPE DESIGN FOR TESTING THE GENERATOR DRIVE
(not for Hudson- Quebec River Voyage)

- Inflatable PVC : light, foldable, relatively strong. Cylindrical tubes with tapered bow and stern. Low cost.
- Catamaran configuration: for stability and cargo space.
- Electric motor outboard drive.
- Motor driven by generator, generator turned by pilot.
- Pedal drive generator can charge the battery (if weather or currents do not permit cruising).
- 5 miles per hour desired vessel speed to enable 50 miles per day maximum.

PARAMETRIC DESIGN STUDY: Influence of hull length, hull separation and speed on total resistance

Resistance data for inflatable cylindrical hulls not available.

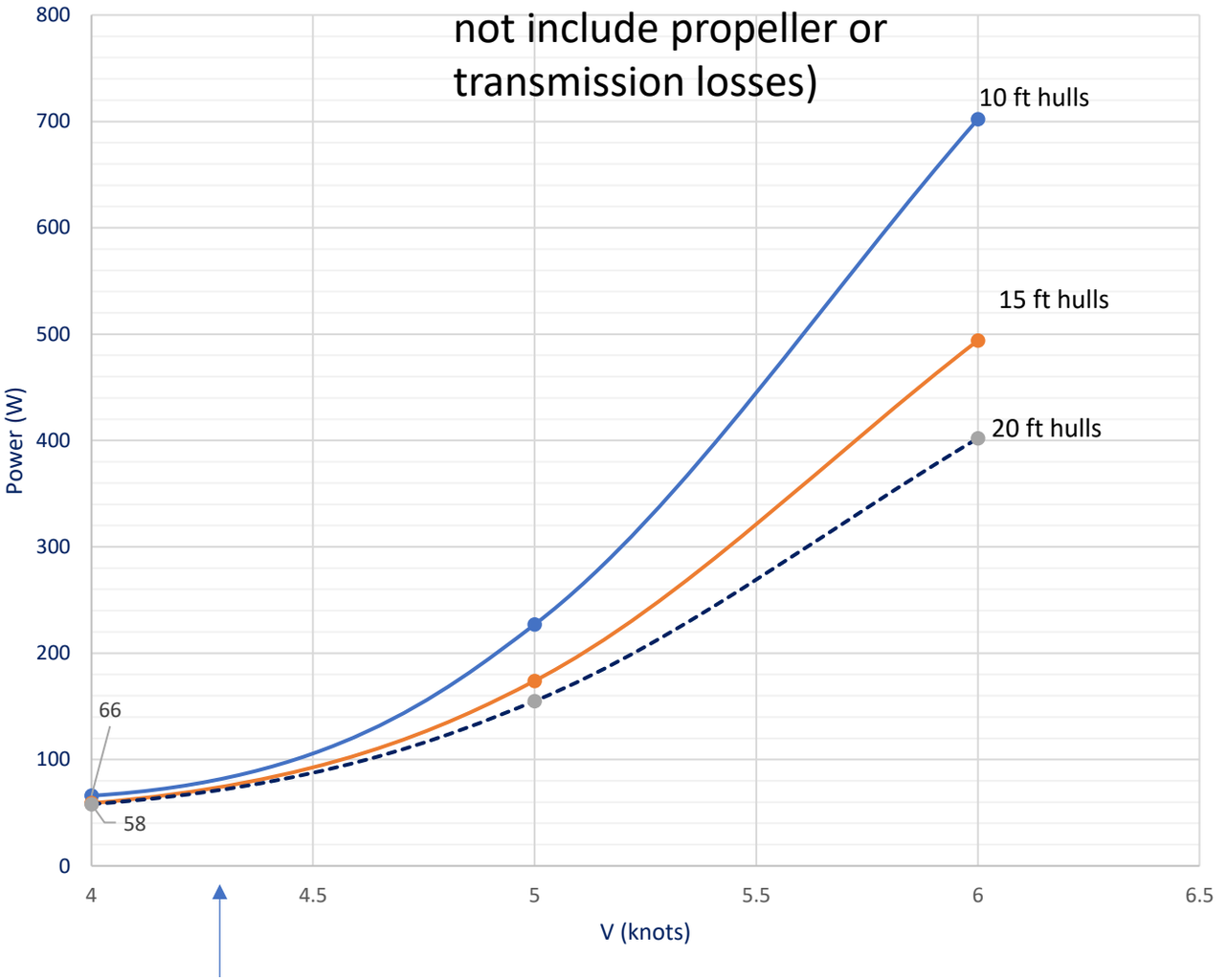
Design study performed by OpenAI by using theoretical estimates of skin, form, and wave-making drag forces (for idealized hulls that were not identical to the prototype), then adjusting the estimate using real-world data (again from hulls that are not identical to the prototype). Results appear reasonable.

Skin and form drag: from Hoerner's Aerodynamics book relating skin drag of symmetrical bodies of revolution to form drag.
Wave-making drag: from Michell's Thin Ship Wave Resistance Integral combined with towing tank data base regressions.
Hull Interference: Using an empirical curve-fit derived from Insel & Molland catamaran database

It is hoped that the trends are accurate. Estimates should be verified by experiments.

300 lb wt, 10 degree hull, 8 ft hull-spacing, 0.3 m hull diam

Effective Power (does not include propeller or transmission losses)



5 miles/hr (4.34 knots

Findings for 300 lb Prototype boat, with 0.3 m cylindrical hulls with 10 degree angle to water at bow and stern, 4.34 knots:

1. 15 ft and 20 ft hulls require the same power
2. Hull Interference is almost zero at >8 ft spacing between hulls, with 15 ft hulls
3. For 15 ft hulls, effective power is about 70 Watts. Power required from pilot would be about 140 W.
4. The 10 ft hulls are adequate, requiring about 80 Watts. but 15 feet may be safer.
5. The angle the hulls make with the water at entry point is important.

Will use 10 ft hulls for Prototype. Considering the efficiency of the propeller (0.7) and generator losses (0.65) through the generator, about 176 Watts will be required from the pilot, or about 0.23 HP. A recreational cyclist in good condition might be able to keep this up all day, but battery assist may be needed.

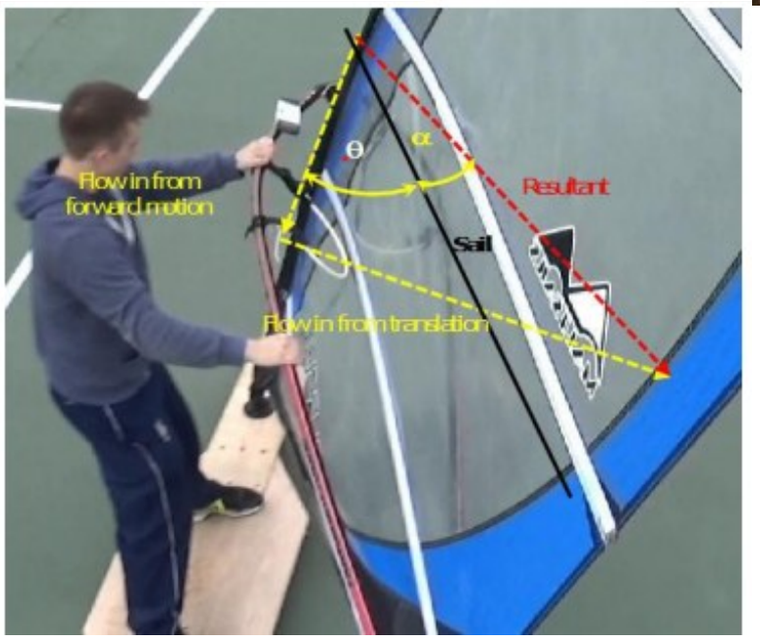
CONSTRUCTION OF PROTOTYPE FOR TESTING THE ELECTRIC PEDAL DRIVE

Began construction in summer of 2026, still a work in progress!

PAST HUMAN-POWERED VEHICLES







https://www.youtube.com/watch?v=VpxNAKokcMg

Strouhal # = Frequency/ (Amplitude x Velocity)

THE PROTOTYPE FOR TESTING ELECTRIC DRIVE CONCEPT

Generator



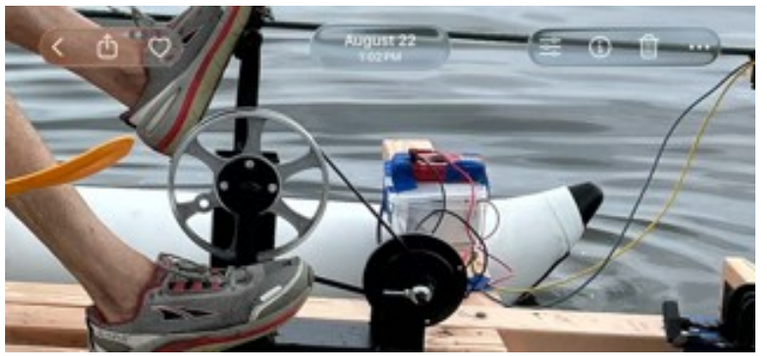
Electric motor
at bow





RESULTS SO FAR (water tests performed summer 2026 at Bar Beach, Port Washington)

- Pedal power with propeller in air: turning the pedals at 90 revs/min spun the propeller at 2000 rpm using about 17 watts and about 10 volts.
- If pedal speed is too low, the propeller turns spasmodically, as if it's turning on cogs. Once pedaling rate is high enough prop spins smoothly.
- Pedaling in the water: Higher rpm required. Could not get out of spasmodic propeller operation phase. Only about 1-2 knots achieved. Could not spin the pedals fast enough.
- Need a higher gear - like changing from 1st to 10th gear on a bike. Wheel needs to be bigger.



- It takes great care to make the two hulls parallel when setting up the boat.
- Inflatable hulls can be inflated quickly with leaf-blower, followed by high pressure hand pump.
- It may take battery assist to start the motor, which can be shut off once propeller is spinning smoothly.
- If we believe the power calculations, electric motor assist may be required to maintain 5 miles/hr.

Presentation now turned over to Midshipmen Isaac Lee and Erik Lunn, who worked on improving the gear ratio of the generator.

DESIGN ITERATION • FALL 2026

Improving the Pedal-Generator Drive

Fusion 360 → 3D printing → assembly → tank testing

MIDN Isaac Lee • MIDN Erik Lunn



Starting Point: The Original Prototype

Why improving the drive ratio became our main objective



Propeller in air

90 pedal RPM produced about 2,000 propeller RPM; about 17 W and 10 V reported.

Propeller in water

Low-speed operation remained spasmodic; initial on-water speed about 1–2 knots.

Our objective

Increase generator speed at a practical pedal cadence and make the test rig more reliable.

Design target from original deck: 4.3 knots (~5 mph), not yet achieved.

Baseline information: original presentation, slide 22

Ideas We Considered

Several mechanical changes were possible; we prioritized a larger drive wheel.

01 **Larger drive wheel**

Raise generator shaft RPM for a given pedal cadence.

02 **Flywheel / rotational inertia**

Smooth rotational speed changes, especially at low pedal RPM.

03 **Pedal and crank changes**

Improve comfort, cadence and input power transfer.

04 **Generator or alternator changes**

Match the electrical machine to the achievable RPM and load.

Belt-drive relationship (assuming negligible slip):

Generator RPM ≈ Pedal RPM × (drive-wheel Ø / driven-pulley Ø)

First Design: Full-Spoked Wheel

The initial Fusion 360 model was mechanically appealing but difficult to manufacture with our available printers.



Original concept

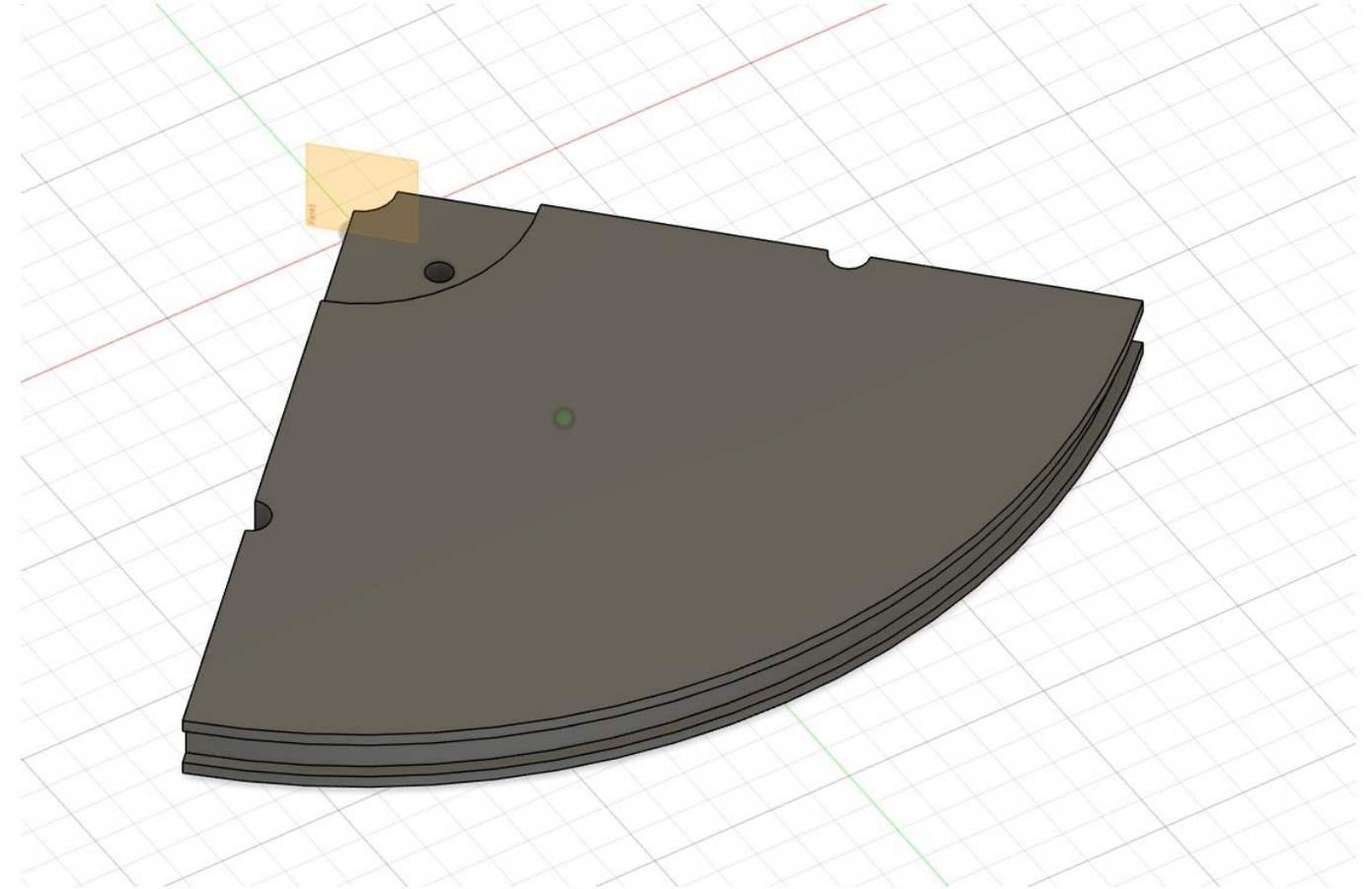
One circular, multi-spoke wheel with a grooved outer rim and central mounting holes.

Issue

Printing all of the individual geometry at this scale was more complicated than necessary.

Redesign: Print Four Identical Quarters

A simpler quarter-wheel design made the new wheel practical to fabricate and assemble.

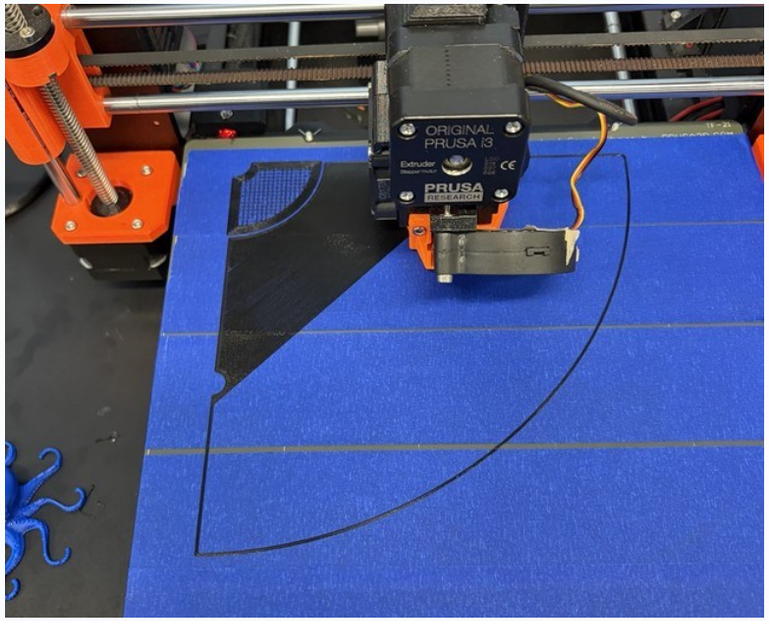


1 QUARTER × 4 PRINTS

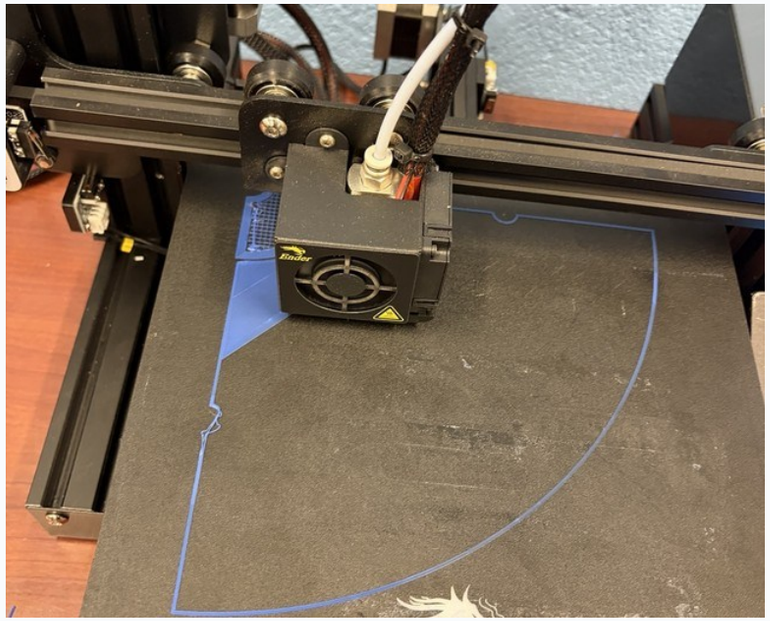
- Reduced each print to a manageable size.
- Repeated the same part four times.
- Joined sections around the existing metal hub.
- Kept the outer belt-contact surface.

Fabrication: From CAD to 3D-Printed Parts

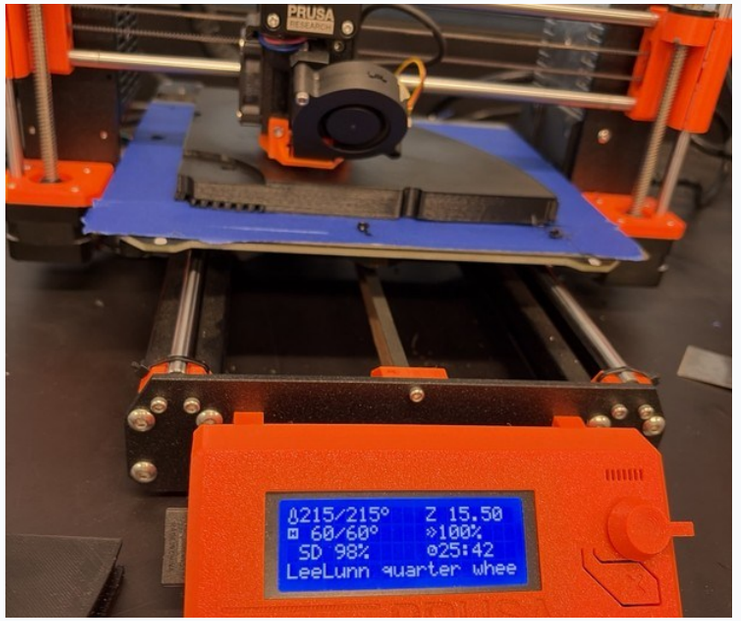
We used available Prusa and Ender printers to produce the segmented wheel.



PRUSA PRINTING



ENDER PRINTER

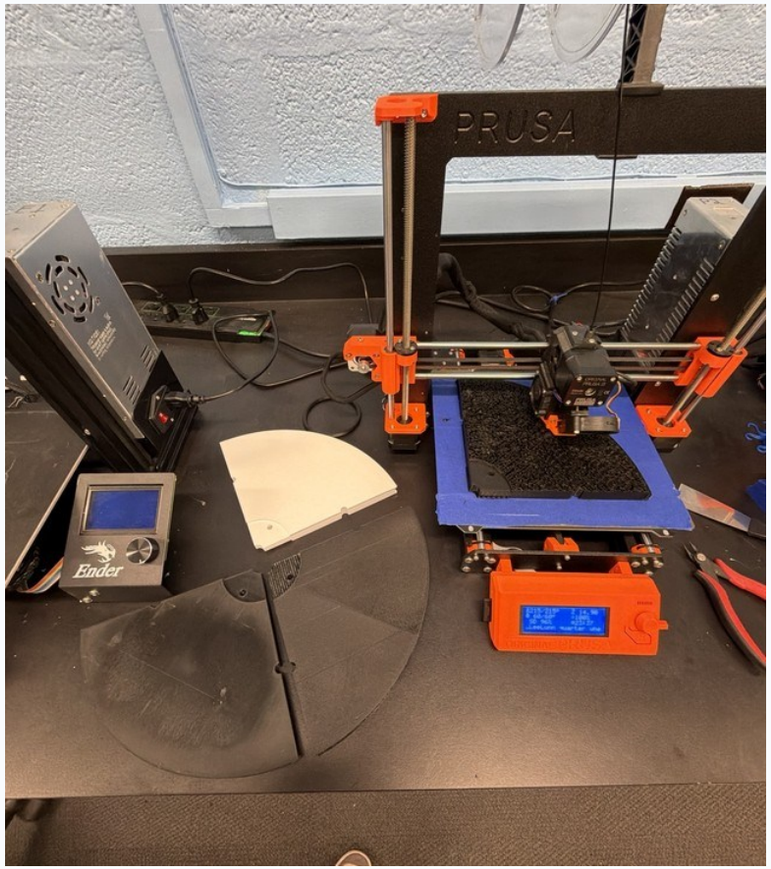


FOUR SECTIONS

Design choice: modular prints were easier to repeat and replace than a single large wheel.

Assembling the New Drive Wheel

Four printed quarters were fitted to the original metal wheel/hub and fastened in place.



PRINTED SECTIONS



NEW WHEEL + OLD WHEEL

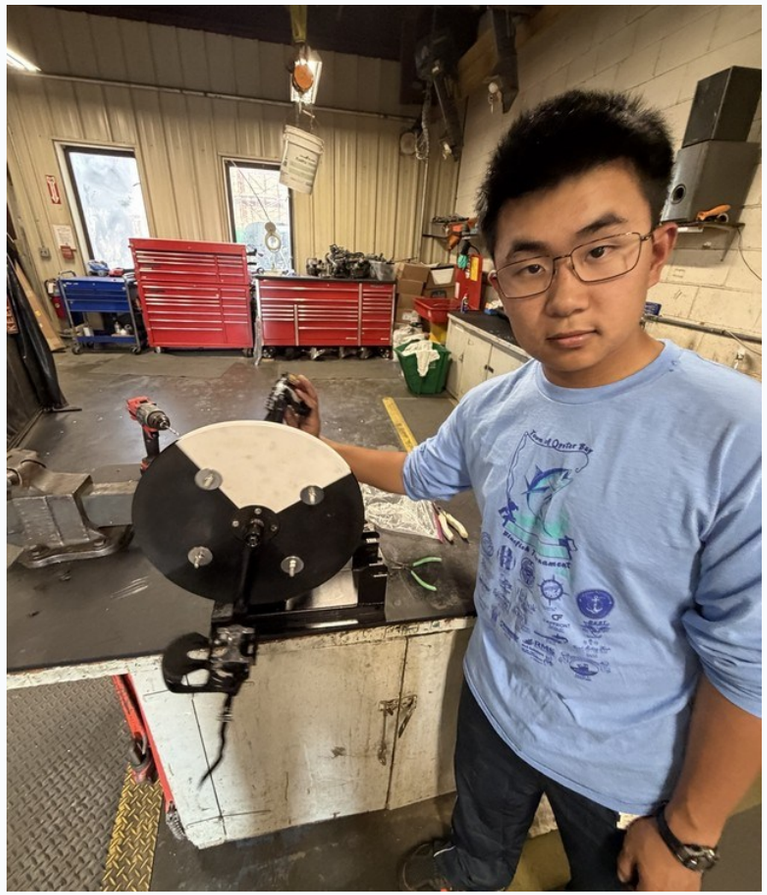


SHOP ASSEMBLY

Engineering Constraint: The Belt Was Too Short

The first full-diameter assembly would not work with the new belt, so the design had to change again.



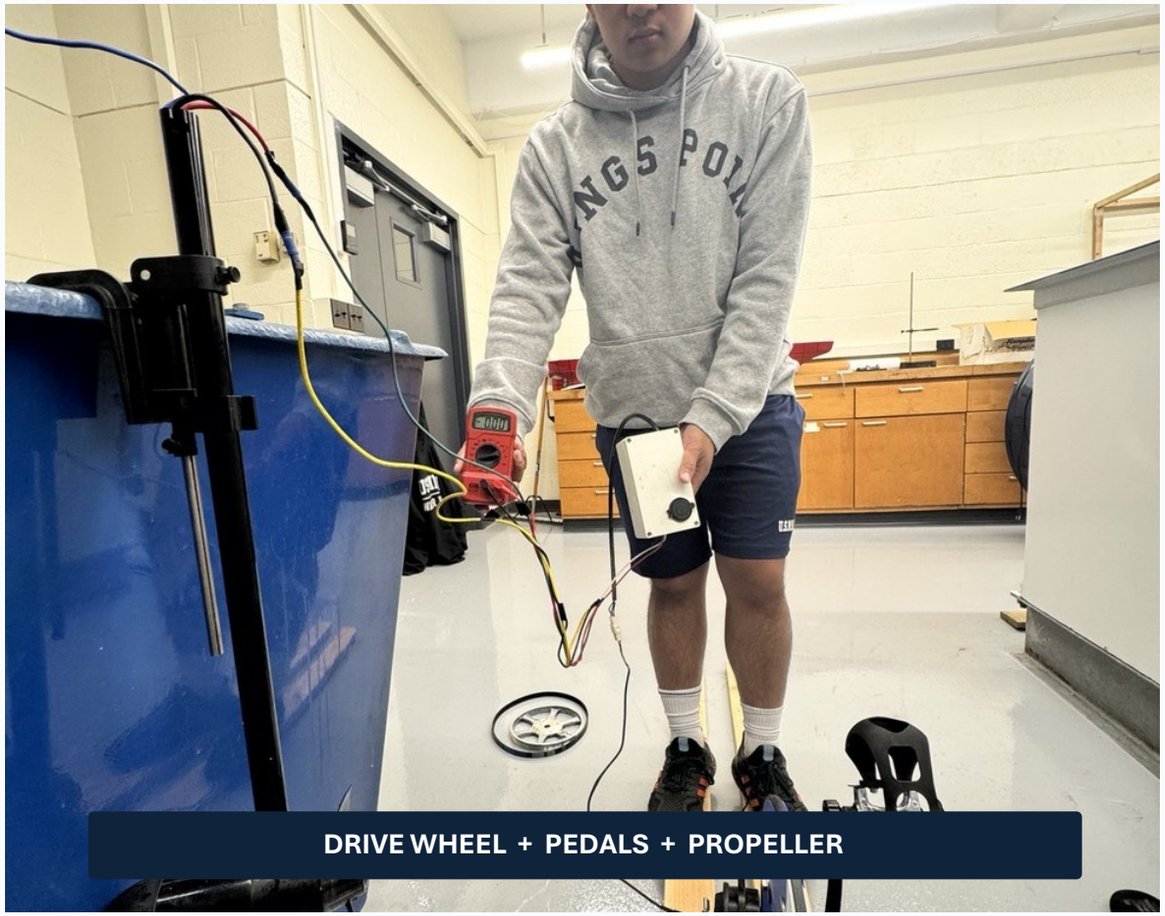


ITERATION

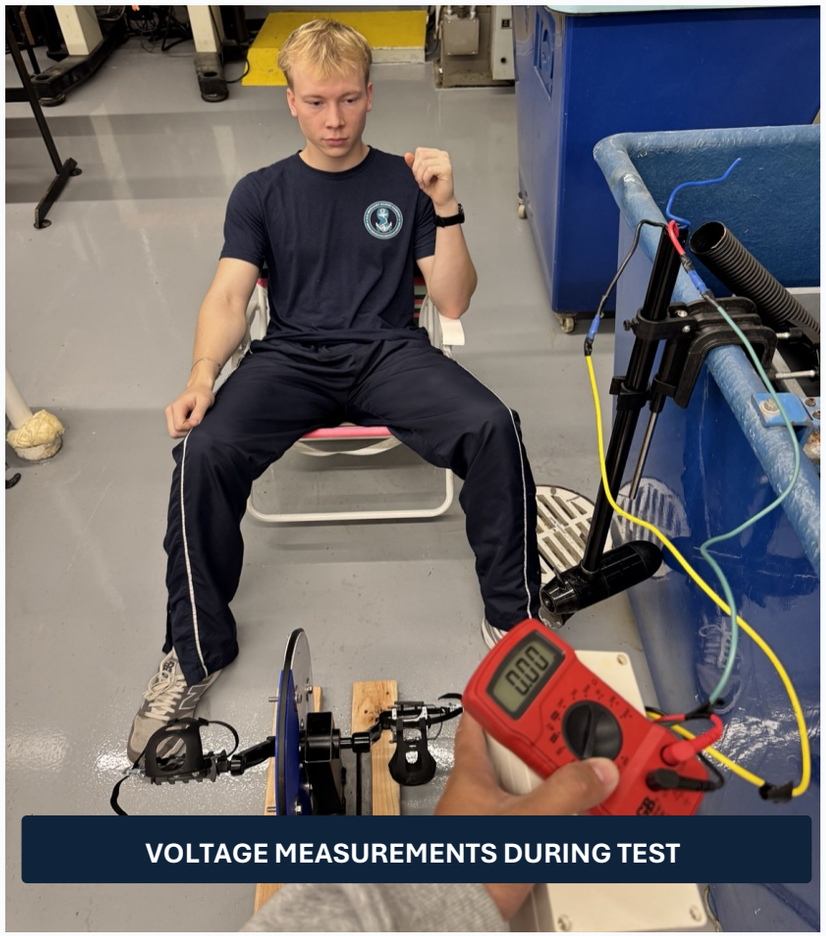
- Full-size wheel increased belt path length.
- New belt could not reach / tension correctly.
- Reduced the outside diameter.
- Retained the principle of increasing the drive ratio.

Bench and Tank Testing

The pedal mechanism was connected to the propeller assembly to study starting, speed and electrical response.



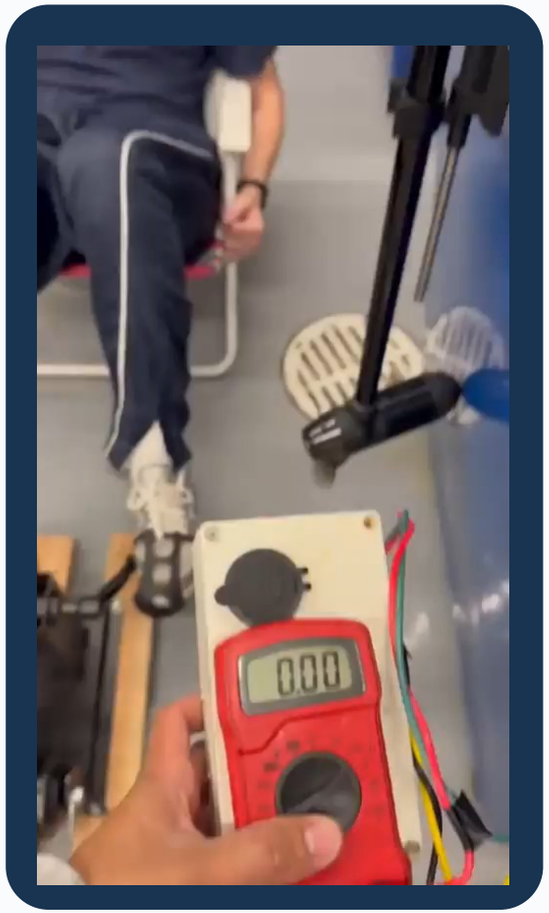
DRIVE WHEEL + PEDALS + PROPELLER



VOLTAGE MEASUREMENTS DURING TEST

Video Evidence: Electrical Output Tests – Propellor Out The Water

Test-frame previews; video clips are available separately.





What to watch for

- The pedal/drive-wheel system rotating together.
- How the propeller responds during startup.
- Uneven motion at low input speeds versus smoother rotation as speed increases.

Video Evidence: Electrical Output Tests – Propellor in the Water

Two clips captured the voltmeter while the pedal-generator drive was being operated.





Sample readings from tests don't shown in video

Clip A $|V| \approx 6.97V$

Clip B $|V| \approx 10.98V$

Field notes

- Tank tests help reveal startup and load behavior that air tests cannot.

Preliminary Results: What the Recordings Show

A higher observed voltage is encouraging, but the two samples are not a controlled efficiency test.

Observed magnitude of displayed voltage



≈57% higher voltage magnitude

Interpretation

- Ratio shown: (10.98 − 6.98) / 6.98.
- Clips do not establish equal pedal speed or load.
- Voltage alone cannot determine output power or efficiency.
- Controlled measurements are the next step.

Human-Input Reference: Pedaling Power and Cadence

Stationary exercise-machine displays provide context, not direct measurements of the prototype generator input.



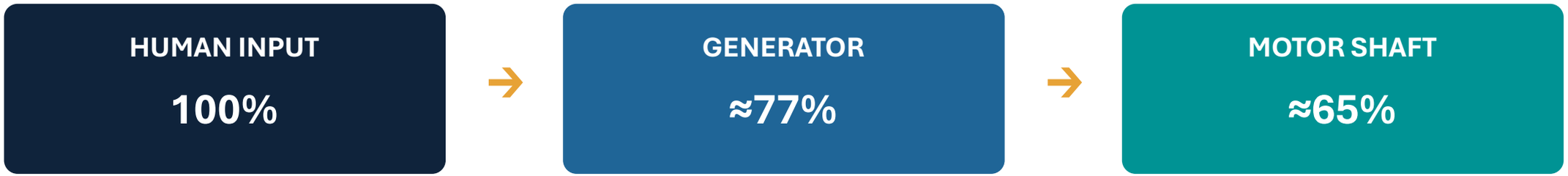


Displayed readings

- 60 W at 38 RPM (exercise bike).
- Approx. 57 W at 37 RPM in another image.
- These values are not measured power delivered to the boat’s generator.

Efficiency: Existing Estimate vs. Actual Measurements

The baseline deck estimated conversion losses; a new wheel changes drive ratio but does not remove those losses.



Original design example: generator 0.77 × motor 0.85 = 0.6545 ≈ 65% combined conversion efficiency.

Gear ratio: changes speed / torque operating point

True efficiency: needs measured input and output power

Efficiency ranges originate from original presentation, slide 12; not a new measured result.

What We Learned

Three rounds of engineering iteration: design, manufacture and fit.

01 Simpler designs can work better

Switching from a full-spoked print to four identical sections reduced fabrication complexity.

02 Real hardware sets the limits

The existing belt length dictated how large a new drive wheel we could use.

03 Testing reveals what CAD cannot

Water load and propeller startup behavior exposed performance limitations.

04 Measurements must be comparable

Voltage snapshots are useful; consistent cadence, torque, current and RPM are needed for efficiency.

The major accomplishment: a manufactured, assembled and tested alternative drive-wheel configuration that did increase efficiency.

Next Steps: Make the System More Effective

Next iteration should be selected using repeatable performance data.

01 Optimize the drive ratio

Test a longer belt or different pulleys so a larger wheel can run without binding or slipping.

02 Reassess the alternator

Consider a different size or lower-speed generator with appropriate torque and electrical characteristics.

03 Investigate smooth startup

Test flywheel inertia and/or controlled battery assist to get past low-speed bucking.

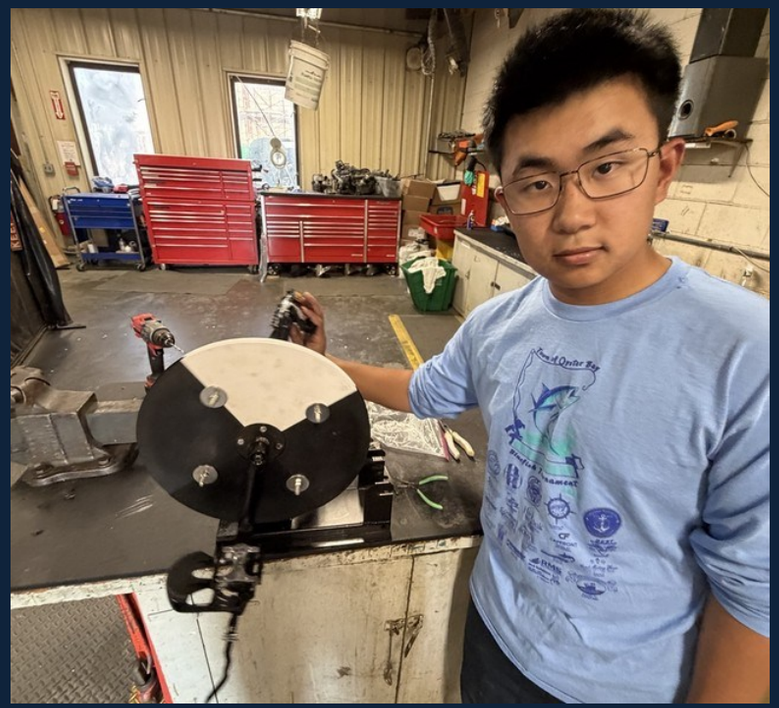
04 Run a controlled comparison

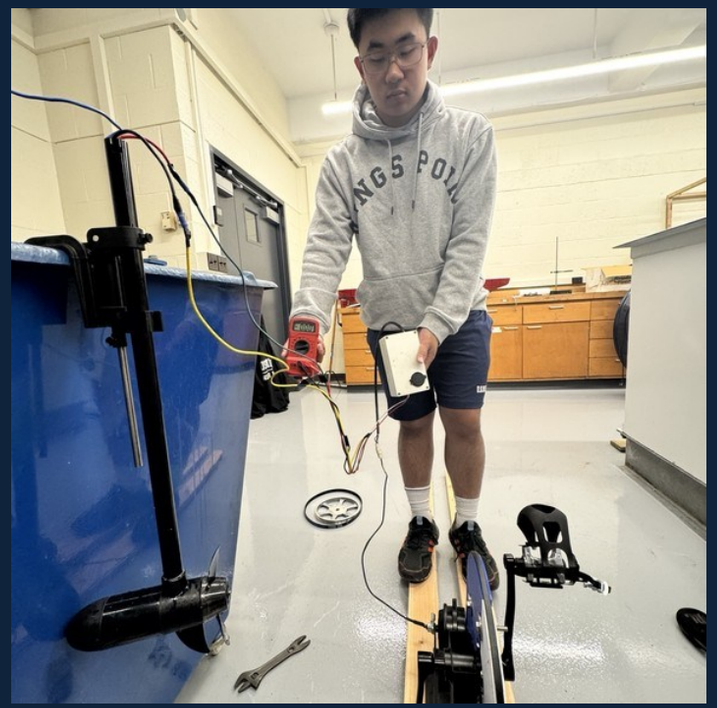
Record pedal RPM, torque, generator RPM, voltage, current, water condition and propeller thrust.

Next test metric: η = Electrical output power / Mechanical pedal input power

FROM IDEA TO HARDWARE

Design → Print → Fit → Test







Isaac Lee | Erik Lunn • Human-Powered Electric Boat Prototype

Reassessing the 32°C Tropical Seawater Design Condition for Ship Machinery Cooling Under Ocean Warming

Spenser Boyd, PhD, CEM

Webb Institute, Glen Cove, NY

SISDO 2026, October 19-20

Outline

1	**Background**	32°C design reference, central cooling plant, prior work
2	**Research Questions**	RQ1–RQ5 and the three study tracks
3	**Study Methodology**	Three study tracks
	A **Study Track A**	Satellite SST analysis
	B **Study Track B**	Heat-exchanger margin
	C **Study Track C**	Shipping presence and timing
4	**Results, Limitations, Conclusions**	Summary results, RQ5 assessment, limitations, conclusions

32°C Seawater Design Reference

Rule text

IACS UR M40 lists +32°C seawater as an ambient condition for machinery in unrestricted service

Purpose

Provides one common severe condition for equipment sizing, without voyage-specific prediction

Interpretation

Design target only, not a restriction. Seawater temperature does exceed 32°C and restricted service may use other values

Where the value appears

Rule	Seawater value
IACS UR M40 (listed 1981)	+32°C, unrestricted service
DNV machinery rules, Pt.4 Ch.1 (2025)	32°C; approved alternatives for restricted service
Lloyd's Register, Pt 5 Ch 1 Sec 3 (2022)	−2 to +32°C; deviation may be considered for restricted service

The margin installed above the reference condition remains a design decision.

Where Does 32°C Come From?

1935

Hillier, Institute of Marine Engineers

Tropical sea temperature “generally taken as 80°F or 85°F” (26.7–29.4°C)

Steam-condenser sizing practice; not a rule.

1954

Ranken, Journal of Naval Engineering

HMS Vidal heat-pump plant designed for seawater at 90°F (32.2°C)

Earliest 32°C-equivalent figure found; single vessel.

1981

IACS UR M40

Listed with date 1981; published text gives seawater +32°C

Earliest formal date found; first issue or revision not stated.

Today

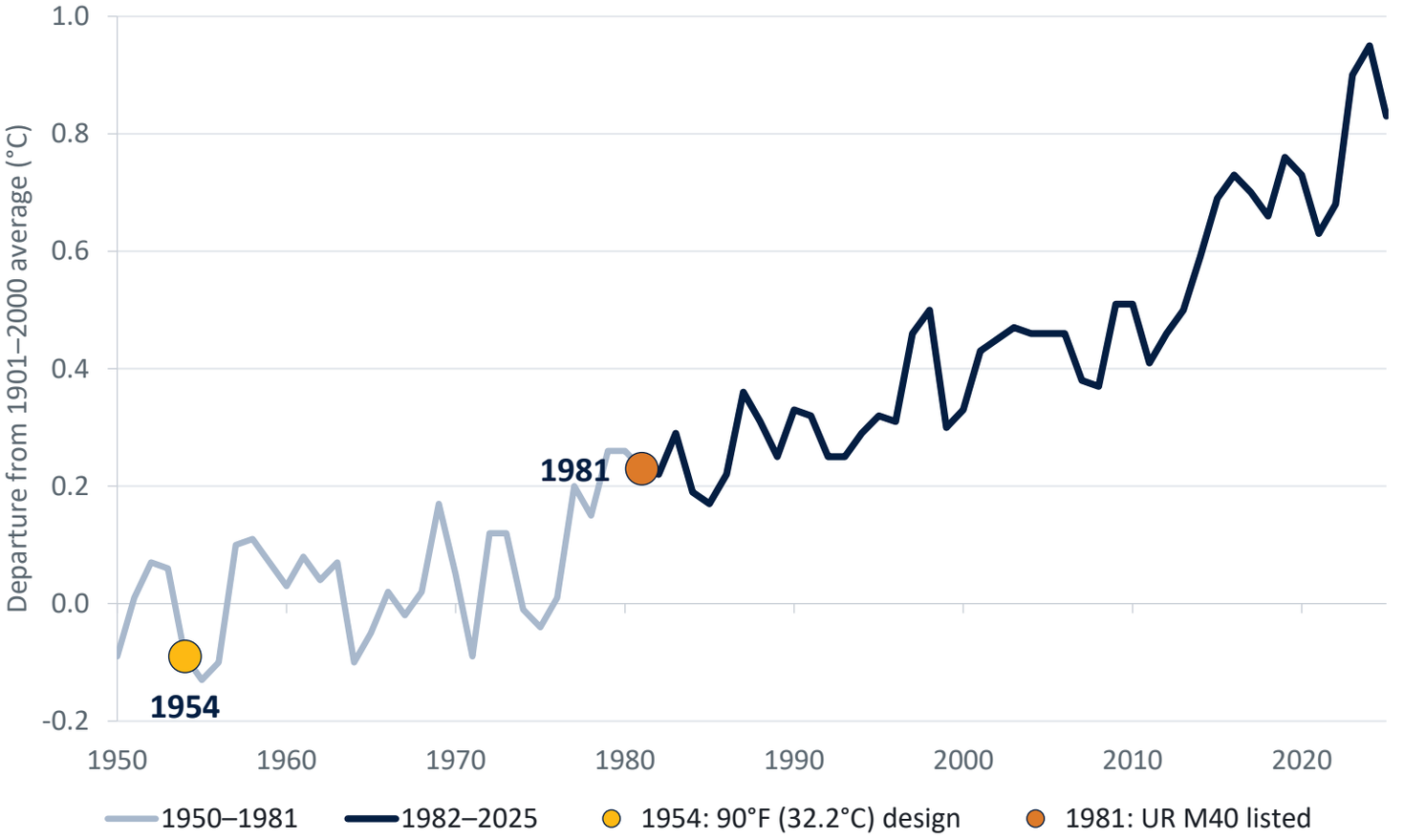
Lloyd’s Register 2022; DNV 2025

Same +32°C carried into current class rules

Restricted service may use other values.

It is unclear why 32°C was chosen, but 1981 is the earliest formal date documented.

Ocean Surface Warming Since 32°C Established



Source: NOAA NCEI Climate at a Glance, global ocean, annual.

SST ≈ 0.00°C

1950s average: ocean near its 20th-century mean at the time of the 90°F design.

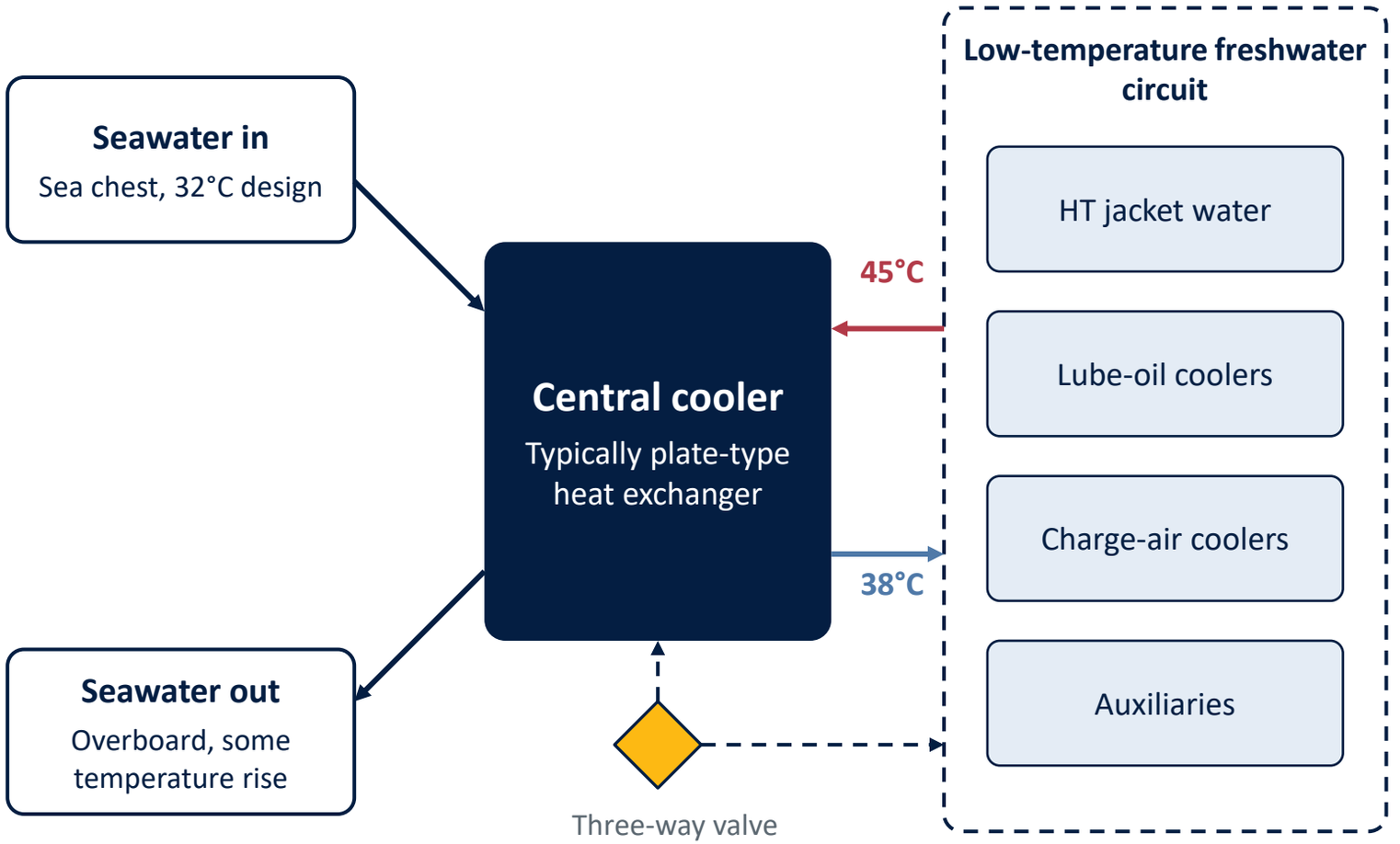
SST +0.23°C

1981, approximate year UR M40 is listed: onset of rise.

SST +0.83°C

2025: up 0.60°C since 1981. IPCC AR6 independently gives 0.60 [0.44–0.74]°C for 1980–2020.

Typical Shipboard Central Cooling Plant



Cool seawater

- Most freshwater bypasses the cooler
- Surplus capacity permits reduced seawater pump speed

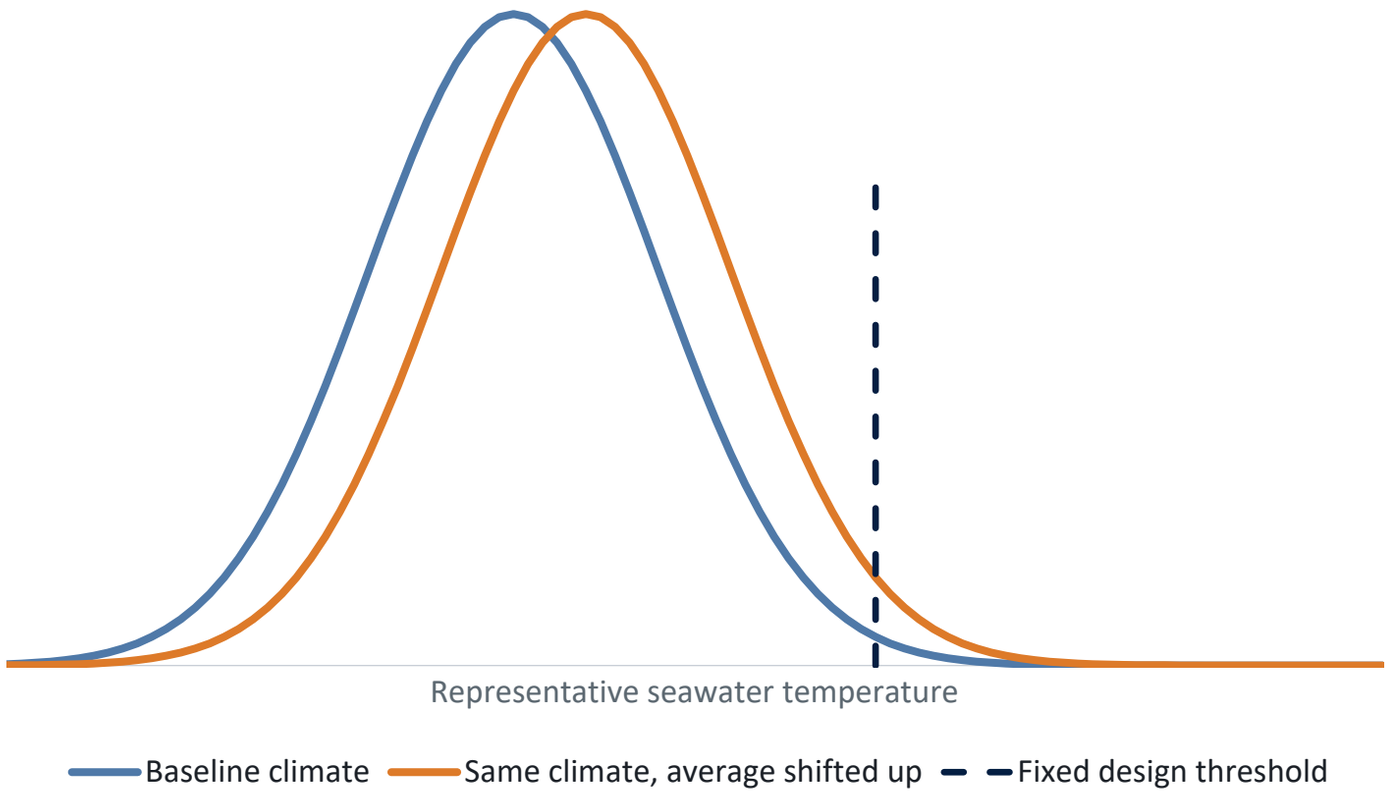
Warming toward 32°C

- The bypass adjusts
- Cooler size, seawater flow and set point determine whether the full heat load can be rejected

At the design point

- Minimum thermal reserve for fouling, high heat rejection load

Small SST Shift May Have Significant Cooling Impact



Representative normal curves only. Shift = 0.5 standard deviations, threshold = 2.5 standard deviations.

3.7×

increase in the share beyond the threshold
(0.6% → 2.3% in this strawman)

- A small shift in the mean produces a disproportionate change in the warm tail.
- Equipment is sized for the tail.
- Raises the question of **how often**, **where** and for **how long** seawater reaches a threshold absolute temperature.
- Global mean SST obfuscates the local detail a ship may actually experience.

Prior Work: Warm Extremes Are Measured as Anomalies

+54%

annual marine heatwave days, 1925–2016: frequency +34%, duration +17%, largely explained by mean ocean warming (Oliver et al., 2018)

≈ 2×

marine heatwave frequency since the 1980s (IPCC AR6, 2021)

Marine heatwave versus design condition

	Marine heatwave	Design condition
Reference	Each place's own seasonal climatology	A fixed absolute temperature (32°C)
Question	How anomalous is current SST at this location?	How often, where and for how long does seawater reach this temperature?
For Ship Cooling	A 1°C anomaly matters only where water is already near 32°C	The temperature difference determines capacity directly

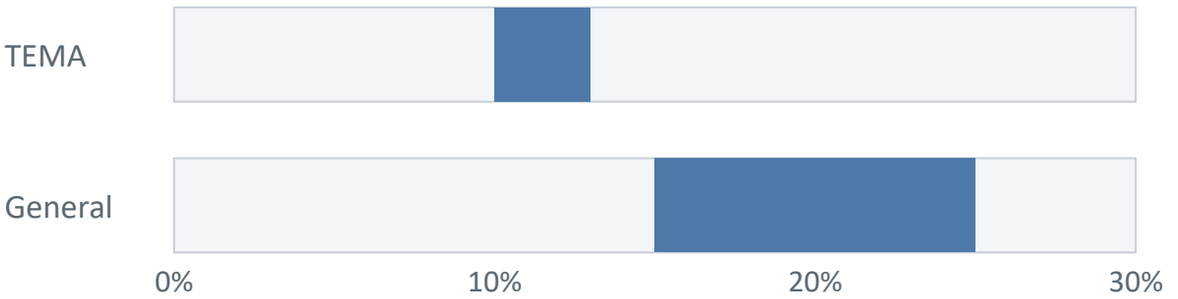
Exposure to a particular absolute temperature threshold (relevant to machinery design), has not been clearly reported in the literature.

Prior Work: Cooling Studies and Design Margin

Cooling studies

- **Kocak and Durmusoglu (2017):** energy saved by variable-speed seawater pumps on a containership.
- **Jeon et al. (2022):** central freshwater-cooling control model of a merchant training ship, validated against ship data.
- Both are ship-specific and address conditions below 32°C, where surplus capacity is exchanged for pump energy savings. **Neither considers the established design condition.**

Design reserve in heat-exchanger sizing



- **TEMA 10/13:** at least 10% surface beyond the clean-plus-fouled requirement; spare duty capped at 13%.
- **General practice:** about 15–25% oversizing; plate coolers typically receive smaller fouling allowances.

Cooling reserve is typically allocated to fouling and degradation, not to warmer seawater at the design point. The rate at which water above 32°C reduces margin has not been clearly quantified.

Prior Work: Open Shipping-Traffic Data

Source	What it measures	Time span	Limit
AIS (SOLAS carriage rules)	Vessel identity, position, course and speed from required transponders	Continuous	Coverage depends on receiver location and recording period
Global Fishing Watch presence	Sessions: vessel entry and exit times for a region, and hours present	2012 onward	Queryable by region and time; reception coverage increased over time
World Bank/IMF shipping density	Hourly AIS positions aggregated at 0.005°; commercial and passenger layers	Jan 2015 – Feb 2021	One static surface; absolute scale undocumented
EMODnet vessel density	Monthly, vessel-type-resolved 1 km grids	Monthly	European and adjacent waters only

Bold rows indicate the two sources used: **where** traffic operates (World Bank/IMF) and **when** it is present (Global Fishing Watch).

Research Questions

RQ1 — **Track A: satellite SST**

How often, for how long and over what area has daily SST approached or exceeded 32°C since 1982?

RQ2 — **Track A: satellite SST**

How has exposure at 30, 31, 32 and 33°C changed between 1982–2001 and 2006–2025, and across the full record?

RQ3 — **Track B: cooler margin**

How much capacity does a representative central cooler lose as seawater warms past 32°C, and how does that compare with conventional design margin?

RQ4 — **Track C: shipping**

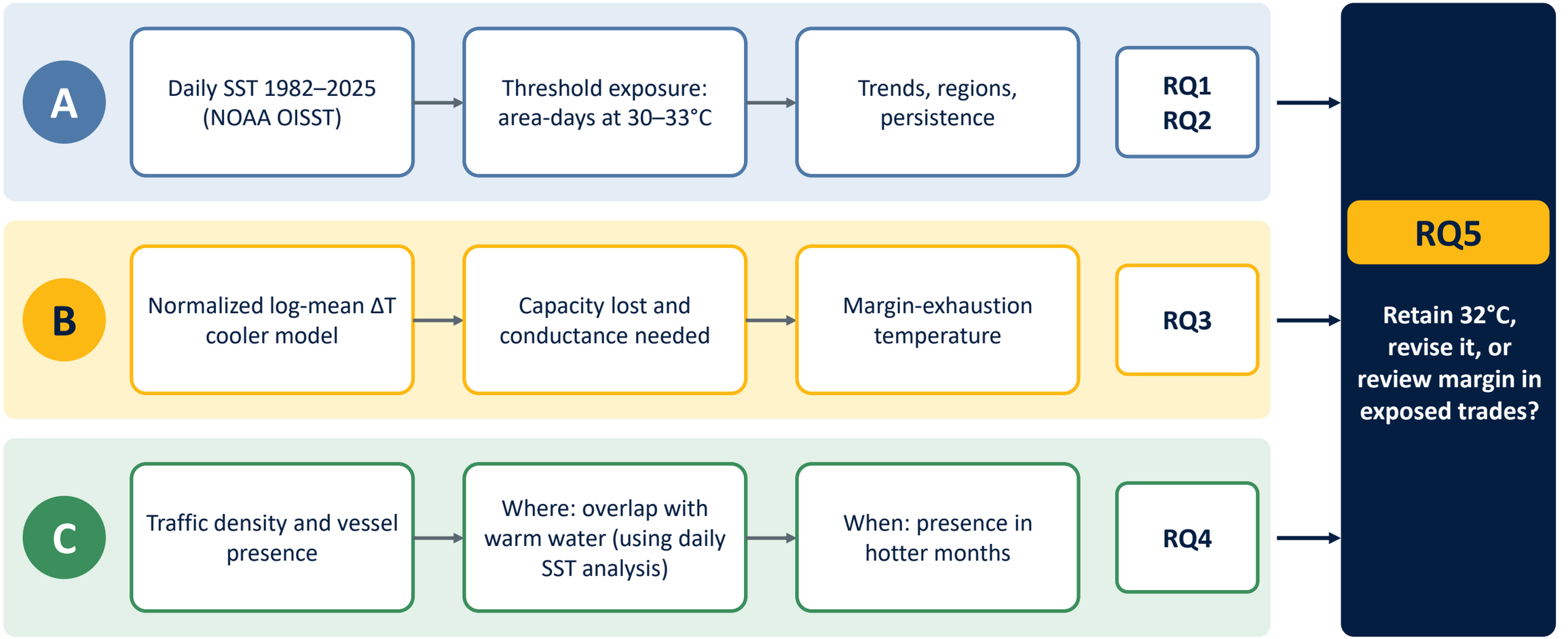
Does commercial shipping operate in the regions, and in the months, where exposure is highest?

RQ5

Do the results support keeping the 32°C reference, revising it universally, or reviewing margin for specific trades?

RQ1–RQ4 provide the evidence; RQ5 addresses the decision.

Three Study Tracks



Track A

Satellite SST Analysis

A

RQ1 How often, for how long and over what area has SST approached or exceeded 32°C?

RQ2 How has exposure at 30–33°C changed between 1982–2001 and 2006–2025?

A Satellite SST | B Cooler margin | C Shipping

Track A Data: NOAA OISST v2.1

A



16,071 maps

1 Jan 1982 – 31 Dec 2025

≈ 28 km

cell width at the equator

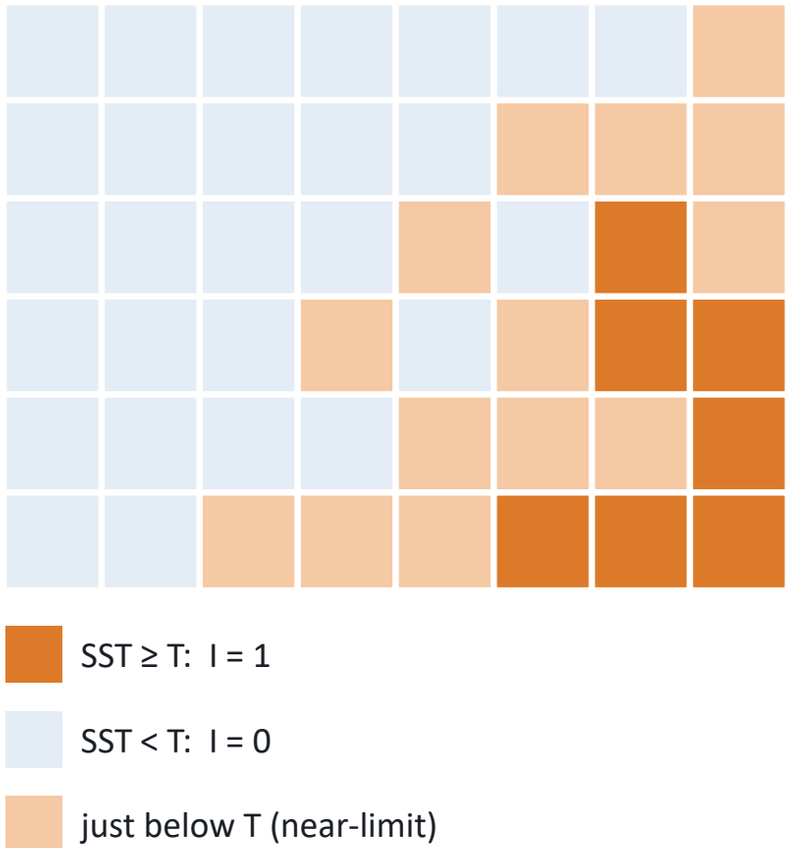
Data Caveats

- Interpolated surface values approximate water drawn into a sea chest below waterline.
- **Cross-check:** 1990 → 2023 warming is +0.67°C in OISST and +0.51°C in ERSSTv5.

SST Map Cell Indicator and Area Weighting

A

One day, ocean subregion (toy example)



Eq. (1) Threshold indicator

$$I_{g,d,T} = 1\left(\mathrm{SST}_{g,d} \geq T\right)$$

The indicator equals 1 when cell g on day d is at or above threshold T (inclusive; exactly 32.0°C is counted). Cells without data are excluded from both numerator and denominator.

Eq. (2) Cell area

$$A_g = R^2 \Delta\lambda (\sin\varphi_N - \sin\varphi_S)$$

Cell area decreases toward the poles. Spherical area, with Earth radius R = 6,371,008.8 m, longitude width Δλ and north and south edges ϕN, ϕS, converts the indicator to square kilometers.

Annual SST Exposure by Area-days and Ocean Fraction

A

Eq. (3) Annual area-days at or above T

$$A_{y,T} = \sum_{g} A_g \sum_{d \in y} I_{g,d,T}$$

Cell area multiplied by days at or above T, summed over all cells, in million km²·day per year.

Eq. (4) Fraction of valid ocean area-days

$$F_{y,T} = \frac{A_{y,T}}{\sum_g A_g N_{g,y}}$$

N is the number of valid days for each cell, missing cells are excluded.

Interpretation

$$\text{average daily area} = \frac{A_{y,T}}{365.25}$$

area at or above the threshold on an average day

$$\text{days per year} = 365.25 \times F_{y,T}$$

days per year at an average location; 10% ≈ 37 days

- Thresholds: 30, 31, 32, 33°C
- Near-limit band: 30°C ≤ SST < 32°C (≥30 total minus ≥32 total)

Twenty-Year SST Comparison

A



Change = mean annual exposure (recent) − mean annual exposure (baseline), in absolute terms and as a % of baseline

Equal windows

Bulk of available data captured in two twenty-year windows.

Four-year separation

2002–2005 arbitrarily separates the windows but is included in the full-record trends.

Approximate effect size

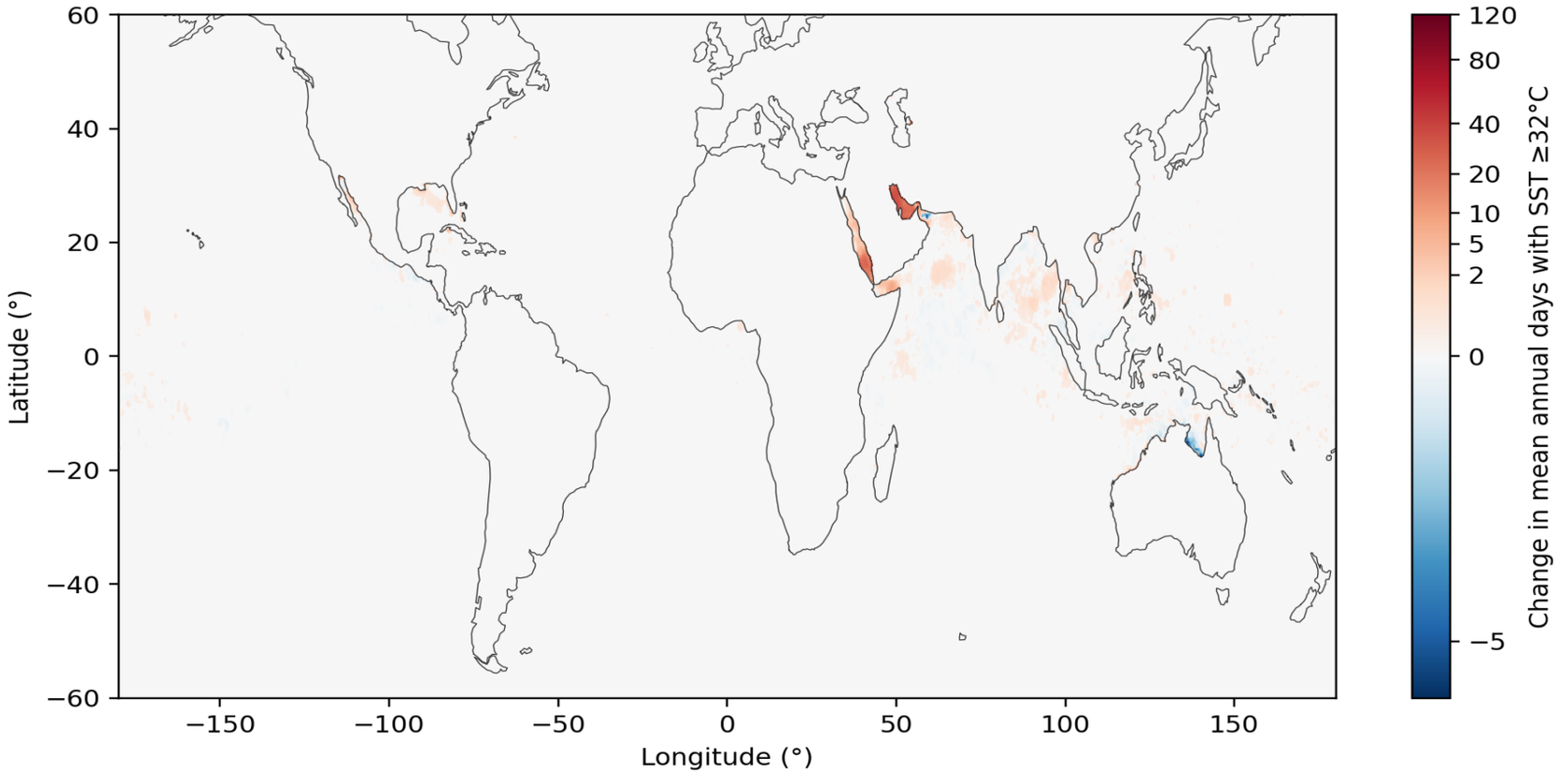
Demonstrates size of effect, full 44-year window used in residual analysis.

Independent check

Global mean SST, 1990 → 2023: OISST +0.67°C consistent with ERSSTv5 +0.51°C.

Global Map of Change in SST Exposure at 32°C

A



Change in mean annual days with SST ≥ 32°C per 0.25° cell, 1982–2001 → 2006–2025. NOAA OISST v2.1, 16,071 daily maps. Color scale compressed at high values so that small increases remain visible.

Reading the map

- Eq. (1) applied to every cell and day, then averaged over each 20-year window
- Red: more days at or above 32°C in the recent window compared to baseline
- Blue: fewer days in recent window compared to baseline
- White: negligible to no change

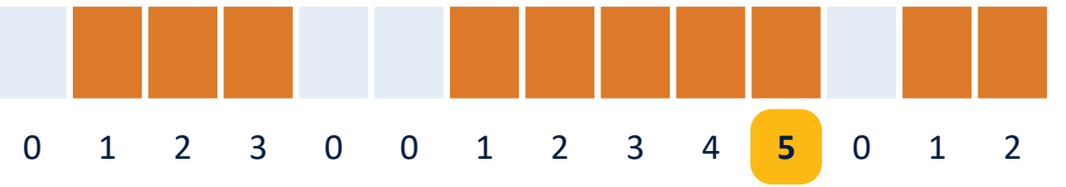
Seven Regions of Interest

A

Region	Longitude (°E)	Latitude (°N)
Persian Gulf	48.0 to 57.5	23.0 to 31.5
Red Sea	32.0 to 44.0	12.0 to 30.0
Arabian Sea	55.0 to 75.0	5.0 to 25.0
Bay of Bengal	80.0 to 100.0	5.0 to 23.0
South China Sea	105.0 to 122.0	0.0 to 23.0
Gulf of Mexico / Caribbean	−98.0 to −60.0	9.0 to 31.0
Western tropical Pacific	130.0 to 170.0	−10.0 to 15.0

Regions captured as map rectangles, not basin outlines.

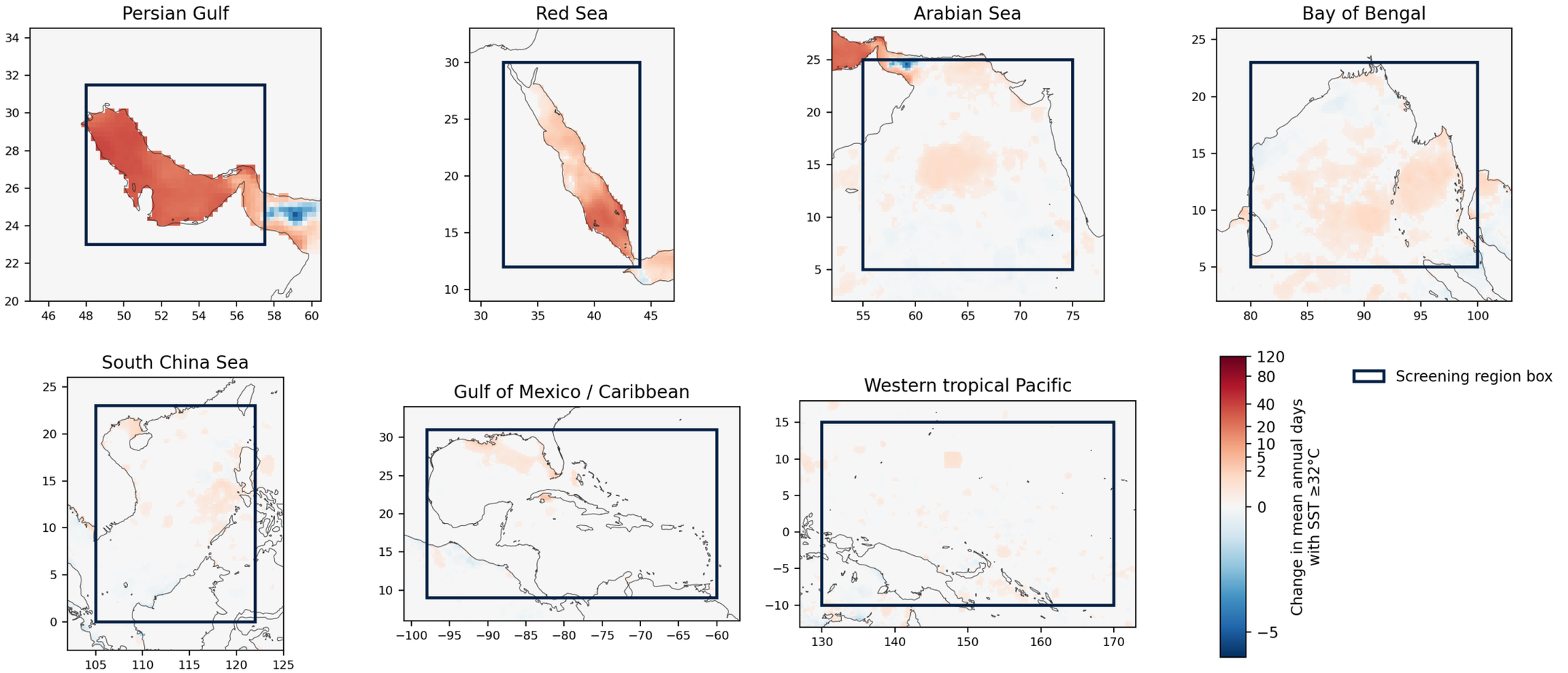
Persistence: longest consecutive run



consecutive days (orange = at or above T)

- The counter increments by 1 for each consecutive day at or above T and resets to 0 on a day below T, at a year boundary, or at a date gap.
- The regional longest run is the largest value at any single cell.
- Characterizes the most persistent local episode.
- Does NOT represent a basin-wide event or a ship transit.

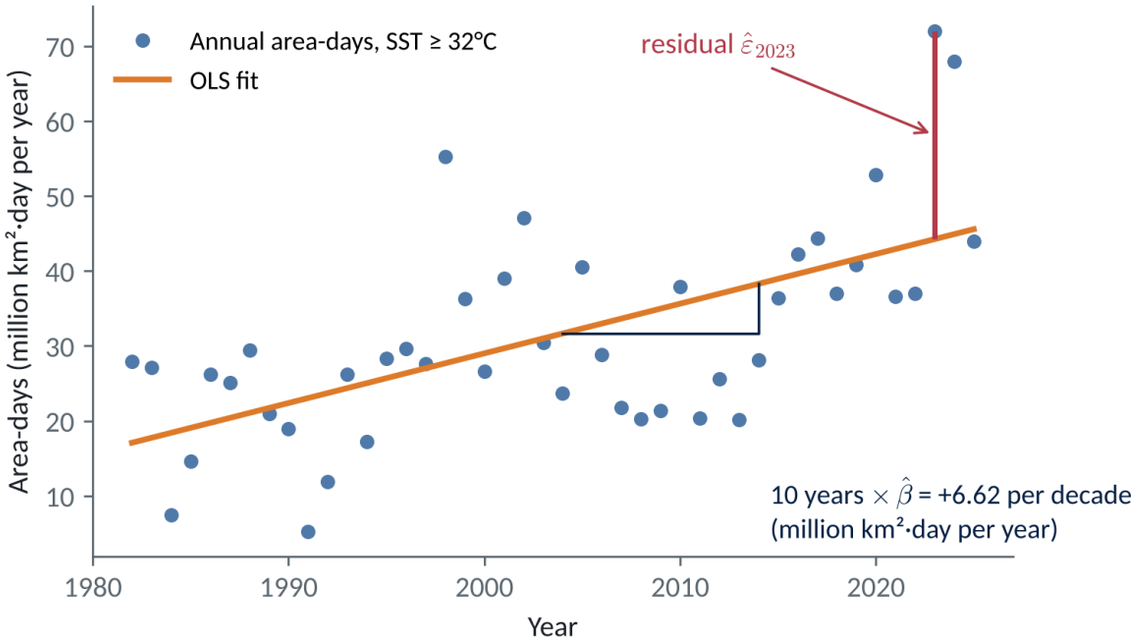
Seven Regions of Interest on the SST Map



Region boxes fixed by coordinates, with 3° of context. Change in mean annual days with SST ≥ 32°C, 1982–2001 → 2006–2025.

Ordinary Least Squares Trend Estimate

A



- **Output:** the slope and the residuals, the inputs to the following statistical tests.
- **Global ≥ 32°C:** trend = +6.62 million km²·day per year, per decade.

Trend model

$$\underbrace{y_t}_{\text{annual exposure in year } t} = \underbrace{\alpha}_{\text{mean level}} + \underbrace{\beta}_{\text{slope per year}} \underbrace{(t-\bar{t})}_{\text{year, centered on the 1982–2025 mean}} + \underbrace{\varepsilon_t}_{\text{residual: year-to-year variability}}$$

Slope estimate

$$\hat{\beta} = \frac{\overbrace{\sum_t (t-\bar{t})(y_t-\bar{y})}^{\text{co-variation of year and exposure}}}{\underbrace{\sum_t (t-\bar{t})^2}_{\text{spread of the 44 years}}}$$

$$\text{trend per decade} = 10\,\hat{\beta}$$

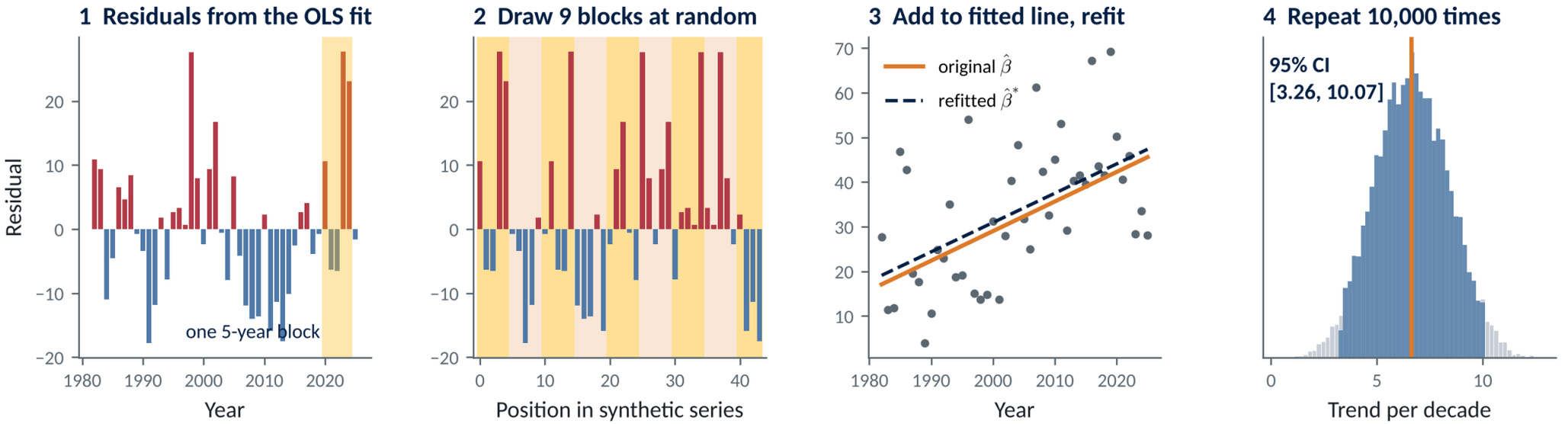
NOTE: Residuals appear autocorrelated

Global ≥ 32°C: $\hat{\rho}_1 = 0.36$, so 44 years carry about 21 independent observations.

$$n_{\text{eff}} \approx n\,\frac{1-\hat{\rho}_1}{1+\hat{\rho}_1}$$

Bootstrapping Moving Block Residual Trend Uncertainty

A



Each replicate

$$\underbrace{y_t^*}_{\text{synthetic series}} = \underbrace{\hat{\alpha} + \hat{\beta}\,(t - \bar{t}\,)}_{\text{fitted trend from OLS (held fixed)}} + \underbrace{\varepsilon_t^*}_{\text{residuals redrawn in 5-year blocks}}$$

$\underbrace{\hat{\beta}_b^*}_{\text{slope refitted to synthetic series } b}$ $\quad b = 1, \ldots, 10\,000$ $\quad$ 95% CI $= [\ \underbrace{\hat{\beta}^*_{(2.5\%)}}_{\text{2.5th percentile}},\ \underbrace{\hat{\beta}^*_{(97.5\%)}}_{\text{97.5th percentile}}\ ]$

- **Blocks of 5 years** cluster warm years.
- **Circular:** a block may wrap from 2025 to 1982.
- **10,000 replicates** with reproducible seed.
- **Output:** 95% CI for the trend. Global ≥ 32°C: +6.62 [3.26, 10.07] per decade.

Autocorrelated Trend t-test: Newey–West HAC test

A

$$t = \frac{\hat{\beta}}{\underbrace{\mathrm{SE}_{\mathrm{HAC}}(\hat{\beta})}_{\text{autocorrelation-robust standard error}}}$$

$$p = 2\left[1 - \underbrace{\Phi(|t|)}_{\text{standard normal CDF evaluated at } |t|}\right]$$

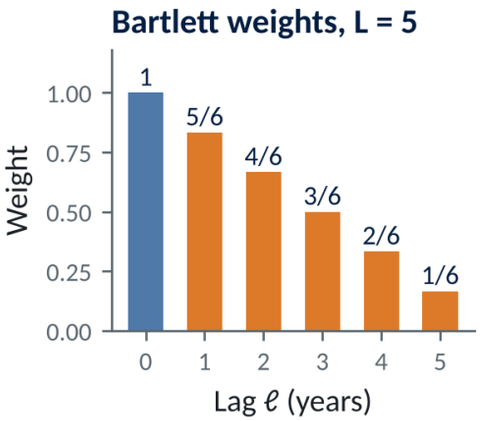
$$\mathrm{SE}^2_{\mathrm{HAC}} = \Big[\ \underbrace{(X^\top X)^{-1}}_{\text{“bread”: depends only on the years}}\ \underbrace{\hat{S}}_{\text{“meat”: built from residual products}}\ \underbrace{(X^\top X)^{-1}}_{\text{“bread”}}\ \Big]_{22}$$

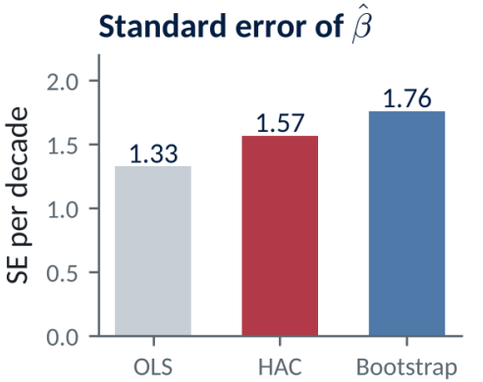
$$\underbrace{X = [\,1,\ t - \bar{t}\,]}_{\text{intercept and centered year}}$$

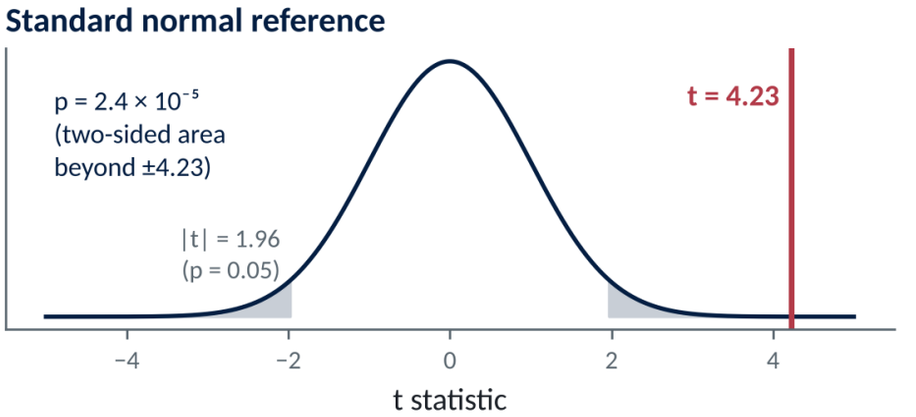
$$\hat{S} = \underbrace{\hat{\Gamma}_0}_{\text{same-year term (lag 0)}} + \sum_{\ell=1}^{L} \underbrace{w_\ell}_{\text{Bartlett weight}} (\hat{\Gamma}_\ell + \hat{\Gamma}_\ell^\top)$$

$$\underbrace{w_\ell = 1 - \frac{\ell}{L+1}}_{5/6,\ 4/6,\ \ldots,\ 1/6 \text{ for } L=5}$$

$$\underbrace{\hat{\Gamma}_\ell = \sum_t \hat{\varepsilon}_t \hat{\varepsilon}_{t-\ell}\, x_t\, x_{t-\ell}^\top}_{\text{products of residuals } \ell \text{ years apart}}$$



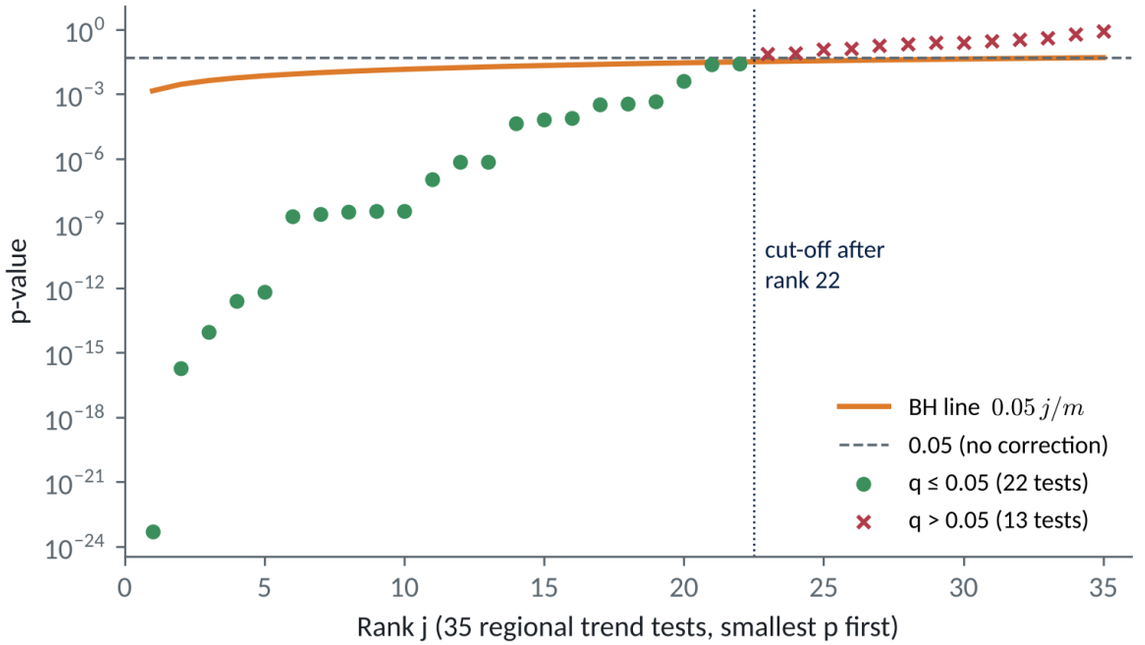




- **Test Matrix:** 5 global tests and 35 regional tests (7 regions × 5 bands), used for FDR correction
- **Global ≥ 32°C:** t = 4.23, p = 2.36 × 10^{-5}

Control Multiple Testing with Benjamini–Hochberg FDR

A



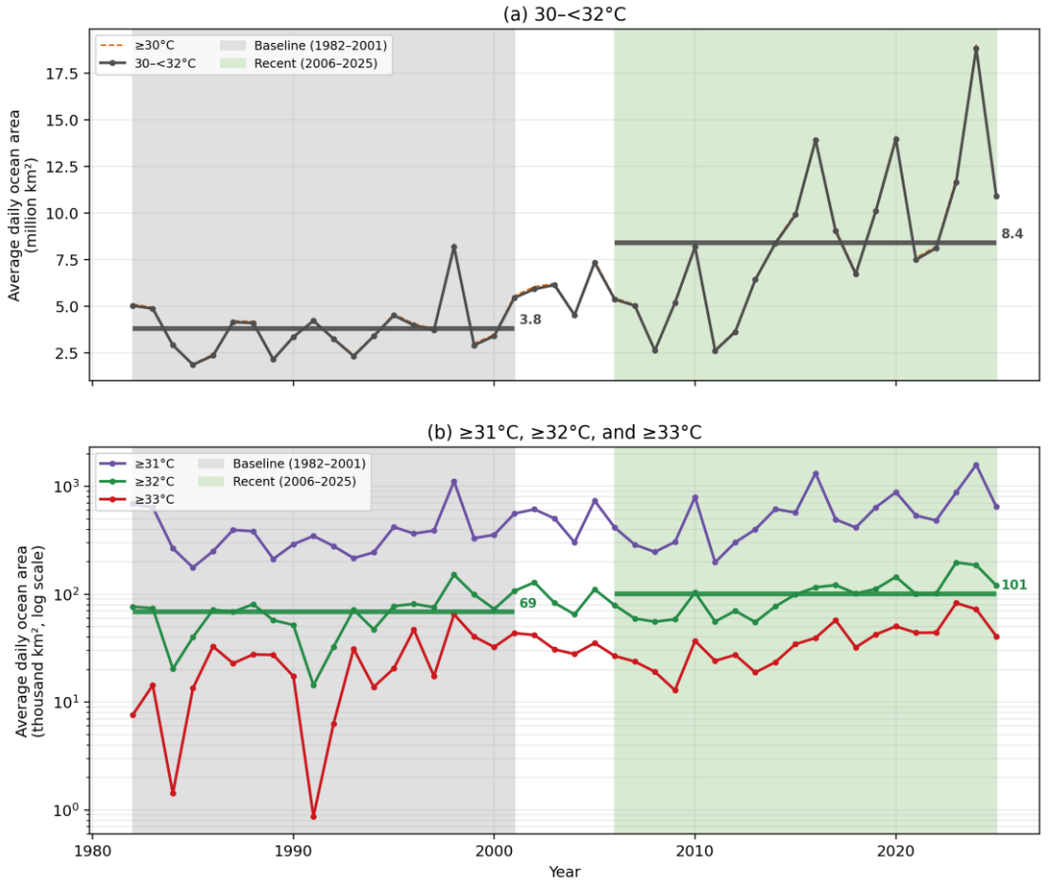
$$\underbrace{q_{(i)}}_{\text{adjusted value for rank } i} = \underbrace{\min_{j \geq i}}_{\text{running minimum from the bottom}} \underbrace{\frac{m}{j}}_{\text{tests in family ÷ rank}} \underbrace{p_{(j)}}_{j\text{-th smallest p-value}}$$

- **Test Matrix:** 5 global tests and 35 regional tests (7 regions × 5 bands)
- **Regional:** 22 of 35 have q ≤ 0.05 (cut-off at rank 22); the same 22 have p < 0.05.

Worked example: 5 global tests (m = 5)

Rank	Band	p-value	q
1	30–<32°C	4.11×10^{-8}	1.04×10^{-7}
2	≥30°C	4.15×10^{-8}	1.04×10^{-7}
3	≥33°C	7.59×10^{-6}	1.26×10^{-5}
4	**≥32°C**	$\mathbf{2.36 \times 10^{-5}}$	$\mathbf{2.96 \times 10^{-5}}$
5	≥31°C	1.54×10^{-3}	1.54×10^{-3}

Track A Result: Global Exposure Increased



Global daily ocean area by threshold; (b) uses a log axis. NOAA OISST v2.1.

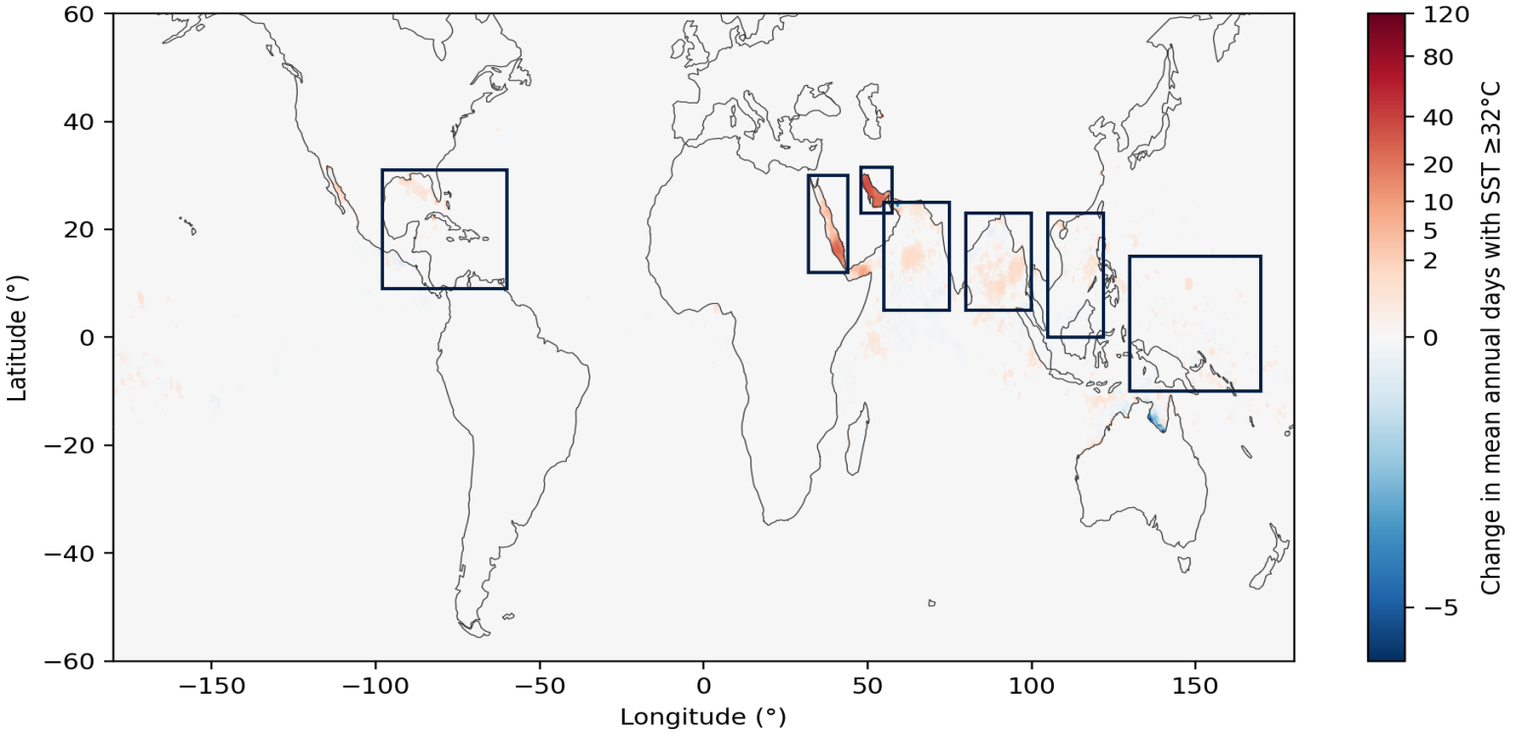
Mean daily ocean area, baseline → recent

Band	Area	Change
30–<32°C	3.8 → 8.4 million km²	+121%
≥31°C	396 → 600 thousand km²	+52%
≥32°C	69 → 101 thousand km²	+47%
≥33°C	24 → 38 thousand km²	+56%

- All five trends are positive, 95% intervals exclude zero, all significant after FDR ($q \leq 0.0015$).
- ≥32°C band covers about 0.03% of the ocean on an average day, large percentage changes impacted by small baselines.
- Increases driven by individual hot years, e.g. ≥31°C in 2024 was 2.6× the recent mean.

Track A Result: Regionally Concentrated Temperature Rise

A



Change in mean annual days with SST ≥ 32°C per 0.25° cell, 1982–2001 → 2006–2025. Color scale compressed at high values so that small increases remain visible.

54 → 78

days per year at ≥32°C, average Persian Gulf location. Trend +3.2 percentage points per decade (95% CI 2.1–4.4)

12 → 20

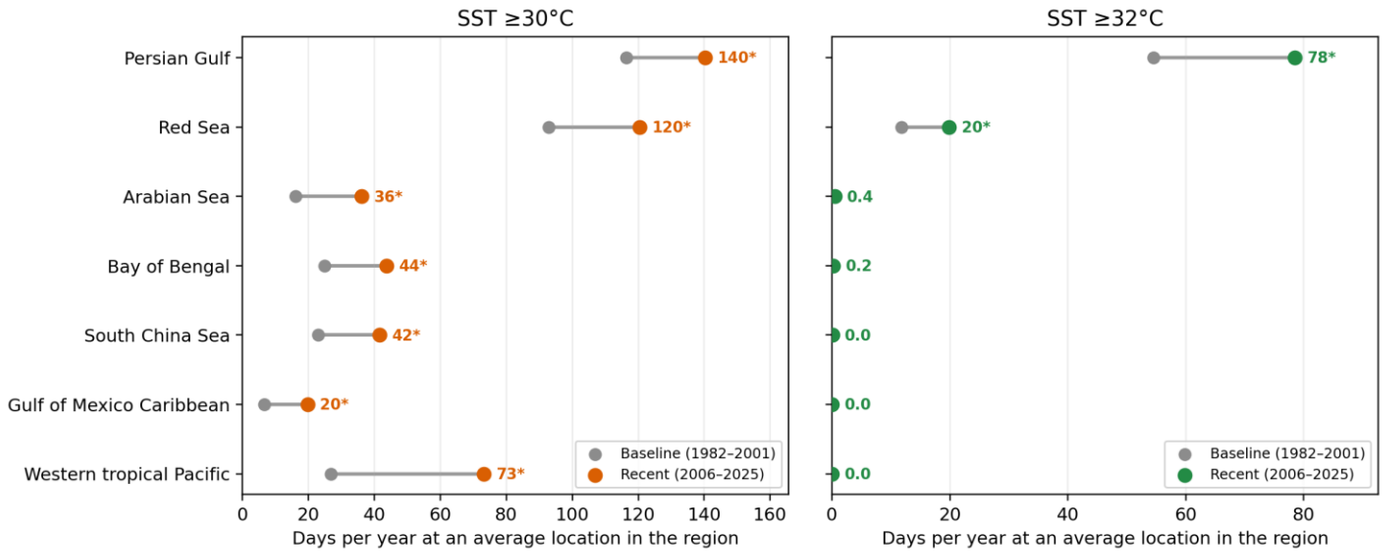
days per year at ≥32°C, average Red Sea location. Trend +1.5 per decade (95% CI 0.5–2.5)

< 1

day per year at ≥32°C at an average location in each of the other five regions

Track A Result: Regional Warm Water Episode Length

A



Days per year at an average location. * = significant after FDR.

- Near-limit exposure increased widely: western tropical Pacific 27 → 73 days a year; Arabian Sea, Bay of Bengal and South China Sea about +20.
- 2023 longest single-cell runs: Persian Gulf 147 days, Red Sea 150.
- 22 of 35 regional trends significant after FDR correction including ≥30°C in all seven regions.

RQ1-2 answer

Water at or above 32°C is globally rare (about 0.03% of the ocean) but 47% larger than in 1982–2001, and the 30–<32°C band has more than doubled. Growth above 32°C is concentrated in the Persian Gulf and Red Sea.

Track B

Heat-exchanger margin

B

RQ3 How much capacity does a representative central cooler lose as seawater warms past 32°C, and how does that compare with conventional design margin?

A Satellite SST

B Cooler margin

C Shipping

Central Cooler Model

B

Eq. (5) Heat rejected = conductance × mean temperature difference

$$\dot{Q} = UA \cdot \Delta T_{\mathrm{lm}}$$

Mean temperature difference: the log-mean temperature difference

$$\Delta T_{\mathrm{lm}} = \frac{\Delta T_1 - \Delta T_2}{\ln\left(\frac{\Delta T_1}{\Delta T_2}\right)}$$

$$\Delta T_1 = T_{\mathrm{fw,in}} - T_{\mathrm{sw}}$$

$$\Delta T_2 = T_{\mathrm{fw,out}} - T_{\mathrm{sw}}$$

Two representative designs

	6°C approach	3°C approach
FW in → out	45 → 38°C	42 → 35°C
ΔT_1 at 32°C	13°C	10°C
ΔT_2 at 32°C	6°C	3°C
ΔT_{lm} at 32°C	9.05°C	5.81°C

- Constant 7°C FW temperature drop.
- The 3°C design has a smaller driving temperature difference, so each degree removes a larger share.
- Each design is normalized to its own value at 32°C.

Reserve Capacity Margin vs. Required Capacity Margin

B

Eq. (6) Existing ship

Fixed cooler: fraction of design capacity remaining

$$M_Q(T) = \frac{\Delta T_{\mathrm{lm}}(T)}{\Delta T_{\mathrm{lm}}(32)}$$

Capacity loss = 1 − $M_Q(T)$

Eq. (7) New design

Fixed heat load: required increase in conductance

$$M_{\mathrm{UA}}(T) = \frac{\Delta T_{\mathrm{lm}}(32)}{\Delta T_{\mathrm{lm}}(T)}$$

Extra conductance = $M_{UA}(T) - 1$

Example Case: 6°C approach at 33°C

ΔT_{lm} decreases from 9.05°C to 8.00°C, giving M_Q = 0.88 (an existing cooler retains 88% of capacity) and M_{UA} = 1.13 (a new design requires 13% more conductance).

Fouled variant: M_Q is multiplied by 0.85 to represent a 15% loss of conductance, applied to capacity only.

Reserve Capacity Margin Depletion

B

A cooler with spare capacity m carries the design duty until:

$$M_Q(T^*) = \frac{1}{1+m}$$

Allowable fractional capacity loss:

$$\text{allowable loss} = \frac{m}{1+m}$$

- A m = 13% margin tolerates an 11.5% loss and a m = 25% margin a 20% loss.
- T* is solved iteratively for m = 10, 13, 15 and 25%.
- Benchmarks: TEMA 10/13 and general oversizing of 15–25%.

Example: a cooler with m = 25% margin



At 32°C: design duty + 25% reserve



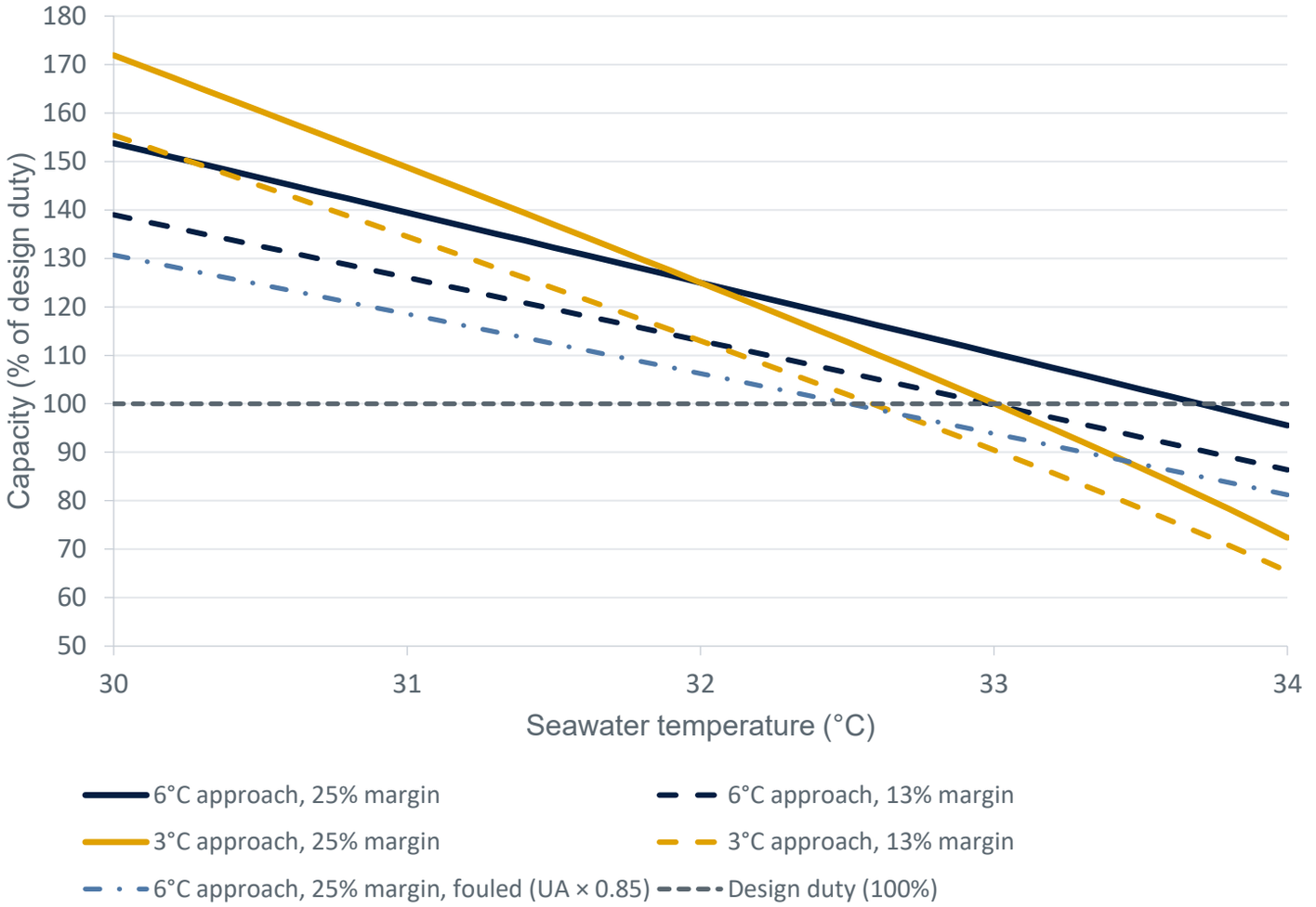
Warmer seawater: design duty + reduced reserve



At T*: reserve exhausted

Track B Result: Design Capacity Sensitivity to Seawater

B



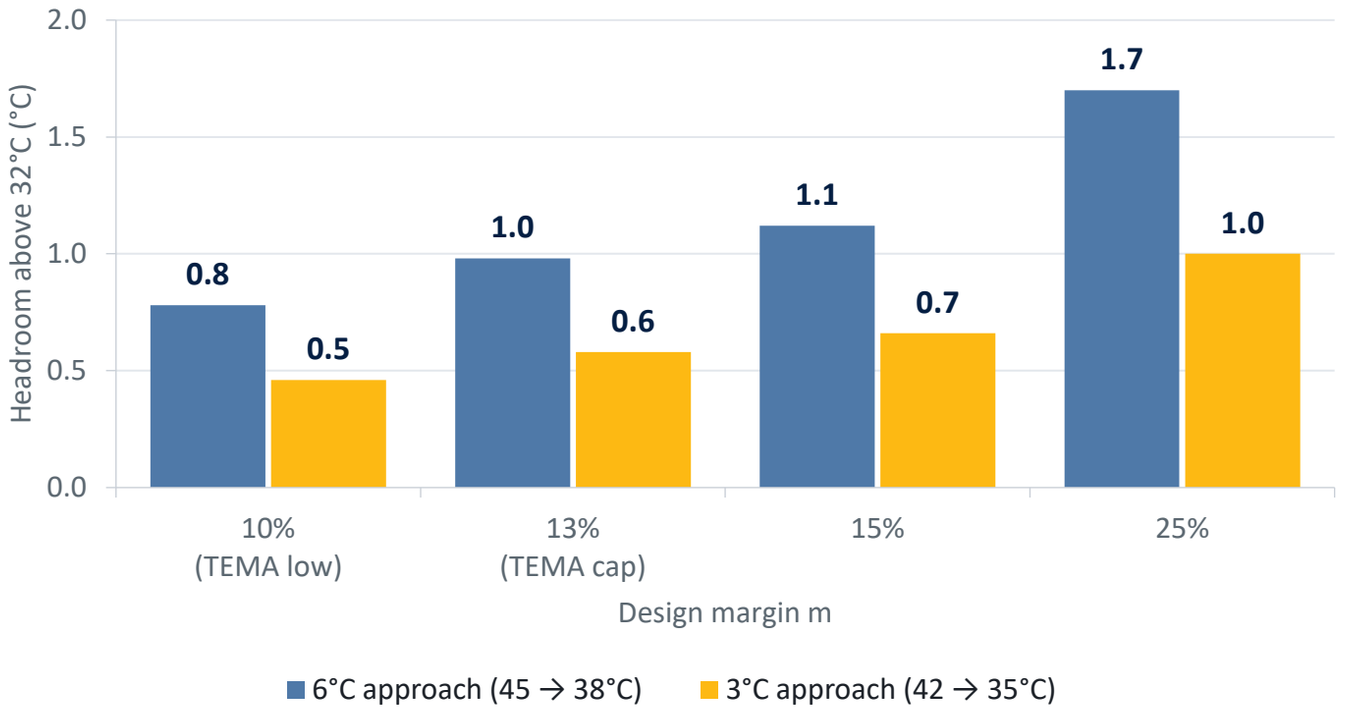
Capacity as % of design duty

Approach, margin	32°C	33°C	34°C	T*
— 6°C, 25%	125%	110%	96%	33.7°C
-- 6°C, 13%	113%	100%	86%	33.0°C
— 3°C, 25%	125%	100%	72%	33.0°C
-- 3°C, 13%	113%	90%	65%	32.6°C
-- 6°C, 25%, fouled	106%	94%	81%	32.5°C

- **100% = design duty:** a cooler sized exactly to the load. Each curve starts at 1 + m at 32°C (113% or 125%).
- **Each °C above 32°C** removes about 12% (6°C approach) to 20% (3°C approach) of installed capacity.
- **T*, crossing 100%,** is margin exhaustion: 32.6–33.7°C for the clean cases.
- **Fouled, 25% margin:** 106% at 32°C, exhausted at 32.5°C. With a 13% margin, a fouled cooler is below duty (96%) at 32°C.

Track B Result: Margin Depletion Above 32°C

B



0.5–1.7°C

headroom above 32°C for a clean, conventionally sized cooler

- Persian Gulf, average location: about 78 days a year at ≥32°C and about 44 at ≥33°C.
- Fouling draws on the same reserve as seawater warming.
- Results quantify lost margin, not failure. Seawater flow, set point, standby coolers and cleaning provide additional mitigation.

RQ3 answer

Each °C above 32°C reduces fixed-cooler capacity by about 12–20%, comparable to the entire 10–13% TEMA margin and a large part of 15–25% oversizing. A clean, conventionally sized cooler reaches margin exhaustion at 32.5–33.7°C.

Track C

Shipping presence and timing

C

RQ4 Does commercial shipping operate in the regions, and in the months, where exposure is highest?

A Satellite SST | B Cooler margin | **C Shipping**

Spatial and Temporal Traffic Presence Data

C

World Bank / IMF traffic density

Static map, Jan 2015 – Feb 2021

- 0.005° fixed map pooled to the 0.25° SST grid
- 97.8% of density lands on valid ocean cells
- Scale undocumented, so only relative density used

Global Fishing Watch presence

Vessel sessions, 2012 – 2025

- Region, dates and hours for each vessel session
- Vessel class from a registry: tanker, cargo, passenger
- Provides timing and vessel class

Eq. (8) Share of traffic density in warm water

$$S_T = \frac{\sum_g V_g \cdot 1\left(D_{g,T} > 0\right)}{\sum_{g \in \text{ocean}} V_g}$$

V_g = traffic density in cell g

$D_{g,T}$ = days cell g reached T in the period

S_T = share of all density in cells that ever reached T

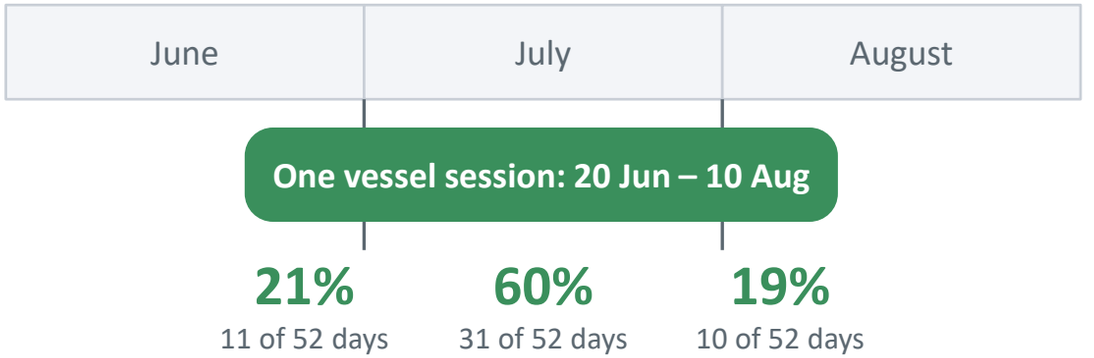
Interpretation: percentage of traffic density in cells that reached T at least once.

Both datasets measure presence in a region and time, not specific position.

GFW Vessel Sessions to Monthly Ship-hours

C

Session hours are allocated across the months covered



- **1,032,363** vessels classified as tanker, cargo, or passenger
- **60.8%** of hours unclassified
- **12.6%** of hours are “matchable” (sessions of 90 days or less)

Monthly allocation

$$h_{r,m} = \sum_{s} H_s \cdot \frac{n_{s,m}}{n_s}$$

H = session hours, n = session days, sum over vessel sessions s that overlap month m in region r.

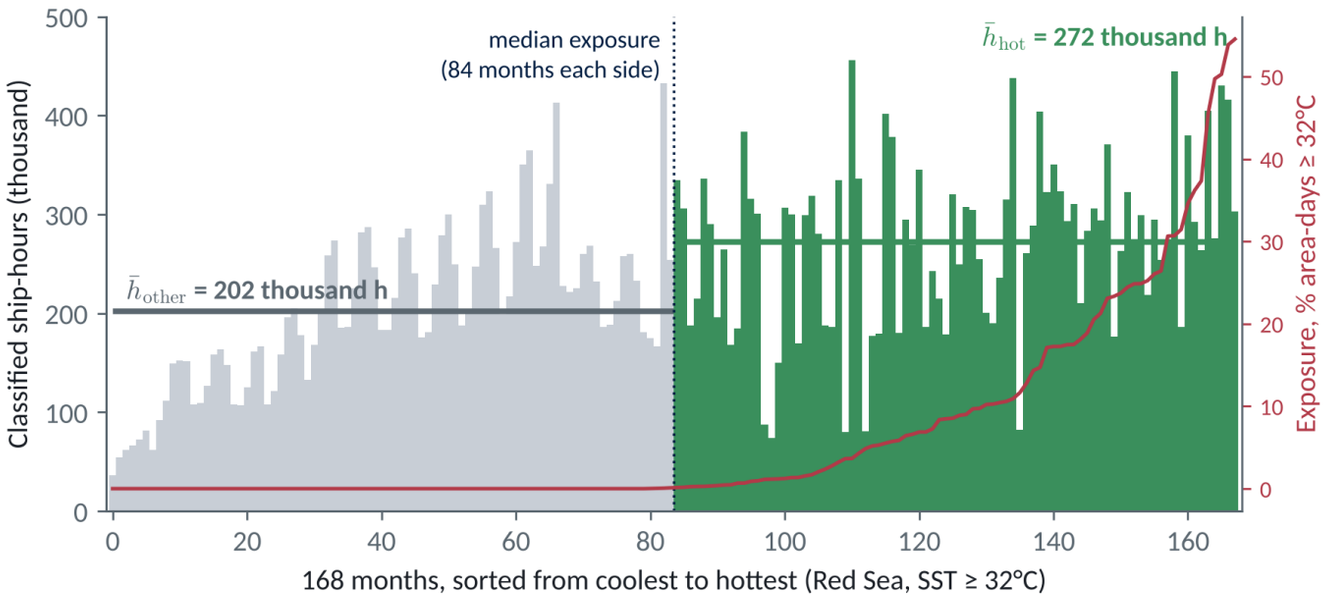
Exposure-weighted presence

$$X_{r,T} = H_r \times F_{r,T}$$

Classified hours H multiplied by area-day fraction F (regional Eq. 4)

Vessel Presence to Month Temperature Median-Split Ratio

C



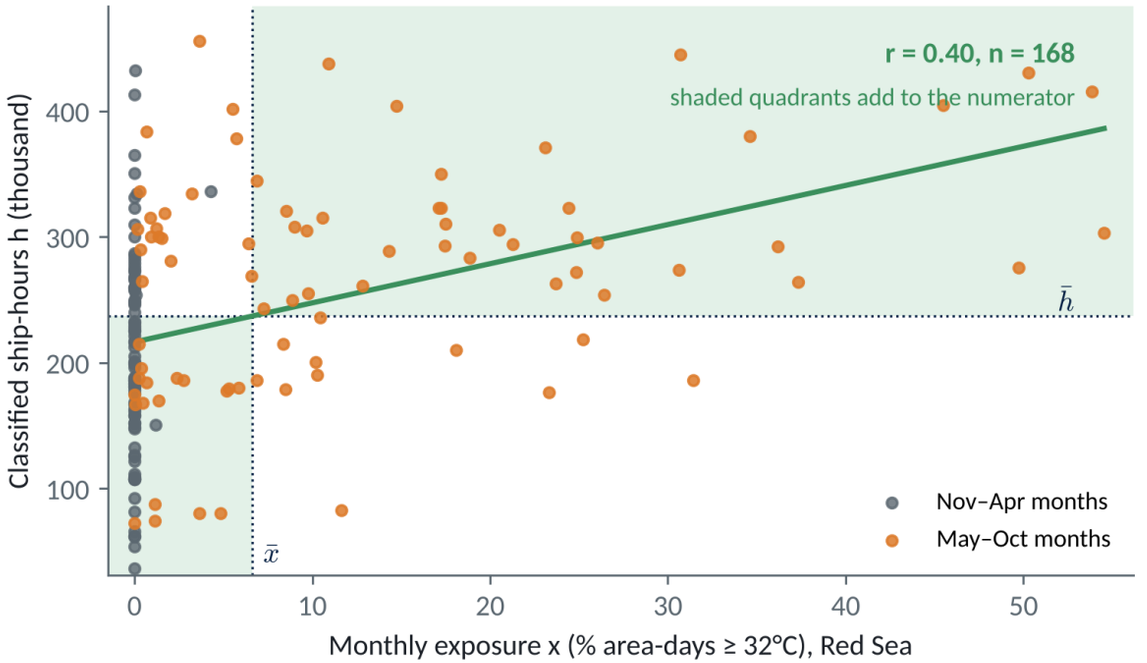
$$R = \frac{\bar{h}_{\text{hot}}}{\bar{h}_{\text{other}}}$$

- Sort the 168 months by exposure x; split at the median.
- **Numerator** (green): mean ship-hours in months above the median.
- **Denominator** (grey): at or below.
- R = 1.3 corresponds to 30% more ship-hours in the hotter half.
- **Red Sea, ≥ 32°C:** R = 272 / 202 = 1.35.

- **Data:** 168 months per region (2012–2025). x = monthly SST exposure (area-day fraction at 30 or 32°C), h = classified ship-hours.
- **Lower Half:** 80 of 168 Red Sea months have zero exposure at 32°C, the median (0.12%) still splits the months 84-84.
- **Limitation:** two groups only, no statistical significance. Pearson correlation uses every monthly value.

Vessel Presence to Monthly Exposure Pearson Correlation

C



co-movement of exposure and ship-hours

$$r = \frac{\overbrace{\sum_m (x_m - \bar{x})(h_m - \bar{h})}}{\underbrace{\sqrt{\sum_m (x_m - \bar{x})^2 \sum_m (h_m - \bar{h})^2}}}$$

product of the two spreads: scales r to $[-1, +1]$

$$t = \frac{r\sqrt{n-2}}{\sqrt{1-r^2}} \quad \text{with} \quad \underbrace{n - 2 = 166}_{\text{degrees of freedom}} \quad \rightarrow \quad \text{two-sided } p$$

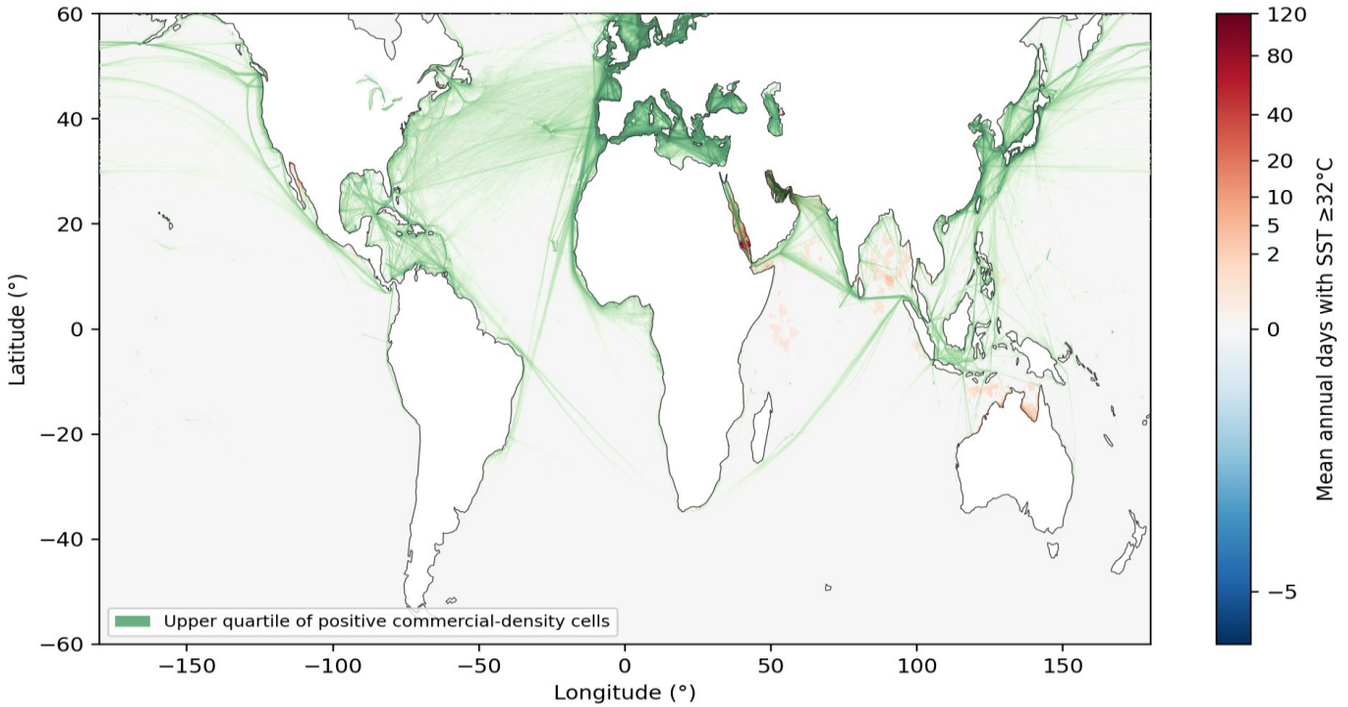
Red Sea, ≥ 32°C: r = 0.40, t = 5.69, p < 0.001; r^2 = 0.16.

CORRELATION CAVEATS

- Both series trend upward from confounding factors (AIS coverage increased, SST warmed), which can produce correlation without a seasonal link.
- Using p-values assumes independent months, but long sessions are allocated uniformly, biasing results toward zero.

Track C Result: Traffic Density in Warm Water

C



Mean annual days with SST ≥ 32°C and the busiest quarter of shipping-density cells, 2015–2021.

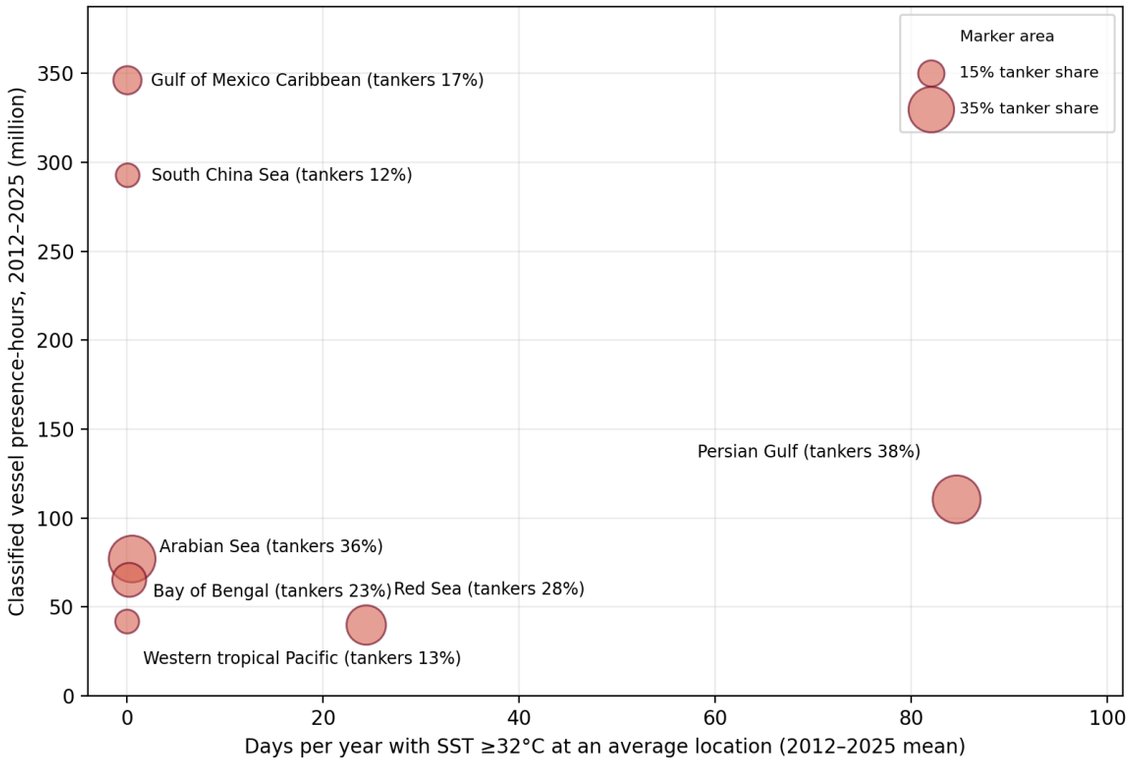
Share of traffic density in warm water

SST	Ever reached	≥ 7 days/yr
≥ 30°C	24.5%	15.9%
≥ 31°C	13.0%	3.8%
≥ 32°C	3.1%	1.75%
≥ 33°C	1.5%	1.06%

- Near-limit water is a regular condition for about a quarter of traffic density.
- Water above 32°C affects only about 3%, on a few routes.
- In the Persian Gulf and Red Sea, the main corridors cross the most exposed water.

Track C Result: Traffic Density and Exposure

C



Days per year at ≥ 32°C versus classified presence-hours, 2012–2025. Circle area increases with tanker share.

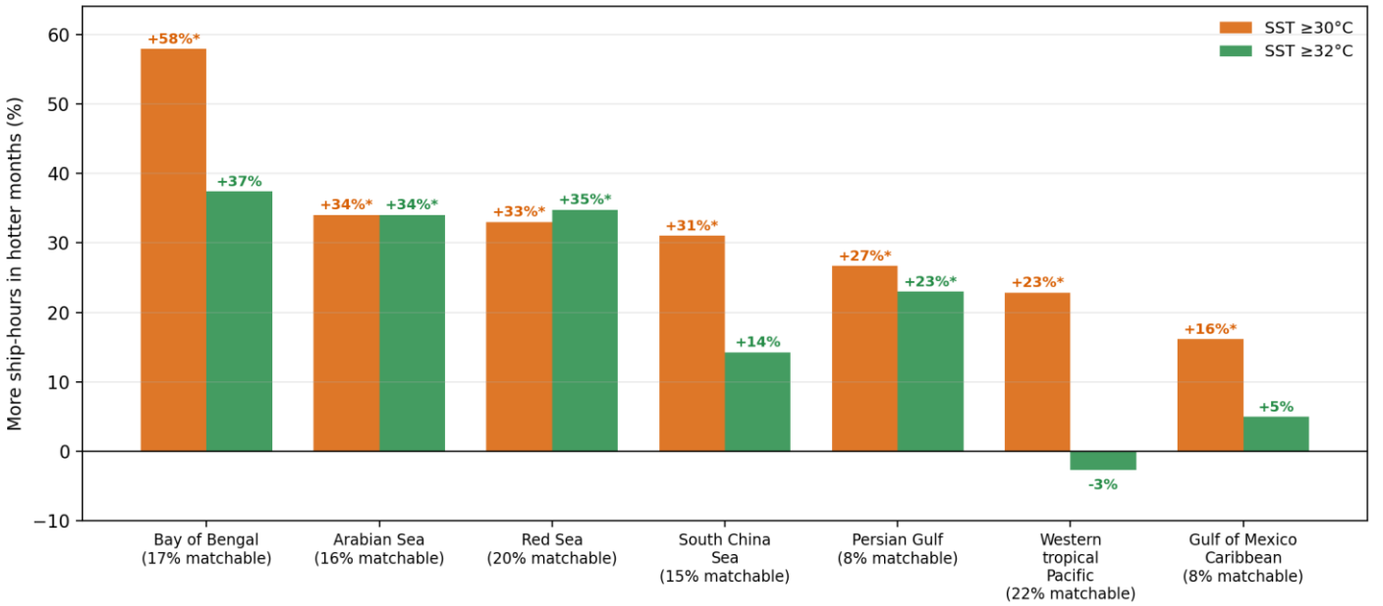
Classified presence-hours, 2012–2025

Region	Total (M h)	Tanker share	Unclass.
Gulf of Mexico / Caribbean	346	17%	47%
South China Sea	293	12%	73%
Persian Gulf	110	38%	67%
Arabian Sea	77	36%	51%
Bay of Bengal	65	23%	35%
W. tropical Pacific	42	13%	58%
Red Sea	40	28%	33%

- **Weighted by thermal exposure, the Persian Gulf ranks first** at every threshold (43.6 vs 42.7 million h at 30°C).
- Presence hours rise 66–124% per decade in every region, confounded with AIS coverage growth.

Track C Result: Presence Higher in Warmer Months

C



*Difference in presence-hours, hotter vs cooler half of months. * = significant (p < 0.05).*

Monthly correlation, ≥ 32°C

Region	Ratio R	Pearson r
Red Sea	1.35	0.40
Arabian Sea	1.34	0.31
Persian Gulf	1.23	0.25
Other four regions	0.97–1.37	−0.10 to 0.15

- At ≥ 30°C: r = 0.22–0.43 in all seven regions.
- Only ~1 hour in 8 is month-matchable, so these figures understate the association.

RQ4 answer

The most exposed regions are not the busiest, but they carry substantial, tanker-heavy traffic, and traffic is heavier in the hot months; significant at 30°C in all seven regions and at 32°C in the three most exposed.

Results Summary

A

RQ1–RQ2

Extent and location of warm water

Daily SST 1982–2025; area-days at 30–33°C; bootstrap, HAC and FDR

- ≥ 32°C water: about 0.03% of the ocean, but +47% in area
- 30–< 32°C band: +121% (3.8 → 8.4 million km²)
- Persian Gulf 54 → 78 days/yr; Red Sea 12 → 20 days/yr

B

RQ3

Cooler capacity loss

Normalized log-mean ΔT model; 6°C and 3°C approach designs

- About 12% (6°C approach) to 20% (3°C approach) lost per °C above 32°C
- Comparable to the entire 10–13% TEMA margin
- Clean, conventional margin exhausted at 32.5–33.7°C

C

RQ4

Ship presence in exposed regions and months

Traffic density and vessel presence; median split and correlation

- 3.1% of traffic density in cells that reached 32°C (24.5% at 30°C)
- Persian Gulf: 38% tankers, first by heat-weighted presence
- Warm-month traffic is higher: r = 0.22–0.43 at 30°C

RQ5: Is a fixed 32°C reference still adequate?

A **Warm water is more frequent and regionally concentrated**

≥ 32°C water +47%

Near-limit +121%

Persian Gulf and Red Sea

B **Warming consumes cooler margin**

12–20% capacity lost per °C

Margin exhausted at 32.5–33.7°C

C **Ships operate there during the hot months**

Tanker-heavy Persian Gulf traffic

Heavier in hotter months

RQ5 Answer

Retain 32°C as the general design basis

Review cooling margin for ships in the most exposed trades (Persian Gulf, Red Sea, similar waters) under combined fouling, degraded flow, high load and seawater above 32°C.

Study Limitations

A Satellite SST

- Interpolated 0.25° surface product, not sea-chest temperature
- Coastal and shallow gradients not resolved
- Intervals reflect annual variability

B Cooler model

- Two assumed designs, fixed freshwater temperatures, steady state
- A sensitivity study, not a ship model
- TEMA margins refer to shell-and-tube coolers, plate coolers use smaller fouling allowances
- Order-of-magnitude benchmark

C Shipping

- Presence matched by region and month, not by precise position
- Static 2015–2021 density
- 60.8% of GFW presence hours unclassified and 12.6% month-matchable
- Ship-hours drift with AIS coverage, pooled months overstate effect size

Broadly, this is an exposure and sensitivity analysis. Identifies where further assessment is warranted, not the conditions experienced by an individual ship.

Conclusions

1. Water at or above 32°C is still rare (about 0.03% of the ocean) but 47% larger in recent decades, and the 30–<32°C band has more than doubled. It is concentrated in the Persian Gulf (54 → 78 days per year) and the Red Sea (12 → 20 days per year).
2. Commercial ships operate in these regions during the hot months: the most exposed seas are not the busiest, but carry substantial, tanker-heavy traffic that increases when the water is hottest.
3. Each degree above 32°C reduces a fixed cooler's capacity by about 12–20%, comparable to its fouling margin. Seawater warming and operational degradation compound capacity loss.
4. No strong evidence to change 32°C as the general design basis. Consider cooling margin review for the most exposed trades (vessels and regions).

Next Steps: Finer SST mapping resolution, detailed cooler and control-system modeling, vessel-level position time in warm water from licensed AIS data.

Thank You and Questions



References (1) design basis, climate and SST

Hillier (1935) “Modern Marine Condensing Plants and Feed Systems,” Institute of Marine Engineers. library.imarest.org/record/1618

Ranken (1954) “Heat Pump in H.M.S. Vidal,” Journal of Naval Engineering. library.imarest.org/record/10226

[1] IACS, Unified Requirement M40: Ambient Conditions – Temperatures. iacs.org.uk/resolutions/unified-requirements/ur-m/ur-m40-new

LR (2022) Lloyd’s Register, Rules for the Classification of Ships, Part 5, Ch. 1, Sec. 3. imorules.com/LRSHIP_PT5_CH1_3.html

[2] DNV, Rules for Classification: Ships, Pt.4 Ch.1 – Machinery Systems, General, Jul. 2025.

[3] G. Kocak and Y. Durmusoglu, “Energy efficiency analysis of a ship’s central cooling system using variable speed pump,” Ships and Offshore Structures, 12(sup1), 43–51, 2017.

[4] T.-Y. Jeon, C.-M. Lee and J.-J. Hur, “A study on the control solution of ship’s central fresh water-cooling system,” J. Mar. Sci. Eng., 10(5), 679, 2022.

[5] B. Huang et al., “Improvements of the daily optimum interpolation sea surface temperature (DOISST) version 2.1,” J. Climate, 34(8), 2923–2939, 2021.

[6] NOAA NCEI, Optimum Interpolation Sea Surface Temperature (OISST). ncei.noaa.gov/products/optimum-interpolation-sst

[7] E. C. J. Oliver et al., “Longer and more frequent marine heatwaves over the past century,” Nature Communications, 9, 1324, 2018.

[8] IPCC, Climate Change 2021: The Physical Science Basis (WG I, AR6), Ch. 9, §9.2.1.1. ipcc.ch/report/ar6/wg1/chapter/chapter-9/

NOAA NOAA NCEI, Climate at a Glance: Global Time Series, global ocean, 1950–2025. ncei.noaa.gov/access/monitoring/climate-at-a-glance

References (2) data, statistics and shipping

Künsch (1989) H. R. Künsch, “The jackknife and the bootstrap for general stationary observations,” Annals of Statistics, 17(3), 1217–1241.

Newey & West (1987) “A simple, positive semi-definite, heteroskedasticity and autocorrelation consistent covariance matrix,” Econometrica, 55(3), 703–708.

Benjamini & Hochberg (1995) “Controlling the false discovery rate,” J. Royal Statistical Society B, 57(1), 289–300. doi:10.1111/j.2517-6161.1995.tb02031.x

Benjamini & Yekutieli (2001) “The control of the false discovery rate in multiple testing under dependency,” Annals of Statistics, 29(4), 1165–1188.

[9] IMO, “AIS transponders.” imo.org/en/OurWork/Safety/Pages/AIS.aspx

[10] Global Fishing Watch, “API v3: Key concepts.” globalfishingwatch.org/our-apis/documentation

[11] World Bank and IMF, “Global Shipping Traffic Density,” World Bank Data Catalog, 2023.

[12] EMODnet Human Activities, “EU Vessel Density Map – Detailed Method,” 2023.

[13] TEMA, Standards of the Tubular Exchanger Manufacturers Association, 10th ed., Para. R-4.22, 2019.

[14] S. Hall, “Rules of thumb: heat exchanger selection,” The Chemical Engineer, no. 976, Oct. 2022.

[15] Natural Earth, “Free vector and raster map data.” naturalearthdata.com

The Case for Powered Propellers on Ship Wingsails

Sergio E. Perez

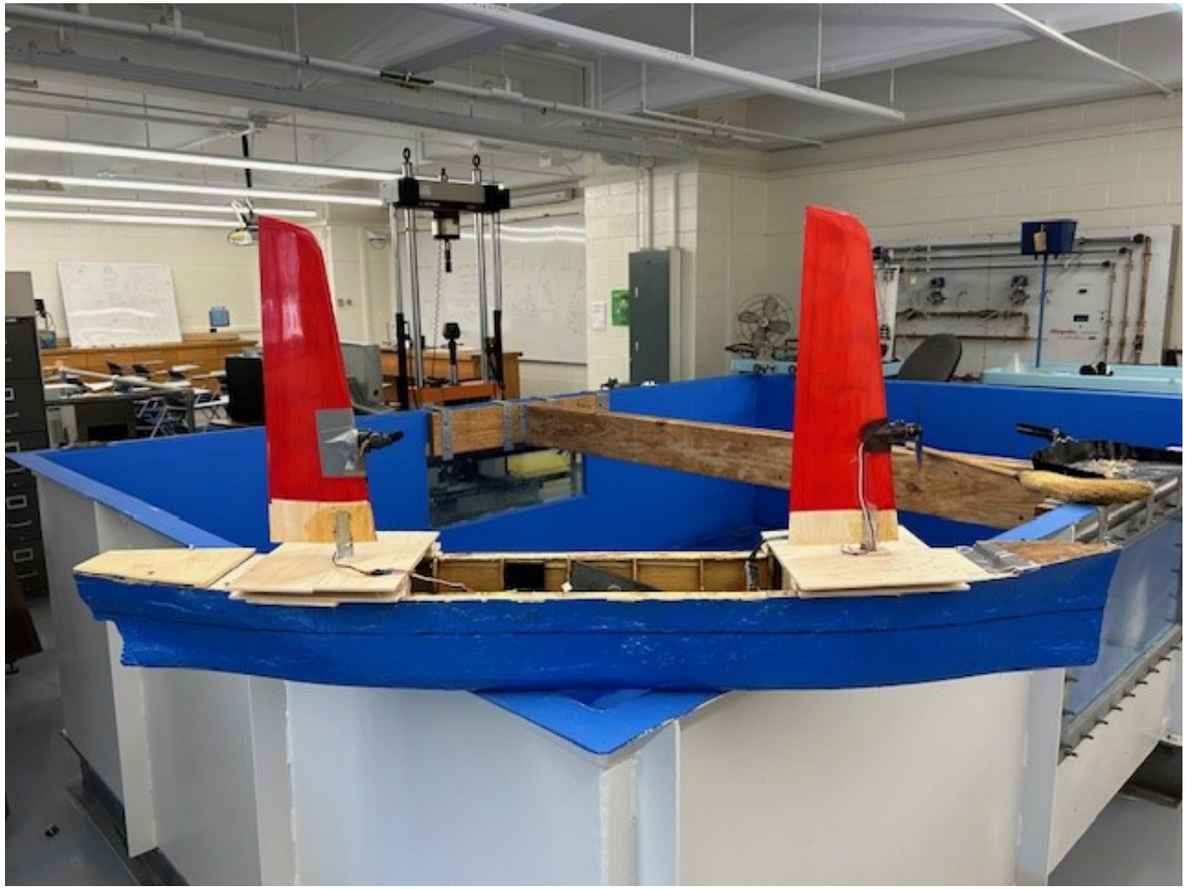


For more details please see: Journal of Sailing Technology 2026, volume 11, issue 1, pp. 115 – 136. The Society of Naval Architects and Marine Engineers.

Powered Wingsails (Propeller-Sails)

(conceived 2023 – still under development)



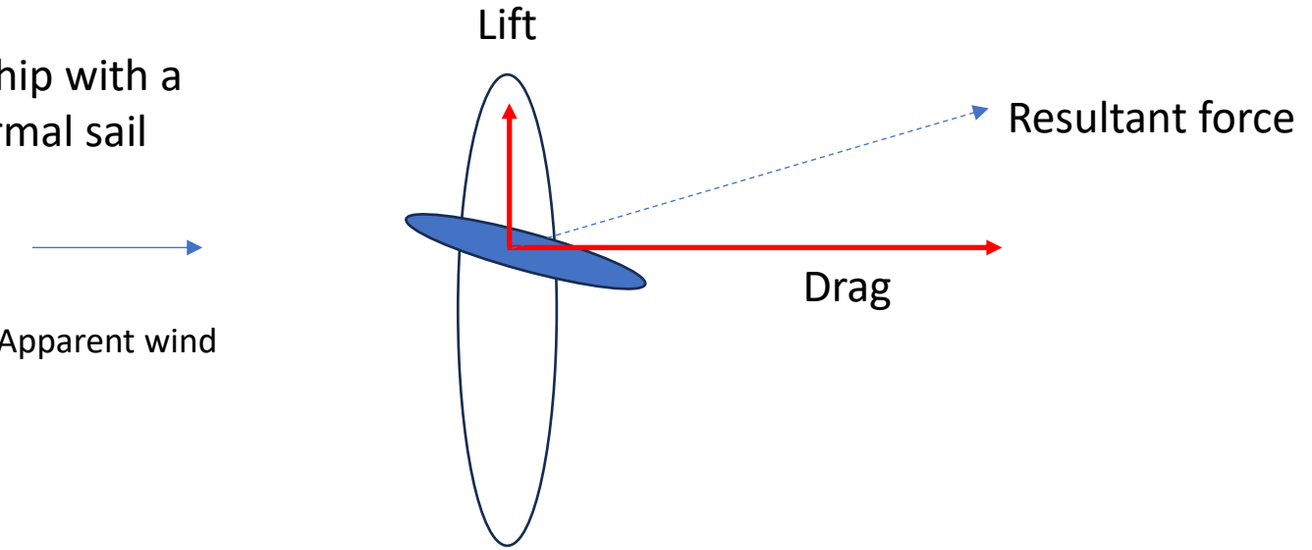


QUESTION TO BE ANSWERED: Should ships use this idea?

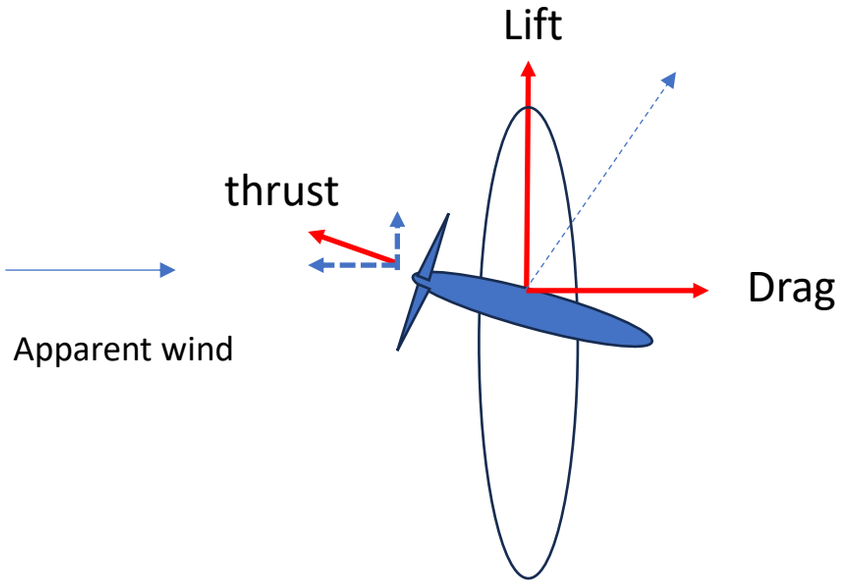
This work is an extension of SISDO 2025 presentation on same topic, with more wing angles of attack and a variety of wing power settings

Propeller-Sail on a Ship (ship moves towards the top of screen)

A ship with a normal sail



A ship with a Propeller-Sail



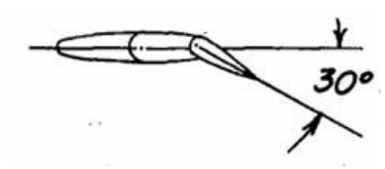
Net effect of propeller:

- Higher lift (Cl as high as 14)
- Lower drag

Higher lift is not just from thrust component up, but also from faster flow speeds over the wing from propeller wake.

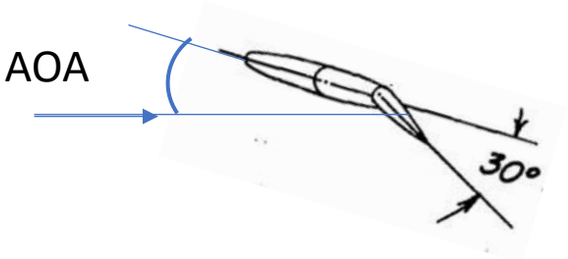
Controlling the Propeller-Sail:

The wing has a flap that can be adjusted



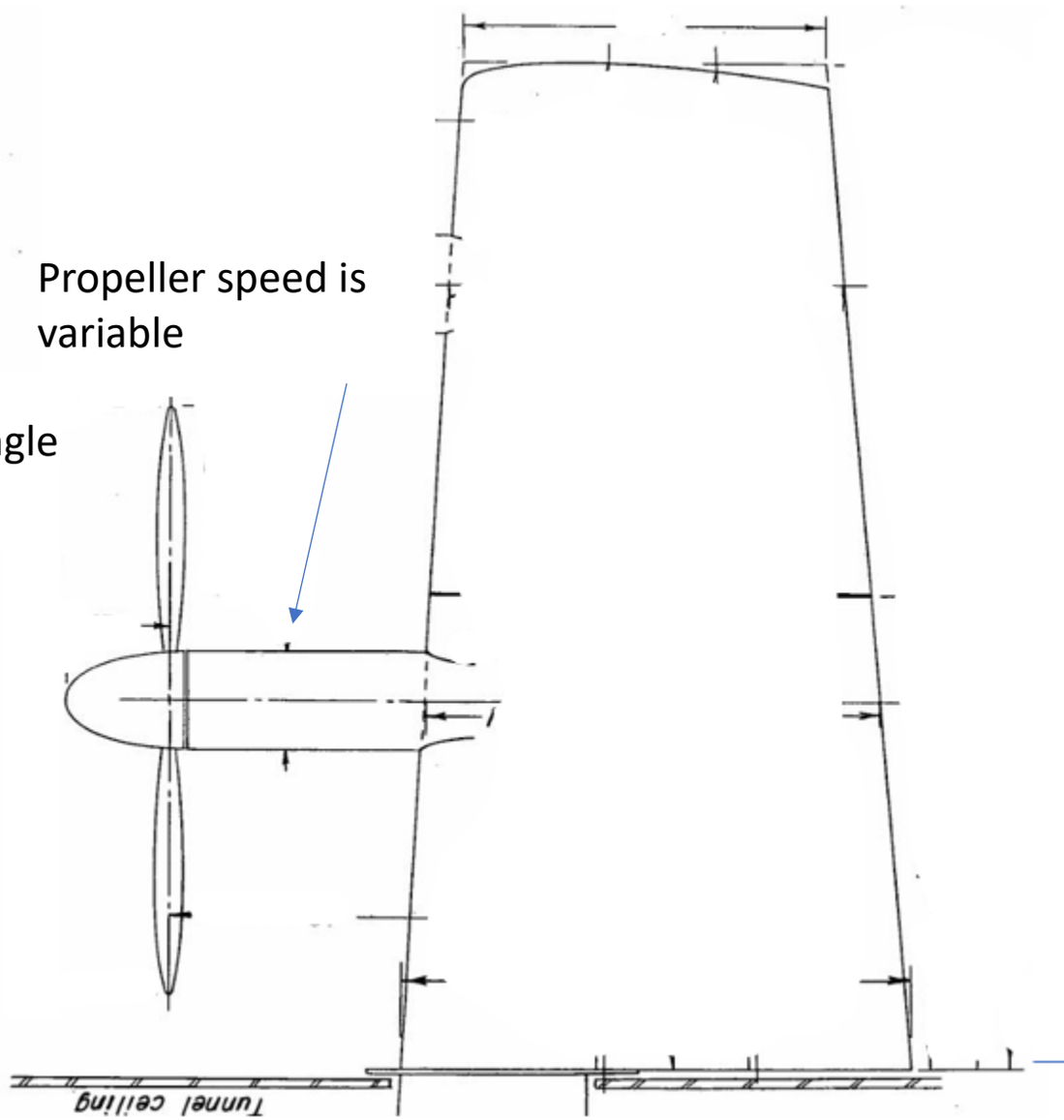
The wing can be angled into the incoming wind. The angle is the angle of attack, or AOA

AOA



If the propeller power is off, the Propeller-Sail acts like a rigid sail (or wingsail) and can still move a ship.

Propeller speed is variable



A simulation was run on a fully-loaded, 37 m Series 60 cargo ship hull with Propeller-Sail in 10 m/s winds

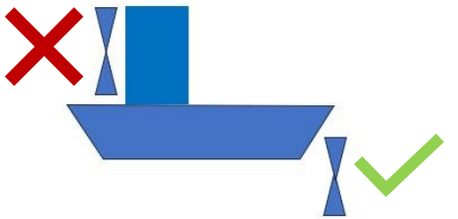
- A Velocity Prediction Program (VPP) OpenVPPimplict was used to determine ship velocity.
- Experiments conducted for Vertical take-off propeller aircraft by Kuhn and Draper were used to calculate wing propeller thrust.
- Lift, drag and power of the Flettner rotor were determined using the results of DeMarco and Trout
- Ship hull drag and lift were taken from Series 60 towing tank results and Wagner's experimental results for hulls at an angle to the incoming flow of water.
- Two vessel speeds were analyzed:
    1) **6 knots**
    2) **9 knots**

Continued on next slide

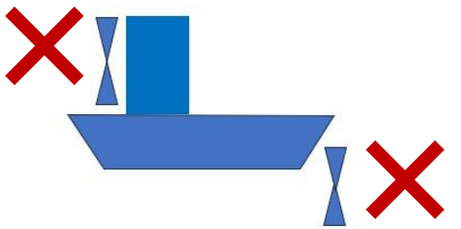
- The Operational modes analyzed:
  - Powered Propeller-Sail: Wing-mounted propeller is powered, ship's engine off

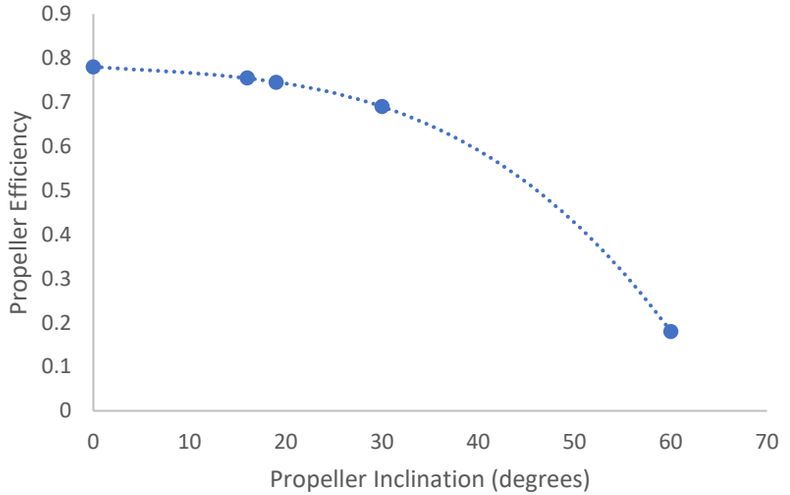


  - Hybrid Wingsail: Wing-mounted propeller is unpowered, ship's engine turns ship propeller at reduced level. The Propeller-Sail acts like a wing-sail with the ship's engine/propeller on.

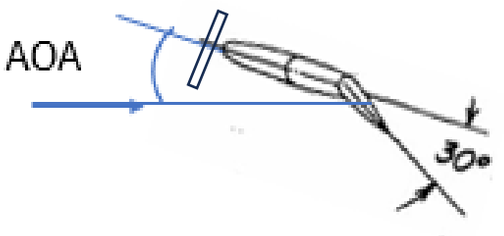


  - Pure-Sailing: Wing-mounted propeller is unpowered and ship's engine is unpowered. Propeller-Sail operates as a wing-sail



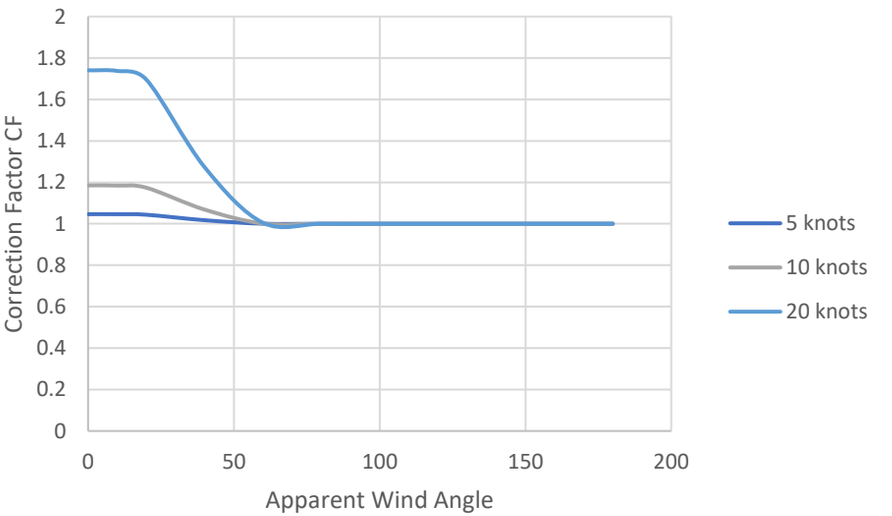


Air Propeller efficiency depends on angle of tilt of prop (Lesley et al. 1937)



Ship propeller efficiency assumed 0.8 when moving straight ahead/

To account for head seas and wind: (Woodward et al.), calm water resistance is multiplied by a correction factor CF:



BEST RESULTS

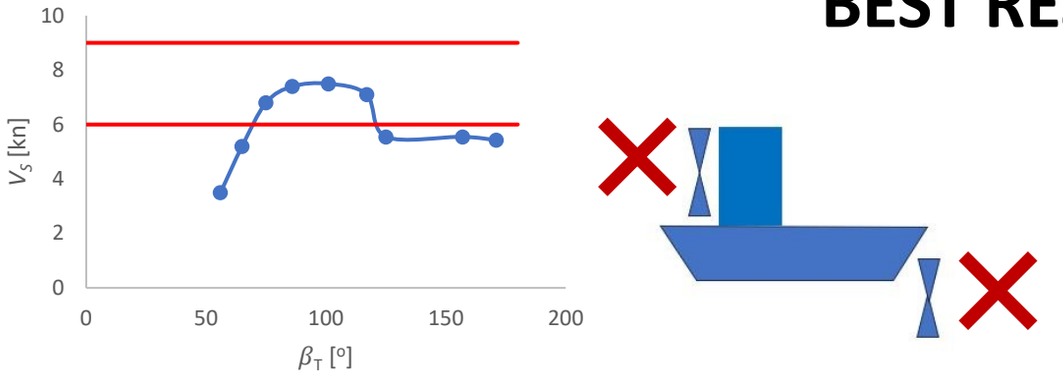


Figure 12. Vessel speed V_S in Pure-Sailing mode in 10 m/s winds, as a function of true wind angle β_T

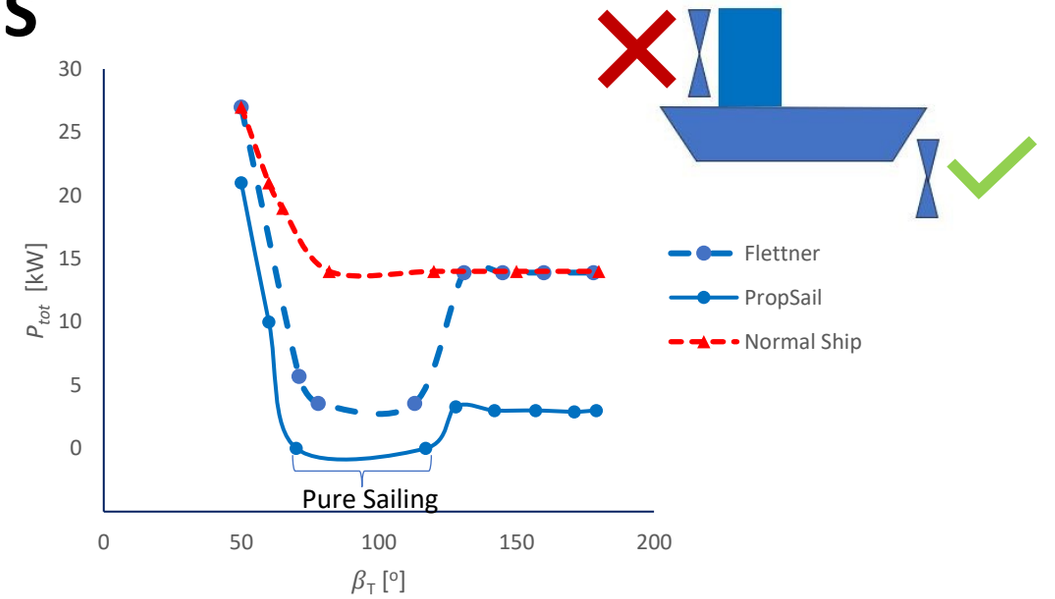


Figure 13. 6 knot results. Total power consumed P_{tot}.

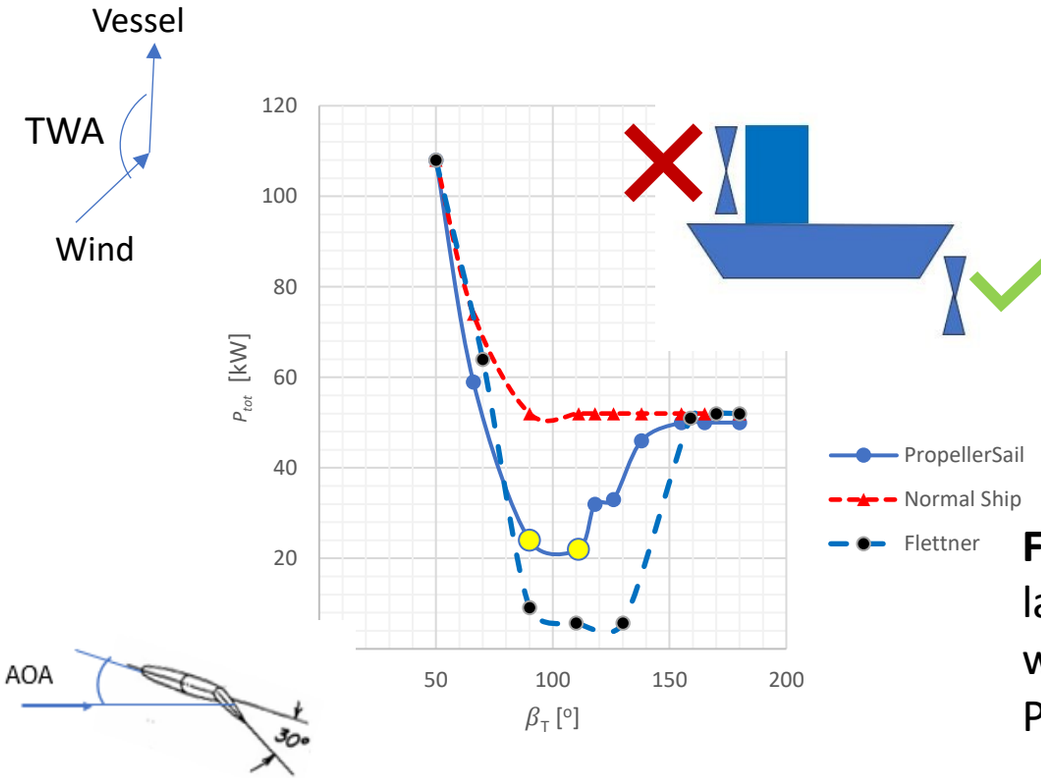


Figure 14. 9 knot results for total power consumed P_{tot}.The two large yellow points on the Propeller-Sail plot were generated with the wing propeller activated in Pure-Sail mode. All other Propeller-Sail points were made in Hybrid mode.

It appears the propeller is not really needed to save fuel! (at 9 knots the savings are small)

But powered wingsails give tremendous maneuverability, comparable to azimuth thrusters.

If both reduced-cost operation and greater maneuverability are required, powering the sails is warranted.

https://youtu.be/8Y-W33zXOMY

Propeller Sail single-prop maneuvering in lab

https://youtu.be/CpEcJ0EMUXE